Towards a Systems Modelling Approach for a Large-Scale Canadian Prairie Watershed

A Thesis Submitted to the College of
Graduate and Postdoctoral Studies
In Partial Fulfilment of the Requirements
for the Degree of Master of Science
In the Department of Civil, Geological, and Environmental Engineering
University of Saskatchewan
Saskatoon, Saskatchewan, Canada

By

Kamrul Hossain

Permission to Use

In presenting this thesis in partial fulfillment of the requirements for a Postgraduate degree from the University of Saskatchewan, I agree that the Libraries of this University may make it freely available for inspection. I further agree that permission for copying of this thesis in any manner, in whole or in part, for scholarly purposes may be granted by the professor or professors who supervised my thesis work or, in their absence, by the Head of the Department or the Dean of the College in which my thesis work was done. It is understood that any copying or publication or use of this thesis or parts thereof for financial gain shall not be allowed without my written permission. It is also understood that due recognition shall be given to me and to the University of Saskatchewan in any scholarly use, which may be made of any material in my thesis.

Requests for permission to copy or to make other uses of materials in this thesis/dissertation in whole or part should be addressed to:

Head of the Department of Civil, Geological, and Environmental Engineering
University of Saskatchewan
57 Campus Drive
Saskatoon, Saskatchewan S7N 5A9
Canada

OR

Dean
College of Graduate and Postdoctoral Studies
University of Saskatchewan
116 Thorvaldson Building, 110 Science Place
Saskatoon, Saskatchewan S7N 5C9
Canada

Abstract

The hydrological processes of a large-scale prairie watershed pose a number of challenges for a modeller, and are difficult to parameterize in a hydrological model. Prairie land surface heterogeneity includes wetland hydrology along with dynamic surface storage capacity and cascading arrangements of depressional surface storages or ponds, which eventually lead to a fill-spill type runoff propagation. Fill-spill runoff is movement of excess rainfall or snowmelt from pond to pond, which is different from traditional runoff propagation methods. For this reason, a special parameterization of fill-spill type runoff propagation as well as land surface heterogeneity is required for model development for a prairie watershed. The probability distribution model (PDM) concept has been tested for the prairies in the past and appears to be suitable to parameterize the runoff propagation. Besides the challenging prairie topography, large watersheds may contain lakes and reservoirs that are used for various purposes like water supply, agriculture, and recreation. Water resources management practices at interconnected, controlled and uncontrolled lake systems also pose challenges to the modellers. The effect of lakes may be insignificant for a prairie watershed located in a headwater area, however, the effects of interconnected lake system are significant and require appropriate parameterization to model. The main objectives of this thesis are to investigate the hydrological connectivity in the context of runoff processes and to assess the effect of water resources management practices in the prairie region of Canada. The Qu'Appelle River basin (QRB), located in the Canadian Prairie region, contains a network of multiple controlled and uncontrolled lakes, and hence is a suitable large-scale watershed for this study.

The prairie hydrological processes in association with the interactions of multiple lakes create a cascading hydrological system in the QRB and a hybrid modelling approach looks to be a promising methodology to develop a systems model for this watershed. Instead of using a

single modelling tool to address this system, two modelling tools are used in this study. MESH (Modelisation Environmentale Communautaire (MEC)—Surface and Hydrology) is a widely used hydrological modelling tool in Canada and contains runoff generation algorithms suited for different types of land surface schemes. For the prairies, an existing runoff generation algorithm was developed using the PDM concept (known as PDMROF). The PDM concept assumes that runoff is a function of dynamic storage capacity, which is represented using a probability distribution function of surface storage capacities. In the direction of simulating prairie runoff processes, there is a scope to improve the parameterization of PDMROF by addressing its limitation of not being able to simulate interflow. An interflow component was added in the parameterization of PDMROF using an approximate solution of Richards' equation that was found in another existing runoff generation algorithm within MESH named 'WATROF'. The algorithm developed in this study is known as 'LATFLOW', which was compared with the existing runoff generation algorithms used in MESH across three different prairie and non-prairie watersheds with areas ranging from 600 to 2500 km^2. Comparison results suggest that LATFLOW performed better than the PDMROF algorithm for simulating streamflow in prairie watersheds and performed also reasonably well in a non-prairie watershed. Owing to the better performance of LATFLOW, it was used in developing a hydrological model for the QRB, which has an area of ~50,000 km^2. Due to the presence of multiple lakes within the QRB, a lake system model was developed using the system dynamics (SD) approach to simulate operations and interactions of the lake system of the QRB. This model was developed using measured outflow from the tributaries and lake water levels. The calibrated SD model was able to simulate streamflow and lake levels to a high degree of accuracy, indicating that the lake system of the QRB is suitable for the task under consideration. In order to combine both MESH and the SD model to simulate streamflow in the QRB, two approaches were implemented, which are named as 'top-down' and 'bottom-up' approaches.

In the top-down approach, simulated outflow from MESH models for the headwater tributaries of the QRB were input to the lake SD model to estimate streamflow at the outlet of the QRB near Welby, which is located near the Saskatchewan and Manitoba border. In the bottom-up approach, naturalized streamflow was generated at the outlet of the QRB by using the lake SD model, and the MESH parameters for the QRB were estimated considering the naturalized hydrological system of the QRB. Results indicate that simulated streamflow is underestimated for some tributaries, but the timing of peak flows is captured. The hybridization of the hydrological model and lake SD model is considered as a viable option when handling watersheds such as QRB where interactions between lakes play an important role in association with complex prairie hydrological processes. Investigations were also carried out to identify the effect of the choice of the calibration period on the model performance, and the results indicate that the QRB exhibits different streamflow patterns at a decadal scale and efficient modelling requires further knowledge about incorporating these patterns within the modelling framework.

Acknowledgements

With gratitude, I acknowledge that this work was supported by the Natural Science and Engineering Research Council (NSERC) Canadian FloodNet (Grant number: NETGP 451456) and the Department of Civil, Geological, and Environmental Engineering, and scholarships received through the College of Engineering. I am also grateful for the computing facilities provided by CANSIM, department of Civil, Geological, and Environmental Engineering, University of Saskatchewan.

I would like to thank my supervisors, Prof. Amin Elshorbagy and Prof. Howard Wheater, for their guidance and technical support in completing this work. I would like to thank my committee members, Dr. Kevin Shook and Prof. Saman Razavi for their support in this work. Lastly, I would like to thank my external examiner Dr. Karl-Erich Lindenschmidt, as well as the committee members, for clarifying much of my work.

This work would not have been possible without the support from friends, colleagues and family. The students of CANSIM and the Global Institute for Water Security have provided invaluable support, and particularly Dr. Raja Bharath, Dr. Bruce Davison, and Mr. Daniel Princz for discussing ideas and motivating me through the past years. I would like to convey my profound gratefulness to my parents (Md. Delwar Hossain and Ms. Roushan ara Begum) for their supports. Special thanks to my loving wife, Ms. Tanzim Sharmila Akther, for her continuous inspiration. Last but not the least, my sincere thanks to my brother, Muhmmad Fakhrul Hossain, for his encouragements.

Table of Contents

List of Figures

List of Tables

Chapter 1: Introduction

The components of the hydrological cycle, i.e. precipitation, evapotranspiration, runoff, storage, act differently based on the hydrological features of a region. It is often observed that runoff response of a watershed is proportional to rainfall (Chow et al., 1988) and a number of mathematical models (for example TOPMODEL, HYMOD, HBV) were developed using this relationship. However, hydrological responses are dependent on the physiographic properties of a watershed (Hewlett and Hibbert, 1967), which are mostly different across the world. For example, a forest dominated watershed would generate greater evapotranspiration compared to a non-vegetative watershed, a cold region watershed exhibits high dependencies on snow related hydrological processes, and a prairie watershed exhibits a variable drainage properties due to increased storage capacity. In this thesis, the hydrological responses of a large-scale prairie watershed are going to be discussed along with suitable modelling approaches.

In a Canadian context, where the country is divided into 15 distinct ecozones (Stelfox et al., 1991), topographic features of the prairie ecozone are mostly different from those of the other ecozones. The provinces of Alberta, Saskatchewan, and Manitoba of Canada contain the prairie region. This region contains millions of small depressions of glacial origin called prairie potholes that provide important wildlife habitats (Johnson et al., 2004; Valk, 1989). These depressions form wetlands, which are hydrologically important due to their surface storage capacity and variable drainage contribution (Van der Kamp and Hayashi, 2009). Many of these wetlands often drain internally and form a temporary storage, which affects the transformation of runoff into streamflow (Hayashi et al., 2003; Shook et al., 2015). Under normal condition internally drained closed basins do not contribute to nearby streams (Pomeroy et al., 2010) and form non-contributing areas (NCAs), defined as a portion of the watershed that does not contribute runoff to the watershed outlet up to 2-year return period events (Prairie Farm

Rehabilitation Administration, 2008). The NCAs are dynamic in nature and vary with the amount of water stored in depressions (Pomeroy et al., 2010; Shaw et al., 2012).

Diverse physiography and unique hydrological features across watersheds, along with the representation of land surface heterogeneity and human interventions, pose challenges to model hydrological processes in such watersheds. The pattern and extent of these challenges change depending on the physiographic properties of a watershed. Because of NCAs, development of a hydrological model for a prairie watershed is complex. Complexity of prairie hydrological modelling is not only limited to variable drainage contribution due to natural topography, but also depends on the modelling of a number of controlled and uncontrolled water bodies that might exist. For similar hydrometeorological conditions, runoff response in a prairie watershed can change from year to year depending on the antecedent soil moisture condition (Stichling and Blackwell, 1957). During wet conditions, a temporary channel is formed by connecting depressional wetlands to one another and runoff from headwater can reach the nearest stream through a 'fill-spill' mechanism (Shaw et al., 2013, 2012). Parameterizing 'fill-spill' type of runoff propagation poses a challenging feature for the development of a hydrological model for prairie watersheds. Moreover, the presence of lakes with complicated operating rules based on downstream demand, natural interactions, and flat topography forms a complex system, which is difficult to formulate and represent in a hydrological model as well. The scale is also an important aspect for a prairie watershed modelling. The scale of a model governs spatial heterogeneity and non-linearity in a watershed for which entities, patterns, and processes is characterized. A large-scale watershed consists of multiple sub-watersheds and the hydrological characteristic of the sub-watersheds often vary from one another. The degree of variation depends on human interventions, and spatial and physiographic properties of the large-scale watershed. For a prairie watershed, the degree of variation is high as prairie physiography presents a high level of heterogeneity and a significant effect of human

intervention may arise due to lake operations. Developing a systems model for a large-scale prairie watershed is done using a hybrid modelling approach by distributing different modelling challenges to different modelling tools and generate a combined simulation considering all the sub-ordinate models. Using a hydrological model (Mekonnen et al., 2015) that has the ability to address fill-spill type runoff propagation with a systems model for lakes that can address the operations and interactions could be one of the suitable approaches to develop a hydrological model of a large-scale prairie watershed.

1.1 Problem Definition

Developing a model for a large-scale prairie watershed is a challenging task because of complex features of prairie topography and anthropogenic activities. One such important large-scale watershed is the Qu'Appelle River basin (QRB), which is located in the southern part of Saskatchewan, encompassed entirely within the prairie ecozone. This is a critical basin of interest for different organizations (such as the Saskatchewan Water Security Agency) as this basin is a home for a large number of people, and is of agricultural, industrial, socio-economic and ecological importance (Lindenschmidt et al., 2012; Saskatchewan Bureau of Statistics, 2012; Water Security Agency, 2014). The main challenge of hydrological modelling for QRB is to address hydrological processes as well as water resources management practices. The hydrological processes of such a prairie watershed are heavily dependent on the appropriate representation of surface storage connectivity (Shaw et al., 2012). Surface storage connectivity is the arrangement of depression storages, which play an important role in draining water from headwater areas to the nearest stream using the 'fill-spill' mechanism of runoff propagation. The effect of storage capacity and connectivity of depression wetland is important as it determines the pattern of hydrological response. Previously researchers used different approaches to address the prairie surface storage connectivity using approaches such as remote sensing based (Shook et al., 2013) and conceptual (Mekonnen et al., 2016, 2014). Both of these

approaches have merits and demerits. The former approach models the actual arrangement of potholes (ponds) and simulates runoff considering actual pothole connectivity, however, this has a limitation that it might not be applicable for a large watershed because of high computational expense. On the other hand, the latter approach attempts to represent the connectivity of a watershed conceptually and simulates runoff. This approach is simpler, requires less data, and is applied over larger watersheds. However, it also suffers from the choice of the conceptualization and the loss of physical information when introduced into hydrological models. There is a necessity to improve the runoff generation parameterization by addressing the limitations of already established approaches or methods to represent surface storage connectivity and improve the modelling capability.

Modelling water resources management practice is an additional challenge in developing a hydrological model for a prairie watershed. The existence of a number of controlled and uncontrolled lakes creates complex and interconnected interactions. Commonly used hydrological modelling tools can simulate simple lake operations, however, in the case of a complex and interconnected lake arrangement, a specialized tool is required to simulate them. It is highly probable that a large-scale prairie watershed contains such a complex and interconnected lake system and developing a hydrological model for such large-scale watershed needs to simulate the lake system with a specialized tool and approach. It is possible to address the challenges (i.e. hydrological processes and water resources management practice) efficiently for a large-scale prairie watershed separately. Developing a hybrid modelling approach to address hydrological processes as well as lake system operations and interactions has a potential to be used as a modelling approach for a large-scale prairie watershed. Such approaches have to account for hydrological processes as well as human interventions simultaneously, and are vulnerable to accumulation of errors during hybridization.

1.2 Objectives

The overall goal of this research is to develop a hydrological model for the prairies with an improved representation of the hydrologic connectivity as well as accurate representation of water management practices for streamflow simulation. The specific objectives are-

1. To investigate runoff processes in the prairie region considering the dynamics in hydrologic connectivity;

2. To assess the effects of water management practices in the context of lake operation in the prairie region; and

3. To conceptualize a modelling approach for prairie watersheds that combines hydrological modelling and water resources management for efficient streamflow prediction.

1.3 Scope of the Research

The scope of this research includes differentiating various components of runoff processes occurring in prairie watersheds, development of a new runoff generation algorithm by addressing the shortcomings of existing algorithms, development of a lake system model, assessment of the naturalized conditions and comparing the effects of lake operations with no operation, and development of integrated hybrid model that has the ability to address challenges in prairie hydrology as well as water resources management practices.

1.4 Layout of Thesis

In Chapter-2, relevant literature is reviewed and discussed. This includes hydrological process modelling in the prairies, lake systems modelling, and hybrid modelling approaches for systems modelling. In Chapter-3, the methodology and processes as well as a brief description of the modelling data are discussed. In Chapter-4, a detailed comparative assessment of existing

and proposed runoff generation algorithms is discussed. The comparison primarily considers model performance across three prairie and non-prairie watersheds and the ability to predict the hydrological response as well as other processes. In Chapter-5, development of a system dynamics model for the lake system operation and the development of the hybrid model using a combination of a hydrological modelling tool and a lake system modelling tool is discussed along with subsequent analysis of results. Finally, an overall summary, conclusion, limitations, and future scope of research are discussed in Chapter-6.

Chapter 2: Literature Review

This research focuses on the development of a systems model for a large-scale prairie watershed by addressing various challenges regarding the hydrology and lake management. The term 'system' holds a variety of classification, however, in this research 'system' refers to 'hydrological system' that has components of the natural hydrological cycle as well as human intervention in a specific river basin. The modelling approach of a system is the development of strategies to represent the dynamics of that system, which could be used to answer questions via analysis and simulation. Before the methodology is presented, some key concepts related to prairie hydrological processes and the subsequent modelling approach are discussed. The literature review covers an introduction of the prairie hydrological processes, an overview of different approaches of hydrological model development, lake systems modelling approach, and a hybrid modelling approach.

2.1 Prairie Hydrological Processes

The hydrology of the Canadian Prairie region is featured by (i) internal drainage occurring in large areas that do not contribute to the major river systems, (ii) long periods of winter with occasional mid-winter melts and blowing snow redistribution, (iii) high surface runoff from the major spring snowmelt event, (iv) high water-holding capacity and high unfrozen infiltration rates of soil mass, (v) extreme precipitation events occurring in spring and early summer from large frontal and convective storms over small areas, and (vi) low levels of soil moisture, plant growth, evaporation and runoff from mid-summer to fall due to low rainfall (Elliott and Efetha, 1999; Fang et al., 2007; Granger and Gray, 1989; Gray, 1973; Gray et al., 1985; Pomeroy et al., 2010). The main hydrological processes in the prairies is divided into winter and summer hydrological processes (Figure 2.1). Lateral hydrological processes that include runoff processes, more specifically overland flow, interflow, and baseflow, play an important role in

the prairie hydrological cycle. Overland flow is explained as a term of infiltration excess (Horton, 1933) or saturation excess (Dunne and Black, 1970). Various definitions of interflow exist in literature such as subsurface stormflow (Weiler et al., 2005), lateral flow, subsurface runoff, transient groundwater, soil water flow, through-flow, unsaturated Darcian flow in the soil matrix or pipe flow in macropores (Dingman, 2002 pp-419). For the present study, interflow is considered as the lateral flow of water between the soil surface and above the water table, where interflow increases with increase in horizontal hydraulic conductivity (Ward et al., 2004). The interpretation of baseflow depends on groundwater dynamics, and different models use simplified concepts to represent baseflow (Clark et al., 2015). This study represents baseflow as the accumulation of infiltrated water, which percolates vertically through the soil column into the groundwater system and drains horizontally as baseflow in the stream. Runoff due to spring melt of the winter snowpack is the major contributor to the streamflow in the prairies (Gray and Landine, 1988). The formation of winter snowpack is the accumulation of snow, which is redistributed by wind and ablated by sublimation and mid-winter melts (Pomeroy and Li, 2000). High surface runoff from the major spring snowmelt event is a result of the frozen state of soils at the time and the relatively rapid release of water from snowpack (Gray et al., 1985). Increased infiltrability and high water storage potential along with inadequate rainfall generates low runoff, which is also prone to increased evapotranspiration rates, in the prairie during summer and fall (Elliott and Efetha, 1999; Granger and Gray, 1989).

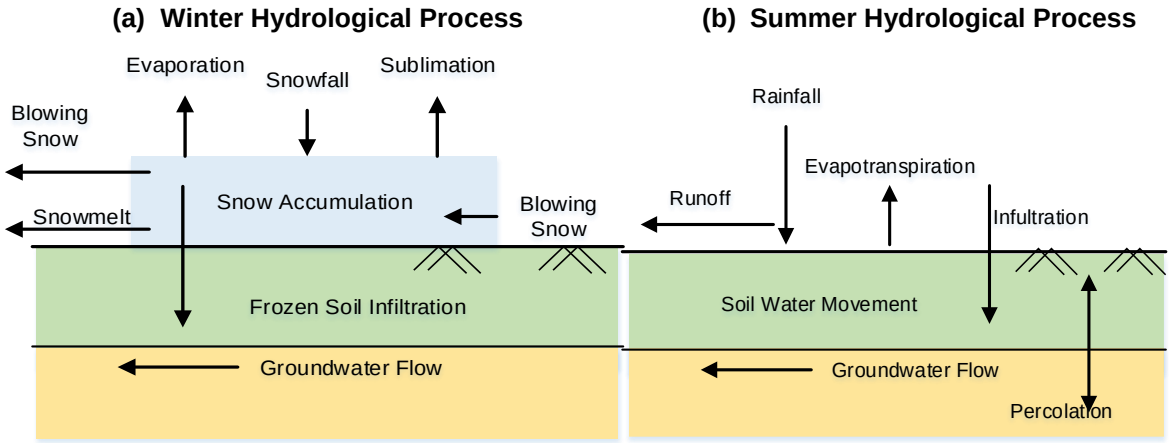

Figure 2.1: Prairie hydrological cycle for (a) winter and (b) summer hydrological processes

The topography of the Canadian Prairie region holds great importance in the prairie hydrological cycle, which is characterized as flat, with glaciated depressions in the forms of moraines, flutings, drumlins, outwash plains, glacial outburst valleys, sand dunes and glacially dammed lake beds (Christiansen, 1979). A large area in the prairies is internally drained to wetlands, which often consists of millions of depressions or 'potholes'. Wetlands have high water holding capacity and intercept runoff transformation into streamflow. Wetlands is defined as an area of hydric soil, hydrophytic vegetation and enhanced biological activities due to the level of ground water table, which normally stays near or above surface for a considerably long amount of time (Tarnocai, 1980). In the prairies, a large amount of snowmelt runoff contributes to the watershed and a major share of it infiltrates and drains thorough near surface routes. For St. Denis National Wildlife area near Saskatoon in Saskatchewan, Hayashi et al. (1998) found that about 30-60% of winter precipitation transfers from the upland into the wetland, and about 75% of snowmelt water and summer precipitation infiltrates from the wetland, which leaves remaining water for evapotranspiration (Hayashi et al., 1998). In wetlands, soil water generally percolates to groundwater very slowly due to low permeability subsurface glacial till (Van der Kamp and Hayashi, 1998). Wetlands also influence the runoff response and timing by storing and delaying arrival of runoff at the basin outlet (Spence, 2000). Surface runoff flows from the upstream area to the wetlands and/or numerous ponds, lakes and

potholes during snowmelt or a heavy rainfall event. Water remains trapped in these areas until seepage, evaporation, and/or spillage takes place. Spillage of excess water after satisfying the water holding capacity of a particular ponds often fills up the neighbouring ponds. The filling up process increases the surface area of individual ponds, and smaller ponds are combined to form larger ponds. When enough ponds are connected, they form a temporary path to the nearest stream and is considered as a fully connected pond network. Additional precipitation or snowmelt water in this interconnected pond network drains to the nearest stream. This is a common phenomenon in the wetlands, which is referred as a fill-and-spill runoff system (Spence and Woo, 2003). This process of runoff propagation is mainly dependent on the location and size of available surface storage in a basin, and it is influenced by other hydrological processes within the landscape in the basin and by inputs from upstream landscape units (Spence and Woo, 2006). Spence (2006) found that the contributing area of a basin varies as a function of connectivity and capacity of depressions or ponds, which also exhibits a hysteretic behavior with regard to drainage contribution. Hysteresis in this context is noted as a looped non-linear response of depressional storage to the connectivity (dynamics of contributing area) during the wetting and drying cycles in the watershed. Shook and Pomeroy (2011) further suggested that the hysteresis and nonlinearity in the relationship between the contributing area and the storage prevent the use of a simple relationship to relate the contributing area to the depressional storage, and also impacts the use of hydrological models, which assume a constant contributing area.

Snow accumulation and snow melt are also important hydrological processes in the prairies, and approximately one third of annual precipitation occurs as snowfall, which produces 80% or more of annual local surface runoff (Gray and Landine, 1988). Blowing snow transport is also a distinct hydrological process of the Canadian prairies. The windblown snow provides an important source of runoff and controls streamflow peak and duration (Pomeroy et al., 2007).

Blowing snow redistribution has an important effect on river flow pattern and surface runoff (Fang & Pomeroy, 2009; MacDonald et al., 2009). This hydrological process uses wind to transport snow and ice from large open areas to vegetative areas or sheltered areas of leeward hill slope during winter (Vionnet et al., 2014). The blowing snow redistribution feature has its effect at sub-grid scale of a distributed hydrological model. From the modelling perspective, blowing snow is a composite process relating sublimation, wind speed, vegetation properties, and downwind landuse, which pose challenges for the modelers (Pomeroy et al., 1993). In addition to these challenges, a significant amount of uncertainty over complex topography and vegetation is also present when parameterizing the blowing snow redistribution process.

The snowmelt process contributes to recharging the soil moisture and groundwater storage through infiltration. Snowmelt also replenishes reservoirs, lakes, and rivers through surface runoff. The amount of water from snowmelt is controlled by energy exchange at the snow surface, and meltwater is produced when the snowpack is isothermal at a temperature of 0°C (Male and Gray, 1981). Rainfall events in the prairies are intermittent and mainly occur in the period from May to early July. Because of increased evapotranspiration rates during summer, most of the rainfall is lost, which often leads to insignificant surface runoff during the summer period (Pomeroy et al., 2010). Infiltration processes in the prairies is divided into winter and summer infiltration processes. Winter infiltration is heavily controlled by an impeding soil layer in the form of an ice lens, which restricts infiltration, leaving a frozen surface mass of ice or snow. Gray et al. (1985) suggested classifying the infiltration capacity of frozen prairie soils into three groups, which are restricted, limited, and unlimited. Zhao and Gray (1999) derived parametric infiltration equations, which are commonly used to parameterize infiltration process through frozen soil. Summer infiltration is often enhanced by the spring thaw condition of the soil, resulting in low surface runoff, which is due to occasional and brief rainfall. The evapotranspiration process is limited during winter and some sublimation occurs from the

accumulated snowpack as well as from the blowing snow content. Evapotranspiration consumes most rainfall on the prairies during summer, including evaporation from water bodies, rainfall intercepted on vegetation, and wet soil surfaces (Granger and Gray, 1989).

2.2 Hydrological Modelling in the Prairies

The purpose of hydrological modelling is to simulate the movement and redistribution of water within a watershed, and researchers in the past have used different approaches to represent the hydrological processes in a hydrological model, which include physically-based (Abbott et al., 1986; Beven, 1989; Freeze, 1972) and conceptual approaches (Crawford and Linsley, 1966; Dawdy and O'Donnell, 1965; Dooge, 1973). Some of the conceptual approaches are tank based (Efstratiadis et al., 2008; Li and Simonovic, 2002; Xu et al., 2001), probabilistic (Mekonnen et al., 2016, Shook et al., 2013, Mekonnen et al., 2014), and hybrid (Díaz-Robles et al., 2008; Mekonnen et al., 2015; Tiwari and Chatterjee, 2010). The modelling input varies with the approach of model development (lumped and distributed). Simpler water balance based models often require temperature and precipitation as input and complex models require a wide variety of input data to parameterize evapotranspiration, snowmelt, and other physically based processes. Typically, when more processes are modeled, more data are required for model calibration and validation (Maclean, 2009). Hydrological modelling is used for many engineering applications such as landuse planning (Lørup et al., 1998), flood forecasting (Papathanasiou et al., 2015; Rao et al., 2011; Refsgaard et al., 1988), and water quality (Abbaspour et al., 2007; Hesse et al., 2008).

Development of hydrological models for the prairies is difficult, because the model needs to address unique prairie features like fill-spill type runoff propagation, surface storage connectivity, and dynamic contributing area. Commonly used modelling tools cannot be applied for a prairie watershed unless these tools have the ability to parameterize the unique

prairie processes. A number of hydrological models have been developed or adapted for Canadian conditions using one or more of the above-mentioned approaches. Li and Simonovic (2002) used a tank based approach in a system dynamics model to predict floods during spring season in the Assiniboine River prairie watershed. Mekonnen et al. (2015) used the Soil and Water Assessment Tool (SWAT) in association with an artificial neural network (ANN) modelling technique to develop a model for the Moose Jaw River watershed in Saskatchewan. The Cold Region Hydrological Model (CRHM) (Pomeroy et al., 2007; Shook et al., 2013) and MEC-surface and Hydrology (MESH) (Davison et al., 2016; Haghnegahdar et al., 2014; Pietroniro et al., 2007) are examples of physically-based models that are widely used the prairie model development. Pomeroy et al. (2007) developed a specialized hydrological model for the Bad Lake in Saskatchewan using CRHM. This model has the capability to address fill-spill runoff propagation, blowing snow redistribution, and other unique prairie features. MESH was evolved from WATCLASS (Soulis et al., 2000) and is being used across Canada. Being a community-based tool, MESH has a comprehensive parameterization approach suitable for large scale model development.

The main challenges for a prairie model development are to simulate the runoff generation process and to parameterize the dynamic drainage contribution by addressing prairie spatial heterogeneity. These challenges are discussed in the following sections.

2.2.1 Runoff Process Simulation Methods

The main challenges for runoff process simulation in the prairies are to simulate the movement of rainfall excess and snowmelt in a watershed under spatial heterogeneity, hydrological connectivity, and topographical complexity. These processes are major integral part of hydrological and land surface models and their applicability varies with respect to different physiographic properties in watersheds. Development of a runoff generation algorithm within

a hydrological model commonly encounters a few complexities and challenges, which include representation of unique lateral hydrological processes and spatial heterogeneity. Overall estimates of runoff include overland flow, interflow, and baseflow. In overland flow, the variable drainage contribution is represented as variable spatial pattern of contributing area, which depends on spatial pattern of storage capacity (Zehe et al., 2005). Interflow is induced by sub-surface saturation increase with the accumulation of infiltrated water, depending on the horizontal hydraulic conductivity (Ward et al., 2004). Accumulated infiltrated water, which percolates vertically through soil column, eventually reaches to the top of impermeable layer and drains horizontally as baseflow. Traditionally runoff is conceptualized as a function of change in storage (Dooge, 1959; Nash, 1957; Wooding, 1966). However, Spence (2010) proposed a paradigm shift concept wherein runoff is a function of threshold-mediated and connectivity-controlled hysteretic process, and storage connectivity is defined by storage heterogeneity in soil, hillslope, and catchments.

To parameterize runoff processes, researchers in the past have used different approaches, which include physically based approaches (Liang et al., 1994; Liu & Todini, 2002; Neitsch et al., 2011) and conceptual approaches (Burnash et al., 1973; Chiew & McMahon, 2002; O'Connell et al., 1970; Post & Jakeman, 1999). The physically based approach uses physical laws, usually represented as differential equations to determine hydrological responses. The parameterization of a physically based hydrological model is reasonably complex and is generally associated with large number of parameters to describe the processes. On the other hand, the conceptual approach uses different techniques and well established hydraulic and statistical concepts to estimate runoff in a watershed. Some of the conceptual approaches are tank based (Li and Simonovic, 2002), remote sensing based (Shook and Pomeroy, 2011), probabilistic (Mekonnen et al., 2016; Mekonnen et al., 2014; Shook & Pomeroy, 2011), and hybrid approach (Mekonnen et al., 2015). The tank based approach is a simplest hydrological

representation where runoff is estimated using interactions of surface storage with other storages (groundwater, canopy, snow, and subsurface storage) using conceptual tanks or buckets assigned for each storage (Li and Simonovic, 2002). The remote sensing based approach for runoff estimation addresses accurate representation of surface storage connectivity. In this technique the actual location of surface storages is identified using a high resolution map and the amount and direction of flow is estimated, which exhibits actual connectivity of surface storages (Shook et al., 2013). However, it is restricted by limited practical application because of great computational expense and limited availability of high resolution data. The statistically based probabilistic approach addresses surface storage connectivity using probability distributions to represent surface storages under varying capacities. This approach is advantageous as it simplifies the surface storage representation and is not computationally expensive. Among various approaches, a physically based runoff generation approach is considered as more accurate and acceptable method for runoff generation (Du et al., 2007; Liu & Todini, 2002; Pomeroy et al., 2007) and probabilistic runoff generation approaches are considered as a better conceptualization of land surface heterogeneity (Mekonnen et al., 2014; Shook & Pomeroy, 2011).

2.2.2 Spatial Heterogeneity

The representation of spatial heterogeneity in a hydrological model is a challenging task. Spatial heterogeneity is classified in different forms of heterogeneity, i.e. variable atmospheric forcing, vegetation type, elevation, slope, and soil moisture (Ghan et al., 1997; Guo et al., 2015). It has considerable effects on fluxes of energy, mass and momentum across the landscape and atmosphere and a range of spatial scales (Ke et al., 2013). The approaches to address spatial heterogeneity in a distributed, semi-distributed, and lumped models are usually different (e.g. Jajarmizad et al., 2012; Karvonen et al., 1999). Mathematical modelling of land surface processes becomes more challenging because of the spatial heterogeneity, and the need

for appropriate assumptions and simplifications by the modeler to represent spatial heterogeneity of the study watershed considering the level of accuracy of input information.

The challenges of representing spatial heterogeneity in a prairie watershed are even more than those in non-prairie watersheds because the prairie land surface consists of millions of depression, which differ in their location and capacity showing unique surface storage connectivity. Because of the variable storage connectivity, model development for a prairie watershed becomes complex and often simple representation of spatial heterogeneity does not work (Mekonnen et al., 2016, 2014). A suitable approach for handling depression storage heterogeneity was proposed by Ullah and Dickinson (1979), which showed that the storage capacity of depressions in the Canadian prairie region followed a probability distribution. It was realised that the probability distribution-based models used to describe heterogeneity in soil moisture storage (e.g. Bell et al., 2009, 2007, Moore, 2007, 1985; Moore and Bell, 2002; Moore and Clarke, 1981) could be used to represent prairie spatial heterogeneity for depression storage (Abedini, 1998). Recently, similar probability distribution based approaches were implemented for the prairie by Mekonnen et al. (2014) using MESH and Mekonnen et al. (2016) using SWAT. The probability distribution model is a conceptual rainfall-runoff model wherein, runoff generation at any point in the watershed is considered as a function of different processes (e.g. canopy interception, surface detention and soil water storage), which is conceptualized as a store with a specific storage capacity. If different points in the watershed have different storage capacities, and is described by a probability distribution, a runoff production model is formulated such that it integrates the point runoffs to produce direct runoff. (Moore, 2007, 1985; Moore and Bell, 2002).

2.3 Lake System Modelling

'System' is defined by a regularly interacting or interdependent group of entities connected in a structure. Lake system consists of one or many controlled and uncontrolled water bodies with corresponding hydrological system, which determines the behavior and purpose of the lake system. Controlled lakes (or reservoirs) is the most important element of complex water resource systems, which represent the intervention of human into a hydrological system. The lake system affects the hydrological system by regulating the flows and lowering and delaying peak flows. A lake system often withstands the adverse effect of flood and replenishes downstream area during dry seasons. Developing a model for a lake system is simplified using a hydrological modelling tool, however, it is possible to develop a specialized lake system model (for example water quality, irrigation, water allocation, and decision support) using different conceptual approaches.

System Dynamics (SD) is a widely used approach to model reservoir operation and their decision support system (DSS), which has been applied in many places (Elshorbagy et al., 2007, 2005; Gonda, 2015; Hassanzadeh et al., 2014; Kotir et al., 2016; Thompson and Bank, 2010; Torretta and Vincenzo, 2014; Turner et al., 2016; Wei et al., 2012). SD is a well known approach of systems thinking, pioneered by Jay Forrester, which was initially used as a tool to understand industrial systems (Forrester, 1961). The application of the SD approach has been a major focus of research in water resources engineering as early as the 1980s with applications to small-scale hydropower analyses (Turner et al. (2016) and references therin). The SD approach for modelling reservoir operations is efficient and simple to use compared with traditional systems analysis techniques and does not require complex mathematical description of the system. This approach is highly applicable to water resources modelling as it is integrated into many user-friendly tools with capabilities to analyze complex system interactions (Mirchi et al., 2012). Owing to the integrative abilities of the SD method to connect physical and social

system components, and visual attractiveness, SD has been an effective approach for water resources management (Fletcher, 1998; Kotir et al., 2016; Simonovic et al., 1997), river basin planning (Palmer, 1994, 1995; Palmer et al., 1993), drought monitoring (Keyes and Palmer, 1993), sea-level rise (Fletcher, 1998), environmental flow analysis (Wei et al., 2012), and policy analysis (Simonovic et al., 1997; Simonovic and Rajasekaram, 2004). SD also provides a strong environment for stakeholder participation (Mirchi et al., 2012; Stave, 2002; Winz et al., 2009) and system validation (Barlas, 1996; Peterson and Eberlein, 1994). Apart from water resources studies, SD also shows its versatility in socio-economic studies, for example, Gastélum et al. (2010) used a SD approach to estimate benefits of agricultural productivity under different water transfer schemes between Mexico and US, and Qin et al. (2011) estimated economic growth in Shenzhen province of China using SD approach.

In the context of the Canadian prairies, SD has been used in the modelling of hydrological processes (Li and Simonovic, 2002) and water resources management (Hassanzadeh et al., 2016, 2015, 2014; Simonovic and Rajasekaram, 2004). SD is one of the initial attempts to develop a hydrological model for the prairies. Li and Simonovic (2002) formulated a bucket model using suitable equations for different prairie hydrological processes. Although the application of SD showed a significant promise in modelling a prairie watershed, no studies focussed on using SD for hydrological modelling in the prairies, and researchers moved to more physically based approaches (Pietroniro et al., 2007; Pomeroy et al., 2007).

Due to the importance of the Qu'Appelle River Basin (QRB), researchers and agencies have worked on developing models for its water resources management over the years. The history of the study on the lake systems of QRB starts from 1970's, when Hammer (1971) conducted a limnological study on the lake drainage systems. Saskatchewan Department of Environment (1975) conducted a detailed conveyance study on the lakes of QRB and recorded area, capacity,

elevation, control structure detailing, rating curves, and area-elevation curves. Based on this document and current water use information, the Saskatchewan Watershed Authority (2012) developed a monthly time scale model, which is one of the DSS tools for QRB used by the Water Security Agency (WSA) to operate the QRB lake system.

2.4 Hybrid Modelling Approach

Hybrid modelling is an integrated modelling structure that may include multiple models based on different modelling paradigms (Mekonnen et al., 2015). Hybrid modelling is suitable for a hybrid system, which is defined as a dynamic system that involves the interaction of different types of dynamics (Lygeros et al., 2008). A dynamic system is classified as a continuous system or discrete system or a combination of both. A hydrological system is considered as a combination of continuous and discrete systems, where soil moisture and atmospheric forcing is considered as continuous system, whereas landcover and soil properties is considered as discrete systems. In this context, a limited number of hybrid hydrological models are found in the literature. These models have included the coupling of ANN with a rainfall-runoff model (Chen and Adams, 2006), the combination of semi distributed process-based and data-driven models (Corzo et al., 2009), the combination of ANN and the kinematic wave approach (Chua and Wong, 2010). The basic motivation behind the hybridization is to improve the capability of a model by addressing its limitations and using another modelling approach to overcome them. For example, Mekonnen et al. (2015) applied a hybrid modelling approach for a prairie watershed by joining ANNs into the SWAT hydrological model, where SWAT represented hydrological processes of the watershed and the ANN component simulates the effect of non-contributing area. Corzo et al. (2009) applied hybrid modelling approach by joining ANN into HBV-M model to improve the representation of flow routing from the sub-basins of a watershed, White et al. (2010) combined SWAT with CE-Qual-W2 model, where SWAT estimates the water and nutrient and CE-Qual-W2 uses this information to asses the water

quality. Combination of different data driven approaches and hydrological models (such as, SWAT-ANN, wavelet–bootstrap–ANN, and ARIMA-ANN) is common for hydrological processes representation (Chen and Adams, 2006; Jain and Srinivasulu, 2006), water quality analysis (Hamilton and Schladow, 1997; Moore et al., 2004), and flood forecasting (Díaz-Robles et al., 2008; Tiwari and Chatterjee, 2010). However, a hybrid hydrological and hydraulic lake model is not very common in the literature. Xu et al. (2007) hybridized a model using a complex link between a runoff model (HSPF) and a lake model (CE-Qual-W2) to develop a hybrid model. The intention was to develop a new approach for calibration and validation of a hybrid model, which consists of two different models, as a whole. Most of the hydrological modelling tools are able to simulate the effect of simple lake operations. However, complex lake management and operations are less likely to be represented by any known hydrological modelling tool, hence a hybridization of a hydrological modelling tool with a suitable lake systems tool being able to simulate complex lake management and operations is proven useful.

Development of a systems model for a prairie hydrological system requires representation of not only prairie hydrological processes, but also the lake system operations which are often specific to events (e.g. diverting high flows into lateral lakes as natural flood dampening) that is difficult to address. A number of studies were found explaining prairie hydrological processes, but very few considered human intervention in the hydrological system of a prairie watershed (Dumanski et al., 2015; Ehsanzadeh et al., 2016; Shook and Pomeroy, 2011). Due to increasing water demands in the prairie provinces of Canada, the need of a hydrological systems model that has the ability to address prairie hydrological processes as well as lake operation and interventions for the prairies is high.

Chapter 3: Materials and Methods

This chapter provides a description of the study area and hydro-meteorological data used for model development. This chapter also provides brief description of the hydrological modelling tool along with emphasis on important hydrological processes, system dynamics (SD) approach for lake systems Modelling, and the proposed hybrid modelling method.

3.1 Study Areas and Data Products

To address objective 1 of this thesis and conduct a comparative study of runoff generation algorithms, three watersheds were selected, namely the White Gull Creek, Brightwater Creek, and Kronau Marsh watersheds (Figure 3.1). The three watersheds are located in the province of Saskatchewan, which contains three ecozones namely prairie, boreal plains, and boreal shield, of which prairie and boreal plain occupy 65% of the province. The White Gull Creek watershed is located in the boreal plain ecozone and the other two watersheds are within the prairie ecozone.

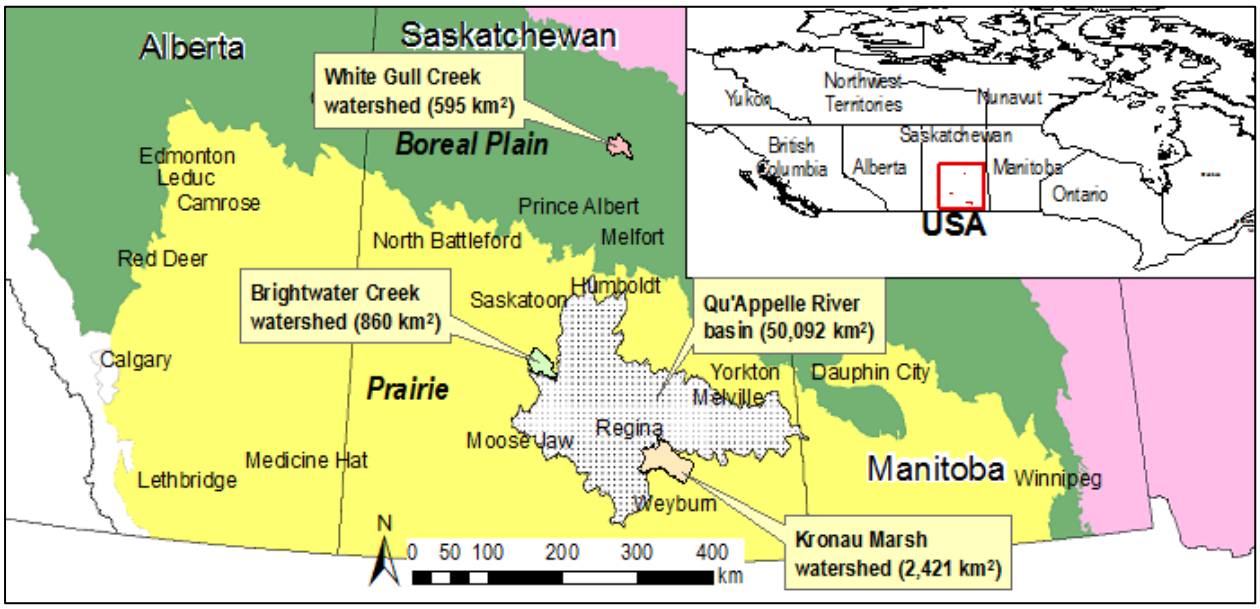

Figure 3.1: Location of the Qu'Appelle River Basin (QRB), White Gull Creek, Kronau Marsh, and Brightwater Creek watersheds in Boreal plain and Prairie ecozone of Canada. Here, Kronau Marsh is a sub-basin of QRB, however, Brightwater Creek is not a sub-basin of QRB.

The White Gull Creek watershed (Figure 3.2a) is located 60 km North East of Prince Albert, Saskatchewan, at the southern end of the Canadian Boreal plain between Latitudes 53.99^{o} N and 54.13 ^{o} N and Longitudes 104.62^{o} W and 105.08^{o} W. The White Gull Creek watershed has a gross area of 595 km^2 and the entire watershed contributes to streamflow. The landuse in the watershed is mostly forest (71% of the area), followed by grass (6%) and wetland (23%) (Natural Resources Canada, 2015). Climate normals for Waskesiu Lake (a community 75 km from the site) obtained from Environment and Climate Change Canada (ECCC) indicate that the average yearly precipitation is 467 mm, 30% of which fall as snow; and annual, January, and July mean air temperatures is 0.4^{o}C, −17.9^{o}C and 16.2^{o}C, respectively. The Kronau Marsh watershed (Figure 3.2b) is located in the upstream of Wascana Lake, about 13 km south-east from Regina, Saskatchewan, at the center of the Canadian prairies between Latitudes 49.5^{o} N and 50.3^{o} N and Longitudes 103.3^{o} W and 104.3^{o} W. According to ECCC, the Kronau Marsh watershed has a gross area of 2,421 km^2 and contains 59% non-contributing wetlands within it, which is about 994 km^2 area effectively contributes runoff to the outlet. Crops are the dominant landuse type (Kulshreshtha et al., 2012). The average yearly precipitation is around 390 mm, 26% of which falls as snow; and the mean annual, January, and July air temperatures are 3.1^{o}C, −14.7^{o}C and 18.9^{o}C, respectively (climate normals from Regina Int'l Airport, a community 50 km from the site; source: ECCC). The Brightwater Creek watershed (Figure 3.2c) is located 80 km south of Saskatoon, Saskatchewan, at the north central part of the Canadian prairies between Latitudes 51.2^{o} N and 51.6^{o} N and Longitudes 106.1^{o} W and 106.7^{o} W. According to ECCC, the Brightwater Creek watershed has a gross area of 860 km^2 and contains about 77% non-contributing wetlands within it, which is about 196 km^2 area effectively contributes runoff to the outlet. The fraction of grass and shrub covers almost 54% and 46% of the watershed, respectively (Peterson et al., 2015). The average yearly precipitation is 298 mm, 26% of which falls as snow; and the mean annual, January, and July air

temperatures are 2.2°C, −15.3°C and 15.1°C, respectively (climate normals from Davidson, a community 32 km from the site; source: ECCC).

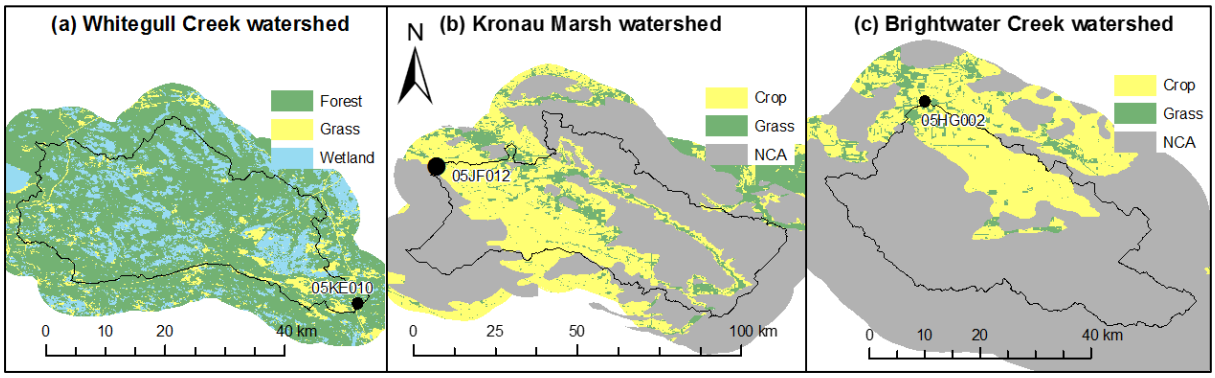

Figure 3.2: Landuse distribution of the (a) White Gull Creek, (b) Kronau Marsh, and (c) Brightwater Creek watershed. NCA is Non-Contributing Area. Black dot is the outlet of the watershed.

To address the second objective of the thesis regarding the effect of reservoir/lake operation on the hydrology of the region, a hydrological model was developed for a large river basin that contains a series of operated lakes. The Qu'Appelle River basin (QRB; Figure 3.1), located in southern side of Saskatchewan within the Prairie ecozone, was selected for this purpose. The QRB is also a basin of interest for the Water Security Agency and the NSERC strategic network on floods (www.nsercfloodnet.ca). The basin is an optimal representation of large prairie watersheds that have all challenging features of prairie hydrology. The Qu'Appelle River extends east from the Qu'Appelle Valley Dam on Lake Diefenbaker to the Manitoba border, and it joins the Assiniboine River near St. Lazare, Manitoba. The Moose Jaw River and Wascana Creek are the major tributaries of the Qu'Appelle River. The basin occupies 50,092 km^2 area, and its landuse map (Figure 3.3) suggests that over 85% of the area is agricultural land. According to ECCC, the average yearly precipitation is 432 mm (Figure 3.4a), and the mean annual, January, and July air temperatures are 3.7°C, −12.5°C and 19.8°C, respectively (Figure 3.4b).

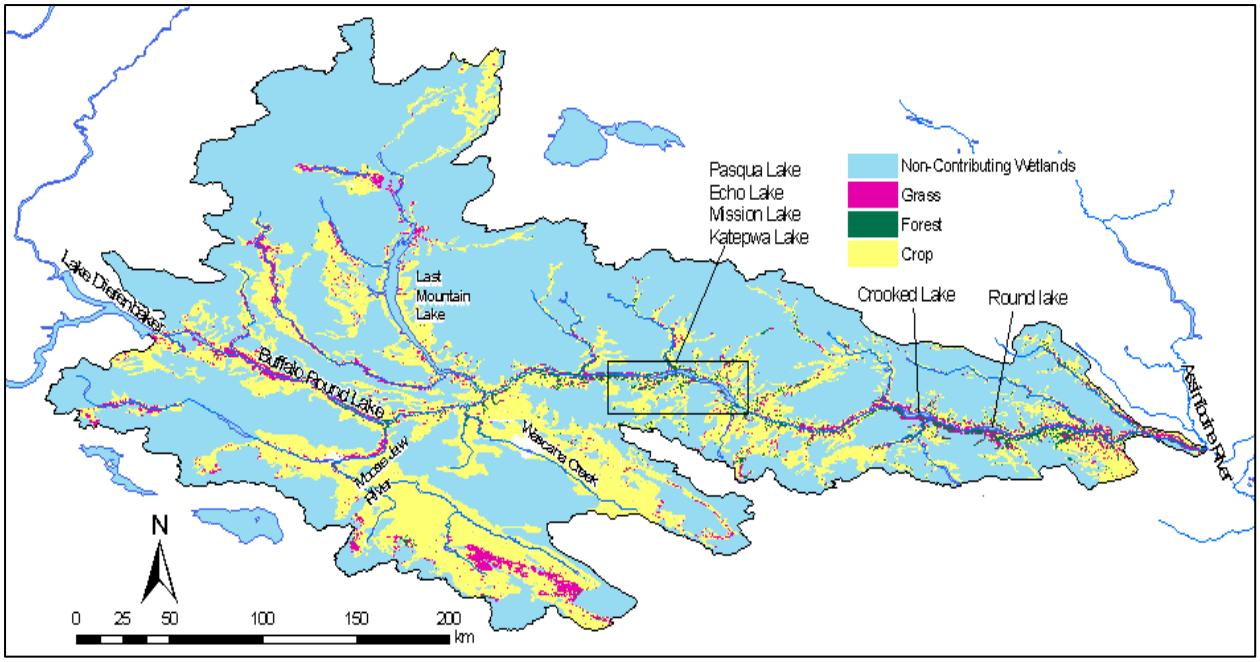

Figure 3.3: Landuse distribution of the Qu'Appelle River basin

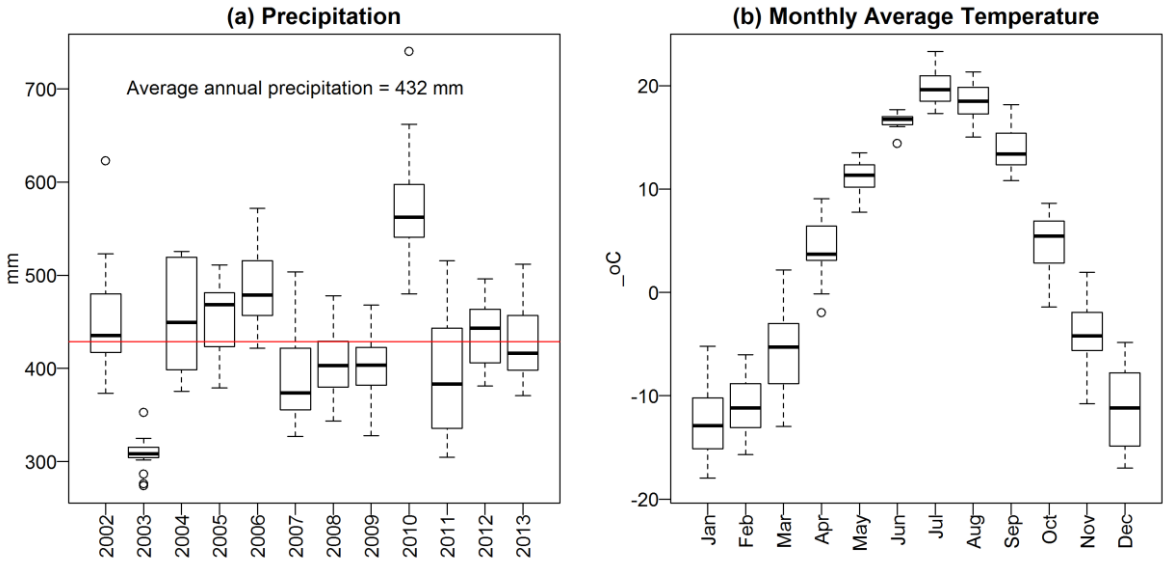

Figure 3.4: (a) Average annual precipitation and (b) monthly temperature distribution of the Qu'Appelle River basin estimated using data from ECCC.

This basin contains eight interconnected lakes (Figure 3.5), which provides a unique situation of lake interactions and dynamics in the form of backwater effects from the river towards upstream lakes. The river system starts at the southern end of Lake Diefenbaker at the Qu'Appelle Dam and Elbow diversion canal and flows eastward. The Moose Jaw River, Last Mountain Lake, Wascana, Loon, Jumping Deer, Indian Head, Pheasant, Kaposver, Ekapo, Cutarm Creeks are the important tributaries for the Qu`Appelle River. Besides these creeks and

lakes, there are a few smaller lakes that have insignificant surface area and have insignificant hydrological effect over the QRB. Water is diverted for agricultural, industrial, and domestic uses from the lakes. According to the 2011 census, the population of the QRB is about 588,000, which is 57% of total Saskatchewan population of the QRB's water is mainly allocated for agricultural purposes. Moreover, industrial demand in potash mines and municipal demand for cities (e.g. Regina, Moose Jaw) require a significant amount of water diverted from the lakes.

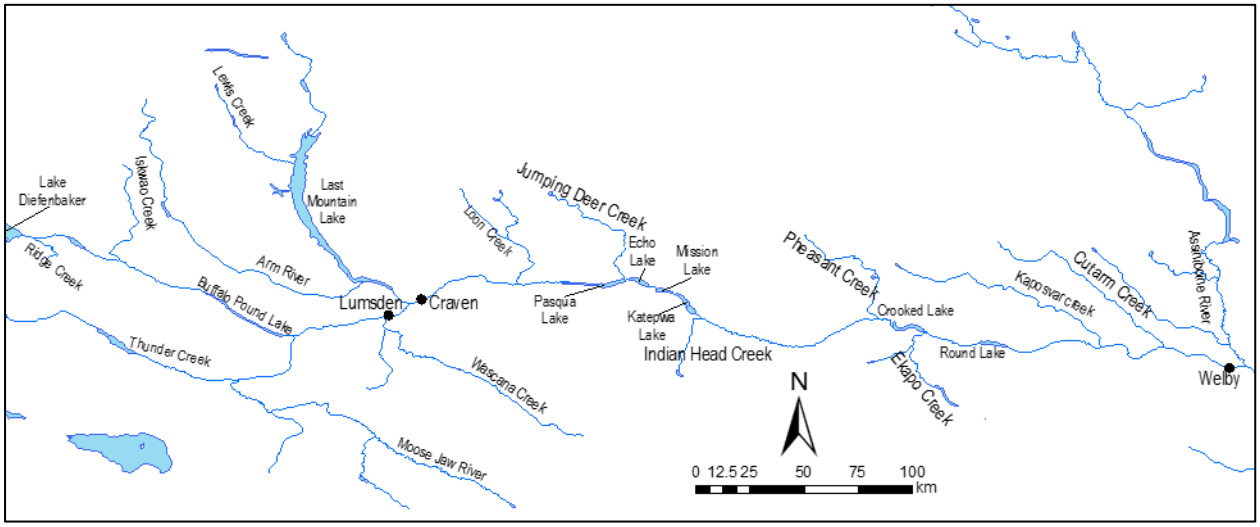

Figure 3.5: Spatial location of different Rivers, Creeks and Lakes in QRB

Hydro-meteorological and physiographic data were collected from different sources. The land cover data for the study areas were derived from the LCC2000-V database of Geobase (http://www.geobase.ca). The topographic data for the study areas were collected from the GeoBase website. Geobase provides the Canadian Digital Elevation Data (CDED), which were extracted from the National Topographic Data Base (NTDB). For this study, the CDED data with a resolution of about 20m were considered as this was the finest resolution available. The Green-Kenue Software (Canadian Hydraulics Center, 2010), which is compatible to generate a database for the MESH hydrological model, was used for drainage database preparation. The same software was used for delineating watershed boundaries using the DEM-based automatic delineation method. The Prairie Farm Rehabilitation Administration (PFRA) developed a Canada wide map to locate the non-contributing area, which was used in this research for

delineation of NCA (Martin, 2001). Soil texture data were extracted from ecological framework attribute data produced by Agriculture and Agri-food Canada (AAFC) (http://sis.agr.gc.ca/cansis/nsdb/index.html).

Hydro-meteorological data for each watershed were sourced from various agencies. Forcing data, namely, incoming shortwave and longwave radiation (Wm^{-2}), air temperature (K), wind speed (ms^{-1}), barometric pressure (Pa), specific humidity ($kg\ kg^{-1}$), and precipitation ($kg\ m^{-2}\ s^{-1}$ or $mm\ s^{-1}$) for all the watersheds were collected from the Global Environmental Multiscale (GEM) model of ECCC and the Canadian precipitation analysis (CaPA) model. GEM is an integrated atmospheric environmental forecasting and simulation system developed by ECCC. The meteorological forcing data were available at an hourly scale from 2002 onward. Precipitation data were collected from the Canadian precipitation analysis (CaPA) model (Mahfouf et al., 2007), which were available at six hourly time-scale. Daily streamflow data at the outlet of all four watersheds were obtained from ECCC (http://wateroffice.ec.gc.ca).

3.2 Methodology

According to the objectives and scope, this research is divided into three major components, which are to (i) investigate runoff generation processes in the prairies, (ii) develop a lake systems model, and (iii) hybridize appropriate hydrological processes model with lake systems model in order to deliver a complete tool that has the ability to simulate a large-scale prairie watershed. The three components are directly related to the three objectives of the study. Figure 3.6 shows the schematics of the methodology adopted to achieve the research objectives. Initial steps of the methodology include selection of appropriate study area and modelling tool. The Qu'Appelle river basin was selected as study area because it is situated in the prairies and it contains an interconnected lake system. MESH was selected as the hydrological model development tool, because of its capability of handling large-scale modelling as well as prairie

hydrological processes. The following step includes investigation of existing runoff generation algorithms and identify to the need for improving the existing ones. A comparative study was conducted to investigate the value of newly proposed runoff generation algorithm over the existing ones. Later, a MESH model for the hydrological processes of the QRB, ignoring the lake system, was developed and combined with another system dynamics model for the lake system to form the hybrid structure to predict the streamflow at the outlet of the QRB (Welby).

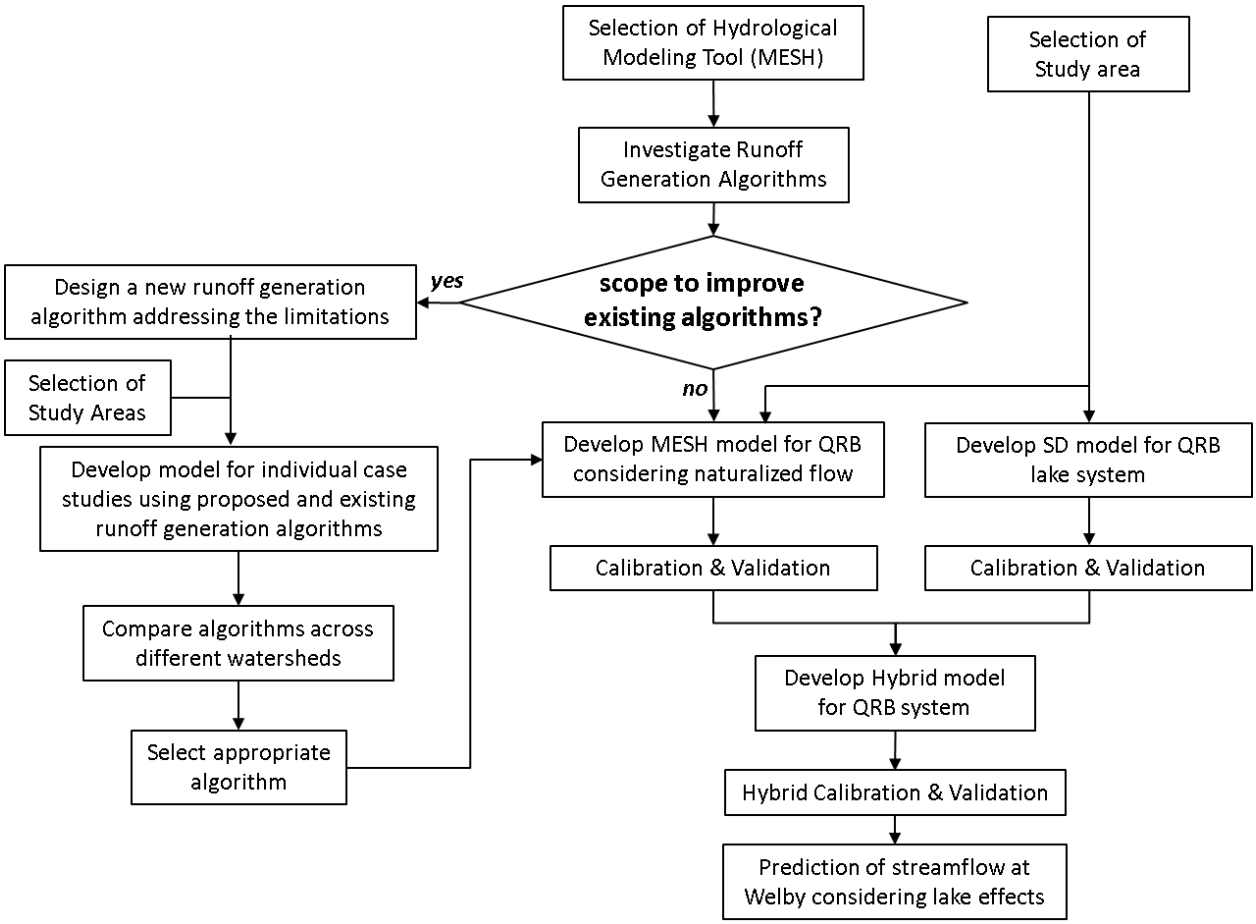

Figure 3.6: Schematics for the complete methodology adopted in this thesis.

A brief description of the hydrological modelling tool is provided in Section 3.3. . A brief description of the lake system modelling approach is provided in Section 3.4.1. These two components are not mutually related; however, the third component connects these two components, which is directly related to the overall goal of this research i.e., the systems modelling approach for a Canadian prairie watershed. This component consists of the

development of a hybrid systems model, structured from a hydrological model and a lake systems model.

3.3 Prairie Runoff Processes Modelling

A well-known hydrological modelling tool, named MESH was selected to model hydrological processes in the watersheds selected for this study. MESH (Modelisation Environmentale Communautaire - Surface and Hydrology) (Pietroniro et al., 2007) is a grid-based stand-alone land surface hydrology modelling tool developed by Environment and Climate Change Canada (ECCC). It is a combination of the Canadian Land Surface Scheme (CLASS) (Verseghy, 1991; Verseghy et al., 1993) and WATFLOOD (a semi-distributed hydrological model, Kouwen *et al.*, 1993). CLASS is a physically based model that utilizes a finite difference solution of Richards' equation to represent the average moisture content in a given soil layer and the movement between soil layers to simulate the energy and water balances of vegetation, snow, and soil. MESH uses the routing component of WATFLOOD, which is known as WATROUTE and the continuity equation together with the Manning's equation to route water from grid-to-grid once it is in the channel. To estimate the generated water within a grid cell and move the water from the land surface to the channel, MESH uses the concept of Grouped Response Units (GRU) from WATFLOOD (Kouwen et al., 1993). Each grid cell can contain a number of GRUs, with each GRU being homogeneous with respect to landuse, soil properties, or other hydrologically relevant properties. A single GRU parameterization is present in multiple grid cells. MESH allows CLASS to run independently on each of the GRUs within each grid-cell. The overall fluxes and prognostic variables of a grid cell involved in the simulation are calculated using the weighted area of each GRU. A GRU is further divided into 'tiles' within which landuse divisions (e.g. needleleaf tree, broad leaf tree, grass, crop, urban) are classified. In the recent past, MESH has been implemented for several Canadian river basins to model various components of water balance (Davison et al., 2016; Haghnegahdar et al., 2015, 2014;

Maclean, 2009; Maclean et al., 2010; Mekonnen et al., 2014; Mengistu and Spence, 2016; Pohl et al., 2004; Yassin et al., 2017).

The MESH modelling system represents three components of hydrological processes: (i) a vertical exchange of water between the soil, plant, and atmosphere; (ii) surface and sub-surface runoff generation; and (iii) routing of lateral fluxes along the stream network. MESH addresses the first component using the one-dimensional Richards' equation (Richards, 1931) to simulate the storage and transmission of water through soils, as shown in Equation 3.1.

$$\frac{\delta\theta}{\delta t} = -\frac{\delta q}{\delta z} + S_{et} + S_{lf} \quad (3.1)$$

where θ is the volumetric liquid water content, q is the vertical flux of liquid water (ms^{-1}), S_{et} is the sink term for evapotranspiration (root water uptake) (s^{-1}) and S_{lf} is the source-sink term for the lateral flux of liquid water (s^{-1}). The vertical flux of water q leads to the moisture-based form of Richards' equation (Richards, 1931) (Equation 3.2).

$$q(z) = -K\,\frac{d\psi}{d\theta}\frac{\delta\theta}{\delta z} + K \quad (3.2)$$

Where, $K=f(\theta)$ is the hydraulic conductivity (ms^{-1}) and $\psi=f(\theta)$ is the liquid water matric potential (m). A detailed explanation of the physical processes involved in determining water balance components for various land surface schemes is found in Clark et al. (2015) and for MESH in Davison et al. (2016).

Within MESH, CLASS simulates soil moisture storage and transport processes using equations (3.1) and (3.2) but is unable to include the upper boundary conditions as represented by the partitioning of surface runoff as well as the lateral flux term (S_{lf}) (Davison et al., 2016). To overcome this limitation, Soulis et al. (2000) introduced the idea of a sloping soil layer with a horizontal hydraulic conductivity. In this interpretation of the runoff generation algorithm, excess surface water drains through a micro-drainage system as overland flow, interflow drains

through the soil matrix and the macro-pore structure to leave the soil column through a seepage face, and base flow drains the accumulated water that occurs at the bottom of the soil column into groundwater system to the stream (Soulis et al., 2011, 2000). This algorithm is known as 'WATROF', wherein overland flow is represented by the Manning's equation and interflow by an approximate solution of the Richards' equation. WATROF manages the upper boundary conditions as represented by the partitioning of surface runoff into overland flow and infiltration, as well as the lateral flux term (S_{lf}) in equation 3.1. The drawback associated with the physically based WATROF algorithm is that it is found to be ineffective in the prairie watersheds where complex terrain and peak runoff due to snowmelt is dominant (Mekonnen et al., 2014).

To improve the performance of MESH in the prairies, Mekonnen *et al.* (2014) adopted the Probability Distribution Model (PDM) concept (Moore, 2007; Moore and Bell, 2002) within MESH, to better represent the variable nature of contributing area dynamics, which is common in many Canadian landscapes, and developed 'PDMROF'. The basic assumption of this concept considers that storage capacities at different points within a computational unit is represented by a probability distribution. PDMROF uses a 'tile' as a computational unit, which simulates sub-grid scale heterogeneity. The standard form of PDM employs a truncated Pareto distribution of storage capacities with probability density function *f(c)* and cumulative distribution function *F(c)* given by

$$f(c) = \frac{dF(c)}{dc} = \frac{b}{c_{max}}\left[1 - \frac{c}{c_{max}}\right]^{b-1} \qquad 0 \le c \le c_{max} \tag{3.3}$$

$$F(c) = 1 - \left[1 - \frac{c}{c_{max}}\right]^{b} \qquad 0 \le c \le c_{max} \tag{3.4}$$

Where *c* is the generic terminology of surface storage capacity of an individual pond, c_{max} is the maximum storage capacity among all the ponds located in a tile, and *b* is the shape factor parameter that controls the degree of variability of storage capacity. A non-zero value of shape

factor (b > 0) represents different pothole connectivity configurations, which is explained in Shaw *et al.* (2012). Low values of b represent a highly disconnected pothole distribution whereas high values of b represent a well-connected pothole distribution. Both probability density and cumulative distribution functions are plotted for a range of values of b in Figure 3.7.

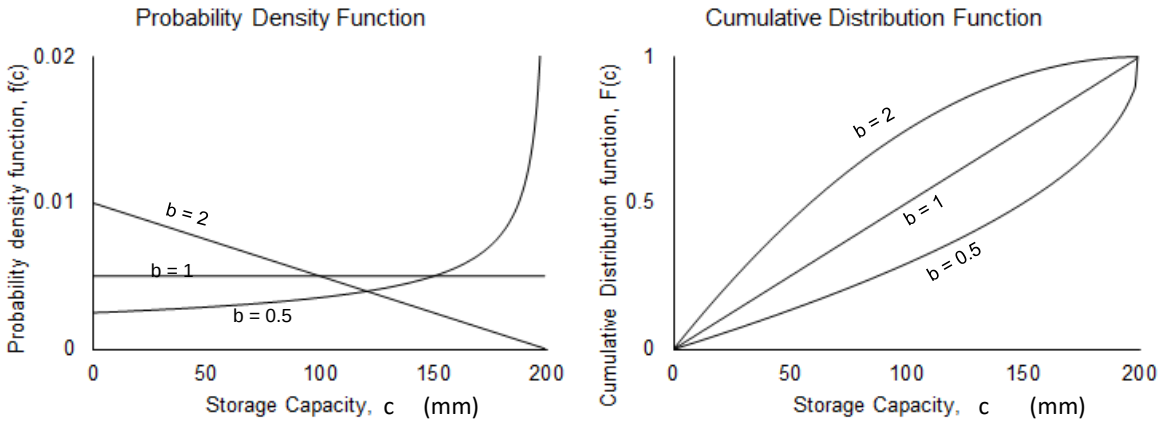

Figure 3.7: Probability density and cumulative distribution functions are plotted for a range of values of b.

At any time t, the depressional storage $S(t)$ in the tile is estimated as the area above the curve upto time t and bounded by the hatched area in Figure 3.8, which is given by Equation 3.5.

$$S(t) = \int_0^{C*(t)} \big(1 - F(c)\big) dc \tag{3.5}$$

Where $F(c)$ represents the proportion of runoff contribution towards outlet. For a given value of storage, $S(t)$, the critical storage capacity, $C^*(t)$, is computed as-

$$C^*(t) = c_{max}[1 - (1 - \frac{S(t)}{S_{max}})^{\frac{1}{b+1}}] \tag{3.6}$$

$C^*(t)$ is a certain storage capacity below which all storages are saturated at time t and generating runoff (Moore, 2007). Total available storage, S_{max}, of a tile is computed as-

$$S_{max} = \int_0^{c_{max}} \big(1 - F(c)\big) dc = \frac{c_{max}}{b+1} \tag{3.7}$$

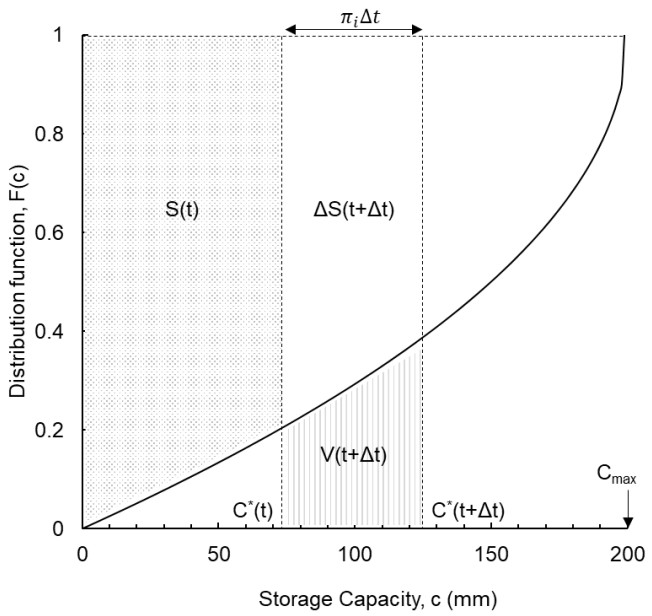

Figure 3.8: Estimation of depressional storage, critical capacity, and direct runoff using storage capacity distribution function. Here, shape factor b<1.0

Total available storage (S_{max}) is visualized as the accumulated storage held within all the ponds in a tile when $C^*(t)$ becomes c_{max}. At a given time t, effective contributing area of a tile, A_c is calculated as-

$$A_c = F(C^*(t)).\ A \qquad (3.8)$$

Where A is the total area of a tile and C^* is critical storage capacity. Over the ith time interval $(t, t + \Delta t)$ with net rainfall π_i, the volume of direct runoff V over the interval $(t + \Delta t)$, per unit area generated from the distribution of storages is-

$$V(t + \Delta t) = \pi_i \Delta t - (S(t + \Delta t) - S(t)) \qquad (3.9)$$

Equation 3.9 is visualized using Figure 3.8. This approach allows the surface storage (commonly known as 'pothole' in the prairies) connectivity dynamics to be represented in a simplified manner that permits the model to mimic the pothole connectivity and the associated fill-spill mechanism of runoff propagation (Mekonnen et al., 2014; Moore, 2007). The optimal values of PDMROF parameters (surface storage capacity (C) and pothole connectivity (b)) are determined by calibration.

After the inception of MESH, a number of improvements of the parameterizations was proposed and tested in different physiographic conditions. There are several other improvements proposed for MESH, which are suitable for cold region hydrological processes parameterization, such as prairie blowing snow model (PBSM) and algorithm for snowmelt infiltration into frozen soil (Mekonnen, 2011). Cold region hydrology is generally seen in a

location where ice and snow play an important role in the local hydrology. MESH contains special parameterization for some of these processes, which is generally developed using special approaches and adopted during the model development for a cold region watershed. Two such special modules were used in this research, which are PBSM and frozen soil infiltration model as the case studies are mainly cold region watersheds. It was observed that inclusion of these modules in MESH improved the model performance, but the degree of improvement is insignificant compared to the improvement in the runoff generation processes. A separate analysis was conducted to understand the effects of PBSM and frozen soil infiltration module and the corresponding results is found in Appendix A.

3.3.1 Development of an Improved Runoff Generation Algorithm

The basic idea for a new runoff generation algorithm evolves from the benefits and limitations of existing algorithms (WATROF and PDMROF). PDMROF assumes no subsurface lateral flow and hence, excludes calculation of interflow from the runoff generation process. Prairie potholes are internally drained by overland and subsurface flows to wetlands. The hydraulic conductivity of the clay- rich glacial till deposits in the prairies increases exponentially in the near surface due to fracturing and macropores caused by weathering (Van der Kamp and Hayashi, 2009). Because of this reason, water in potholes as well as wetlands percolates to groundwater very slowly and a small amount of lateral flow is initiated through seepage, which shows weak sub-surface connections across the prairies (Hayashi et al., 2016; Van der Kamp and Hayashi, 2009, 1998). Brannen et al. (2015) found that shallow groundwater flows from beneath the hillslopes to the wetlands can contribute significantly to surface storage, and plays a role in sustaining surface connections between ponds and generating streamflow. The subsurface runoff is a small component of the water budget of prairie wetlands in dry condition, but it is a large component compared to other fluxes under wet conditions (Brannen et al., 2015). After a rainfall or snowmelt event, the potholes and wetland of prairies are prone to

create a scenario of wet shallow subsurface and high near surface water tables, which have a great potential to trigger lateral subsurface flow. It is probable that excluding subsurface connection and subsurface runoff or interflow from runoff estimation may deteriorate the prediction performance of recession flow and summer runoff in a prairie hydrological model. Therefore, there is a need to investigate the effect of including interflow component on the modelling skill of prairie hydrological models.

To incorporate interflow into the previously developed PDMROF, a blend of WATROF and PDMROF is proposed in this study to develop an improved algorithm. PDMROF's ability to capture prairie surface runoff estimation considering the fill-spill mechanism of prairie potholes and WATROF's ability to estimate interflow and groundwater flow are combined in the improved algorithm. This improvement is proposed to account for the existence of sub-surface connections between neighboring potholes by lateral seepage of water in the prairies. To improve the representation of overland flow in MESH, the default ponding depth in CLASS (used in WATROF) is replaced by that estimated using PDMROF. It uses the PDM concept to estimate excess available water for runoff, with Manning's equation used to obtain overland flow on the land surface to a micro-drainage network within each model grid. This allows for variable contributing area and provides a better representation of surface connectivity in the prairies. To include interflow, an approximate solution of Richards' equation (Richards, 1931), used to calculate interflow in WATROF is utilized. The runoff generation approach developed in this study is henceforth referred to as LATFLOW due to its ability to simulate lateral sub-surface flow. The difference between LATFLOW and WATROF is the threshold in surface water holding capacity. WATROF has a constant threshold capacity across the topography of the watershed, while LATFLOW uses a variable threshold capacity as in PDMROF. The calibration parameters of LATFLOW are the combination of the parameters of WATROF and PDMROF. LATFLOW is included in MESH as a switch to replace the existing overland and

subsurface lateral flow algorithms. Schematics of the proposed runoff generation scheme along with existing schemes considered in this study are shown in Figure 3.9. It clearly represents the distinctions between the three runoff generation algorithms considered in this study along with information on required hydrometeorological data. Hydrometeorological and topographical data (DEM and land-cover information) are passed to CLASS subroutines to calculate different components of the water balance (except runoff). Either WATROF, PDMROF, or LATFLOW is used within each grid cell to estimate runoff and route across grid cells using continuity and Manning's equation, which eventually estimates streamflow.

The parameterization of MESH consists of a number of governing equations for different hydrological processes. A detailed description of all the parameters is found in CLASS documentation (Verseghy, 2011) and https://wiki.usask.ca/display/MESH. The parameters used in MESH is divided into different categories as shown in Table 3.1. Within MESH, vegetation parameters control evapotranspiration and interception; drainage and soil parameters control runoff, soil moisture storage, and ponding of water; snow parameters control snow accumulation, redistribution, storage, and snowmelt; routing parameter is used for routing of streamflow; and initial condition parameters are used to initiate the model run. Some of the parameters (river channel roughness factor, porosity, saturation during snowmelt, and opportunity time of infiltration) are not affected by the variation of landuse type (GRU independent).

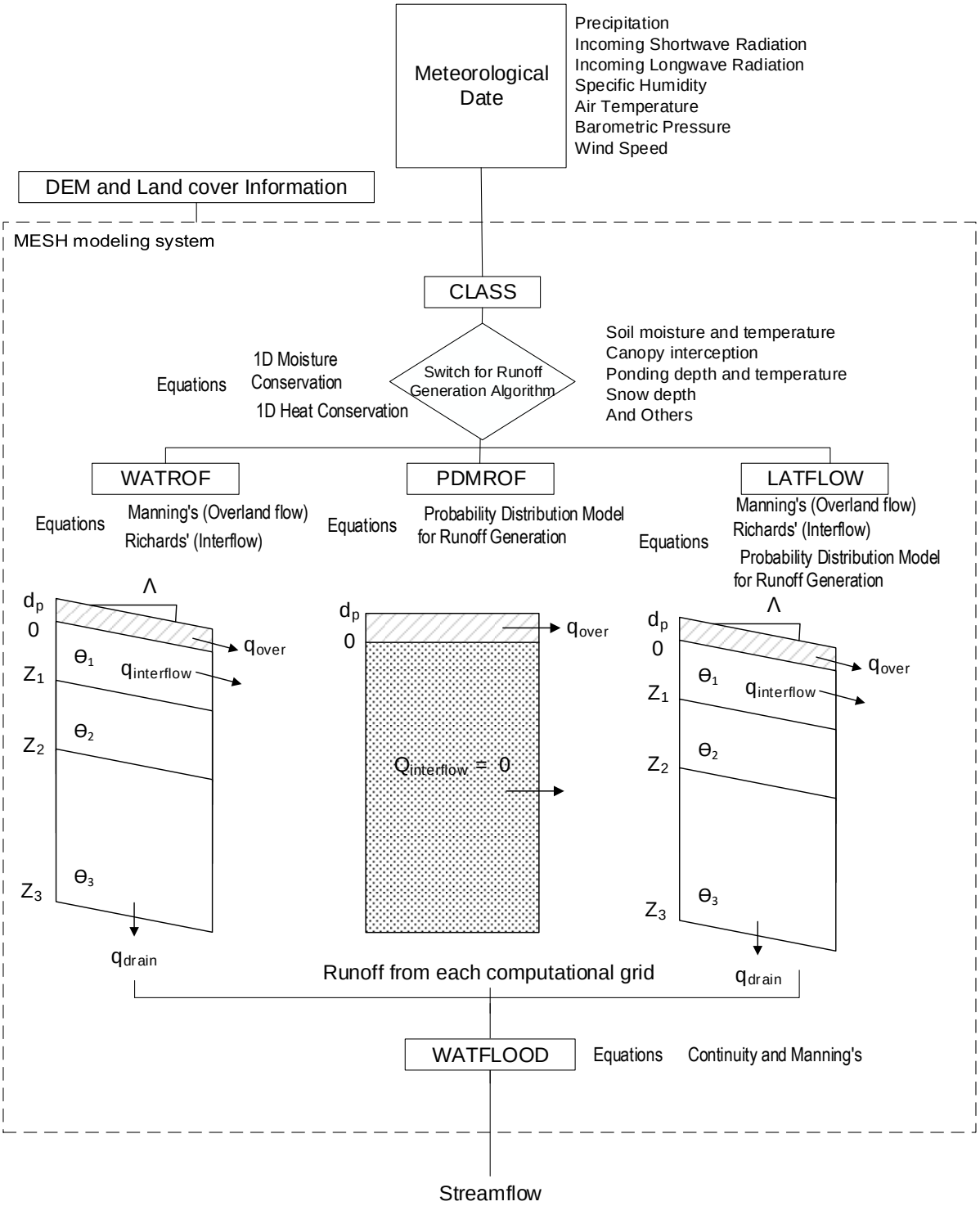

Figure 3.9: Detailed schematic of MESH Modelling system, a linked representation of atmospheric-hydrologic-land surface model. Acronym 'Z' is depth, 'q' is runoff, 'θ' is soil moisture content, 'dp' is ponding depth, and 'Λ' is slope

Table 3.1: All parameters used in MESH

Vegetation Parameters	Drainage Parameters	Soil Parameter	Snow Parameter	Routing Parameter	Initial Condition
○ Vegetation type ○ Leaf area index ○ Roughness length ○ Visible and near-infrared albedo ○ Biomass density ○ Rooting depth ○ Stomatal resistance	○ Drainage index to control seepage from the bottom of the soil column ○ Permeable depth ○ Drainage density ○ Overland slope ○ Saturated surface soil conductivity ○ Manning's n ○ Average slope ○ Surface Storage connectivity (shape factor) ○ Surface Storage capacity	○ % sand, clay and silt ○ % organic matter ○ Porosity	○ Limiting snow depth ○ Depth in snow-covered areas ○ Depth in snow-free areas ○ Saturation during melt ○ Opportunity time of infiltration ○ Fetch ○ Vegetation height and density ○ Snow distribution factor	○ River channel roughness factor	○ Temperature of soil, canopy, and ponded water ○ Volumetric liquid and frozen water content ○ Depth of ponded water ponded ○ Intercepted liquid and frozen water

3.3.2 Model Run Configurations for Runoff Generation Algorithm Comparison

Regarding the comparative study of the runoff generation algorithms (Objective-1), three different model configurations using existing algorithms, i.e. WATROF and PDMROF, and the proposed LATFLOW, were examined to analyze the influence of runoff distribution between overland flow and interflow in different watersheds, and to assess the limitations of runoff generation algorithms used in MESH. The idea was to compare three model configurations with different runoff generation algorithms, with all other model components unchanged. Initial conditions assigned to the model before calibration were an important attribute, as they fix the value of state variables (variables that determine the current state of the model) prior to a calibration run. Theoretically, it was possible to achieve the amount of water stored in watershed by spinning up the model for a few years. Previous studies (Davison

et al., 2016; Mengistu and Spence, 2016) suggest that the selection of two years as spin up period in MESH would achieve a stable state, close to the actual state of the watershed, and provide reasonable initial conditions for a calibration run. For each watershed, the first two years were considered as spin-up period, the final two years were considered as a validation period, and the number of years in between were considered as the period for calibration. The state variables (volumetric soil moisture of different layers of soil) of each watershed were assigned high values at the beginning of spin-up indicating near saturated conditions. This soil condition allows the model to drain during the spin up period to acquire acceptable initial conditions for calibration as MESH simulates draining water process more quickly compared to filling up process. The models for White Gull Creek, Kronau Marsh, and Brightwater Creek watersheds were run from October 1st, 2002 to October 1st, 2010. The modelling time step was based on the available temporal resolution of meteorological data for individual watersheds (hourly time step). Output information was stored at a daily time step in order to match the temporal resolution of the observed streamflow data. All the configurations of MESH were setup using grids of $0.1^{o} \times 0.1^{o}$ (approximately 10 km × 10 km) as shown in Figure 3.10. For the White Gull Creek watershed 16 grid cells were divided into three GRUs, for the Kronau Marsh watershed 45 grid cells into three GRUs, and for the Brightwater Creek watershed 19 grid cells into three GRUs. The number of GRUs were fixed based on the types of landcover and fraction of non-contributing areas within each watershed. The existence of millions of depressions in the non-contributing area redefines the soil properties despite the area may be defined as cropland or grassland in the ECCC maps. So, considering non-contributing area as an individual GRU provides the flexibility to estimate the parameters more accurately for separate GRUs. Detailed delineation of the three watersheds are presented in Figure 3.10. Three soil layers were defined in the model: from 0 to10 cm, 10 to 60 cm, and 60 to 410 cm below ground level to adequately reproduce the soil thermal regime, based on Verseghy (1991). Here

the first shallow surface layer stores diurnal temperature changes, the second layer resolves the temperatures in the middle vegetation rooting zone, and the third layer stores annual variations of temperature change.

Wetland hydrological processes have great impact over the hydrology of prairie watersheds. The proportion of wetland is high in the prairies and during the wet season, a significant portion of watershed appears as bog, which holds the water until evaporation takes place (Van der Kamp and Hayashi, 2009). A synthetic bog condition was created in the model configurations of the prairie study watersheds (Brightwater Creek and Kronau Marsh) by considering no baseflow from the soil column. The soils of the prairie region are underlain by glacial tills, which exhibit very low hydraulic conductivities. This phenomenon is responsible for very low groundwater recharge rates, which occur generally below the wetlands (Hayashi et al., 2016; Van der Kamp and Hayashi, 1998). As a result, baseflow is generally non- existent in small streams and lateral movement of water is only possible as overland flow and interflow. In case of high water table conditions, interflow may have a contribution from near-surface groundwater flow (Hayashi et al., 2016), however, MESH considers this combined flow as interflow. No flow is observed during dry seasons in the prairie watersheds, which also verifies no baseflow contribution under normal conditions.

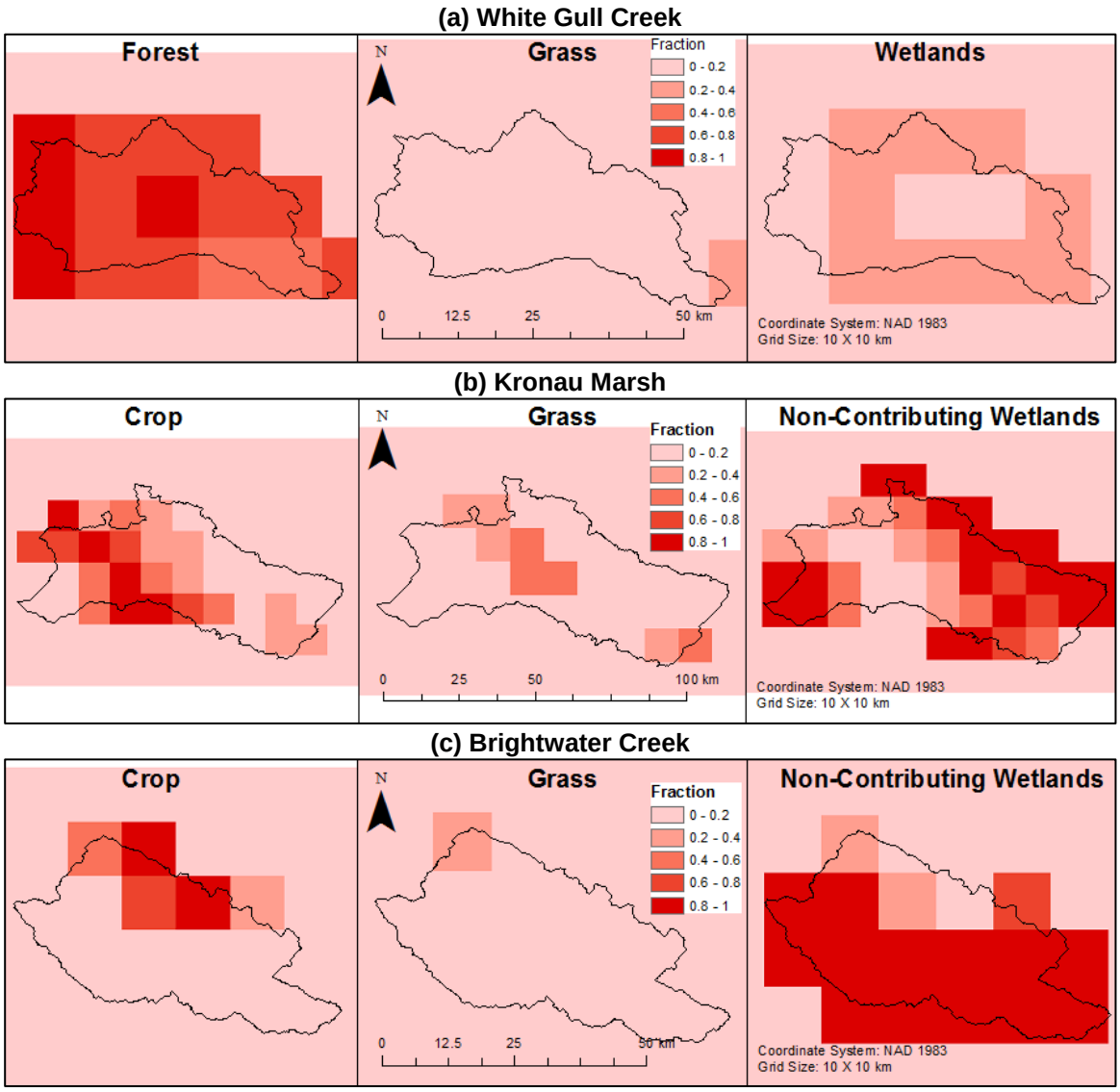

Figure 3.10: Delineated GRU using landuse information for (a) White Gull Creek, (b) Kronau Marsh, and (c) Brightwater Creek watersheds

To represent the spatial distribution of soil information, a probable fraction of soil texture was estimated by averaging the detailed and spatially distributed soil information. Averaging of detailed soil composition information poses a potential uncertainty that could affect the soil heterogeneity. Hence, soil composition was considered as a calibration parameter to account for the uncertainty associated with soil composition. Soil composition was perturbed within a user-defined range (~15%) of the base average value, which is determined by analyzing the range of different soil types located within a watershed.

3.3.3 Calibration and Validation

A split sample approach for calibration and validation was considered in the present study. This approach is often employed to obtain unbiased estimates of future performance of a model (Klemeš, 1986). A multi-objective optimization technique was adopted here to calibrate the model using streamflow at the outlets of respective watersheds. For a multi-objective calibration technique, maximization of both NSE and $Log(NSE)$ was used as objective functions. NSE and $Log(NSE)$ is formulated below-

$$NSE = 1 - \frac{\sum(Q_{obs} - Q_{sim})^2}{\sum(Q_{obs} - \overline{Q_{obs}})^2} \quad (3.10)$$

$$Log(NSE) = 1 - \frac{\sum[\log(Q_{obs}) - \log(Q_{sim})]^2}{\sum[\log(Q_{obs}) - \log(\overline{Q_{obs}})]^2} \quad (3.11)$$

where Q_{obs} is observed flow, Q_{sim} is simulated flow, and $\overline{Q_{obs}}$ is mean of observed flows. Both NSE and $Log(NSE)$ are unitless and ranges from $-\infty$ to 1, where 1 is the highest efficacy. Based on the formulation of NSE and $Log(NSE)$, NSE is an efficient error indicator for high flow conditions and $Log(NSE)$ is efficient for low flow conditions. A multi-objective approach using both NSE and $Log(NSE)$ is likely to address both high and low flow conditions simultaneously. For multi objective optimization, the Pareto Archived Dynamically Dimensioned Search (PADDS) (Asadzadeh and Tolson, 2012) algorithm was used. This algorithm evolved from the Dynamically Dimensioned Search (DDS) algorithm (Tolson and Shoemaker, 2007) and designed to be applied in a multi-objective optimization process. PADDS inherits the simplicity and parsimonious characteristics of DDS. PADDS initiates the search with a robust initial value and it does not show any oscillating behavior during convergence. The DDS is a stochastic global search algorithm designed for optimization problems with multiple parameters. It is a single-solution based heuristic search algorithm and finds a good global solution within a limited number of evaluations. The approach does not intend to optimize all parameters within a fixed neighbourhood, as is the case of most heuristic

optimization approaches. Instead, it automatically sets the size of search region according to the current iteration count and user-specified maximum number of model evaluations (Chu et al., 2015). DDS starts searching for a solution globally and transitions to a local search as it approaches a user-specified maximum number of objective function evaluations. The transition from global to local search is achieved by dynamically and probabilistically reducing the number of dimensions in the search neighbourhood (i.e., the set of decision variables modified from their best value). The probability of choosing each decision variable (model calibration parameters) to search based on a function of iteration count in the DDS algorithm is calculated as:

$$P(i,j) = 1 - \frac{ln(j)}{ln(N)} \tag{3.12}$$

where $P(i,j)$ is the probability of choosing decision variable x_i to search on iteration, and N is the total number of iterations. DDS has grown popular because of its simplicity and high applicability. A number of studies (Dornes et al., 2008; Haghnegahdar et al., 2014; Haghnegahdar et al., 2015) have shown the ability of DDS in finding good solutions in complex models when limited calibration budget is available. PADDS algorithm uses the basic mechanism of DDS as a search engine and archives all non-dominated solutions during the search. This search algorithm provides additional benefit of low computational budget with an efficient way of generating non-dominant solutions in comparison with other multi-objective search algorithms (such as SPEA2, NSGAII) (Asadzadeh and Tolson, 2012).

The purpose of multi objective optimization (MOO) is to minimize or maximize two or more objective functions subject to a set of constraints. Multi-objective optimization techniques are widely applied in hydrology and water resources management, where optimal decisions need to be taken in the presence of tradeoffs between multiple conflicting objectives. In the model response space, often non-dominated objective function solutions create a line or surface,

which is known as ‘pareto front’. Modern evolutionary algorithms (such as PADDS) operates in such a way that it creates a pareto front initially and as it progresses it tries to converge towards the perfect solution. The convergence process of PADDS includes (i) creation of a preliminary non-dominant solution set, (ii) picking up a non-dominated solution and updating the solution by perturbing parameter values. In case an updated solution is found, the solution set gets updated and it converges towards the desired values of the objective functions. The level of convergence of the Pareto front depends on the model parameterization, choice of search algorithm, number of optimization runs, and starting condition of optimization.

To compare the existing and proposed runoff generation algorithms, only drainage, snow, and routing parameters (Table 3.1) of MESH are were perturbed during optimization process. The values of other parameters, i.e. vegetation parameters, soil properties and initial conditions were kept fixed. The idea is to observe the change in drainage conditions due to the change in drainage and storage related parameters (which are part of runoff generation algorithms). If other parameters are also perturbed, the result will be affected by all types of parameters used in MESH, which makes it difficult to understand the actual change in the drainage conditions due to differences of runoff generation algorithms. The following drainage parameters are perturbed during optimization runs in different runoff generation algorithms.

1. River roughness factor
2. Surface storage capacity
3. Surface storages connectivity coefficient or shape factor
4. Limiting snow depth below which coverage is less than 100%
5. Water ponding depth for snow covered areas
6. Water ponding depth for snow free areas
7. Manning's n for overland flow

8. Drainage index to impede baseflow
9. Permeable depth of the soil column
10. -Hydraulic conductivity at saturation at the surface
11. Drainage density
12. Fraction of the saturated lateral surface soil conductivity

Surface storage capacity (c) and surface storages connectivity coefficient or shape factor (b) were explained previously. *River roughness factor* is a combined representation of channel roughness and width, which is explained using Manning formula. It is a function of roughness, drainage density, and shape of elementary cross section of drainage channel. River roughness factor ranges from 1.0 for impervious surfaces in urban areas to approximately 100 for forested areas. These values serve only to show the relative effects of surface roughness and drainage density. Because of its nature, *river roughness factor* can only be evaluated through calibration. *Drainage index* is used where it is desired to suppress drainage from the bottom of the soil profile (e.g. in bogs, or in deep soils with a high-water table). The value of *drainage index* ranges from 0 to 1, where '0' is complete suppression of water from the bottom of soil column and '1' is no suppression. The *soil permeable depth* is the existence of impermeable soil layer or bedrock within soil column. The depth to bedrock may be less than the modelled thermal depth of the soil profile, which provides a range from zero to the total depth of soil column. *Drainage density* is the density of channel with respect to surface area. It is defined as-

$$DD = \sum \frac{L}{B} \ (\text{km/km}^2) \qquad (3.13)$$

Where, L is the length of stream segment and B is the area. Theoretically this can range from 0 to ∞. However, for this study a logical range from 50 to 120 km/km^2 was used. *Limiting snow depth* is the minimum snow depth when it is considered that soil surface is completely covered with snow. This is a storage parameter and indicates the storage capacity in ice form. A higher value indicates high snow water equivalent (SWE) capacity of soil. In this case more

water is stored in ice form and exhibits delayed response to the temperature rise. As soon as ice starts melting, sharper and steeper rise in the hydrograph is observed compared to the lower *limiting snow depth* value. Theoretically, it can range from 0 to ∞, however, for this study a reasonable range of 5 cm to 30 cm was used. During the snow melting period, two additional types of storage are also observed within the snow surface (Figure 3.11). When ground ice and snow starts melting, open patches are observed in different places of ground. This is primarily happening because of different intake rates of energy in solar radiation form. Water is ponded over the snow-covered area as well as snow free patches. These two storages are parameterized using $zplg$ (maximum water ponding depth for snow covered areas) and $zpls$ (maximum water ponding depth for snow free areas). The main difference is the energy intake based on surface albedo, where open patches tend to receive more energy and snow-covered area receives less energy.

Manning's n for overland flow was used for runoff routing. It was used for runoff water to travel to the nearest channel. It can range from 0.02 to 0.05 sm^{-1}. Soulis et al. (2000) introduced a sloped soil column concept instead of the flat soil column concept previously used in CLASS and used the Manning formula to estimate overland runoff in association with a mild soil slope. This parameter is an integral part of overland drainage properties. Information on selected parameters and the range for each configuration (MESH-WATROF, MESH-PDMROF, and MESH-LATFLOW) is presented in Table 3.2. Initial parameter values and calibration ranges (Table 3.2) were decided based on CLASS technical documentation (Verseghy, 2011), literature (Dingman, 2002, Davison et al., 2016,

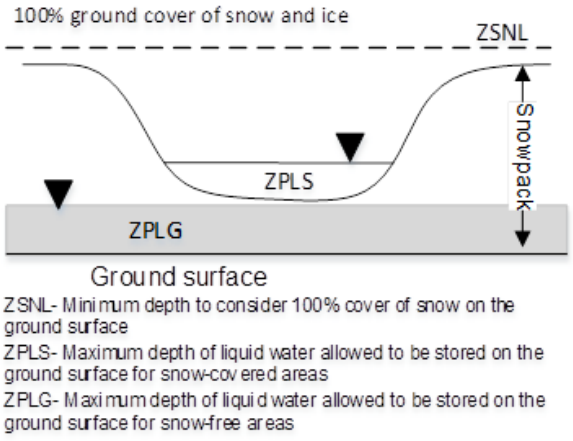

Figure 3.11: Water content of snow covered and snow free areas

2006, Haghnegahdar et al., 2015, 2014; Mekonnen et al., 2014) and expert opinion in case of unavailability of information from literature.

Table 3.2: Calibration parameters, along with their descriptions and ranges

Description	GRU	Lower limit	Upper limit	Model Configuration
River roughness factor [$m^{0.5}s^{-1}$]	-	0.3	2	WATROF, PDMROF, LATFLOW
Surface storages connectivity coefficient or shape factor	crop/ grass/ forest	0	30	WATROF, PDMROF, LATFLOW
	NCW	0	5	
Maximum surface storage capacity [m]	crop/ grass/ forest	0	5	WATROF, PDMROF, LATFLOW
	NCW	0	10	
Limiting snow depth below which coverage is less than 100% [m]	crop/ grass/ forest	0.05	0.3	WATROF, PDMROF, LATFLOW
	NCW	0.05	0.3	
Maximum water ponding depth for snow covered areas [m]	crop/ grass/ forest	0.05	0.25	WATROF, PDMROF, LATFLOW
	NCW	0.05	0.25	
Maximum water ponding depth for snow free areas [m]	crop/ grass/ forest	0.05	0.25	WATROF, PDMROF, LATFLOW
	NCW	0.05	0.25	
Manning's n for overland flow [$ms^{-1/3}$]	crop/ grass/ forest	0.01	0.05	WATROF, LATFLOW
	NCW	0.01	0.05	
Drainage index to impede baseflow	crop/ grass/ forest	0	1	WATROF, PDMROF, LATFLOW
	NCW	0	0.1	
Permeable depth of the soil column [m]	crop/ grass/ forest	0	total soil depth	WATROF, PDMROF, LATFLOW
	NCW	0		
Saturated surface horizontal soil conductivity [ms^{-1}]	crop/ grass/ forest	0.0001	0.01	WATROF, LATFLOW
	NCW	0.0001	0.01	
Drainage density[km/km^2]	crop/ grass/ forest	50	120	WATROF, LATFLOW
	NCW	50	120	
Fraction of the saturated lateral surface soil conductivity	crop/ grass/ forest	0	0.8	WATROF, LATFLOW
	NCW	0	0.1	

*NCW- Non-contributing Wetlands

3.3.4 Model Performance Evaluation

Performance evaluation of the model during the validation periods for streamflow simulation was carried out using guidelines developed by Moriasi *et al.* (2007) who recommended the use of Nash-Sutcliffe efficiency (NSE) (Equation 3.10) and percent bias ($PBIAS$) (Equation 3.14) for this purpose. Percent bias ($PBIAS$) is expressed as,

$$PBIAS(\%) = \frac{\sum(Q_{obs} - Q_{sim})}{\sum Q_{obs}} \times 100 \quad (3.14)$$

Where Q_{obs} is observed flow, Q_{sim} is simulated flow. PBIAS ranges from -100% to +100% with these extremes indicating over estimation and under estimation of the flow volumes, respectively. Because Objective-1 of this study is to evaluate and compare runoff generation algorithms in different watersheds for streamflow simulation, the performance indices were also estimated and analyzed for streamflow only. However, MESH also calculates intermediate water balance components such as evapotranspiration, overland and subsurface storage, and snow water equivalent (SWE) in arriving at streamflow. A better understanding of the bias or discrepancies in estimates of these intermediate processes would aid in locating variables for which physically unrealistic values were assigned during calibration. In this direction, it was understood that drainage and storage related parameters are primarily responsible for runoff process and there is no point perturbing other types of parameters (such as evapotranspiration, soil property, snow accumulation, and initial condition related) because these parameters are modeled by CLASS, which is common in each model configuration (i.e. WATROF, PDMROF, and LATFLOW model configurations). High bias would indicate inaccurate representation of the runoff process in MESH when a particular runoff generation algorithm is used. For this purpose, comparison between measured and simulated values of one or more water balance components was carried out over watersheds where measured data were available.

It is possible that the model outcome is influenced by the number of parameters used in the optimization process. To investigate the influence of number of parameters, Akaike information criterion (AIC) (Akaike, 1974) was chosen as a performance measure. AIC deals with the trade-off between the goodness of fit of the model and the increase in the number of parameters, and it includes a penalty, which is a function of the number of estimated parameters (Remesan and Mathew, 2015). AIC is expressed as,

$$AIC = n\, ln\left(\frac{\sum(Q_{obs}-Q_{sim})^2}{n}\right) + 2m \tag{3.15}$$

where, m is the total number of parameters used in the model, and n is the sample size. AIC is the relative measure that compares performance across models. Low values of AIC indicate better performance across the compared models. In the present study, AIC was used to compare different runoff generation algorithms in an individual watershed to assess the effect of increased number of parameters.

3.4 Lake System Modelling of the Qu'Appelle River Basin

The lake system of the QRB consists of eight lakes (i.e. Buffalo Pound, Last Mountain, Pasqua, Echo, Mission, Katepwa, Crooked, and Round Lake) connected in a series and parallel arrangement. Out of eight, six lakes have a stop-log control structure in their downstream end. The overall goal of the QRB lake operation is to dampen the spring peak flow and replenish the lake storage to maintain socio-economic activities around the lakes. The Buffalo Pound Lake (BPL) lies at the beginning of the QRB lake system and it is the most important lake in terms of municipal, agricultural, and commercial water supply in the basin. At the beginning of the spring peak runoff season, BPL water level is dropped to the lower limit of its operating range, either through increased outflows from the lake or reduced diversions from Lake Diefenbaker (or a combination of the two). During peak flow events, the gates at the Buffalo Pound Dam remain closed to limit the amount of water backing up into the Lake from the Moose Jaw River, which joins the Qu'Appelle River a short distance below the lake. Once the tailwater conditions at the dam equalize or drop below the lake level, the gates are then opened fully to allow flood waters to flow out of the reservoir. Once the Ridge Creek, a tributary of BPL, starts contributing runoff to the lake, diversions from the Qu'Appelle Dam on Lake Diefenbaker are terminated. These diversions are only reinitiated when required to support environmental flows of the river or when required to meet downstream demands (irrigation or to maintain BPL water levels). The Last Mountain Lake (LML) is the biggest lake in the system, and it acts as a natural flood dampener. This lake lies in parallel to the QRB lake system

and there is a control structure just downstream from the confluence of the Qu'Appelle River and LML to divert most of the spring runoff towards the Last Mountain Lake by raising and lowering the control structure level. In the months leading up to a flood event, the water level of LML is lowered to free up flood storage. During peak flow events, the control structure is opened fully, to allow a natural flow of the Qu`Appelle River to split. Initially some of the flow will divert naturally into LML. When the levels in Qu'Appelle River lowers, water in LML flows out into the river. The Echo Lake, Crooked Lake, and Round Lake structures are left wide open until lakes return to their normal operating ranges following the peak flow event. The operating rules of the QRB lakes are summarized in the Table 3.3, and Figure 3.12 shows a simple schematic of the lakes arrangements in the QRB system.

Table 3.3: Operating rules of the lakes in the QRB (Source: Water Security Agency).

Name	Winter	Spring	Summer	Fall
Buffalo Pound Control Structure	Maintains a small release, typically between 0.2 and 0.5 m^3/s to meet the downstream needs.	Operated to help maintain the water levels in the lake within the desirable operating range. The releases are adjusted to maintain the lake level. During high flow events, overflow from the Moose Jaw River backs into the lake, filling the lake well above desired levels.	Releases adjusted as required to maintain desired lake levels.	Releases reduced to 0.2 - 0.5 m^3/s.
Valepoint (or Last Mountain lake) Control Structure (located in the downstream end of LML)	Structure typically wide open.	During expected average or high runoff events the structure is totally opened, during low runoff events the structure is closed to create an artificial backflow.	Structure is typically open.	Structure is typically opened.
Echo Lake Control Structure	Structure typically wide open.	During expected average or high runoff events the structure remains totally open. During very low runoff years, the structure is closed during or even prior to the spring runoff event.	Structure is partially open, passing some downstream flows.	Structure is typically opened.
Katepwa Control Structure	Structure is closed.	Structure is generally closed. During high runoff events, the structure may be opened to help pass the inflows into the lake.	Structure is closed.	Structure is closed.

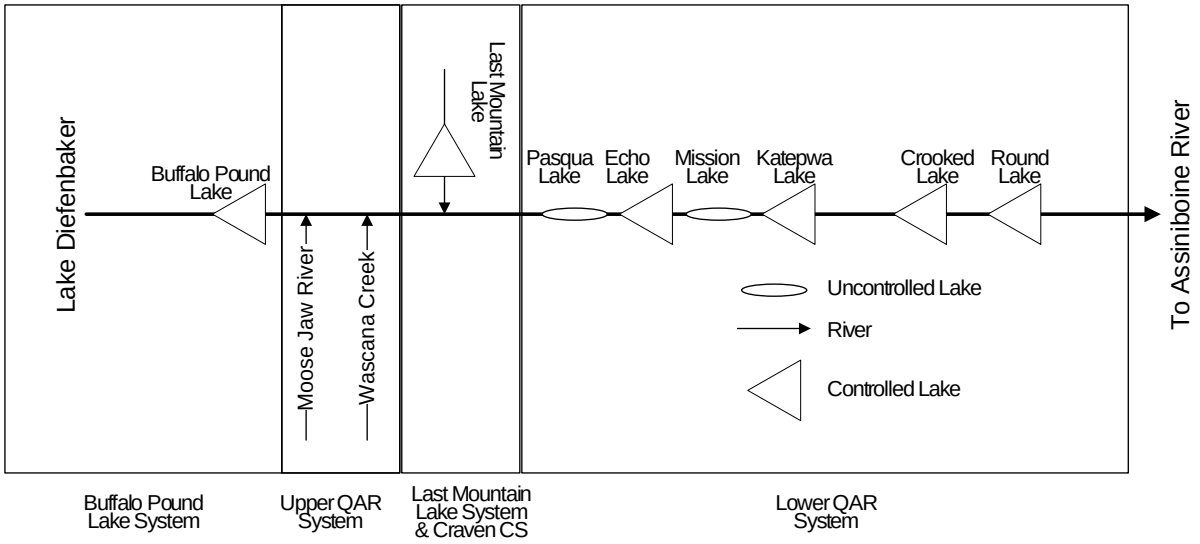

Figure 3.12: Simple schematics of the QRB lake system arrangement.

The entire QRB lake system is divided into four sub-systems, i.e. Buffalo Pound Lake system, upper Qu'Appelle River system, Last Mountain Lake system, and lower Qu'Appelle River system. The total upstream watershed area of BPL is 3,344 km^2. Besides inflow from Elbow, BPL also receives streamflow through tributaries and from upstream watershed. Among the tributaries, outflow from Iskwao and Ridge Creek are gauged, which covers 821 km^2 (25%) of the watershed. The remaining 75% of the watershed is ungauged. Upper Qu'Appelle River system mainly consists of BPL release and outflows from the Moose Jaw River (corresponding watershed area is 9,230 km^2) and the Wascana Creek (3,850 km^2). The total upstream watershed area of LML is 14,732 km^2. The lake receives water from the northern watershed as well as from the Qu'Appelle River. A number of tributaries feed the lake, among them Lanigan Creek (2,283 km^2), Lewis Creek (572 km^2), and Saline Creek (950 km^2) are important and measured outflow is available, however, over 70% of the upstream watershed is ungauged. The lower Qu'Appelle River system consists of six connected lakes. This system primarily receives outflows from Loon Creek, Jumping Deer Creek, Pheasant Creek, Ekapo Creek, and Cutarm Creek (Figure 3.5).

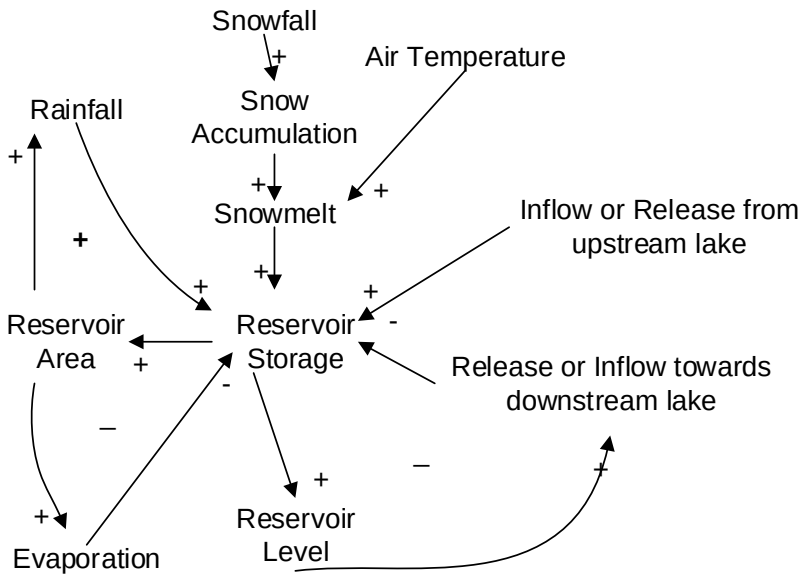

Figure 3.13: Causal Loop Diagram (CLD) of a Lake

3.4.1 System Dynamics for Lake Modelling

System Dynamics (SD) is selected as the platform for the lake systems model. A simple example is used here to illustrate how SD functions. Figure 3.13 shows a causal loop diagram (CLD) for a single lake. A CLD is a simple way to show connections and feedbacks within a system. An arrow ending with '+' sign represents a positive relationship (increase in one variable leads to an increase in another, or decrease in one leads to a decrease in another) and a '-' sign represents a negative relationship (as one variable increases, the other decreases). For example, as inflow increases the amount of lake storage increases (positive), and as release increases lake storage decreases (negative). Feedbacks are represented as loops. The looped '+' represents a positive feedback, e.g. lake storage increases with the lake area and rainfall volume. The opposite occurs for negative feedbacks, as seen for evaporation and release.

Lake systems model development includes (i) identification of modelling schematic, (ii) collection of background information and operating rules, (iii) identification of the interactions of the lakes, and (iv) formulation of the interactions in the SD environment. Modelling schematic is the collection of system elements representing all important structures and

components essential for operation. Streamflow in the QRB is heavily controlled using stop-log structures at the downstream of Buffalo pound, Echo, Katepwa, Crooked, and Round Lakes. The following information was collected and used to identify and formulate the interactions between the lakes: (i) tributary inflows, (ii) precipitation rate, (iii) storage characteristics, (iv) desired operating level, and (v) release criteria. A lake model was developed by Saskatchewan Watershed Authority (2012) at a monthly scale to simulate the water yield and within the QRB and to allocate water based on target levels and demands. This model was used as the guide for the development of the lake SD model at a daily scale as the monthly scale model would not be useful for the present study. Existing operating rules for diversions and lake releases are important as they affect the historical flows, and impact the overall reliability of water supply. The rules is defined as seasonal target levels. Releases are driven by both the downstream demands and the target levels, but limited by the capacity of outlet structures.

The SD model of a reservoir or a lake is constructed graphically on the screen by an SD simulation environment, e.g. STELLA 10.1 software (ISEE Systems Inc., 2013). STELLA facilitates the use of the fundamentals of systems dynamics concept and allows users to run models created as graphical representations of a system using four fundamental building blocks (stocks, flows, converters, and connectors) (Elshorbagy et al., 2005; Forrester, 1961). Population, soil moisture storage, and reservoir can all be considered as stocks as they increase or decrease over time. In the reservoir model, the storage is represented as a stock. Varying inflows and outflows cause changes in storage volume over time. Flows are specified as a rate of increment or reduction of stocks, for example birth rate, death rate, runoff, reservoir release, and water withdrawal. To ensure the consistency of flows and make a compatible structure of model, modifications are required, such as converting reservoir storage to area, or by setting conditions for the stocks and flows, which is known as converters. Converters can also store

data and logical/mathematical functions to operate the system. Reservoir operating rules are also implemented through converters. Converters are linked to stocks and flows through connectors, displayed as arrows, and show how variables are connected.

The simulation model uses differential equations to describe the complex dynamic systems. These equations are solved numerically using Euler's method. Due to the modular nature of the simulation tool, the reservoir model is developed in sectors (Figure 3.12). Flow from all tributaries directly contributing to the reservoir is considered as inflow to the system. Inflow data are provided to the model as input. Total reservoir outflows consist of reservoir releases and lake evaporation. Every lake in the QRB system has its own characteristics, which are available in terms of stage-storage-release relationship (Figure 3.14) and these information is provided in the model to develop individual lakes. Lake releases are controlled by a monthly operating rule, which is available in terms of monthly elevation.

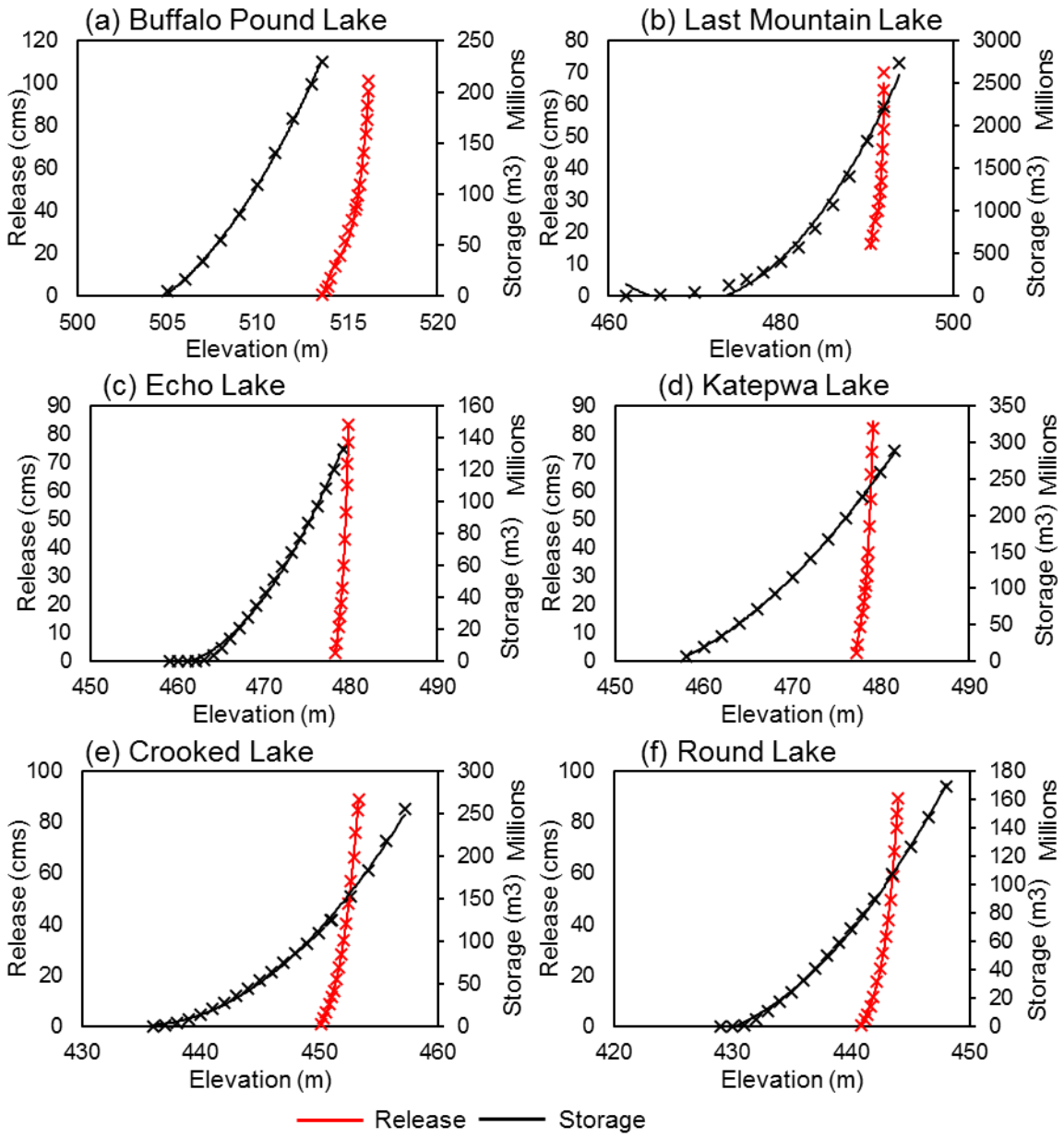

Figure 3.14: Stage-Storage-Release relationship of different lakes in QRB

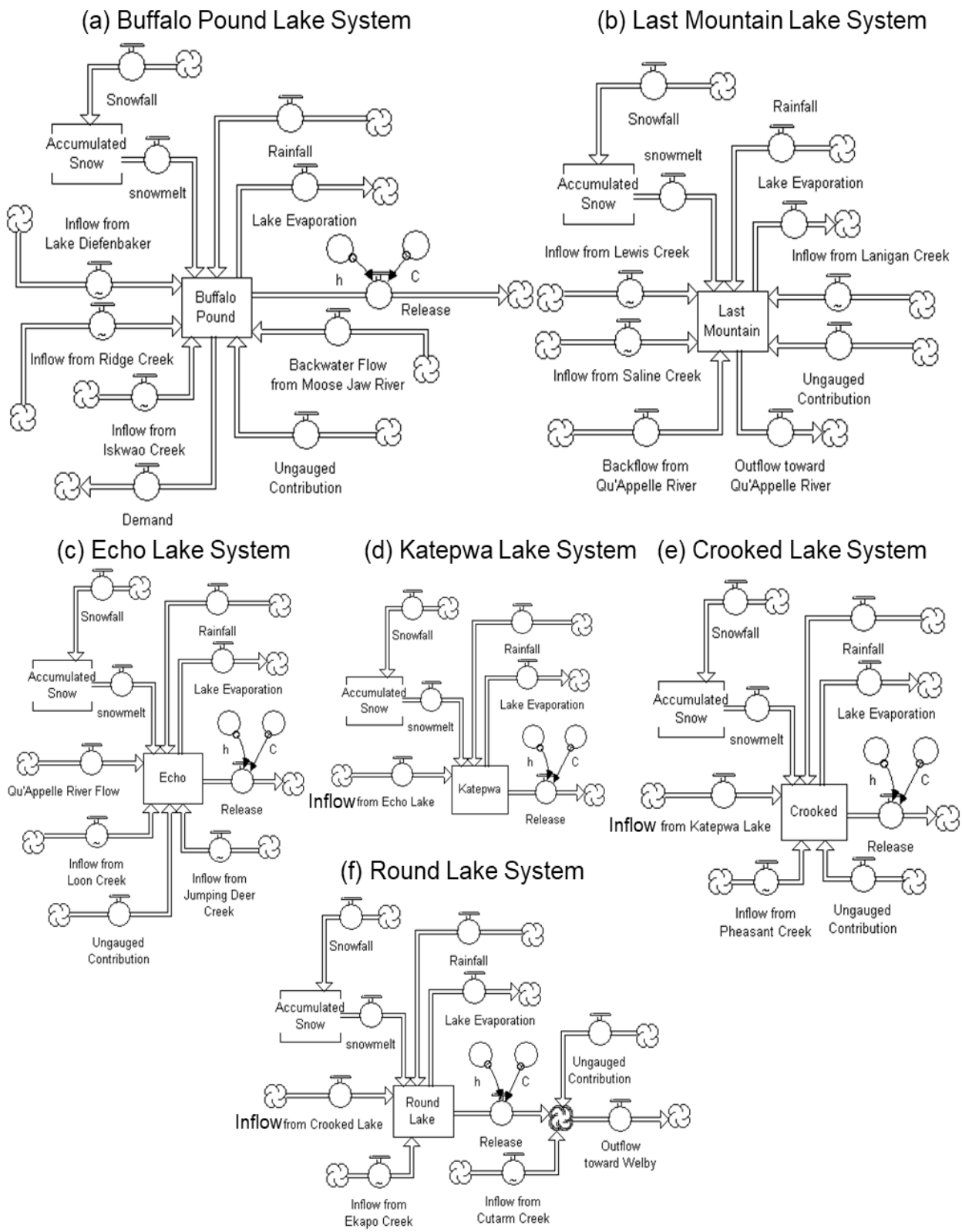

Figure 3.15: Schematics of multiple lake systems used in the SD model

3.4.2 Parameterization of Lake SD model

Water balance components of the lakes of QRB were parameterized in order to develop the lake system SD model. It is important to identify the significant and insignificant water balance components and required detailing of the hydrological processes. Moreover, reasonable assumptions and provisions to account for uncertain and unknown components (e.g. drainage contribution from ungauged watersheds, weir dimensions, temperature threshold for rainfall and snowfall segregation) are also important. Water balance of BPL system (Figure 3.15a) is formulated as-

$$Rainfall_{lake\ surface} + Snowmelt_{lake\ surface} + Inflow_{Lake\ Diefenbaker} + Inflow_{Iskwao\ Creek} + Inflow_{Ridge\ Creek} + Inflow_{ungauged\ basin} + Backwater\ flow_{Moose\ Jaw\ River} - Evaporation_{lake\ surface} - Withdrawal = \Delta storage \quad (3.16)$$

Available precipitation data consist of rainfall and snowfall as snow water equivalent (SWE). A temperature threshold is used to separate rainfall and SWE. A small range of temperature threshold is used from -3^{o}C to 0^{o}C. BPL lake evaporation (E_L, mm/day) was estimated using Meyer's formula (Meyer, 1915). This equation is formulated as:

$$E_L = K_M(e_w - e_a)[1 + \frac{u_9}{16}] \quad (3.17)$$

where, u_9 is the monthly mean wind velocity in km/h at about 9 m above ground and K_M is coefficient accounting for various other factors with a value of 0.36 for large deep and 0.50 for small shallow waters, e_w and e_a is saturated and actual vapor pressure (mb). Snow accumulation was modeled using a separate storage. If air temperature falls below the temperature threshold, then it was considered as snowfall and stored as SWE. Physically, snow accumulation storage resides on top of the lake surface and once melted, it contributes to the

lake volume. Degree-day method was adopted to estimate snowmelt runoff from the snow accumulation storage. Snowmelt (M, mm/day) is formulated as-

$$M = C_M(T_a - T_b) \quad (3.18)$$

where, C_M is the degree-day coefficient in mm/day/°C, T_a is mean daily air temperature °C, and T_b is base temperature °C. The value of C_M varies from 4 to 8 mm/day/°C (Dingman, 2002). Information of BPL abstraction was collected from Saskatchewan Watershed Authority (2012).

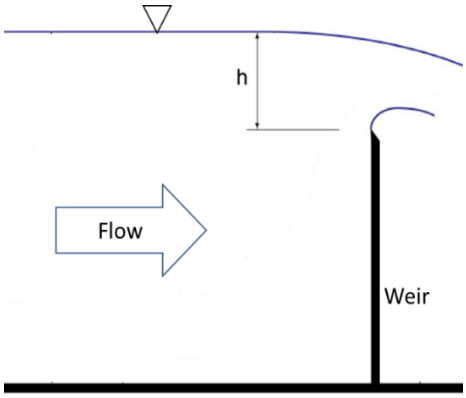

Figure 3.16: Schematics of weir operation

BPL lake release uses the weir equation of rectangular sharp crested weir, which is-

$$Q = CBh^{3/2} \quad (3.19)$$

where, Q is discharge in m^3/s, B is top width of weir (entire channel width is considered as B and estimated using GIS), h is the height difference between the weir and the top of the lake surface (desired operating level is considered as weir height), and C is a coefficient of discharge, which considers the effects of surface tension, contraction of the flow over the weir, energy losses, and the velocity head of the approach flow (Figure 3.16). An experimental value of C was determined as 1.837 when other parameters are in SI unit (Horton, 1907). However, fixed C value appeared to be unsuitable for BPL system because (i) ideal conditions for the sharp crested weir are not available here, (ii) BPL weir has an energy dissipation mechanism, which was not considered in the equation, and (iii) unavailability of weir measurements (width calculated using Google Earth, and depth was assumed). For this model, calibrating C was considered as suitable approach.

A vast 2,523 km^2 of upstream watershed area is ungauged and a significant amount of its runoff contributes to BPL (Figure 3.5). A simple linear assumption was considered to estimate the ungauged contribution (UC) for BPL, which is –

$$UC = A_{BPL} \times (Inflow_{Iskwao\ Creek} + Inflow_{Ridge\ Creek}) \quad (3.20)$$

The coefficient 'A_{BPL}' represents the proportion of ungauged area to gauged area. The basic idea is to estimate the amount of runoff from ungauged areas. For example, gauged outflow in the BPL catchment is from 821 km^2 whereas ungauged outflow is from 2,523 km^2 upstream watershed. Under the assumption that the drainage properties of BPL headwater area are distributed evenly over the entire watershed, the drainage response from 2,523 km^2 of ungauged watershed is considered to be proportional to the 821 km^2 of gauged watershed, which suggests that ungauged watershed is going to contribute about ($\frac{2{,}523}{821} = 3.07$) $\approx$ 3 times more water than gauged watershed. However, this estimation does not account for non-contributing area, which may reduce the ungauged-gauged proportion of watershed. For this reason, 'A' was considered as a calibration parameter within a range from zero to proportion of ungauged and gauged watershed contribution (for BPL, which is 3.0).

Measured water level and storage-area-elevation relationship are available for BPL system; however, measured lake release is not available. Release was estimated using continuity of measured streamflow at Lumsden subtracted from Moose Jaw River flow and Wascana Creek flow. The outlet of this system lies in the Lumsden flow station, where measured flow data are available. Inflow from Moose Jaw River and Wascana Creek were added to the simulated outflow from the lake and the combined flow was compared with the measured flow near Lumsden. In case of water flowing back towards the lake during high flow seasons, a fraction of water coming from Moose Jaw River diverts to the lake and the remaining water flows towards Lumsden. The amount of backwater flow was estimated using a tailwater rating curve

provided by the Water Security Agency with the incoming water from Moose Jaw River (Figure 3.17). An IF-ELSE switch is developed to initiate any backwater flow in the BPL based on the comparison between tailwater elevation and lake elevation. If tailwater rises over the lake elevation at the outlet then backwater flow is allowed into the lake, otherwise BPL outlet is releasing water. The water balance of the Upper Qu'Appelle River System primarily consists of three rivers, i.e. the Qu'Appelle River, Moose Jaw River, and Wascana Creek. Moose Jaw River and Wascana Creek are tributaries that flow into the Qu'Appelle River. During a flood year, a portion of water from Moose Jaw is diverted towards the BPL, which is considered as backwater flow. The water balance of this system is shown as-

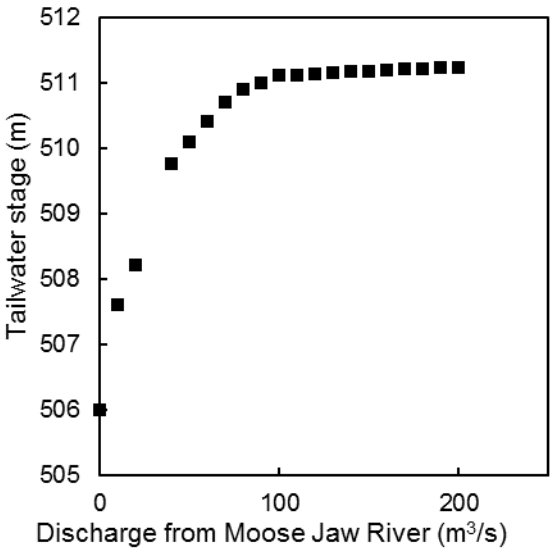

Figure 3.17: Tailwater rating curve

$$Flow_{Lumsden} = Inflow_{Wascana\ Creek} + Inflow_{Moose\ Jaw\ River} + Release_{BPL} - Backflow_{Moose\ Jaw\ to\ BPL} \quad (3.21)$$

The Last Mountain Lake (LML) flows southbound and joins the Qu'Appelle River near Craven. Basic water balance for LML system (Figure 3.15b) is-

$$Rainfall_{lake\ surface} + Snowmelt_{lake\ surface} + Inflow_{Lanigan\ Creek} + Inflow_{Saline\ Creek} + Inflow_{Lewis\ Creek} + Inflow_{ungauged} + Inflow_{Qu'Appelle\ River} - Evaporation_{lake\ surface} - Release = \Delta\, storage \quad (3.22)$$

A vast area of 10,927 km^2 upstream of LML is ungauged and contributes a significant amount of water to LML. A simple assumption was considered to estimate the ungauged contribution (UC) for LML, which is –

$$UC = A_{LML} \times (Inflow_{Lanigan\ Creek} + Inflow_{Lewis\ Creek} + Inflow_{Saline\ Creek}) \quad (3.23)$$

Here, A_{LML} was estimated using similar method of BPL and used as a calibration parameter. The Qu'Appelle River flow near Craven has a complicated two-way relationship with LML, because LML both drains and receives water from the river. A multiple regression analysis was conducted using the information of the Qu'Appelle River and LML considering that the Qu'Appelle River flow near Craven ($Flow_{Craven}$, m^3/day) is a linear function of lake elevation ($Lake_{Elevation}$, m), inflow from tributaries towards the lake ($\text{Inflow}_{\text{Gauged}}$, m^3/day), and inflow from Lumsden ($Inflow_{Lumsden}$, m^3/day). As the characteristics of the interaction between the lake and the river changes during open water and ice seasons, two separate regression models were developed. The developed equations are:

For the winter season (November to March):

$$Flow_{Craven} = \max(0, 0.488 \times Inflow_{Gauged} + 2.744 \times Inflow_{Lumsden} - 8.8 \times 10^4)$$

$$[\ for\ Lake_{Elevation} > 489.87\ m\ ] \quad (3.24)$$

For the spring and summer seasons (March to November)

$$Flow_{Craven} = \max(0, 1.2 \times 10^6 \times Lake_{Elevation} + 0.092 \times \text{Inflow}_{\text{Gauged}} + 0.369 \times \text{Inflow}_{\text{Lumsden}} - 9.3 \times 10^8) \quad (3.25)$$

Figure 3.18 shows the outcome of LML water level simulation using the aforementioned approach. Water level simulation was able to maintain a linear relationship between observed and simulated water levels without large bias, however, simulation during ice season are

underestimating water levels while water levels during summer season are generally overestimated by a small margin.

The lower Qu'Appelle River system (Figure 3.15c, Figure 3.15d, Figure 3.15e, and Figure 3.15f) consists of Pasqua, Echo, Mission, Katepwa, Crooked, and Round Lake. Pasqua and Mission Lake do not have any stop-log control structure at their downstream end and the lake SD model considers Pasqua and Echo Lake as one lake. Similarly, there is no control structure in the Mission lake, and this lake was integrated with Katepwa Lake into one lake. The basic water balance of the lower Qu'Appelle River system is similar to the water balance of BPL, except that there is no water withdrawal from any of the lake system. The parameterization of the lower Qu'Appelle River system is also similar to BPL, therefore, the only difference between the BPL and the lower Qu'Appelle River system is the source of inflow. In addition to inflow into the lakes from the Qu'Appelle River, gauged inflow from Loon Creek, Pheasant Creek, and Ekapo Creek was considered as additional lateral inflow for Echo lake; Crooked lake; and Round lake respectively. The Katepwa lake does not have any gauged tributary. The Cutarm Creek joins the Qu'Appelle River in the downstream of Round lake and the contribution of this Creek is significant. This channel was considered as a tributary of the Qu'Appelle River and contributes outflow just upstream of the outlet of the QRB.

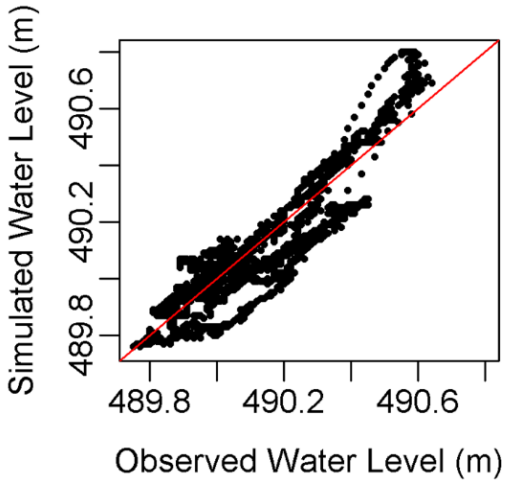

Figure 3.18: LML water level simulation scatter plot. $R^2 = 0.82$

3.4.3 Model Architecture, Setup, Calibration and Validation

The development of a model that has the ability to deal with reservoir operation was conducted using the SD approach. The lake SD model was developed for the daily timescale, where inflow

and forcing data were provided for each day from 2002 to 2015. The modelling process started from October 2002, and the first year was used as spin up. A split sample approach for calibration and validation was considered in the study. The model was calibrated from October 2003 to September 2008 and validated from October 2008 to September 2014. Calibrated parameters and corresponding ranges are shown in Table 3.4. A single-objective optimization technique was adopted using the measured and simulated streamflow at Welby. For the calibration, maximizing NSE (Equation 3.10) for the streamflow at the outlet near Welby was used as the objective function. The Dynamically Dimensioned Search (DDS) (Tolson and Shoemaker, 2007) was used as the automatic search algorithm for calibration. The model was evaluated using simulation of streamflow on the main channel of the Qu'Appelle River at three stations. The first station is located near Lumsden, just downstream of the confluence of the Qu'Appelle and Wascana Creek (Figure 3.5) and accounts for inflow from the BPL system, Moose Jaw River, and Wascana Creek. The second station is located near Craven, just downstream of the confluence of the Qu'Appelle River (Figure 3.5) and Last Mountain Lake and accounts for inflow from the Qu'Appelle River from Lumsden and LML system. The final station is located near Welby (Figure 3.5), which is the outlet of the QRB system, near the Saskatchewan-Manitoba border. Performance evaluation of the model during the validation period for streamflow simulation was carried out using guidelines developed by Moriasi *et al.* (2007) who recommended the use of NSE (Equation 3.10) and percent bias ($PBIAS$) (Equation 3.13). Besides streamflow, the model was further evaluated for the simulated lake elevations and NSE was used as the performance measure for this purpose. $PBIAS$ was not considered for lake water level simulation as it fluctuates over a small range, and PBIAS does not show anything meaningful in the direction of water level simulation.

Table 3.4: Parameter name, description, and ranges used in the lake systems model

Name	Parameter	Lower limit	Upper limit	unit	Source
TT	Temperature Threshold to separate rainfall and snowfall	-3	1	^{o}C	User defined
C	Weir release coefficient	1.8	6	$sm^{1/2}$	User defined
C_m	Degree-day coefficient	4	8	$mm/day/^{o}C$	Dingman (2002)
K_m	Lake evaporation coefficient	0.36	0.60		
A_{BPL}	Ungauged contribution from the watershed where measured streamflow is unavailable	0	3.00		GIS defined
A_{LML}		0	2.85		
A_{EL}		0	0.30		
A_{CL}		0	3.00		
A_{Welby}		0	4.20		

3.5 Hybridization of MESH and SD Modelling Tool

In a large-scale prairie watershed, handling the surface storage connectivity and water resources management of lakes together pose different challenges to the modellers. In the process of SD model development for the lakes, prediction of incoming water from the headwater areas is a challenging task. The hydrological model is aimed to simulate the streamflow prediction from the headwater regions addressing the prairie hydrological processes, while the effect of lake management and operation is simulated by the lake SD model. Specialized hydrological modelling tool, like MESH, has the capability to address prairie surface connectivity. However, in the case of large-scale prairie watershed, a hydrological modelling tool has to deal with a number of interconnected lake system, which is often not well simulated by a model like MESH. For example, the reservoir module of MESH is based on a simple storage-discharge relationship of a single reservoir. This module is not fully developed yet to simulate a complex interconnected lake network. The coupling of MESH and the lake SD model appears to be a necessity in order to develop a prairie systems model with the ability to address the prairie runoff process as well as lake interactions. Figure 3.19

provides a framework and different potential approaches to address the challenge of modelling a large-scale prairie watershed. The basic concept is a two-fold approach. The initial step is to identify the challenges (i.e. to estimate runoff from the headwater region of the prairie watershed and operation of interconnected lakes) and to distribute different challenges to specialized tools, and the second step is to combine the outcome of the models to predict the streamflow near the outlet. In this study, the hydrological model MESH) was used to estimate the water outflow from the headwater tributaries, and lake SD model was used to route the outflows from the tributaries toward the outlet of the whole QRB.

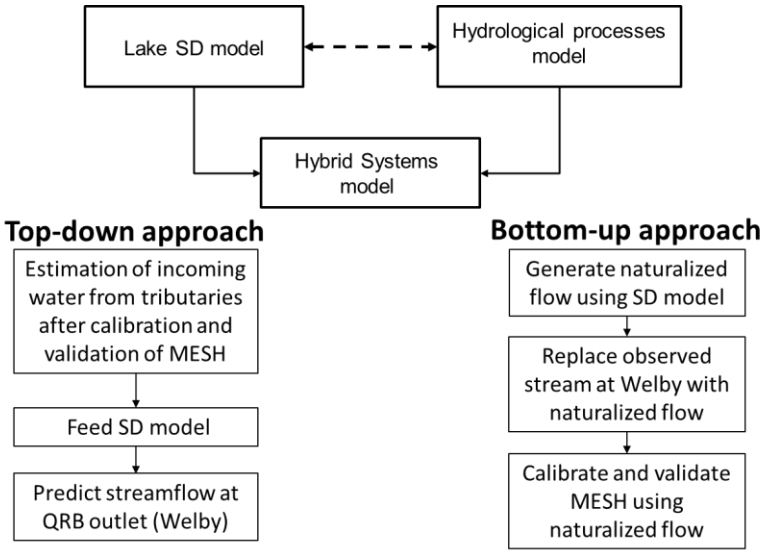

Figure 3.19: Hybrid modelling framework and approaches

Two potential approaches are shown in Figure 3.19, which are 'Top-down' approach and 'Bottom-up' approach. These two approaches are discussed in the following two sections.

3.5.1 'Top-down' Approach

The 'Top-down' approach is estimating outflows from the tributaries of the Qu'Appelle River, feeding the estimated outflow to the lake SD model, and finally route the water using the lake SD model to predict the streamflow at the outlet. Estimation of outflow from the tributaries was simulated by MESH as it was developed in this study to estimate runoff in prairie watersheds and the lake operation was simulated by the SD model. The challenging part was

to transfer information between two models (MESH to the SD model) in different platforms, and this was simulated by developing *R* and *BASH* scripts for this specific purpose. The runoff generation algorithm LATFLOW, that was identified as a suitable algorithm to model prairie runoff generation processes (explained in Chapter-4) was selected to be used in MESH for the hybrid model. The 'top-down approach required developing the MESH model in sub-basin scale in order to estimate outflow from the tributaries (headwaters). In this study, two possible options were implemented-

I. Setting up a model for the QRB and optimize for multiple sub-basins based on multi-site calibration;

II. Setting up individual models for each sub-basin and optimize them separately.

Option-I assumes that the hydrological properties and land surface heterogeneity are identical across all the watersheds of QRB. However, if this underlying assumption appears to be invalid, a more detailed approach is required, which is Option-II. The latter approach is complex and considers different patterns of hydrological properties and land surface heterogeneity across different sub-basins of the QRB. The final step of the top-down approach is to feed the estimated outflow to the lake SD model and predict the outflow at the outlet.

Model Setup, Calibration and Validation

The first step of the MESH model development was to delineate the basin and sub-basins and define the drainage properties using DEM and landuse information. The gross drainage area of the QRB system is about 50,900 km^2 and four distinct landuse types were identified in this system, which are crop, grass, forest, and non-contributing wetland. The last one is not a generic landuse type used in a hydrological model, however, non-contributing wetland is a unique surface type in the prairies, which is primarily wetlands and do not act as an active

contributor to the nearest stream until a temporary connection evolves. Non-contributing wetland was used as a separate landuse in this study, because this area exhibits different hydrological properties compared to conventional landuse types (such as, crop and grass) and it adds further meaningful detailing in the drainage definition for a prairie watershed. Figure 3.20 shows the delineated landuse types used in the QRB. The purpose was to estimate outflows from each sub-basin of the QRB by a multi-site calibration approach.

The modelling approach for Option-II is different. Here 10 individual sub-basins were selected based on the availability of measured streamflow at the respective outlet. These sub-basins were simulated separately and 10 separate MESH models were developed for these individual watersheds (Figure 3.21) using similar process to that adopted for the Kronau Marsh watershed. As the Kronau Marsh watershed is a sub-basin and a developed MESH model was already available (discussed in chapter - 4), the remaining nine sub-basins were considered for model development. The area of the selected sub-basins is given in Table 3.5. Among all the sub-basins the Moose Jaw River watershed is the largest and has a significant impact over the entire QRB.

For MESH, all the models (QRB for Option-I and 10 sub-basins for Option-II) were run from October 2002 to October 2014. The first two years (October 2002 – October 2004) were used as spin-up period, October 2004 to October 2008 was selected as a calibration period, and the remaining time period was used as validation period (October 2008 - October 2014). The modelling time step was based on the available temporal resolution of meteorological data (hourly time step). Output information was stored at a daily time step in order to match the temporal resolution of the observed streamflow data. All the models were setup using grids of $0.1^{o} \times 0.1^{o}$ (approximately 10 km × 10 km) as shown in Figure 3.20.

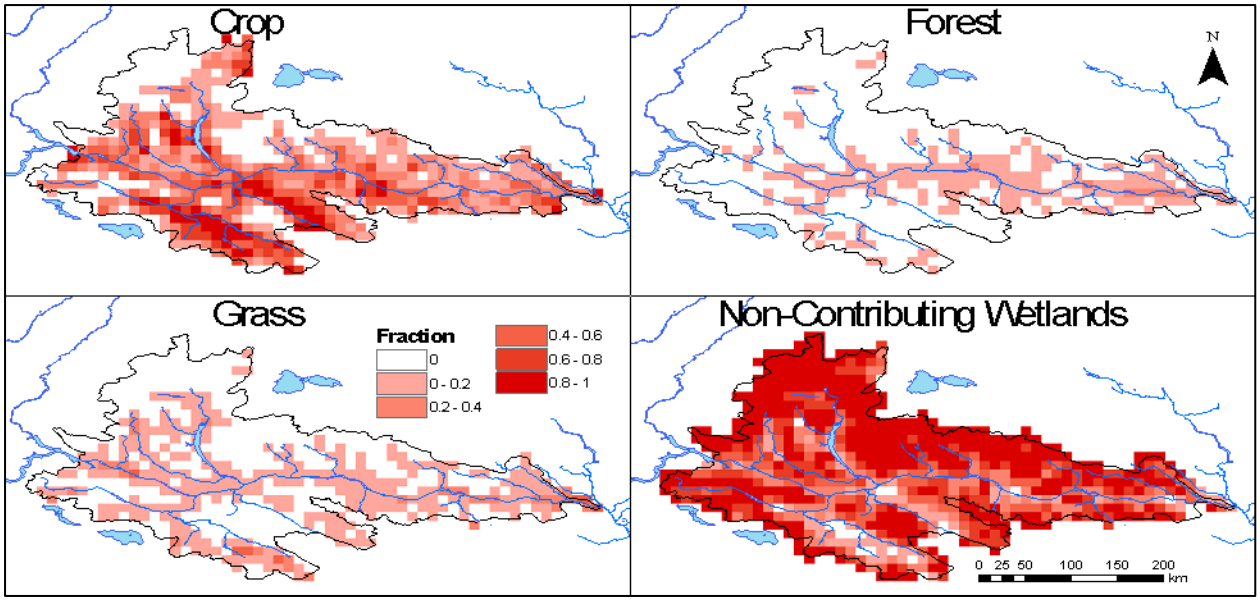

Figure 3.20: GRU discretization using landuse type

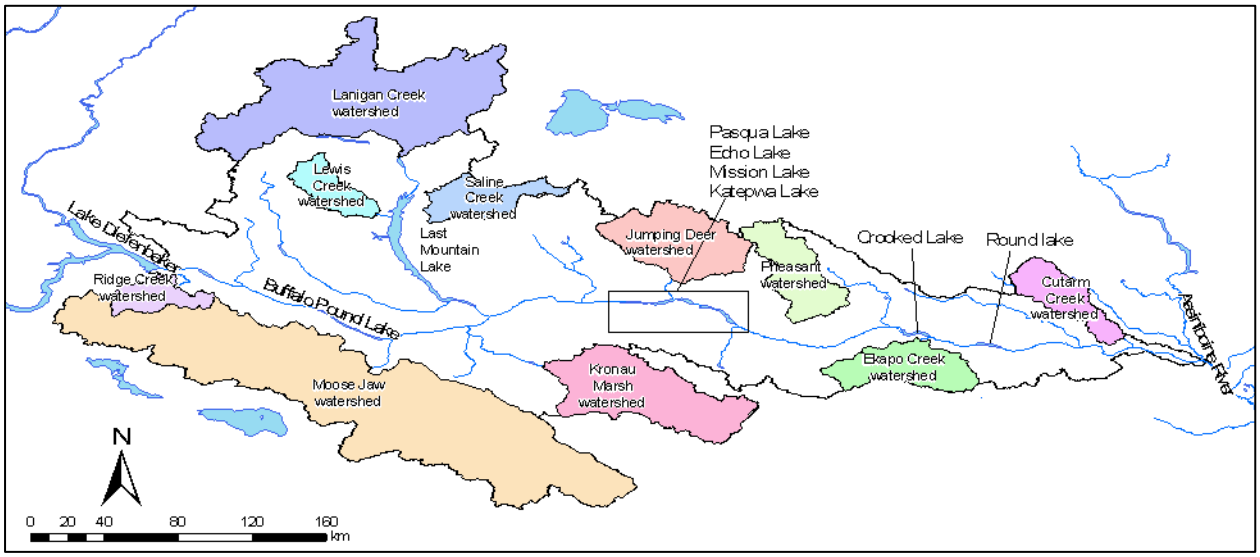

Figure 3.21: The locations of ten selected sub-basins of QRB

Table 3.5: Selected gauged sub-basins for MESH modelling and corresponding area

Name	Drainage area (km^2)	Name	Drainage area (km^2)
Moose Jaw River	9,230	Lewis Creek	593
Kronau Marsh	2,340	Ridge Creek	541
Ekapo Creek	1,138	Pheasant Creek	1,116
Cutarm Creek	845	Jumping Deer Creek	1,675
Saline Creek	813	Lanigan Creek	4,620

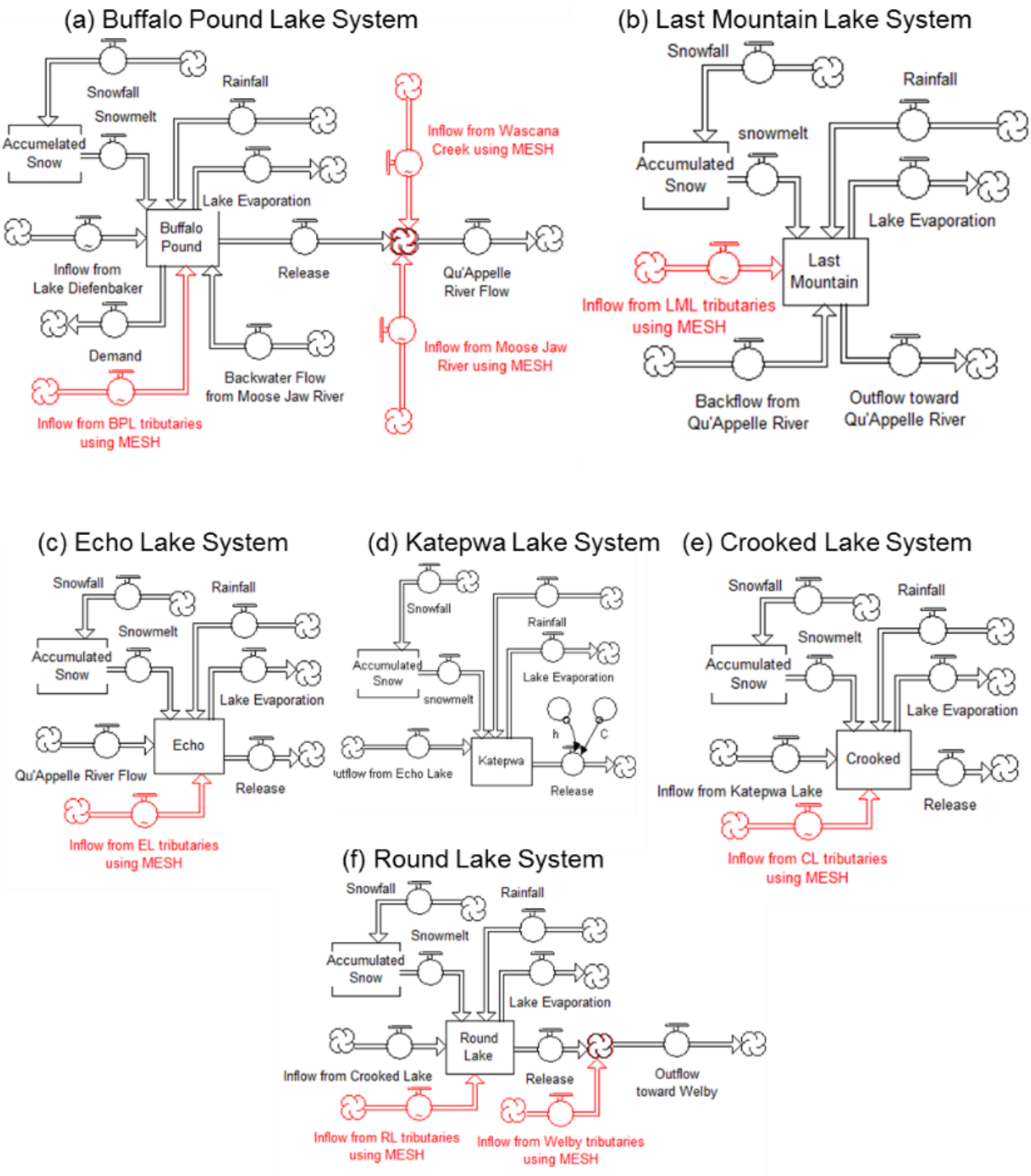

Figure 3.22: The lake SD model used for the hybrid model. The flows with red color indicate predicted inflows using MESH. The accounted area for the tributaries, Moose Jaw River, and Wascana Creek is illustrated in Figure 3.23

The lake SD model for the hybrid structure (Figure 3.19) is the SD model discussed in section 3.4.2 modified to consider flows in the tributaries that were extracted at specific 'pick up' points (Figure 3.23) using MESH model. The 'pick up' points were fixed at the outlet of each sub-system of QRB (i.e., BPL, LML, EL, KL, CL, and RL). Here 'pick up' points indicate the

outlet of individual tributaries of the QRB, where the outflow from the tributaries are fed into the lake SD model as inflow. This lake SD model was suitable for the Option-I of 'Top-down' approach mentioned above. Schematics to illustrate the input of flows estimated using MESH into the lake SD model is presented in Figure 3.22 and the accounted area for individual tributaries is shown in Figure 3.23. For Option-II, the measured streamflow of each sub-basin that was used in the lake SD model (Figure 3.15) was replaced with the simulated streamflow generated using MESH model for individual sub-basins.

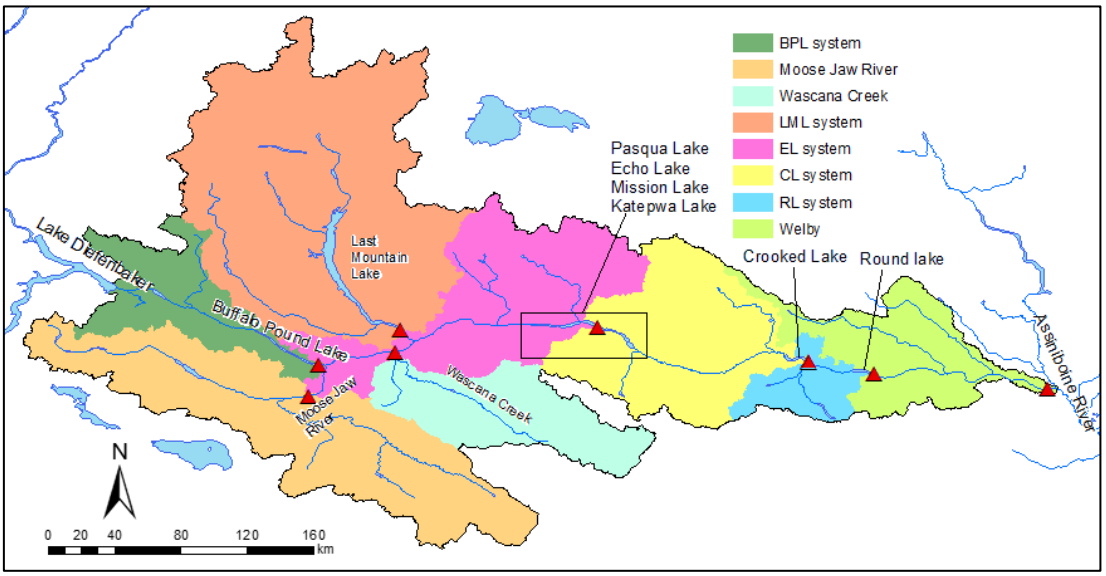

Figure 3.23: Sub-basins of QRB used in this study. Red triangles indicate the 'pick up' points for individual systems. 'Pick up' points are the location of outlet of individual sub-basins of QRB, which are selected as input for the lake SD model.

Calibration of the hybrid model required a two-fold optimization technique (Figure 3.24). First, MESH model was optimized using a multi-objective optimization technique. For Option-I of 'Top-down' approach, the following objective functions were used-

$$Maximize, Z_1 = \sum_{i=1}^{n=10} NSE_i\,, \qquad where\ \infty < Z_1 < 10 \qquad (3.26)$$

$$Maximize, Z_2 = \sum_{i=1}^{n=10} \mathrm{Log}(\mathrm{NSE}_i)\,, \qquad where\ 0 < Z_2 < 10 \qquad (3.27)$$

Here 10 sites were selected for model calibration (where measured streamflow was available). This multi objective optimization was carried out using the Pareto Archived Dynamically Dimensioned Search ($PADDS$) (Asadzadeh and Tolson, 2009) algorithm. Next, the second optimization process was conducted for the lake SD model. Similar to the optimization technique used for the SD model discussed in section 3.3.3, a single objective optimization technique (DDS automatic search algorithm) was used to maximize NSE (equation 3.10). It was understood from a number of preliminary model runs that the simulation of low flows were mostly satisfactory all the time and emphasising on simulation of high flows was a priority, which is why a single objective optimization technique was used. The model validation was similar to that used in section 3.3.4.

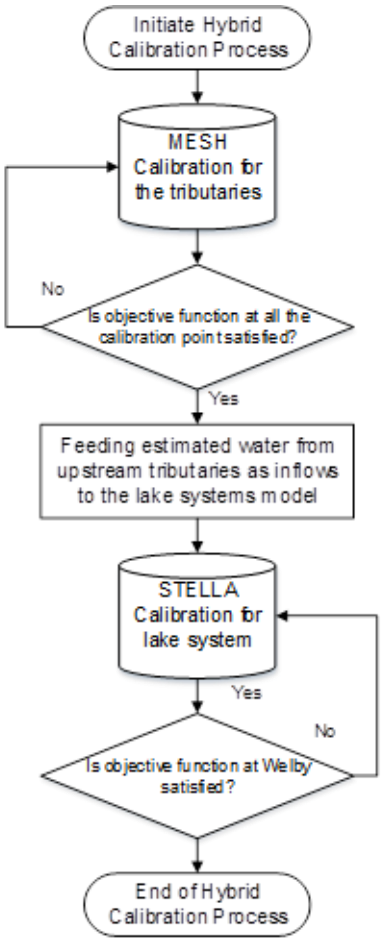

Figure 3.24: Hybrid optimization process involving MESH and STELLA.

Initial parameter values and calibration ranges, used in the MESH modelling part of the hybrid model (Table 3.6), were decided based on CLASS technical documentation (Verseghy, 2011), literature (Dingman, 2002, Davison et al., 2016, 2006, Haghnegahdar et al., 2015, 2014; Mekonnen et al., 2014) and expert opinion in case of unavailability of information from literature, which was similar approach discussed in section 3.3.3.

Table 3.6: Calibration parameter range used in 'Top-down' and 'Bottom-up' approach of hybrid model

Description	Units	GRU	Lower limit	Upper limit	Source
River roughness factor that incorporates a channel shape and width to depth ratio as well as Manning's n	[m0.5s-1]	-	0.3	2	User defined
Surface storages connectivity coefficient or shape factor	[]	forest	0.01	30	Mekonnen (2014)
		NCW	0.01	5	
		crop	0.01	30	
		grass	0.01	30	
Maximum surface storage capacity	[m]	forest	0.01	5	

Description	Units	GRU	Lower limit	Upper limit	Source
		NCW	0.01	10	Mekonnen (2014)
		crop	0.01	5	
		grass	0.01	5	
Maximum leaf area index	[]	forest	2	10	Verseghy (2011)
		NCW	4	6.5	
		crop	2	4	
		grass	2	4	
Minimum leaf area index	[]	forest	1.6	10	Verseghy (2011)
		grass	2	4	
		NCW	2	4	
Annual maximum canopy mass	[kg/m2]	forest	15	50	Verseghy (2011)
		crop	2	5	
		grass	1.5	3	
		NCW	1.5	3	
Annual maximum rooting depth	[m]	forest	1	5	Verseghy (2011)
		crop	1.2	5	
		grass	0.2	5	
		NCW	0.2	5	
Natural log of roughness length	[]	forest	-0.22	0.4	Verseghy (2011)
		crop	-2.53	-1	
		grass	-1.66	-1	
		NCW	-1.66	-1	
Average visible albedo when fully-leafed or of the land cover	[]	forest	0.02	0.04	Verseghy (2011)
		crop	0.04	0.08	
		grass	0.04	0.08	
		NCW	0.04	0.08	
Average near-infrared albedo when fully-leafed or of the land cover	[]	forest	0.13	0.33	Verseghy (2011)
		crop	0.26	0.46	
		grass	0.26	0.46	
		NCW	0.26	0.46	
Limiting snow depth below which coverage is less than 100%	[m]	forest	0.05	0.3	User defined
		NCW	0.05	0.3	
		crop	0.05	0.3	
		grass	0.05	0.3	
Maximum water ponding depth for snow covered areas	[m]	forest	0.05	0.25	User defined
		NCW	0.05	0.25	
		crop	0.05	0.25	
		grass	0.05	0.25	
Maximum water ponding depth for snow free areas	[m]	forest	0.05	0.25	User defined
		NCW	0.05	0.25	
		crop	0.05	0.25	
		grass	0.05	0.25	
Manning's n for overland flow	[ms-1/3]	forest	0.01	0.05	Dingman (2002)
		crop	0.01	0.05	
		grass	0.01	0.05	
		NCW	0.01	0.05	
Permeable depth of the soil column	[m]	forest	0.01	4.1	User defined
		crop	0.01	4.1	
		grass	0.01	4.1	
		NCW	0.01	4.1	
Saturated surface horizontal soil conductivity	[ms-1]	forest	0.0001	0.01	User defined
		crop	0.0001	0.01	
		grass	0.0001	0.01	
		NCW	0.0001	0.01	
Drainage density, equal to the length of the stream divided by area drained by the stream	[km/km2]	forest	50	120	User defined
		crop	50	120	
		grass	50	120	
		NCW	50	120	

Description	Units	GRU	Lower limit	Upper limit	Source
Fraction of the saturated surface soil conductivity moving in the horizontal direction	[]	forest	0	0.8	User defined
		crop	0	0.8	
		grass	0	0.8	
		NCW	0	0.1	
Soil drainage index. Index 1 allows the soil physics to determine drainage and index 0 completely impede drainage	[]	forest	0	1	User defined
		crop	0	1	
		grass	0	1	
		NCW	0	0.1	
Percent content of sand in Layer-1		forest	5.8	77.8	User defined
Percent content of sand in Layer-2			6.9	72.1	
Percent content of sand in Layer-3			7.5	76	
Percent content of clay in Layer-1			6.4	78.4	
Percent content of clay in Layer-2			10.8	75.6	
Percent content of clay in Layer-3			12.2	73.8	
Percent content of sand in Layer-1		NCW	2	75	User defined
Percent content of sand in Layer-2			2	75	
Percent content of sand in Layer-3			2	75	
Percent content of clay in Layer-1			20	80	
Percent content of clay in Layer-2			20	80	
Percent content of clay in Layer-3			20	80	
Percent content of sand in Layer-1		crop	5.8	77.8	User defined
Percent content of sand in Layer-2			6.9	72.1	
Percent content of sand in Layer-3			7.5	76	
Percent content of clay in Layer-1			6.4	78.4	
Percent content of clay in Layer-2			10.8	75.6	
Percent content of clay in Layer-3			12.2	73.8	
Percent content of sand in Layer-1		grass	5.8	77.8	User defined
Percent content of sand in Layer-2			16.9	72.1	
Percent content of sand in Layer-3			7.5	76	
Percent content of clay in Layer-1			6.4	78.4	
Percent content of clay in Layer-2			10.8	75.6	
Percent content of clay in Layer-3			12.2	73.8	
Height of vegetation	[m]	crop	0.05	0.3	PBSM Documentation
		grass	0.2	0.8	
		NCW	1	2	
		forest	2	20	

3.5.2 'Bottom-up' Approach

The 'bottom-up' approach is development of a single hydrological model for the QRB using the naturalized flow at Welby instead of the measured flow. Naturalized flows are adjusted historical streamflow data by removing the effects of water resources management (Kim and Wurbs, 2011). It is formulated as-

$$Naturalized\ flow = Measured\ flow + Flow\ adjustment \quad (3.28)$$

$Flow\ adjustment$ is computed by subtracting regulated flows from naturalized flows and adding storage shortages and diversion shortages associated with reservoirs. In this study, the

lake SD model was used to generate naturalized flow for the Qu'Appelle River. The process included (i) using the measured historical streamflow from the tributaries in the lake SD model, (ii) removing the hydraulic structures or weirs used in the lake SD model as control structure to ensure that streamflow is not obstructed by any human intervention, and (iii) estimating the streamflow at the outlet, which is assumed as naturalized streamflow. The removal of the weir was achieved by lowering the weir level to the bed level and there was no diversion from any of the lakes of the QRB (water withdrawal from municipal and agricultural use was already considered in the lake SD model). Using the naturalized flow in a hydrological model suggests that the river is not interrupted by any control or diversion structure and the amount of water generated from the headwater, is reaching the outlet with a natural time lag. The bottom-up scenario is not natural and depends on the processes of generating naturalized flow.

The naturalized flow at Welby enables the possibility to estimate the parameters for MESH model of the QRB without the effect of these reservoirs. Estimation of parameters using this approach can exhibit a different picture for the tributaries, because the approach prioritizes the streamflow prediction performance of Welby, which may lead to different estimated outflows from the tributaries leading to an inaccurate hydrological scenario of the tributaries. In simple words, the accuracy of the simulated streamflow at Welby comes at a cost of accuracy tradeoff with the headwater tributaries. The Bottom-up approach creates a natural condition for QRB, not actual condition, and for this reason the estimated parameter values are suitable for a hypothetical natural condition. In order to achieve the actual flow from naturalized flow, a relationship between actual flow and naturalized flow is required, which is easily formulated using the lake SD model. Generation of naturalized flow using this approach carried forward the errors and uncertainties associated with the lake SD model. Naturalized flow of the Qu'Appelle River from any other source was unavailable, and for this reason the performance and accuracy of naturalized flow cannot be tested.

Model Setup, Calibration and Validation

The model setup for the bottom-up approach was similar to the top-down approach, however, instead of considering sub-basins, the entire QRB system was considered for calibration of MESH. Before calibration of MESH, the measured streamflow at Welby was replaced with the generated naturalized flow. During the peak flow season, a certain portion of water diverts into the Last Mountain Lake (LML) system from the Qu'Appelle River. This is a natural phenomenon and the arrangement of the lakes allows this diversion. As water is not withdrawn from the LML system, this diversion is considered as temporary flood dampening. Figure 3.25 shows the generated naturalized flow for the QRB at Welby. Distinct peaks is observed occurring just before measured peak flow. For the flood of year 2011, it is observed that the combined lake effect lowers the peak flow from 400 m^3/s to 250 m^3/s (Figure 3.25c). Similar pattern is observed for the peak flow of year 2006 and 2014 flood.

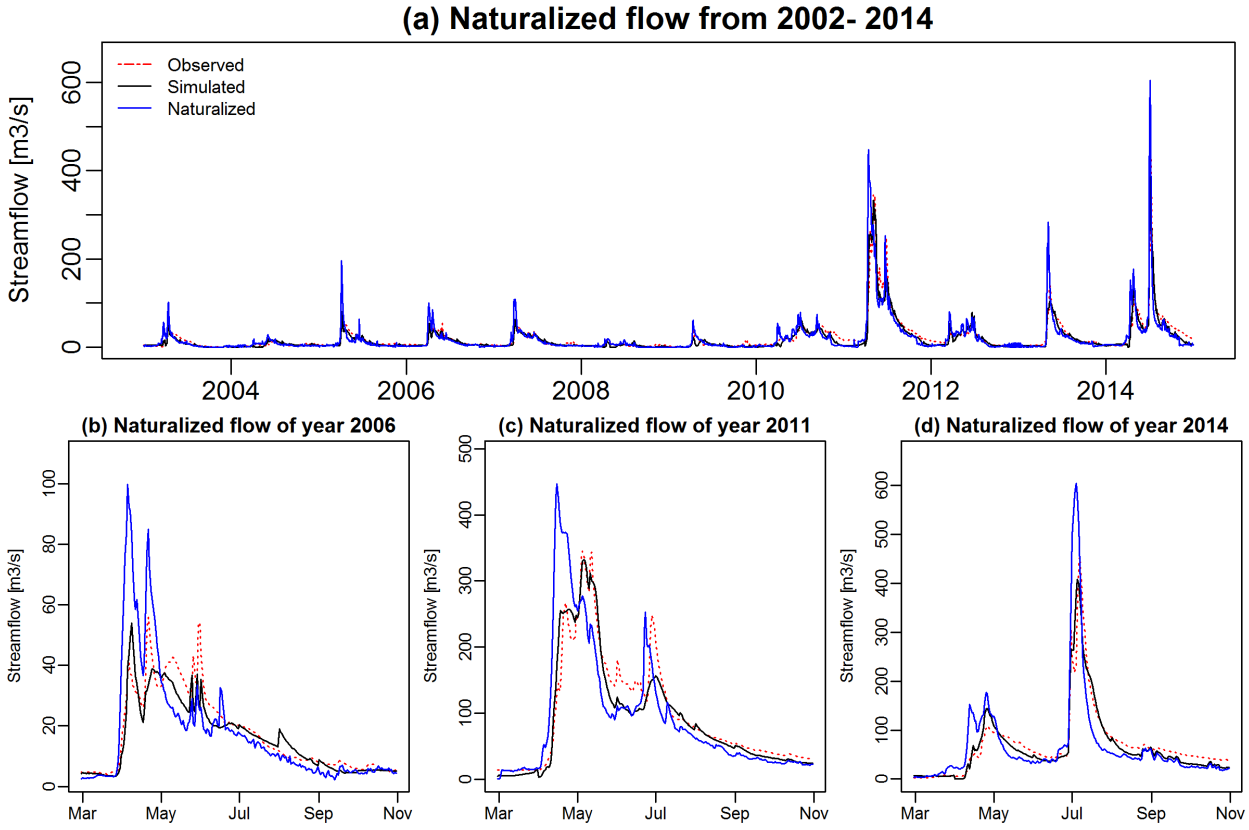

Figure 3.25: (a) Observed, simulated and generated naturalized flow. Flow simulation accounts for combined lake effects and naturalized flow was generated by removing all the obstruction in the river. Figures (b), (c), and (d) magnify all types of flow at year 2006, 2011, and 2014, respectively.

Meteorological data, watershed delineation, and number of calibration parameters for the bottom-up approach was maintained as the same for the top-down approach. The multi-objective optimization technique Pareto Archived Dynamically Dimensioned Search ($PADDS$) was used to maximize objective functions NSE and $Log(NSE)$.

3.6 Parameter Identifiability and Sensitivity

Parameter identifiability is a way to determine how well the system is parameterized by the model, which is implicitly assessed by the performance of the model (Remesan and Mathew, 2015). It enables the modeller to identify a range for the parameters within which, the model is expected to generate a behavioral response. For a physical system, determining appropriate parameterization for the right model equations is difficult and also accounts for different types of uncertainties. Poor parameter identifiability indicates that the solution contains considerable uncertainty in the model outputs and it might be inappropriate to relate the optimized parameter values with the observable characteristics of the basin (Vrugt et al., 2005). The method used for parameter identifiability in this research is straightforward. Behavioral sets of parameters were identified using a threshold that was fixed based on different guidelines and literature. The actual values of the parameters then undergo a normalization process to visualize their comparative band of behavioral value. Box plots were used in this research to visualize the median, first quadrant, third quadrant, and the outliers. A narrow band of first and third quadrant of the box plot of a particular parameter is a more identifiable nature while a wider band is unidentifiable nature of a parameter.

The definition of sensitivity is ambiguous and performing sensitivity analysis is often a challenging task to achieve with a limited computational budget, therefore, the objective and intended definition of sensitivity changes in different context of research (Razavi and Gupta, 2015). In a simple term, sensitivity of a parameter is referred to as the pattern of model response

with respect to the change of parameter value. The question regarding the importance and justification of a particular parameter is showed using a comprehensive sensitivity analysis. It is possible to analyse a set of parameters considering their local and global effect using different techniques of sensitivity analysis, which are referred to as local sensitivity and global sensitivity. Global sensitivity techniques are often preferred over local ones, because they illustrate an integrated view of the model response due to the change of the value of a parameter and the associated effect of other parameters. To assess parameter sensitivity, a simple technique was employed here, which is known as 'Elementary Effect Test (EET)' or alternatively 'Morris Method' of SA (Morris, 1991). This is a derivative-based global SA approach, meaning that the search for a parameter sensitivity is conducted using the derivatives of the output with respect to the parameter, which is dependent on the step size (or the distance between two subsequent parameter values) in the parameter space. The SAFE (Sensitivity Analysis For Everybody) toolbox (Pianosi et al., 2015), a MATLAB-based toolbox for SA, was used in this study. The term 'Elemental Effect' refers to an average of derivatives over the space of parameter (Saltelli et al., 2008). If a model consists of k independent parameters $X_i, i = 1,2, \dots, k,$ which vary across p levels. The parameter space is a discretized p-level grid Ω. For a given value of $\boldsymbol{X}$, the elementary effect of the i^{th} parameter is defined as

$$EE_i = \frac{[Y(X_1,X_2,\dots,X_{i-1},X_i+\Delta,\dots,X_k)-Y(X_1,X_2,\dots,X_k)]}{\Delta} \tag{3.29}$$

Here, Y is the response variable (streamflow) and Δ (or step size) is a value in $\{\frac{1}{(p-1)}, \dots, 1 - \frac{1}{(p-1)}\}$ where p is the number of levels and a convenient choice for p is an even number (often ranges from 4 to 8) and $\Delta = p/2(p-1)$. Fixing Δ using this technique has an advantage to maintain a certain symmetric treatment of parameters although the design sampling strategy does not guarantee equally probable sample (Campolongo et al., 2007; Morris, 1991). EET is a One-At-a-Time (OAT) based SA and the distribution of elementary effects associated with

the input parameters are obtained by Latin-hypercube OAT sampling technique (Saltelli et al., 2008). EET uses two separate sensitivity measures to identify sensitivity, namely μ_i^* and σ_i. The μ_i^* is formulated as-

$$\mu_i^* = \frac{1}{r}\sum_{i=1}^{r}|EE_i| \tag{3.30}$$

where, EE_i is individual elementary effect of the ith parameter, and r is total number of elementary effects. The sensitivity measure σ is the standard deviation of EE. To estimate $\mu_i^*$and σ_i , sampling of r elementary effects via an efficient construction of r trajectories of $(k+1)$ points in the parameter space are suggested (Campolongo et al., 2007; Morris, 1991), and thus total cost of the experiment is $r(k+1)$. The range of $\mu_i^*$and σ_i are zero to infinity with zero indicating no elemental effect and large values indicating significant effect. The sensitivity of a particular parameter is determined by looking at the value of μ_i^*. A high value of μ_i^* indicates high sensitivity and vice versa. The value of σ_i estimates the ensemble of the elementary effects of a parameter due to interactions with other parameters. A low value of σ_i indicates that the elementary effect of a parameter is almost independent of the values taken by the other parameters, because the value of an elementary effect is strongly affected by the choice of the other parameters (Saltelli et al., 2008).

Chapter 4: Simulation of Prairie Runoff Processes

Prairie runoff processes are complex in nature because of the existence of non-contributing drainage area and dynamically connected millions of depressions, which create a complicated surface storage connectivity scenario in the prairie land surface. In this chapter, a comparative study of the performance of existing and newly proposed runoff generation algorithms was conducted.

4.1 Model Simulation Results

MESH Model simulation results are analyzed using the time series and scatter plot of the model outputs. Figure 4.1 shows the outcome of the optimization process of the three watersheds in the form of Pareto front of non-dominated solutions. Multi-objective optimization uses error indicators of NSE and $Log(NSE)$, which show the predictive capability of the model in both high flow and low flow conditions. To find behavioral solutions, a threshold for the behavioral pattern was set to be > +0.50 (Moriasi et al. 2007). For low flow estimation, no guidelines were found in the literature, which leads to an assumption of a reasonable $Log(NSE)$ threshold of +0.30. According to the behavioral criteria optimization results satisfying NSE > +0.50 and $Log(NSE)$ > +0.30 were considered as behavioral solutions and considered for further analysis. Figure 4.1a shows the Pareto front of multi-objective optimization using different runoff generation algorithms in the White Gull Creek watershed. Non-dominated NSE values exhibit a narrow band compared to $Log(NSE)$, suggesting similar capability of high flow estimation of all the runoff generation algorithms, however, LATFLOW exhibits slightly improved *NSE* compared to the others. All the runoff generation algorithms show a wide band of $Log(NSE)$ optimized solutions, suggesting the absence of tradeoff between improving high and low flows. Based on the results shown, it was understood that WATROF is suitable to predict streamflow in White Gull Creek watershed. The proposed algorithm LATFLOW

provides good results, indicating that it could be considered as an alternative runoff generation algorithm even in non-prairie watersheds.

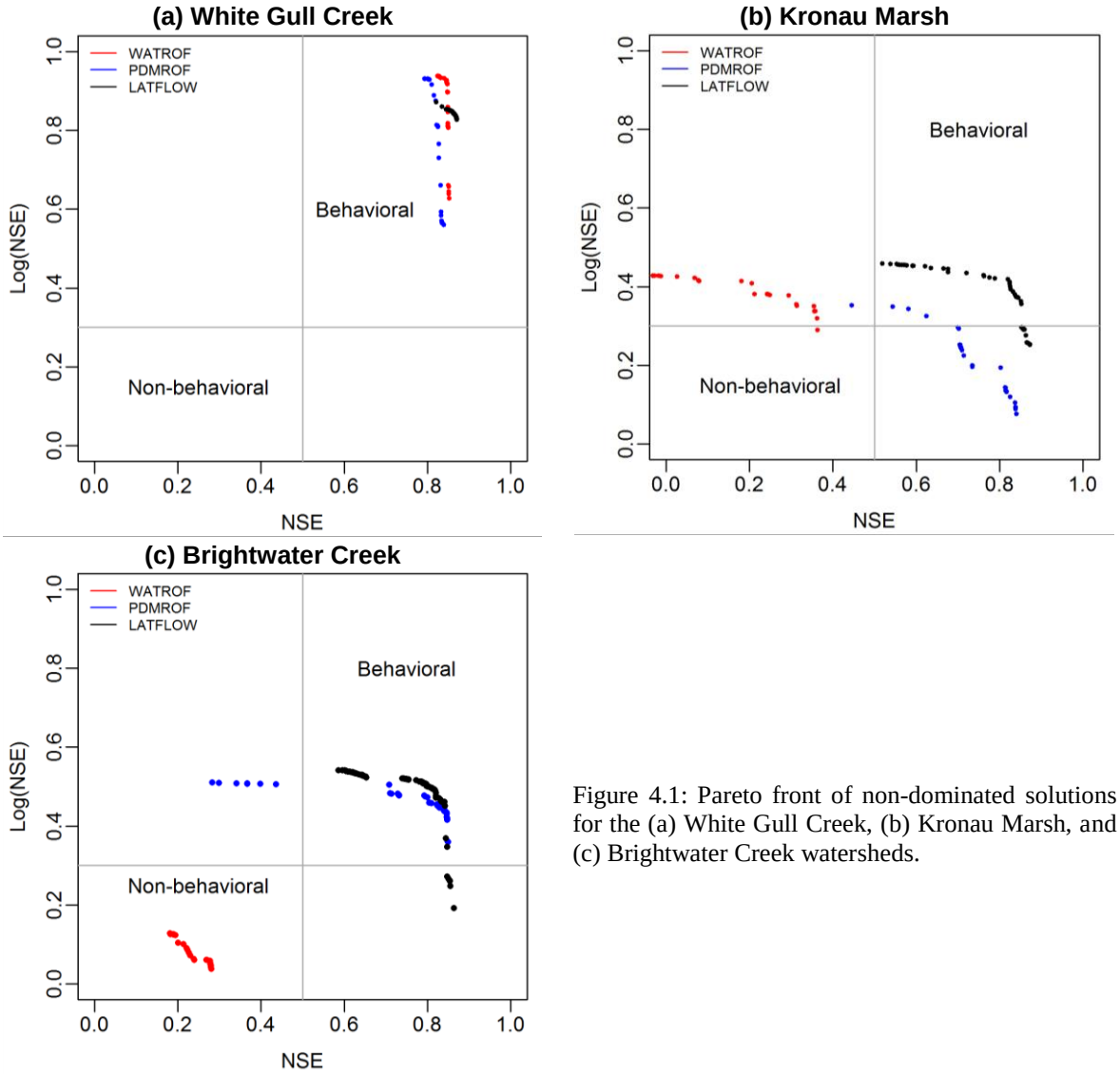

Figure 4.1: Pareto front of non-dominated solutions for the (a) White Gull Creek, (b) Kronau Marsh, and (c) Brightwater Creek watersheds.

Figure 4.1b and Figure 4.1c shows the Pareto front of multi-objective optimization using different runoff generation algorithms in the Kronau Marsh and Brightwater Creek watersheds, which are prairie watersheds. LATFLOW shows better convergence towards the perfect solution and WATROF fails to exhibit behavioral pattern. In the context of PDMROF and LATFLOW distinction, a clear improvement is observed for the Kronau Marsh watershed, however, both PDMROF and LATFLOW exhibit similar convergence for the optimization of the Brightwater Creek watershed, although LATFLOW converges better than PDMROF. WATROF, being a traditional rainfall-runoff algorithm, is unable to simulate fill-spill type

runoff propagation and it is inefficient for addressing the surface storage connectivity as it assumes complete connectivity within a grid cell. For this reason, WATROF is not considered in the comparison of runoff generation algorithms for the prairie watersheds (i.e. Kronau Marsh and Brightwater Creek watersheds). A detailed comparison between WATROF and PDMROF for prairie watersheds is found in Mekonnen et al. (2014). Detailed discussions on the best performing models and results related to individual modelling components are presented in the following subsections. Estimated parameter values for individual watersheds along with lower and higher limits of parameter values considered for calibration is found in Appendix B.

4.1.1 Streamflow

In the comparison study of runoff generation algorithms, high flow estimation capability is prioritized over low flow estimation capability, which leads to the selection of the behaving optimization solutions with maximum high flow estimation capability. This is a specific optimized solution is selected, which has highest NSE value with $Log(NSE) \geq +0.30$. The simulated and observed streamflow for the Boreal Plain White Gull Creek watershed for each configuration are presented in Figure 4.2. The values of performance measures are also provided in the figure. For the calibration period, all three MESH configurations show $NSE >$ +0.80, which is well calibrated models. Validation NSE varies in different model configurations and it appears that WATROF shows the highest validation NSE (= +0.675) compared to LATFLOW (NSE = +0.569) and PDMROF (NSE = +0.365). Validation of PDMROF appears to be unsatisfactory ($NSE <$ +0.50). According to the guidelines of Moriasi et al. (2007), $PBIAS$ of all the configurations are satisfactory (< 25%). However, Figure 4.2a suggests that WATROF is able to model high flow accurately and both PDMROF and LATFLOW exhibit low accuracy in estimating high flow during validation. The results indicate that the underlying concept of WATROF is suitable to predict streamflow in the White Gull Creek watershed.

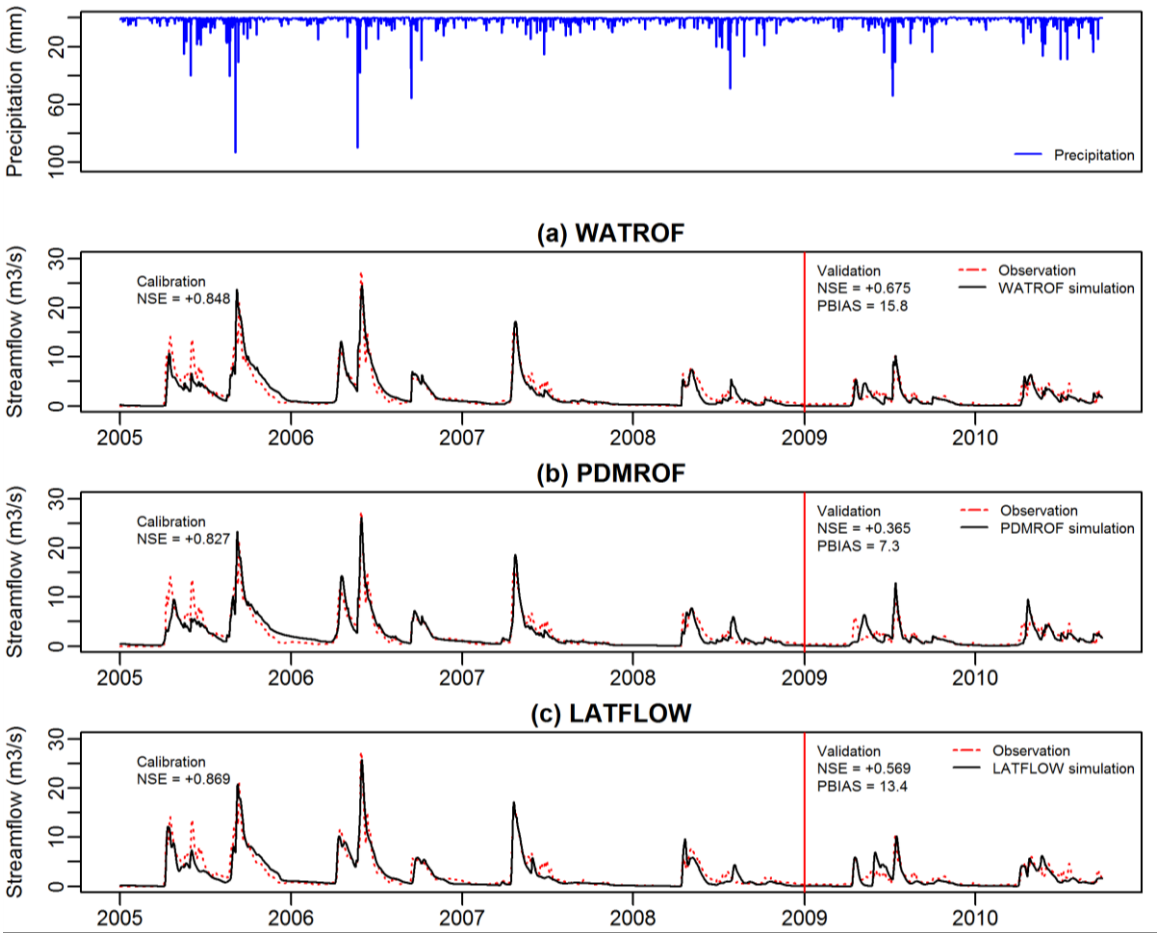

Figure 4.2: Observed and simulated hydrographs for White Gull Creek watershed using (a) WATROF, (b) PDMROF, and (c) LATFLOW configuration.

Figure 4.3 shows the simulated and observed streamflow for PDMROF and LATFLOW configurations in the Kronau Marsh prairie watershed. For the Kronau Marsh watershed, LATFLOW configuration shows the highest NSE values (+0.849 and +0.668) in calibration and validation followed by PDMROF (+0.704 and +0.179). The timing of spring peak flow is well captured in both LATFLOW and PDMROF configurations in both calibration and validation periods. $PBIAS$ in the validation period appears to be unsatisfactory (> 25%) for both the configurations (according to Moriasi et al. (2007), satisfactory PBIAS threshold is ±25%). Figure 4.3b suggests that LATFLOW can successfully simulate flows > 2 m^3/s and PDMROF shows a consistent bias simulating such flows. If flows less than $2m^3/s$ are discarded from the time series, $PBIAS$ for LATFLOW becomes -17.7%, which is considered as satisfactory. However, $PBIAS$ for PDMROF also improves (-36.4%) after discarding the low

flows from the time series, but it is still unsatisfactory suggesting that using PDMROF results in a consistent underestimation of streamflow in the validation period. The underlying concept of LATFLOW is found to be suitable to predict streamflow for the Kronau Marsh watershed.

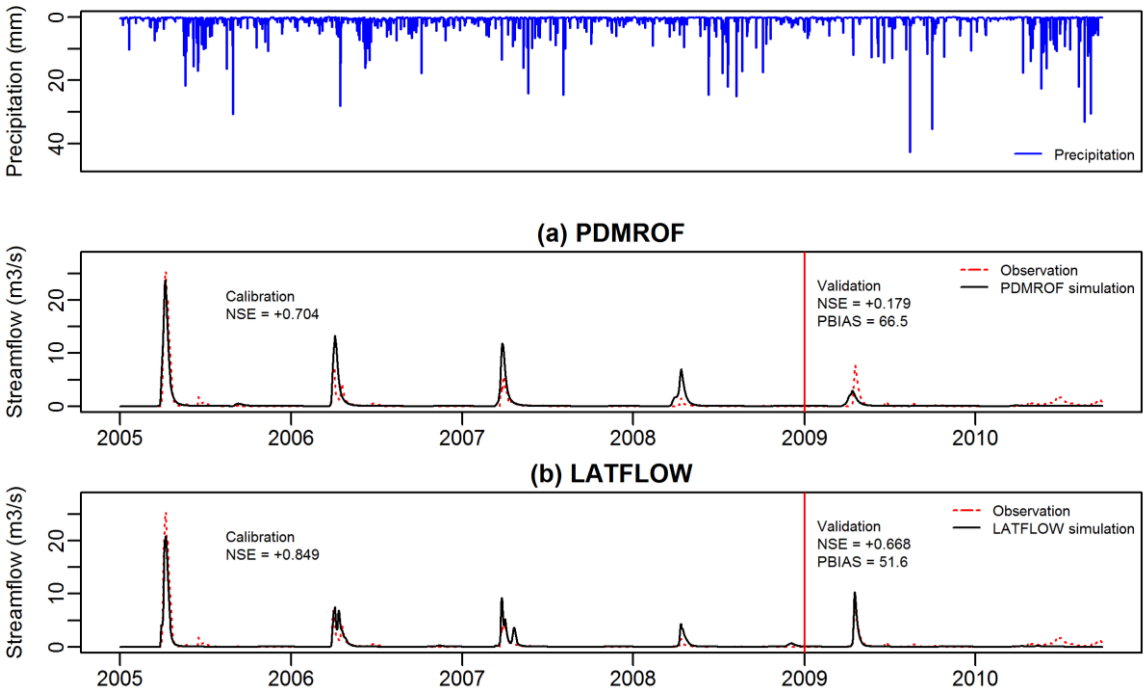

Figure 4.3: Observed and simulated hydrographs for Kronau Marsh watershed using (a) PDMROF, and (b) LATFLOW configuration.

Figure 4.4 shows the simulated and observed streamflow for PDMROF and LATFLOW configurations in the Brightwater Creek prairie watershed. For the Brightwater Creek, LATFLOW configuration shows the highest NSE value (+0.848 and +0.573) in calibration and validation, respectively, followed by PDMROF (+0.829and +0.549). The timing of spring peak flow is well captured using both LATFLOW and PDMROF. $PBIAS$ in the validation period appears to be unsatisfactory (> 25%) for both the configurations (Figure 4.4c). However, the magnitude of streamflow during validation period is very low and most of the time there is no flow in the stream. Both PDMROF and LATFLOW are showing similar performance in streamflow simulation of the Brightwater Creek watershed. Based on the results for both prairie watersheds, the underlying concept and parameterization of LATFLOW is likely to be suitable to predict streamflow in the Kronau Marsh and Brightwater Creek watersheds efficiently.

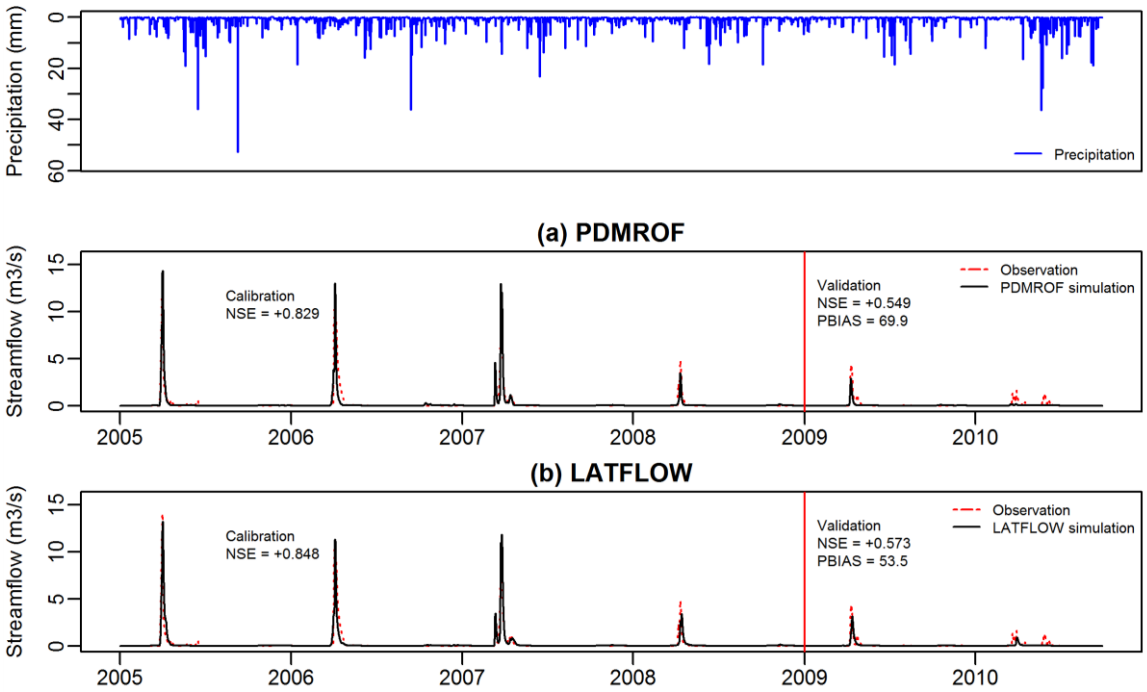

Figure 4.4: Observed and simulated hydrographs for Brightwater Creek watershed using (a) PDMROF and (b) LATFLOW configuration.

To understand how the design of PDMROF and LATFLOW affect the runoff transformation into streamflow, generation of surface runoff and interflow need to be analyzed. Figure 4.5 shows the differences between PDMROF and LATFLOW in runoff generation processes in the prairie watersheds (Kronau Marsh watershed) for a chosen hydrograph during the snowmelt period. It is observed that PDMROF and LATFOW are able to simulate the snowmelt event efficiently. The snowmelt event is slightly underestimated by both PDMROF and LATFLOW (Figure 4.5). Underestimation of the peak flow by both algorithms could be attributed to the underestimation of soil moisture prior to the preceding winter by MESH during simulation. LATFLOW is able to represent the recession limb of the peak hydrograph more accurately as there is a significant contribution of sub-surface flow. The hydrograph obtained using PDMROF appears to be narrower than that obtained using LATFLOW, which is the result of the assumed no contribution of subsurface flow. In most of the measured streamflow hydrographs during snowmelt, a smaller peak or ‘spike’ is seen in the recession limb (Figure 4.5) that may be induced by interflow due to snowmelt infiltration. The efficiency of simulating the peak flow by PDMROF and LATFLOW is comparable and depends on the estimation of

drainage and snow related parameters of MESH. However, the second 'spike' is often not simulated by PDMROF because of the absence of interflow parameterization. LATFLOW is able to improve the representation of the recession limb of the peak flow hydrograph. Although the efficiency of simulating streamflow by either PDMROF or LATFLOW depends on the parameter estimation process, the physical representation of runoff processes appears to be more reasonable in LATFLOW when compared to PDMROF.

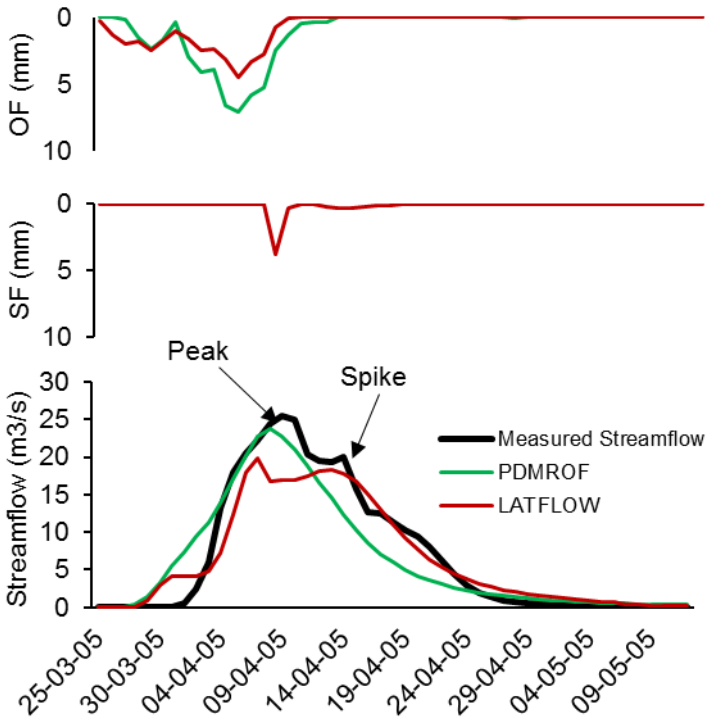

Figure 4.5: Differences among physical processes of PDMROF and LATFLOW for a streamflow event in the Kronau Marsh watershed during snowmelt and summer rainfall events. Here abbreviation 'OF' indicates overland flow and 'SF' indicates 'sub-surface flow'.

4.1.2 Storage

Storage includes liquid water and snow water equivalent (SWE) content in the form of soil moisture and ice within soil column, ponded water, snow on the ground, and intercepted water and snow content in vegetation. The amount of intercepted water and snow in vegetation is insignificant compared to other storage components, therefore, their contribution to the total storage is ignored. Generated runoff varies in magnitude and frequency using the optimized models of different configurations (i.e. WATROF, PDMROF, and LATFLOW). Other components of water balance (i.e., evapotranspiration, snow accumulation, soil moisture, and snowmelt) are also affected during the model calibration. Figure 4.6 shows soil moisture content and ponding depth for the White Gull Creek, Kronau Marsh, and Brightwater Creek watersheds. LATFLOW tends to store more water (5% and 2% more than WATROF and PDMROF) for the White Gull Creek (Figure 4.6a). Excess water is primarily stored as soil

moisture, and not much ponded water is available for LATFLOW. The Amount of accumulated SWE is not very different from each other as runoff generation algorithms do not have any direct effect over it. Both Kronau Marsh and Brightwater Creek watersheds exhibit similar storage pattern (Figure 4.6b and Figure 4.6c). For both the cases, LATFLOW shows sub-surface storage that is 3.0-3.5 times more compared to PDMROF as PDMROF allows more water to be stored overland due to the lack of interflow as drainage mechanism. It was observed that PDMROF tends to store more water overland as ponded water rather than within soil column. Similar to White Gull Creek watershed, the amount of accumulated SWE is not significantly different across various model configurations for the Kronau Marsh and Brightwater Creek watershed. Also, total storage shows a constant pattern suggesting a regular draining and replenishment of storage. WATROF, PDMROF, and LATFLOW algorithms use different approaches to estimate overland and sub-surface flow, which is the prime reason for the difference in estimation of water balance components. PDMROF does not have any interflow component resulting in high overland drainage, and ponding depth, whereas these processes in WATROF and LATFLOW are well simulated due to overland and sub-surface connectivity. This observation shows that incorporation of sub-surface drainage along with the PDM parameterization of overland runoff is physically plausible for the prairies, and this makes LATFLOW a more suitable runoff generation algorithm for the prairies.

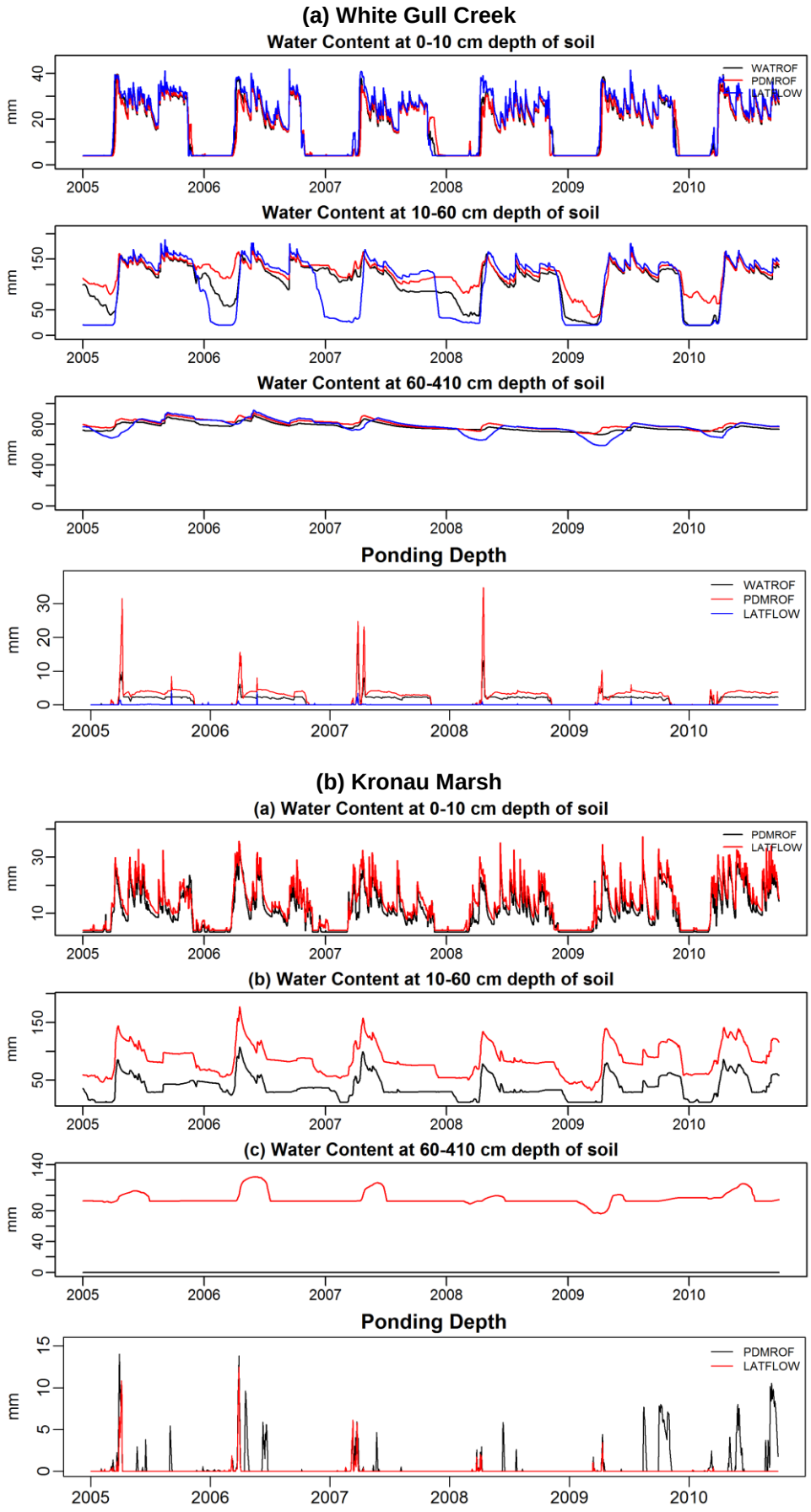
(a) White Gull Creek
Water Content at 0-10 cm depth of soil
WATROF
PDMROF
LATFLOW
mm
0
20
40
2005
2006
2007
2008
2009
2010
Water Content at 10-60 cm depth of soil
mm
0
50
150
Water Content at 60-410 cm depth of soil
mm
0
400
800
Ponding Depth
WATROF
PDMROF
LATFLOW
mm
0
10
20
30
(b) Kronau Marsh
(a) Water Content at 0-10 cm depth of soil
PDMROF
LATFLOW
mm
10
30
(b) Water Content at 10-60 cm depth of soil
mm
50
150
(c) Water Content at 60-410 cm depth of soil
mm
0
40
80
140
Ponding Depth
PDMROF
LATFLOW
mm
0
5
10
15

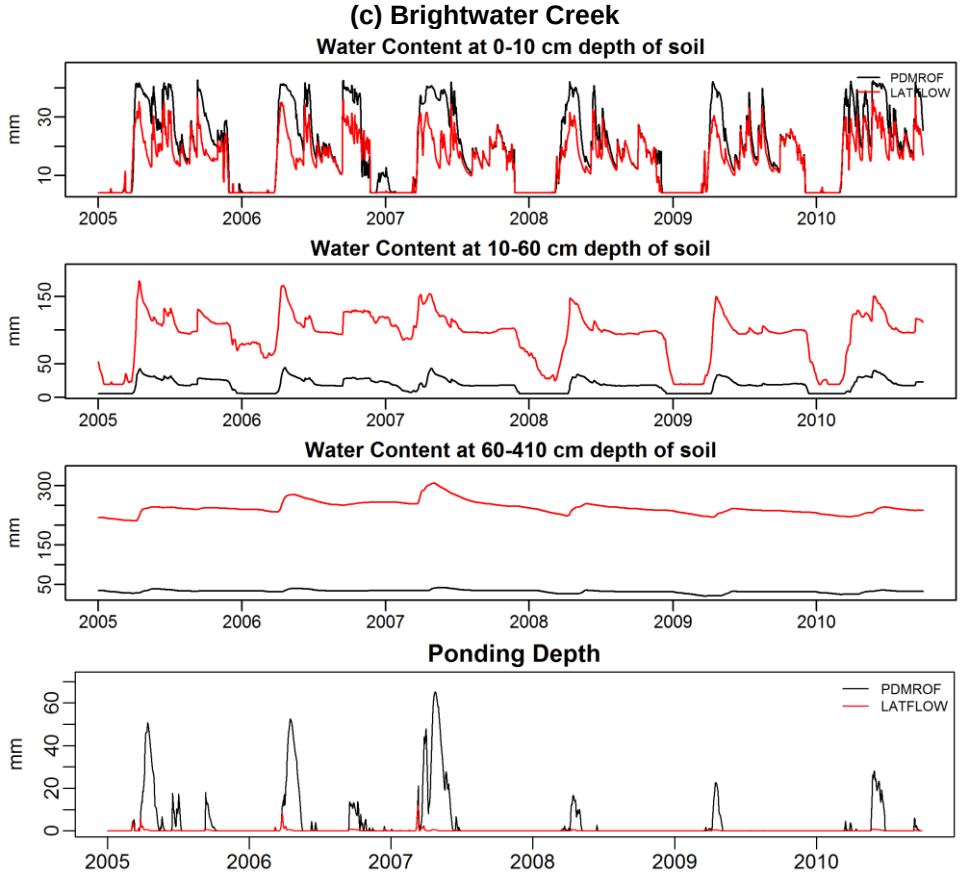

Figure 4.6: Simulated soil moisture content and ponding depth for White Gull Creek watershed using different runoff generation algorithms from 2005 to 2011.

Table 4.1: AIC values for the White Gull Creek, Kronau Marsh, and Brightwater Creek watershed in calibration and validation period

	Calibration period			**Validation period**		
Watershed	WATROF	PDMROF	LATFLOW	WATROF	PDMROF	LATFLOW
White Gull Creek	1061.9	1225.6	864.8	-152.8	298.2	57.7
Kronau Marsh	-	484.2	-397.9	-	-506.1	-1115.5
Brightwater Creek	-	-1849.0	-1996.7	-	-2036.1	-2050.8

The number of calibration parameters used in LATFLOW configuration is high (34) compared to WATROF (28) and PDMROF (22), which raises the question that LATFLOW might perform better just because it uses a higher number of parameters, not because of the incorporation of an additional process (interflow) in it. To investigate the influence of the increased number of parameters on the model performance, AIC was calculated for each calibration and validation across different watersheds (Table 4.1). It appears that for the White

Gull Creek watershed, AIC value for LATFLOW is the lowest compared to WATROF and PDMROF, showing that LATFLOW is a suitable runoff generation algorithm that achieve better calibration. However, WATROF appears to be the best algorithm during the validation period as the AIC value is the lowest during the validation period compared to PDMROF and LATFLOW. For Kronau Marsh watershed, LATFLOW shows lower AIC value compared to PDMROF during both calibration and validation, which suggests that LATFLOW is the appropriate runoff generation algorithm for the watershed. Incorporation of an interflow mechanism realistically represents the drainage mechanism in the Kronau Marsh watershed, and the increased number of parameter does not seem to be the major role for better prediction capability. A similar behavior is observed for the Brightwater Creek watershed, where AIC values for LATFLOW exhibit better performance compared to PDMROF during both calibration and validation periods, suggesting that LATFLOW is the appropriate algorithm. Therefore, the incorporation of interflow component of LATFLOW has the advantage of suitable physical representation of drainage mechanism for the selected prairie watersheds.

4.2 Effect of Differences in Runoff Generation Algorithms

In section 4.1, the MESH model was calibrated individually using the three runoff generation algorithms. These algorithms have a few parameters that are common but vary in their final calibrated values. To assess the effect of runoff generation algorithms on hydrological processes other than streamflow, they should be compared using a parameter set that is common across the algorithms. MESH model calibrated using LATFLOW as the runoff generation algorithm contains all the parameters that are present in WATROF as well as PDMROF. For this reason, the calibrated values for MESH-LATFLOW were taken as the base values to run the MESH model using WATROF and PDMROF. This enables us to have a direct comparison of differences in runoff generation algorithms and their effect on components such as overland runoff, interflow, baseflow, soil moisture, ice-content and ponding depth.

Figure 4.7a shows the overland flow, interflow and baseflow components of total runoff using different runoff generation algorithms for the White Gull Creek watershed. It is observed that WATROF and LATFLOW primarily allow water to be infiltrated and using sub-surface route to drain water as interflow and/ or baseflow. The White Gull Creek watershed being a forest dominated area, contains increased infiltration capability due to high sand content in this watershed. The sand content in the first soil layers of the White Gull Creek is relatively high (about 60%), which allows increased infiltration capability. So, during a high rainfall event (as seen for years 2005 and 2006), all of the algorithms allows more water in the soil column. WATROF is draining water from the side of the soil column as interflow and due to lack of this mechanism in PDMROF, it drains water as overland flow. Figure 4.7a also shows the soil moisture, ice content in the soil column, and ponding water depth for different runoff generation algorithms, which is relate with corresponding runoff generation processes. It is observed that in the first layer (0-10 cm), soil moisture content in not very different for the algorithms. However, some fluctuation is observed in the second (10-60 cm) and bottom (60-410 cm) layer of soil. A 15 mm drop in moisture content is observed in WATROF for year 2007, which happens because of a rainfall event in the late summer of year 2007 (Figure 4.7a). In response to the specific rainfall event, WATROF drains 15 mm of additional water as interflow from the soil column compared to PDMROF and LATFLOW, which drains from the second layer of soil. This phenomenon leaves less amount of water in the soil column to be developed as ice content for the next winter season, which can also be observed in Figure 4.7a.

Two types of ponding is observed, i) ponding is due to snowmelt during spring, and ii) ponding is due to intense rainfall event. Both types of ponding is observed in the White Gull Creek. For year 2005 and 2006, intense summer rainfall events are observed, which create increased amount of ponding depth as well as runoff. High ponding depth also replenish soil moisture, which is observed in Figure 4.7a.

Figure 4.7b shows overland runoff, interflow and baseflow components of total runoff using different runoff generation algorithms for the Kronau Marsh watershed. This is a prairie watershed dominated by 'non-contributing wetlands'. Only interflow is allowed as subsurface lateral drainage to represent realistic soil structure, because of insignificant baseflow in the prairies. WATROF is unable to estimate overland runoff during spring snowmelt, allowing infiltration and drainage as interflow, which is because of its inability to simulate dynamic storage capacity. Moreover, WATROF responds to the summer rainfall events sharply (year 2005 and 2009) and generats overland runoff. However, this is inaccurate representation of prairie runoff generation process, because summer or late summer rainfall event often do not satisfy critical ponding depths and reach the nearest stream, but remains on the ground and either evaporates or increase antecedent soil moisture for following spring melt. Due to lack of interflow mechanism, PDMROF primarily drains water as overland runoff. LATFLOW generats interflow, which complements the peak flow hydrograph in recession period. Figure 4.7b also shows the soil moisture, ice content in the soil column and ponding water depth for different runoff generation algorithms, which is related with corresponding runoff generation processes. It is observed that first and second layer soil moisture content is not very different for the algorithms. However, some fluctuations is observed in the bottom layer of soil (year 2006 and 2007). During the spring runoff, WATROF generates increased amount of interflow just after spring snowmelt and drains as overland runoff. Results indicate that WATROF drains water laterally from the bottom layer of soil. Lack of mechanism to simulate the prairie surface connectivity results in WATROF ponding more water overland and drain as interflow. LATFLOW inherits this capacity of WATROF, and allows a small amount of water to drain as interflow during recession period. For LATFLOW, it provides a flexibility to adjust total runoff and represent prairie runoff processes accurately.

Figure 4.7c shows overland runoff, interflow and baseflow components of total runoff using different runoff generation algorithms for the Brightwater Creek watershed. Being another prairie watershed, it exhibits similar runoff generation behavior of the Kronau Marsh watershed. Similar ineffectiveness of WATROF is observed here as it inaccurately responds to high summer rainfall events. Both PDMROF and LATFLOW estimat similar overland runoff. However, a small amount of interflow is observed during year 2008 and 2009. Figure 4.4 shows that streamflow simulation of PDMROF and LATFLOW is good (based on calibration and validation performance), which verifies that overland runoff is the principal contributor of streamflow in the Brightwater Creek watershed. Figure 4.7c shows the soil moisture, ice content in the soil column and ponding water depth for different runoff generation algorithms, which is relate with corresponding runoff generation processes. For this watershed moisture and ice content at every layer is indifferent. Ponding of water using PDMROF and LATFLOW occurr at the same time. A delayed ponding is observed for WATROF, which is responsible to drain inaccurately as interflow. These results could not be validated with actual observations due to lack of data related to these components in the study areas considered. Hence the discussion mainly focusses on model outputs and the physical processes is verified if such data were available.

(a) White Gull Creek

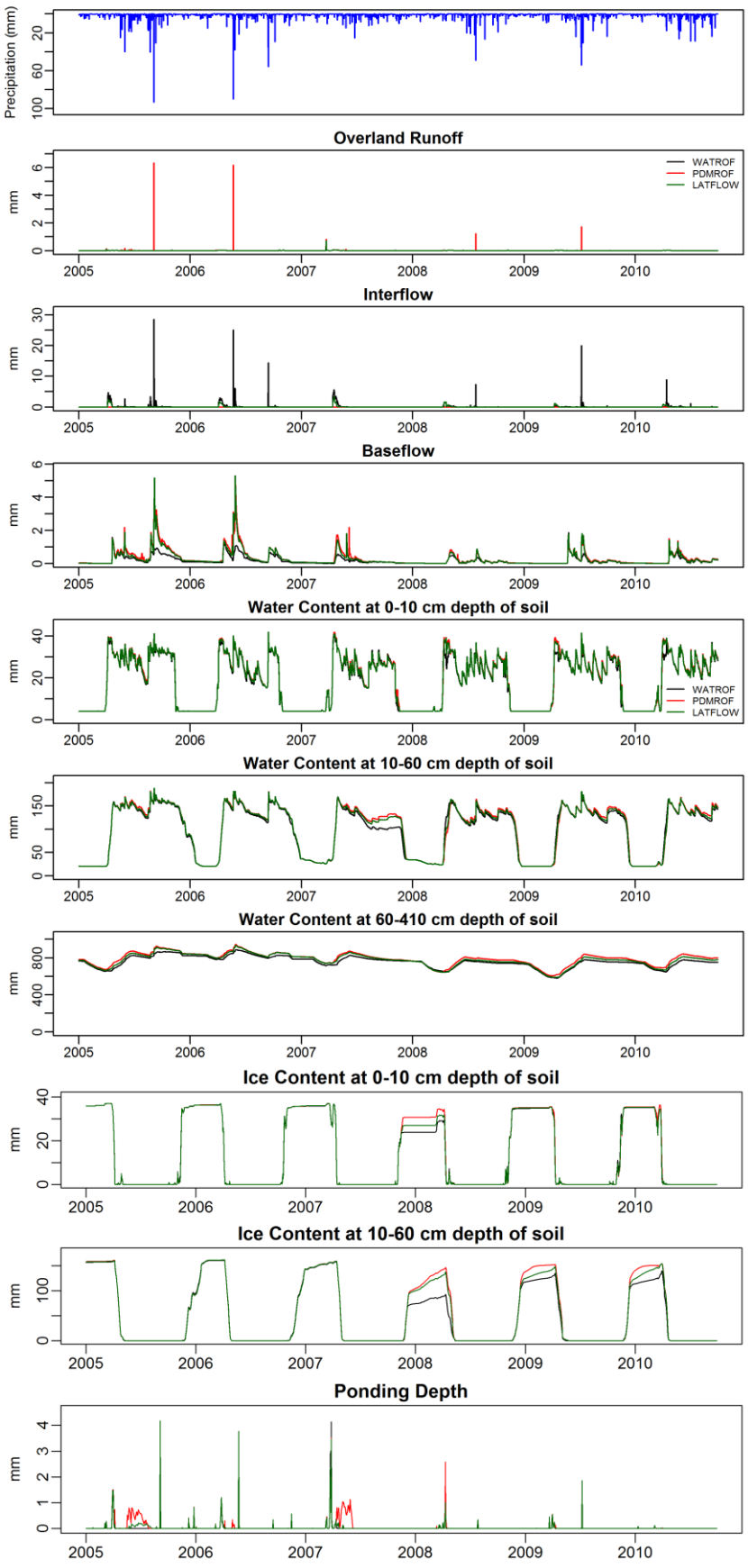

(b) Kronau Marsh

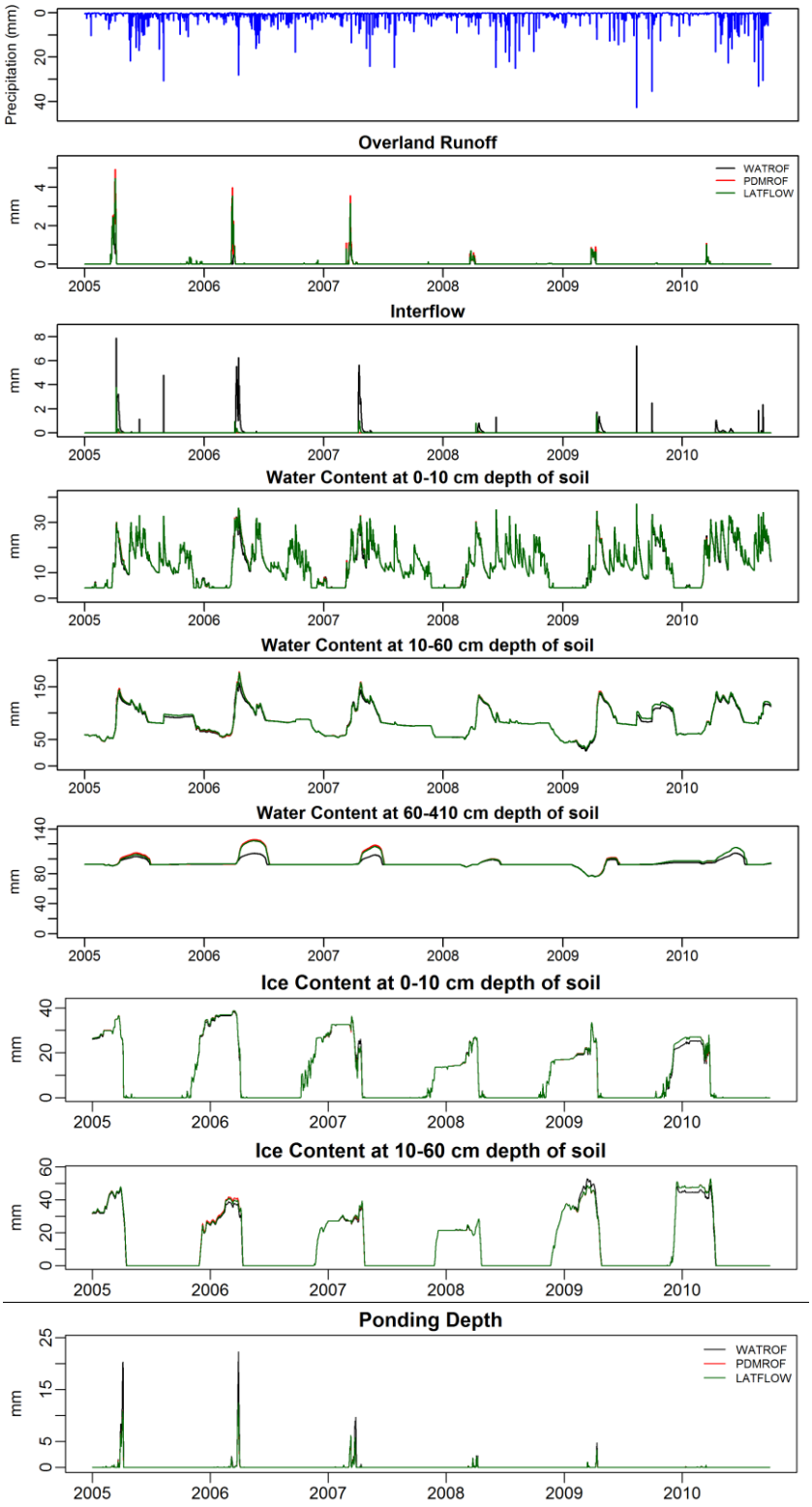

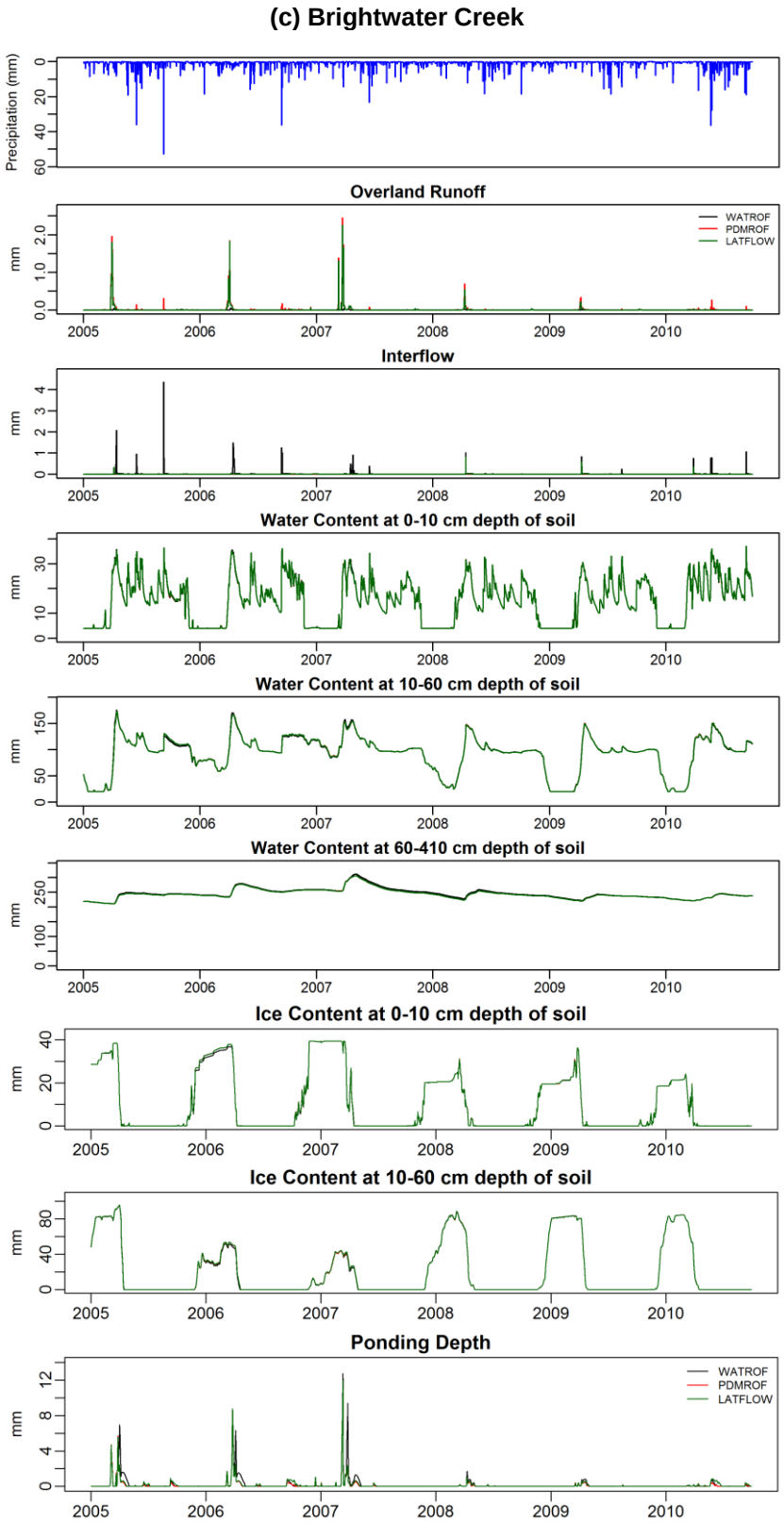

Figure 4.7: Runoff generation processes, soil moisture and ice content in soil layer as well as ponding depth across different runoff generation algorithms in the (a) White Gull Creek (b) Kronau marsh, and (c) Brightwater Creek watershed. Blue lines in the top chart is precipitation.

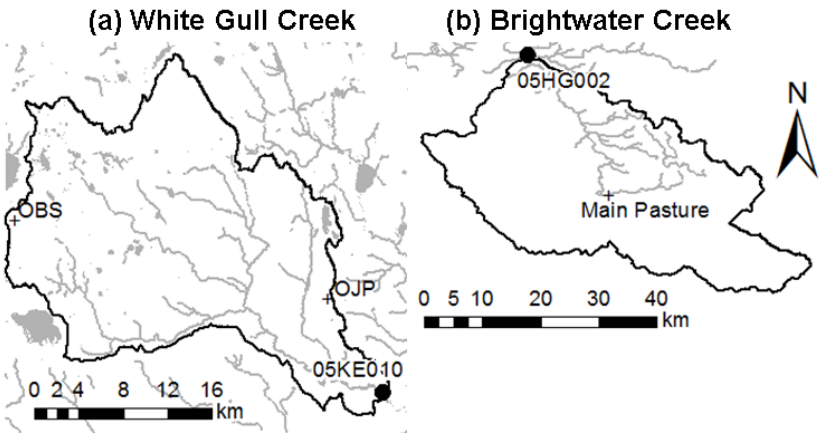

Figure 4.8: Location of (a) OBS and OJP in the White Gull Creek and (b) Main pasture in the Brightwater Creek watershed.

To validate the model configuration for evapotranspiration (ET) during the calibration and validation periods in the White Gull Creek watershed, cumulative plots are considered as visualization indicators. Measured ET was available for White Gull Creek watershed, where latent heat and observed temperature at the flux tower sites (OBS and OJP sites for the White Gull Creek watershed) (Figure 4.8a) were used to compute evapotranspiration, in conjunction with the latent heat of vaporization. Measured ET was also available for the Brightwater Creek watershed at Main Pasture (MP) flux tower (Figure 4.8b), however, data are available from year 2009 onward. A detail methodology for the ET calculation is found in Davison *et al.* (2016), which was adopted for this study. Figure 4.9 shows a plot of cumulative daily evapotranspiration values for the OBS and OJP stations and three model configurations for basin average value from 2005 to 2010. ET simulation for individual model configuration (i.e. WATROF, PDMROF, and LATFLOW) appears to be inseparable. ET is primarily simulated by the vegetation parameters used in MESH and runoff generation algorithms do not have any explicate effect over ET estimation. It is also observed (Figure 4.9a) that ET closely aligns with the measurements for the OBS station compared to OJP station. OJP station is located in the White Gull plains, which exhibits dry nature of watershed compared to the upstream zone. Wetland processes dominate the upstream zone, where OBS station is located. ET estimation at OBS station appears to have good match with observed measurements, which suggests that

MESH is able to simulate ET process well in this location. Due to the dry nature of the OJP site, it is possible that the model results are influenced by the lack of moisture available for ET. Figure 4.9b shows cumulative plots of the daily evapotranspiration values for the Main Pasture station located in the Brightwater Creek watershed (figure 4.7b) from October 2009 to October 2010. In all model runs (Figure 4.9), the cumulative ET estimated from the model is greater than the observations. This could be attributed to the erroneous value for vegetation parameters, which overestimates ET and leaves less amount of soil moisture content.

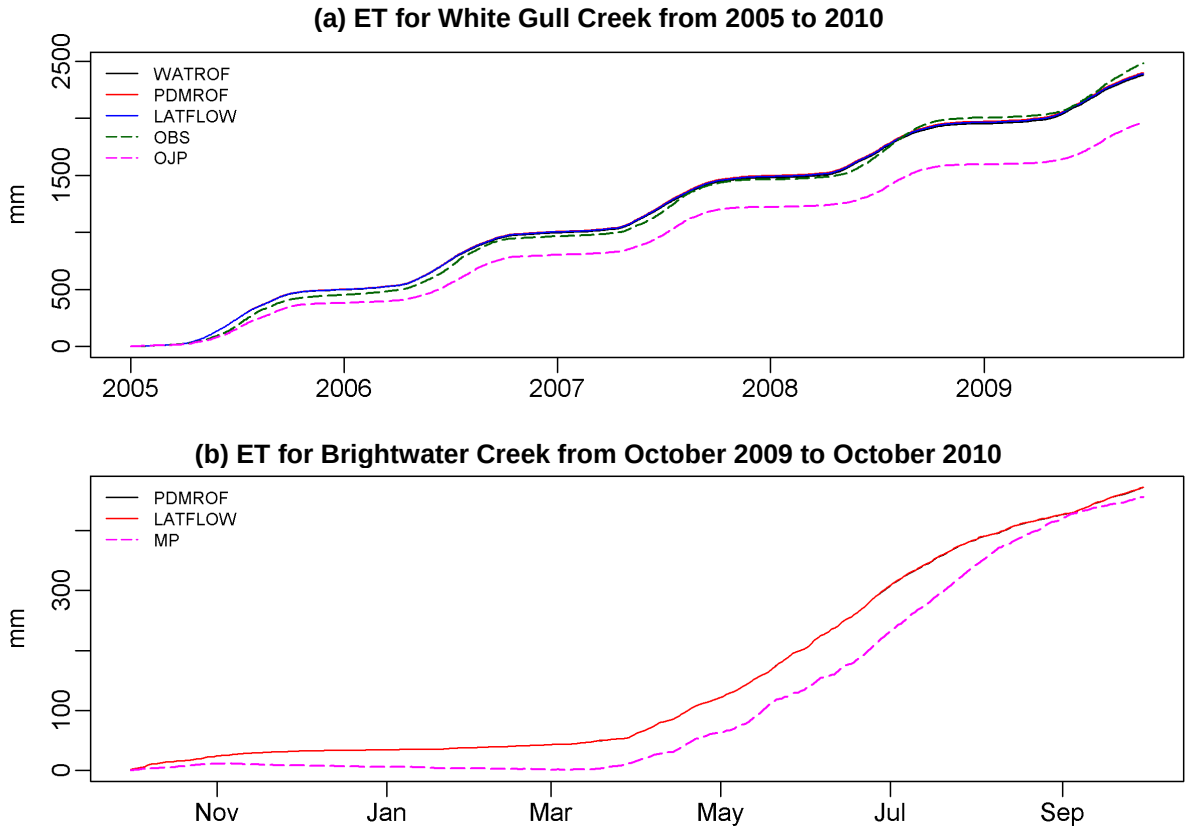

Figure 4.9: Measured and simulated evapotranspiration (ET) for the (a) White Gull Creek and (b) Brightwater Creek watersheds.

The results regarding the simulation of streamflow, storage, and other important hydrological processes indicate that the proposed LATFLOW algorithm performs well in prairie watersheds (Kronau Marsh and Brightwater Creek) and WATROF is suitable for the non-prairie watershed (White Gull Creek). It was also observed that the LATFLOW algorithm was able to simulate streamflow reasonably well in a non-prairie watershed, indicating that the approach could be

applied outside of the prairies as well. The reason behind the effectiveness lies in the basic differences between the runoff generation algorithms (WATROF, PDMROF, and LATFLOW), which are the use of limiting ponding depth, routing of surface runoff, and interflow or near surface runoff. WATROF is considered as a conventional runoff generation algorithm, which was proved to be applicable for most of the small to large scale watersheds in Canada. PDMROF assumes that the surface storage connectivity follows a probability distribution function over time and space. Although few studies (Mekonnen et al., 2014; Mengistu and Spence, 2016; Yassin et al., 2017) showed successful model development using PDMROF, there are scopes to improve the runoff estimation process by addressing its limitations, some of which was implemented in LATFLOW.

4.3 Parameter Identifiability

A complete set of behavioral solutions (NSE>+0.5 and $Log(NSE)$>+0.3) was identified (based on Figure 4.1) for all the watersheds in separate analysis and runoff generation algorithms. Corresponding parameter values for each algorithm were normalized and represented in the following box plots (Figure 4.10, Figure 4.11, and Figure 4.12). As the number of calibration parameters used in different runoff generation algorithms are not same and individual runoff generation algorithms use different parameterization of physical processes, the total number of parameters are not the same in those figures. However, by design, LATFLOW is parameterized in such a way that it represents all the processes used in WATROF and PDMROF, therefore, LATFLOW contains all the parameters used in both WATROF and PDMROF.

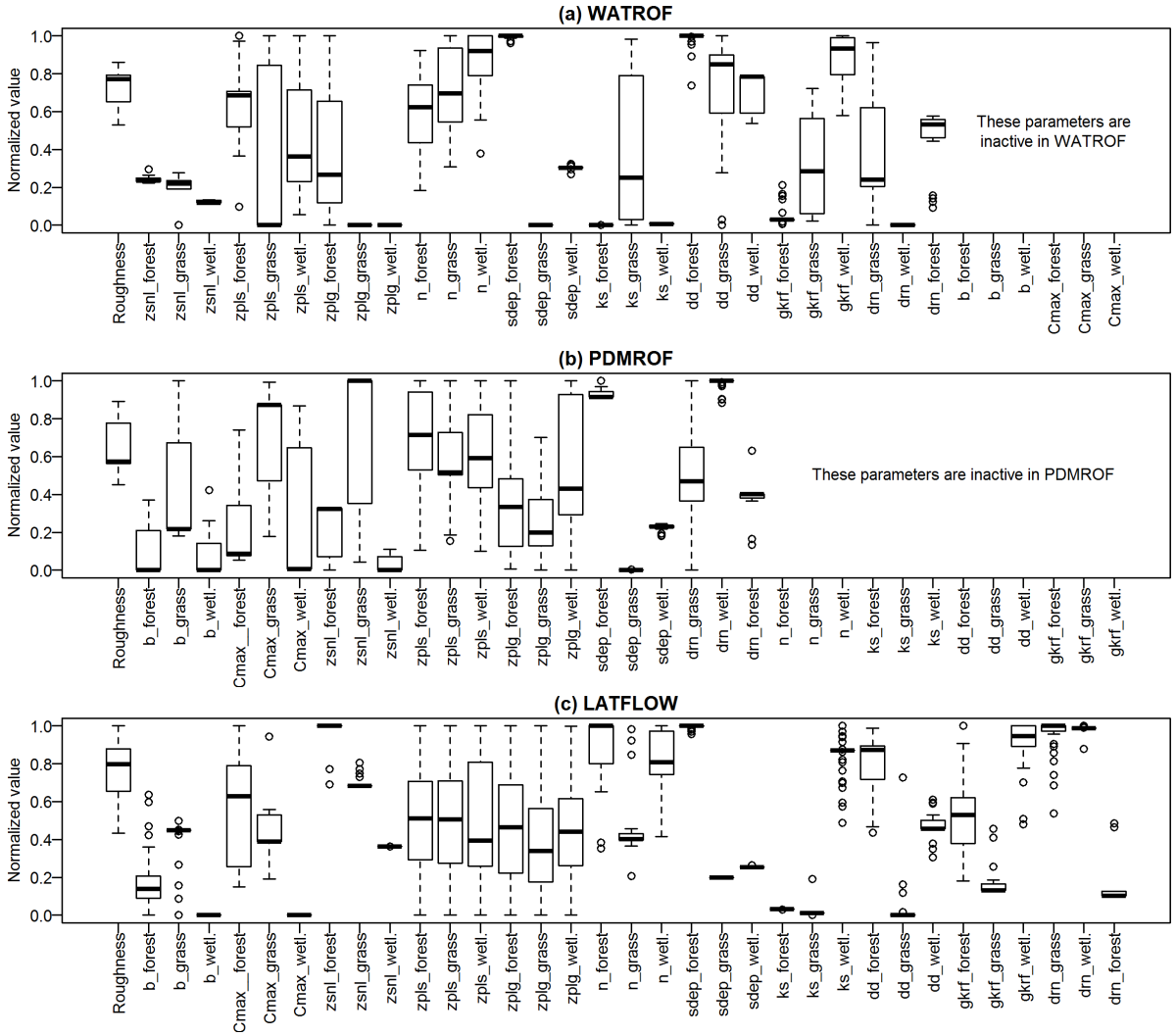

Figure 4.10: Parameter identifiability for the pareto optimal solutions of the White Gull Creek watershed using (a) WATROF, (b) PDMROF, and (c) LATFLOW configuration. The text before '_' is parameter type and after '_' is the GRU type.

According to Figure 4.10, permeable soil depth ($sdep$) for all types of GRU (forest, grass, and wetlands) appears to be identifiable for all the runoff generation algorithms in the White Gull Creek watershed. More number of parameters appear to be identifiable in LATFLOW (59% of total drainage parameters) compared to WATROF (46%) and PDMROF (23%), which suggests that the model is less uncertain in LATFLOW compared to other algorithms. It is not just the number of identifiable or unidentifiable parameters that governs uncertainty, but the pattern and the degree of identifiability also indicates the level of uncertainty. In PDMROF, except permeable soil depth and drainage index in forest and wetland, the rest of the parameters appear to be unidentifiable. It was also observed in Figure 4.2 that PDMROF performs poorly in the

White Gull Creek watershed. Both WATROF and LATFLOW exhibit some common identifiable (such as limiting snow depth ($zsnl$), permeable soil depth ($sdep$), saturated hydraulic conductivity (k_s) and unidentifiable parameters (such as, $zpls$, $zplg$, $Roughness$). The PDM parameters, C_{max} and b (except C_{max} for forest), in LATFLOW appear to be identifiable, suggesting appropriate use of PDM parameters in the White Gull Creek. Moreover, being a forest dominated watershed, subsurface drainage is the primary driver of the runoff process, which is observed in the identifiable nature of soil drainage properties (mainly permeable soil depth and saturated hydraulic conductivity). It is probable that, lack of efficient subsurface drainage mechanism (absence of interflow algorithm) makes PDMROF perform poorly in this watershed.

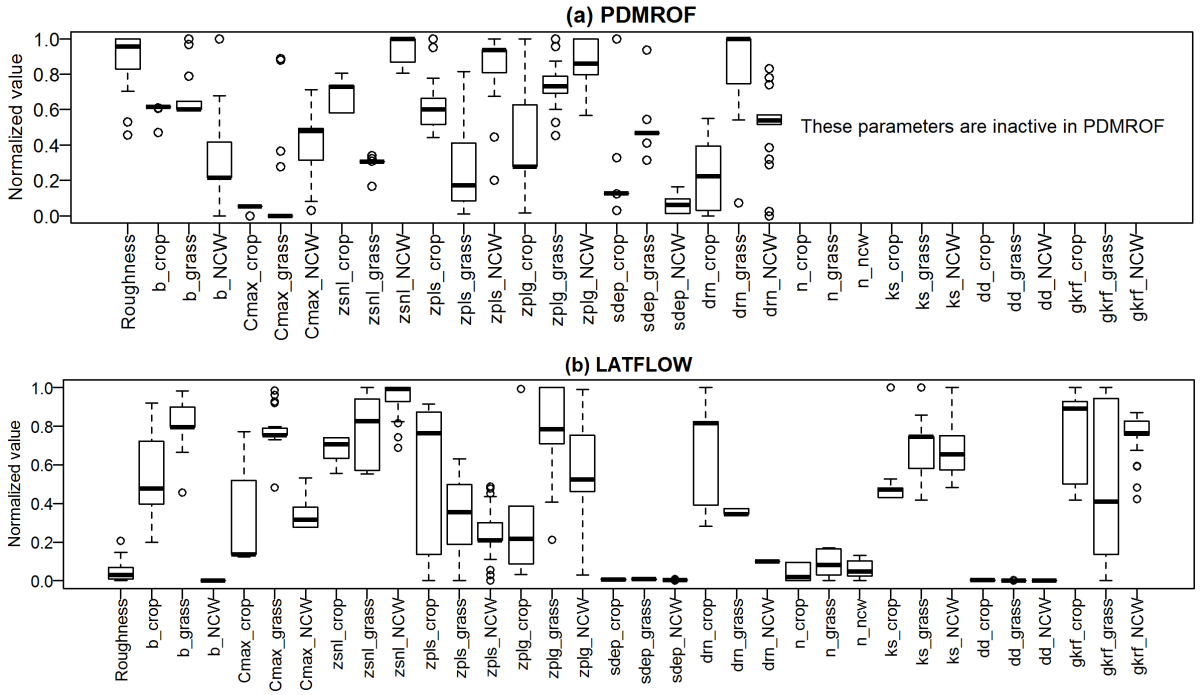

Figure 4.11: Parameter identifiability for the pareto optimal solutions of the Kronau Marsh watershed using (a) PDMROF and (b) LATFLOW configuration. The text before '_' is parameter type and after '_' is the GRU type.

Figure 4.1b and Figure 4.1c already showed the non-behavioral pattern of WATROF, for which it was discarded from the identifiability analysis for both the prairie watersheds. According to Figure 4.11, permeable soil depth ($sdep$) for all types of GRU (crop, grass, and non-contributing wetlands) and limiting snow depth ($zsnl$) appear to be identifiable for both the

runoff generation algorithms in the Kronau Marsh watershed. More parameters appear to be identifiable in LATFLOW (59%) compared to PDMROF (36%). PDM parameters are mostly identifiable in both PDMROF and LATFLOW (except for GRU-Crop in LATFLOW). Drainage parameters (manning's n, saturated hydraulic conductivity, drainage density, and permeable soil depth) appear to be identifiable, which justifies the addition of interflow component in LATFLOW algorithm as identifiable parameter with less uncertainty. Snow parameters $zpls$, $zplg$ appear to be mostly unidentifiable in both algorithms, raising doubts regarding the use of these parameters, which means that these parameters ($zpls$ and $zplg$) is excluded from the calibration process by assuming a constant reasonable value or these parameters needed to be reassessed before using in the model.

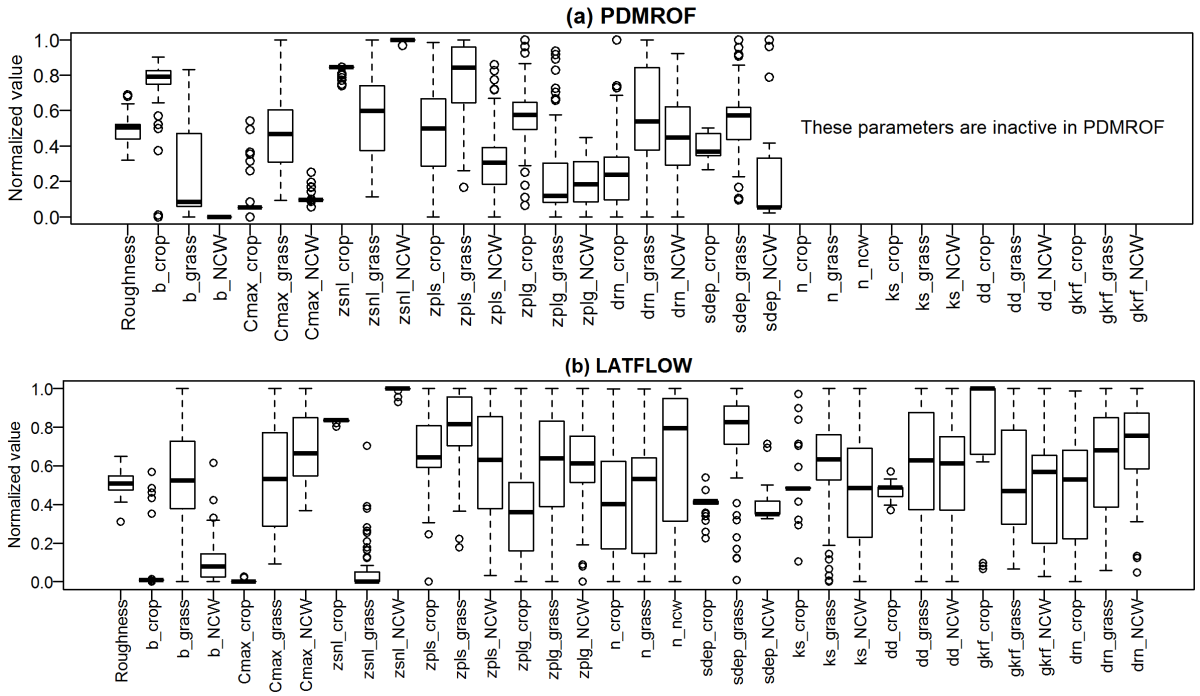

Figure 4.12: Parameter identifiability for the pareto optimal solutions of the Brightwater Creek watershed using (a) PDMROF and (b) LATFLOW configuration. The text before '_' is parameter type and after '_' is the GRU type.

It was observed in Figure 4.4 that the performance of both PDMROF and LATFLOW for streamflow simulation of the Brightwater Creek watershed is similar. According to Figure 4.12, more parameters appear to be identifiable in PDMROF (40%) compared to LATFLOW (34%). Less identifiable nature of parameters in LATFLOW suggests that the addition of interflow

does not add any benefit for this watershed. Both Figure 4.11 and Figure 4.12 indicate that the application of LATFLOW might be useful over PDMROF, depending on the type of the prairie watershed based on the pattern and distribution of non-contributing wetlands, land cover, and dominating drainage properties (which are the differences between the Kronau Marsh and Brightwater Creek watersheds). PDM parameters, permeable soil depth ($sdep$), and limiting snow depth ($zsnl$) for GRU-Crop appear to be identifiable. The parameters for grass and non-contributing wetlands appear to be mostly unidentifiable for both the algorithms, indicating that the GRU delineation is likely to be inefficient. This leads to an argument whether an unidentifiable parameter should or should not be considered in the model discretization process (GRU definition). From the modelling point of view, a well distributed model is always preferable. If the computing facility, availability of physiographic information, and parameterization scheme (the equations used) of model allows, it is preferable to include every available detail into model discretization process, which is done in this study. Even though a few parameters are unidentifiable according to the analysis, they cannot be excluded from the parametrization process as they are integral to the MESH modelling framework. However, this analysis could lead us to reduce the number of parameters required to be calibrated.

The underlying concept of parameter identifiability is to show the context, appropriateness, and uncertainties of parameters used in a model (Vrugt et al., 2005). It was observed that soil permeable depth ($sdep$) is the most identifiable parameter across all the model configurations used in all the watersheds, suggesting that the parameter is well devised to estimate sub-surface runoff (in WATROF and LATFLOW) as well as soil moisture storage (in all three algorithms). Parameter identifiability results for the White Gull Creek watershed suggest that the PDM parameters (C_{max} and b) are unidentifiable, indicating that the PDM concept does not represent runoff processes of a boreal forest watershed well. Water ponding depth in snow covered and snow free areas ($zplg, zpls$) are unidentifiable in all models across different watersheds, which

is that the use of these parameters in these watersheds are likely to be unsuitable. The identifiability nature of the parameters is used to adjust the parameterization processes for future model development in these watersheds.

4.4 Parameter Sensitivity

Parameter sensitivity analysis (SA) examines the output variation of a model, which is attributed to variations of its input parameters. The purpose of SA includes uncertainty assessment, diagnostic evaluation, dominant control analysis and robust decision making (Pianosi et al., 2014). Some of the outcomes from parameter identifiability and sensitivity are the same, i.e. both the procedures can identify unimportant as well as uncertain parameters from the modelling point of view. Besides the screening of unimportant parameters, sensitivity analysis is able to rank the parameter set according to their influence on the model. In this section, SA for each of the model configurations is conducted separately. NSE was used as the model response metric and SA was conducted from 2005 to 2008 (during the calibration period) for each model.

Two different plots were used here for SA, a pie chart using μ^* for each parameter, indicating the rank and importance of a certain sensitive parameter, and a scatter plot using μ^* and σ value of a particular parameter, indicating the overall influence over the model response as well as the effect due to the interaction with other parameters, respectively. According to Figure 4.13, permeable soil depth ($sdep$) for GRU-Forest is one of the most sensitive parameter across all the runoff generation algorithms in the White Gull Creek watershed, which was an identifiable parameter (Figure 4.10). Some of the parameters exhibit high sensitivity in all the algorithms, such as permeable soil depth ($sdep$) and limiting snow depth ($zsnl$), which is similar to the outcome with parameter identifiability in this watershed. Most of the identifiable parameters show high sensitivity. However, PDM parameters show high sensitivity for PDMROF,

although they were not identifiable parameters (Figure 4.10). This outcome may be misleading because PDMROF does not perform well in the White Gull Creek watershed (Figure 4.2b).

According to Figure 4.14, permeable soil depth ($sdep$) for GRU-Crop is the most sensitive parameter across all the runoff generation algorithms in the Kronau Marsh watershed, which was an identifiable parameter (Figure 4.10). Similar to the outcome of the White Gull Creek watershed, identifiable parameters show high sensitivity in this watershed as well. It is also observed that C_{max} for GRU-Crop shows comparatively high sensitivity in PDMROF, which might be attributed to the high dependency on overland drainage in the absence of interflow mechanism.

For the Brightwater Creek watershed, a different rank of sensitive parameters is observed, although the model performance using PDMROF and LATFLOW is considered similar (Figure 4.4). Permeable soil depth ($sdep$) for GRU-Crop and GRU-NCW is considered as sensitive parameters. The sensitivity of parameters for the Brightwater Creek watershed is similar to that of the Kronau Marsh watershed. The remaining outcome of SA is similar to the other watersheds, i.e. identifiable parameters show high sensitivity. From the outcome of parameter identifiability and sensitivity analysis, it is understood that both methods complement each other and they show the robustness of the parameter estimation procedures.

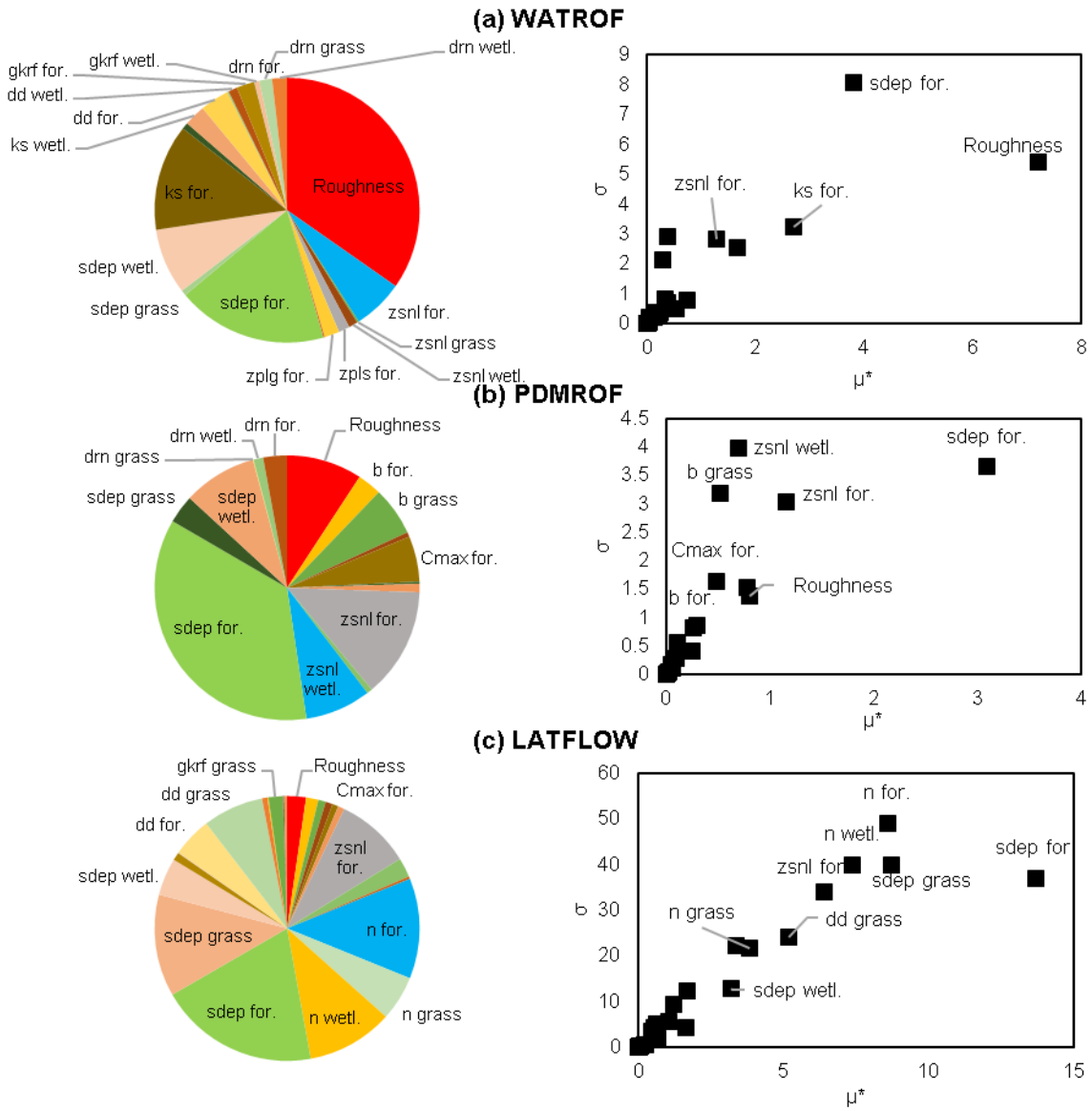

Figure 4.13: Parameter sensitivity of the White Gull Creek watershed using (a) WATROF, (b) PDMROF, and (c) LATFLOW. The acronym ‘for’ and ‘wetl.’stands for ‘forest’ and ‘wetlands’

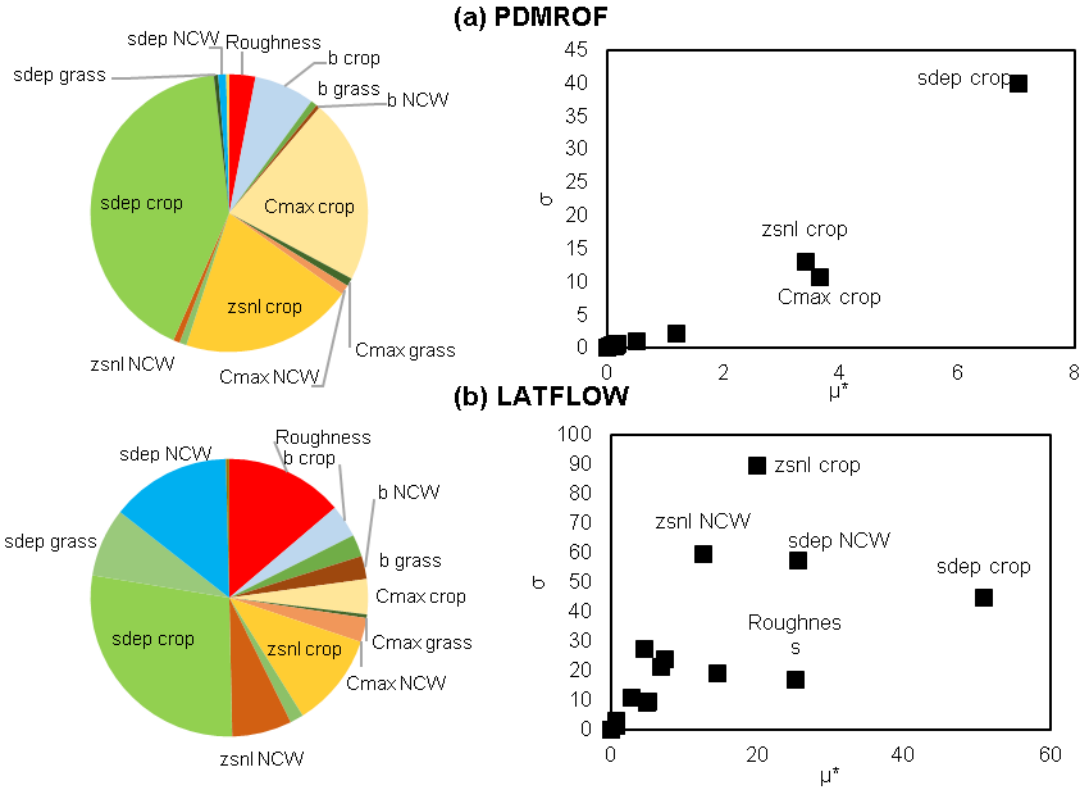

Figure 4.14: Parameter sensitivity of the Kronau Marsh watershed using (a) PDMROF and (b) LATFLOW.

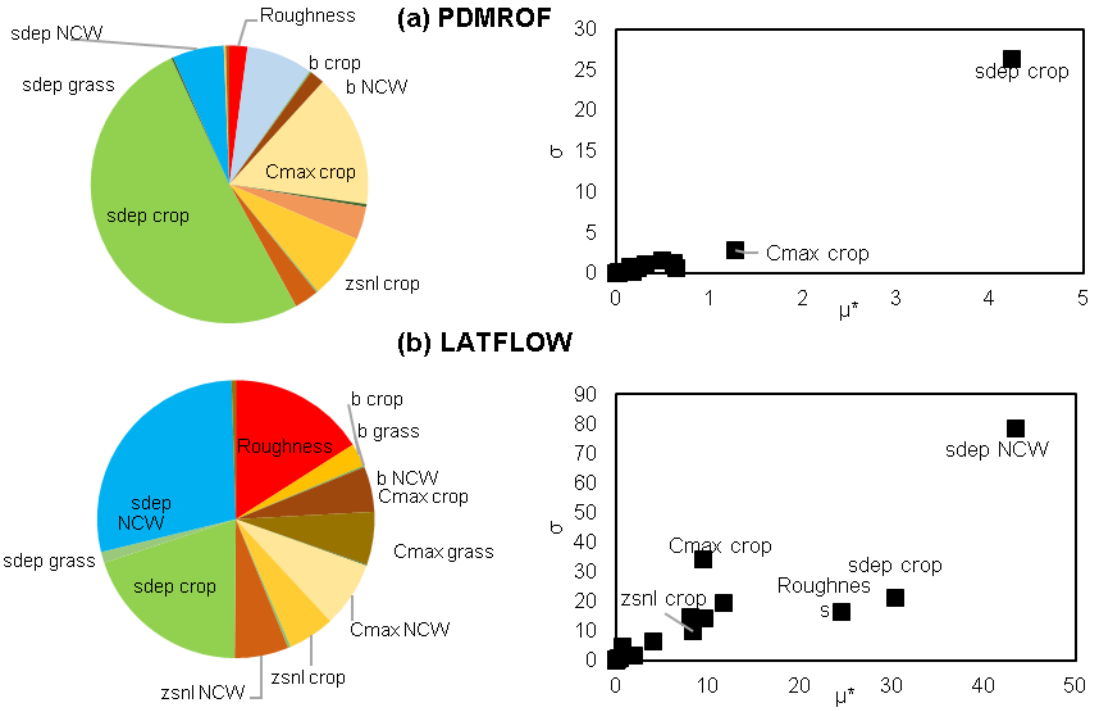

Figure 4.15: Parameter sensitivity of the Brightwater Creek watershed using (a) PDMROF and (b) LATFLOW.

Chapter 5: Hybrid MESH-SD Modelling

Developing an integrated model by joining a hydrological model and a system dynamics model (SD) in order to estimate the streamflow at the outlet of a large-scale watershed is referred to as hybrid modelling in this study. Located in the Canadian prairie ecozone, the Qu'Appelle River basin (QRB) exhibits all the challenging features of prairie watershed Modelling, such as land surface heterogeneity, dynamic drainage contribution, hydrological connectivity, high streamflow flow variability, lack of precise hydro-meteorological information, and effects of human intervention. It is difficult to address all the hydrological features in a single tool, and efficient hybridization of multiple modelling tool is essential to address most of the challenges. To show that such a hybrid approach is possible, there was a need to set up a model to simulate the lake system within the QRB. Once, such a calibrated model was setup, it was coupled with a hydrological model to estimate the streamflow at the outlet of the QRB. This chapter provides results of the SD model and the subsequent hybridization that was carried out to model the QRB.

5.1 Lake SD Model Simulation Results

The Lake SD model simulation was analyzed using time series plots of model runs. Streamflow simulation was analyzed on the main channel of the Qu'Appelle River at Lumsden, Craven, and Welby. Besides streamflow, water levels at individual lakes were also analyzed. Six controlled lakes (Buffalo Pound, Last Mountain, Echo, Katepwa, Crooked, and Round lakes) were considered for this analysis.

5.1.1 Streamflow Simulation

The lake SD model is considered as well calibrated at every station based on Figure 5.1. All the calibration NSE values are well over the satisfaction level (> +0.50) and is considered as

'very good'. The model validation performance was also considered as 'very good' based on both NSE and $PBIAS$ as NSE and PBIAS at all the stations were >+0.65 and < 25%, respectively. The lake SD model, showing good results for both calibration and validation period, runs using measured historical flows from the tributaries. In the direction of hybrid model development, a high performing lake SD model is needed because this model is required to represent the lake interactions and operations correctly so that the errors and uncertainties regarding lake operation during the development of the hybrid model is minimized. Errors and uncertainties are expected to be carried forward from the MESH model during the estimation of the tributaries flows in the hybrid model, and the lake SD model is expected to cause additional error while predicting streamflow at the QRB's outlet near Welby.

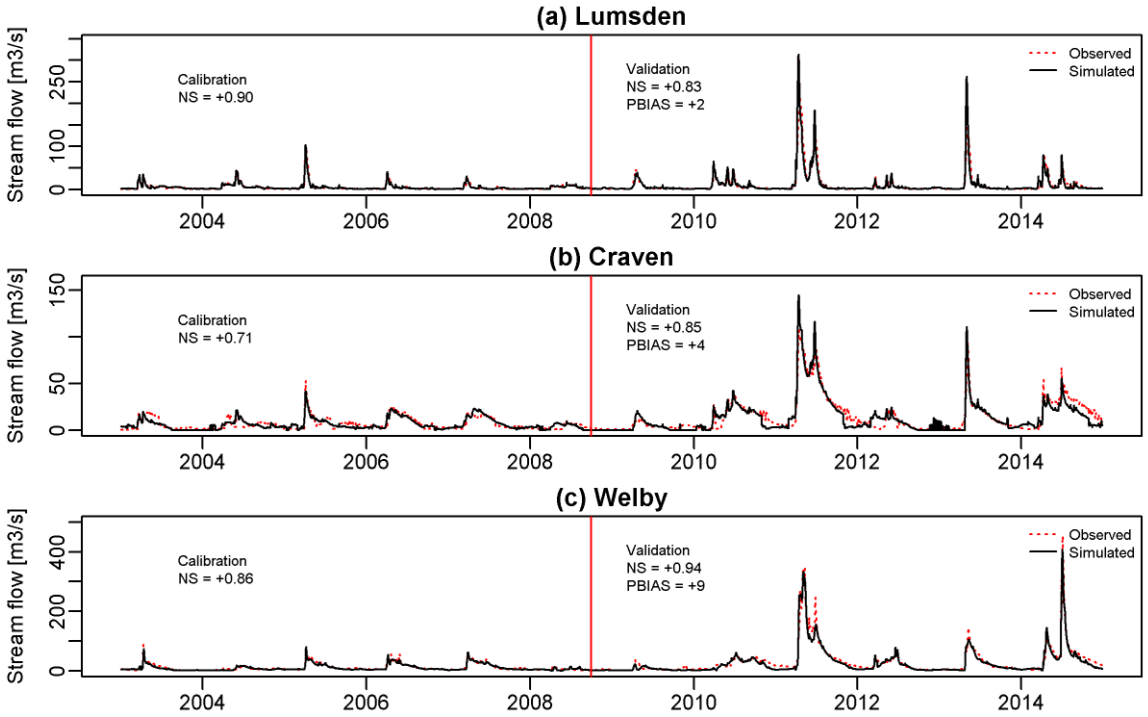

Figure 5.1: Observed and simulated daily hydrographs using the lake SD model at (a) Lumsden, (b) Craven, and (c) Welby.

5.1.2 Lake Water Level

The lake SD model provides the simulated lake elevation for individual lakes in the QRB system. Daily simulated and measured lake water levels from January 2003 to December 2014 was compared and checked for the model's ability to simulate lake water level (Figure 5.2).

NSE was used as a performance measure indicator here. Although the guideline of Moriasi et al. (2007) was mainly developed for watershed response, researchers often use the same guideline for lake model simulation (Muvundja et al., 2014) and the same guideline was used here to evaluate mean monthly lake water level simulation.

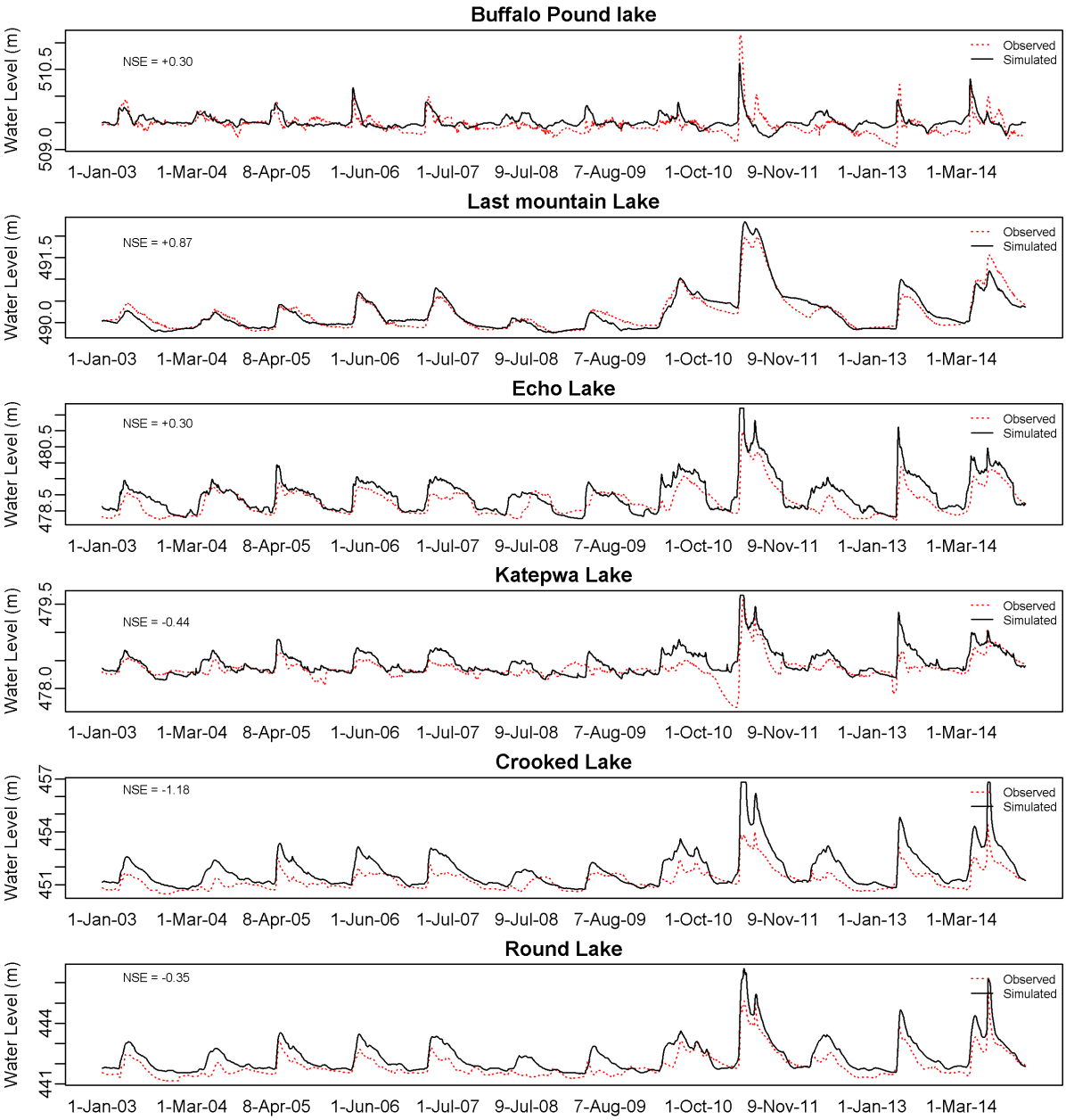

Figure 5.2: Measured and simulated water levels using lake SD model at all the lakes of QRB system.

According to Figure 5.2, it is noticed that the water levels in the lake were not simulated as accurately as the streamflow. Except for the Last Mountain Lake, the model was not able to achieve high NSE values. This reduction of accuracy could be attributed to unavailability of

lake release information, which could have been useful in calibrating the model for lake levels, and human interventions were incorporated as operating rules in the development of the model on monthly basis. However, operating rules is modified anytime within the month based on situational demand and this information could not be accounted in the model. The main purpose of the lake SD model is to simulate the streamflow at Welby efficiently, accounting for all possible lake related processes and operating rules. From this point of view, the model serves its purpose. In order to simulate lake water level efficiently, the parameterization of the lake SD model needs to account for the unaccounted features as well as include the water level simulation into the calibration process.

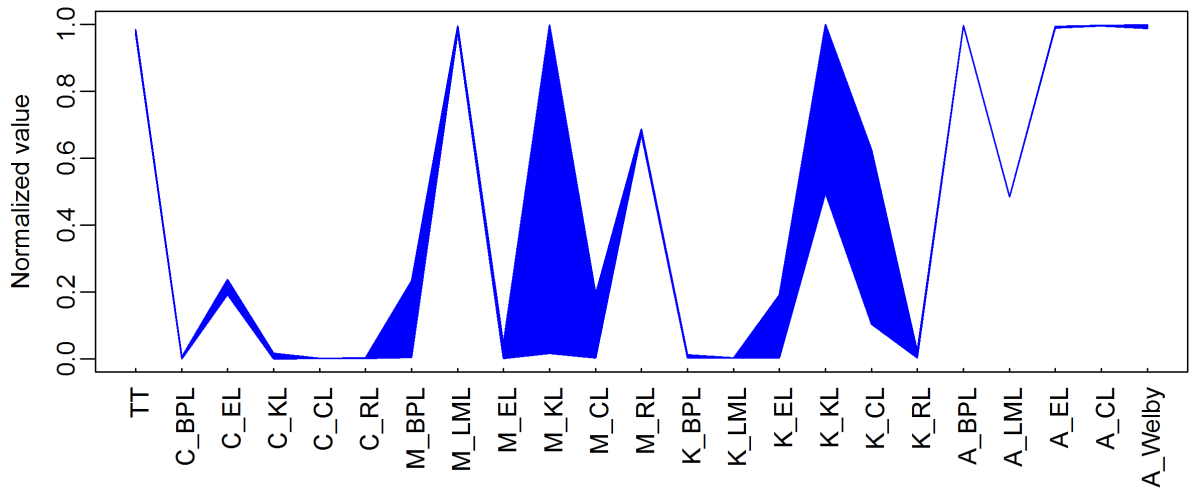

Figure 5.3: Parameter identifiability of the lake SD model. Here '*BPL', 'LML', 'EL', 'CL'*, and '*RL'* indicate lake systems, '*TT'* is temperature threshold, '*C'* is weir release coefficient, '*M'* is degree-day coefficient, '*K'* is lake evaporation coefficient, and '*A'* is co-efficient for ungauged contribution

Figure 5.3 shows the parameter identifiability pattern, constructed using the top 200 simulations. According to this figure, degree-day coefficient (M) and lake evaporation coefficient (K) for Katepwa Lake is unidentifiable, suggesting that the representation of snowmelt and evaporation processes in this lake needs to be improved. Beside these parameters, lake evaporation coefficient (K) for Crooked Lake also appears to be unidentifiable. The rest of the parameters is considered as identifiable parameters, justifying the selection of appropriate equations to represent different processes on the lakes of QRB.

Parameter sensitivity is shown in Figure 5.4 and it shows that ungauged contribution multiplier 'A' for the LML system to be the most sensitive parameter. Although the QRB system contains a number of lakes, apart from BPL and LML, most of them do not have significant surface area to produce a significant amount of snowmelt or evaporation and for this reason snowmelt and lake evaporation parameters appear to be insensitive in this model. It is also observed that the ungauged contribution multipliers for most of the lakes are highly sensitive because the amount of ungauged watersheds for each lake system is considerably high compared to gauged areas. This finding establishes a strong dependency of the model on the water estimation from ungauged area of the QRB. A well calibrated and validated MESH model is required to estimate water coming from gauged and ungauged areas of QRB for good hybrid model and feed it to the lake model.

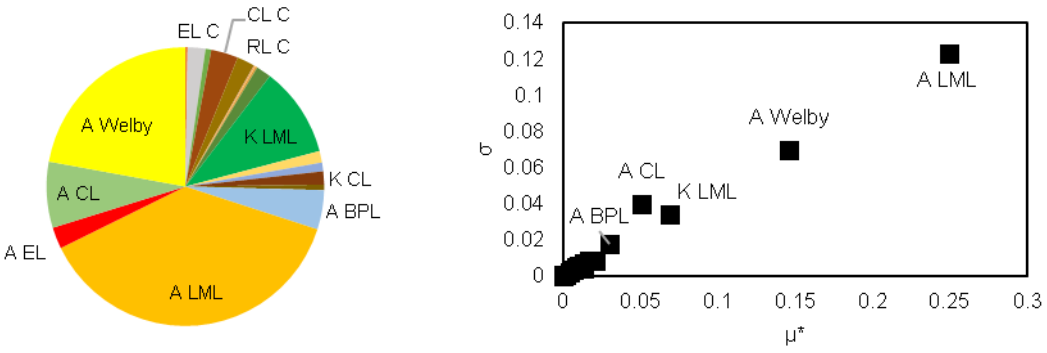

Figure 5.4: Parameter sensitivity of the lake SD model using multiple lake systems model.

The main purpose of the Lake SD model is to model the operations and interaction of multiple lakes of QRB. The model appears to be performing well in the context of streamflow simulation at outlet as well as intermediate locations. Based on the outcome, it is said that this particular lake SD model is able to simulate the operations and interaction of the complex lake arrangement of QRB.

5.2 Hybrid MESH-SD Model Simulation Results

In this study, large-scale modelling of the QRB was simulated by joining a MESH model and a lake SD model in a hybrid structure. The efficiency of the QRB hybrid model depends on the

performance of both MESH model lake SD models individually as well as in a coupled framework. Different approaches of hybridization are possible; however, two approaches were tested for this study named ‘top-down’ and ‘bottom-up’ approach. The naming of these approaches evolves from the style of addressing the hybrid modelling of QRB.

5.2.1 Model Simulation of Top-down Approach

In this case, two possible options were implemented-

I. Setting up a MESH model for natural processes of the QRB and calibrate for multiple sub-basins using a multi-site calibration/optimization technique.

II. Setting up individual models for the sub-basins and calibrate/optimize them separately.

Simulation results for the hybrid model was analyzed in two steps. In the first step, model simulations of the MESH models for both options (option- I and option – II) for the tributaries were analyzed, and in the second step, model simulations of the lake SD model were analyzed using time series plots. Model evaluation criteria were similar to the criteria used in the comparison study (using NSE and $PBIAS$ for the validation run). Figure 5.5 shows the Pareto front of non-dominated solutions of the QRB using Option-I of the top-down approach. A reasonable optimization solution was selected from the Pareto front, which exhibits comparatively high NSE along with high $Log(NSE)$ (NSE = +5.703 and $Log(NSE)$ = +2.104). The uncommon values of the NSE and $Log(NSE)$ are a result of summing up the values of the 10 sub-basins. Figure 5.6 shows the calibration and validation results of the selected sub-basins using Option-I of the top-down approach. The calibration for all the sub-

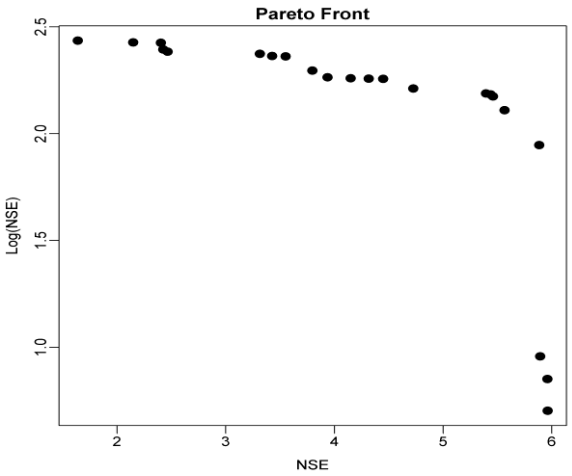

Figure 5.5: Pareto front of non-dominant solution of QRB using Option-I of 'Top-down' approach

basins appears to be satisfactory (NSE>+0.50) except Ridge Creek and Ekapo Creek. The reason for Ridge and Ekapo Creek calibrating poorly may be related to the optimized values of parameters for each GRU. As the QRB contains four GRUs, the sub-basins of QRB may contain four or less than four GRUs. Also, the same optimized values for each GRU was used in each sub-basin. For example, Lewis Creek and Ekapo Creek both contain 'crop' GRU, and the simulation of both these sub-basins use the same optimized values for 'crop' GRU. This was the underlying assumption of Option-I, where the land surface heterogeneity was similar across the QRB. Based on the observation of calibrated NSE of Ridge and Ekapo Creek, it was understood that the land surface heterogeneity of these watersheds was not well represented using Option-I of the top-down approach, which resulted in unsatisfactory calibration. However, in the context of NSE and $PBIAS$, none of the sub-basins shows satisfactory performance during validation. The probable reasons are (i) the underlying assumption of Option-I of the top-down approach is invalid, (ii) calibration of the sub-basins suffered from over fitting, and (iii) hydro-meteorological data were problematic. During the validation, year 2011 and 2013 showed distinct peak flows for all the sub-basins, and it is observed that the magnitude of the peak flow of year 2011 is relatively greater or equal to the magnitude of peak flow of year 2013. However, the validation of model simulations exhibits opposite pattern where the magnitude of peak flow of year 2013 is often greater than the peak of year 2011. This is inaccurate estimation of parameters for QRB sub-basins using Option I. Moreover, simulation of the peak flow of year 2010 and 2014 were mostly poor.

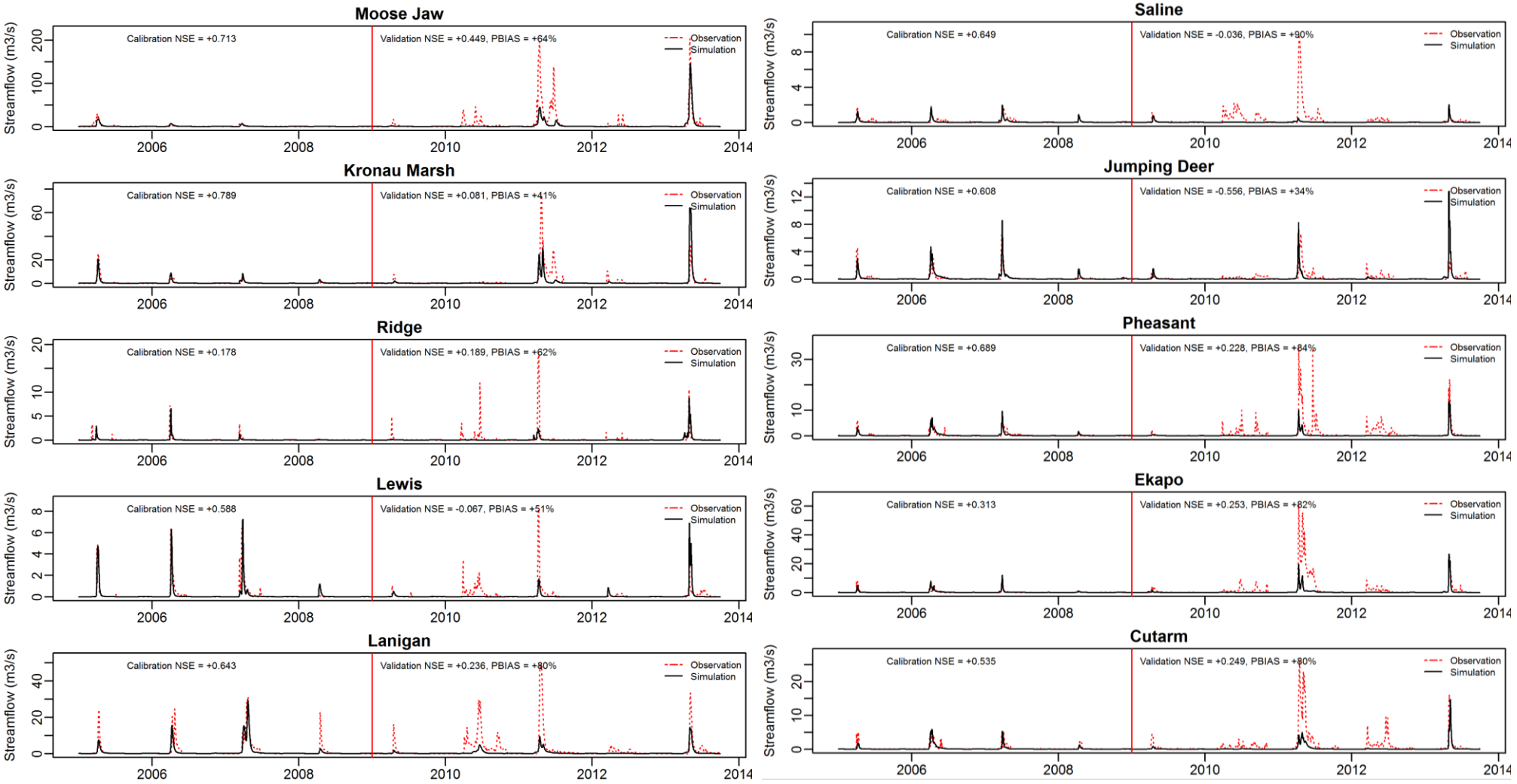

Figure 5.6: Streamflow simulation using Option-I of 'Top-down' approach.

The model performance of MESH for the tributaries are not satisfactory (NS values between -0.557 and +0.449), which affects the performance of the hybrid model. Figure 5.7 shows the calibration and validation of the hybrid model at the outlet of the QRB near Welby, and it appears that the hybrid model was unsatisfactory, which was developed using Option-I of the top-down approach. The simulation of flood peaks during the calibration period contains both magnitude and timing error, which leads to a poor NSE. The performance of the model in the validation period is similar to the performance of MESH models of the tributaries.

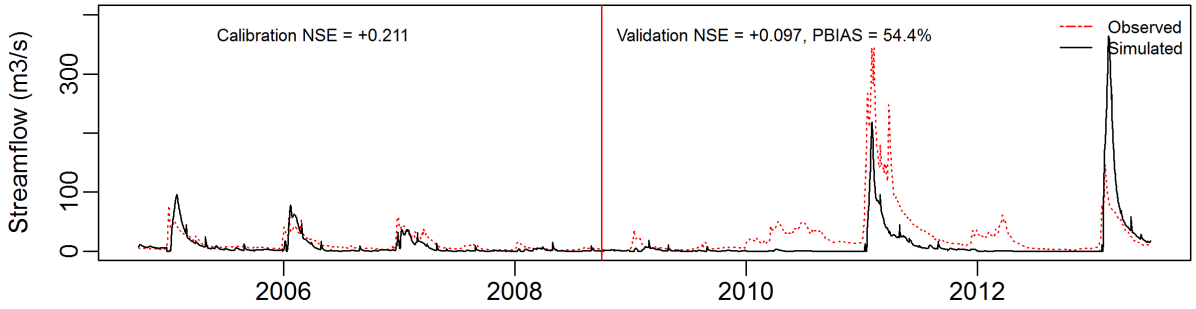

Figure 5.7: Observed and simulated hydrographs for the QRB near Welby using Option-I of the top-down approach.

Option-II allows for assuming non-uniformity of land surface heterogeneity across the sub-basins of the QRB. Figure 5.7 shows the Pareto front of non-dominated solutions of the QRB using Option-II of the top-down approach. Here the objective functions were to maximize NSE and $Log(NSE)$ of the 10 selected sub-basins separately. Similar to the approach adopted in the comparison study (discussed in Chapter-4), a behavioral threshold was set as NSE>+0.50 and $Log(NSE)$>+0.30. It is observed that the optimization of all the sub-basins achieved behavioral solutions except Ridge Creek. The low flow simulations for Ridge Creek is poor ($Log(NSE)$ < 0.0), however, high flow simulation is considered as satisfactory (Maximum NSE = +0.50 was achieved). Reasonable optimized solutions for each watershed was selected from respective pareto fronts, giving priority for high NSE with reasonably high $Log(NSE)$.

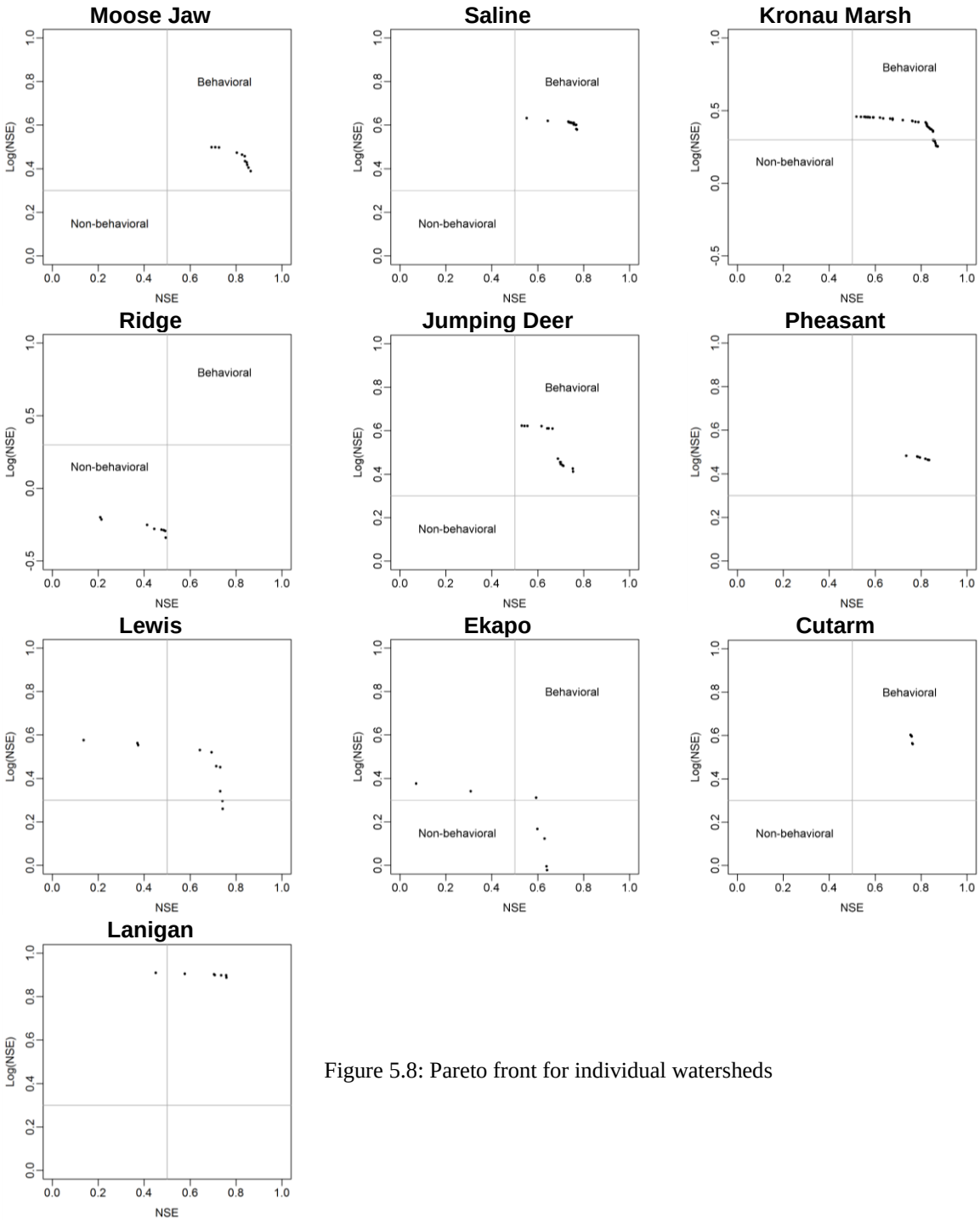

Figure 5.8: Pareto front for individual watersheds

Figure 5.9 shows the calibration and validation results of the selected sub-basins using Option-II. The calibration for all the sub-basins appears to be satisfactory (NSE>+0.50) except Ridge Creek. All the tributaries show 8% to 160% improvement in calibration, suggesting that the assumption of detailed definition of land surface heterogeneity is able to improve the performance of the optimization. Both Ridge Creek and Ekapo Creek did not achieve a satisfactory calibration in Option-I, but these watersheds show significant improvement (160%

and 107%, respectively) in Option-II, which suggests that the land surface heterogeneity is different in these watersheds compared to other sub-basins. However, the validation of the tributaries do not show any improvement over the validation of Option-I. Similar patterns and errors are observed for Option-II, which might be related to the over fitted calibration. Figure 5.10 shows the calibration and validation of the hybrid model at the outlet of the QRB near Welby, and it appears that hybrid model was still unsatisfactory, which was similar to Option-I of the top-down approach. Calibration NSE of the hybrid model using Option-II improves compared to Option-I, which is mainly because of improved calibration NSE of the tributaries. However, validation of the hybrid model using Option-II did not show any improvement over the validation of Option-I. Only the peak flow of year 2013 shows good prediction, but all other years are show underestimated peak flows. It is apparent that none of the options of the top-down approach leads to a satisfactory hybrid model and the main reason is the underperforming MESH models of the tributaries. The lake SD model was shown to be able to simulate the lake interactions and operating rules and predicted streamflow at the outlet of the QRB near Welby with high efficiency. Therefore, developing better MESH models for the tributaries is the primary challenge. It was shown in this analysis that this approach of hybridization allows for connecting two different modelling platforms to simulate hydrological processes and lake operations separately and simulate streamflow at the outlet of a large-scale watershed. Estimated parameter values for the selected optimal solution using Option-I and Option-II is presented in Appendix C.

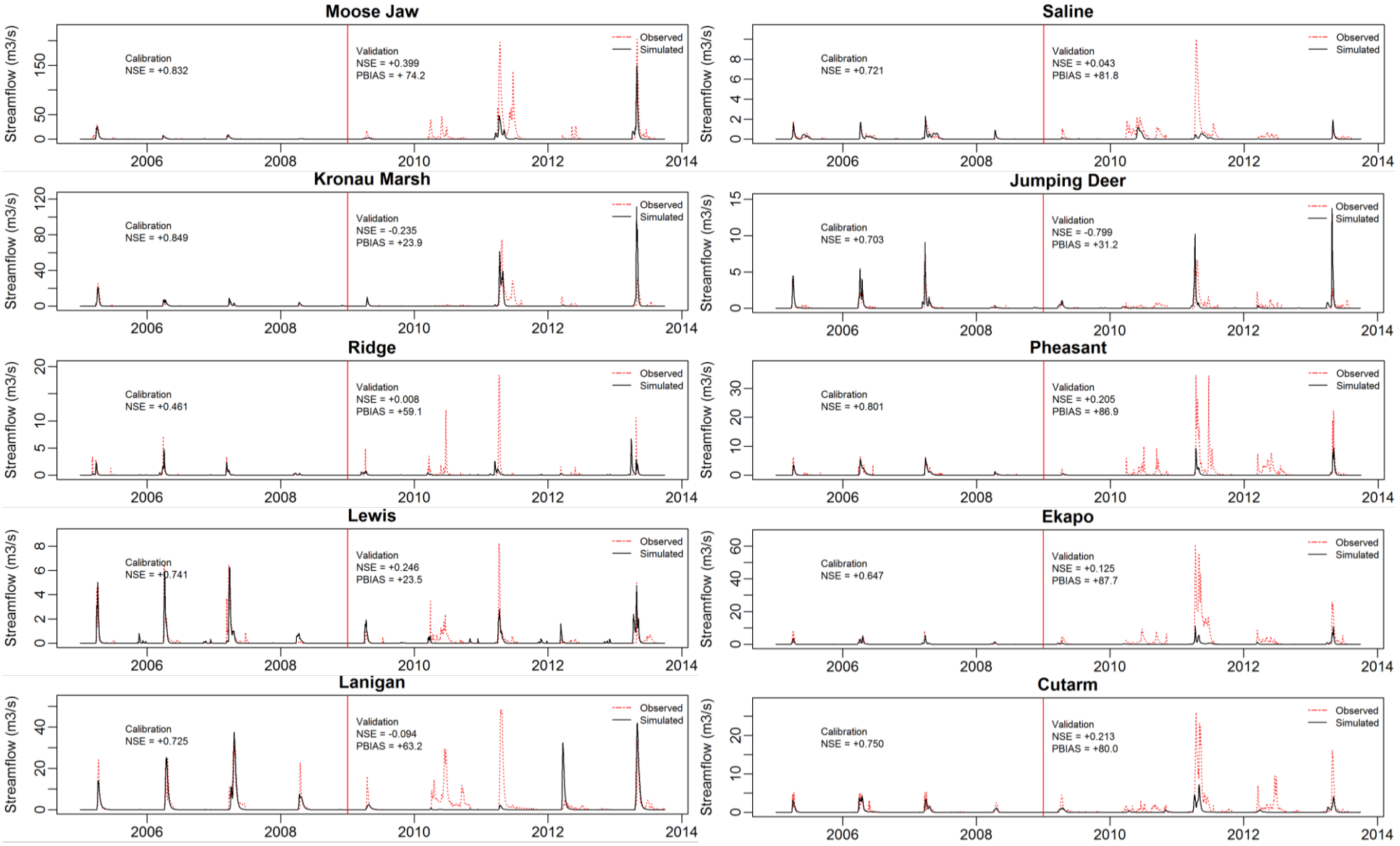

Figure 5.9: Simulated streamflow for individual sub-basins of the QRB.

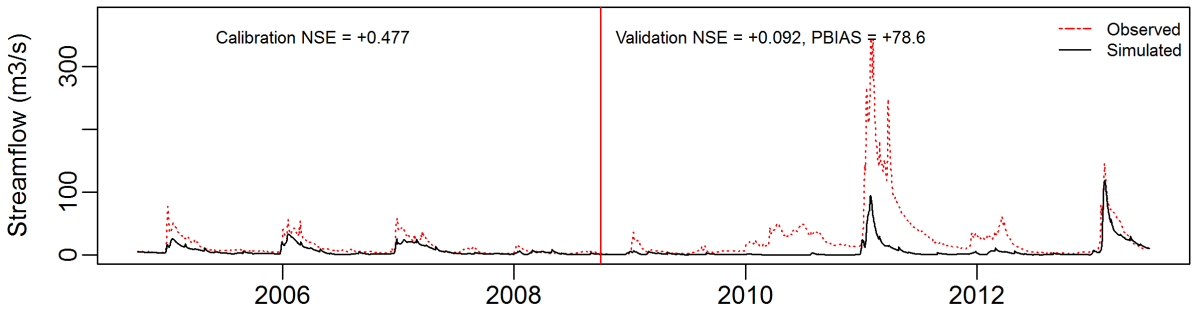

Figure 5.10: Observed and simulated hydrographs for the QRB near Welby using Option-II of the top-down approach.

5.2.2 Model Simulation using Bottom-up Approach

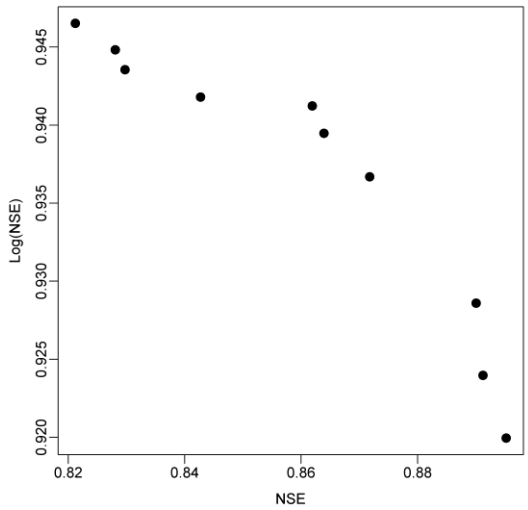

Figure 5.11: Pareto front of non-dominated solutions of QRB using bottom-up approach.

Figure 5.11 shows the Pareto front of non-dominated solutions of the QRB using the bottom-up approach. Here all non-dominated solutions exhibit behavioral solution (NSE > +0.50 and $Log(NSE)$ > +0.30). A reasonable optimization solution was selected from the Pareto front, which exhibits comparatively high NSE along with high $Log(NSE)$ (NSE = +0.84 and $Log(NSE)$ = +0.93). Figure 5.12 shows the calibration and validation results of QRB at Welby using the bottom-up approach. The calibration is considered as satisfactory (NSE > +0.50), however, validation performance is unsatisfactory with NSE and PBIAS values of 0.21 and 68.5%, respectively.

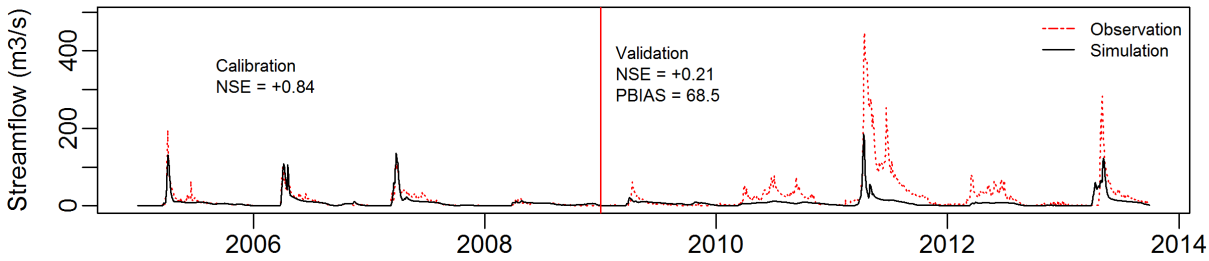

Figure 5.12: Measured and simulated hydrograph of the QRB system near Welby using 'Bottom-up' approach.

Figure 5.13 shows the model performance at different tributaries and it is clear that streamflow simulated at the QRB's tributaries are unsatisfactory (NSE < 0.5) during both calibration and validation periods. Although high NSE (= +0.84) was achieved during the calibration of the model at Welby, the performance of the tributaries is not satisfactory, which is the model optimization process adjusted the outflows from tributaries to improve the model performance at the outlet of the QRB. The bottom-up approach of hybridization is suitable for streamflow simulation at the outlet of the QRB, but it does not simulate sub-basins efficiently. If the generated naturalized flow is validated and adjusted to lower the amount of errors and uncertainties then the bottom-up approach is used for streamflow simulation at the outlet, ignoring the model efficiency at sub-basins level.

It appears that the model performance using the bottom-up approach produced similar outcomes compared to the top-down approach. The simulated streamflow during validation shows a different pattern compared to the top-down approach. The simulated peak flow for year 2011 is estimated greater than that of year 2013, which was opposite for the case of the top-down approach. Validation NSE (=+0.21) in the bottom-up approach is also greater than that of the top-down approach, although not satisfactory. However, the peak flow of year 2010 and 2014 were not captured in this approach either. It is possible that the reasons for unsuccessful validation of the bottom-up approach is similar to those of the top-down approach. Estimated parameter values for the selected optimal solution using 'Bottom-up' approach and 'Top-down' (Option-I) is presented in Appendix D.

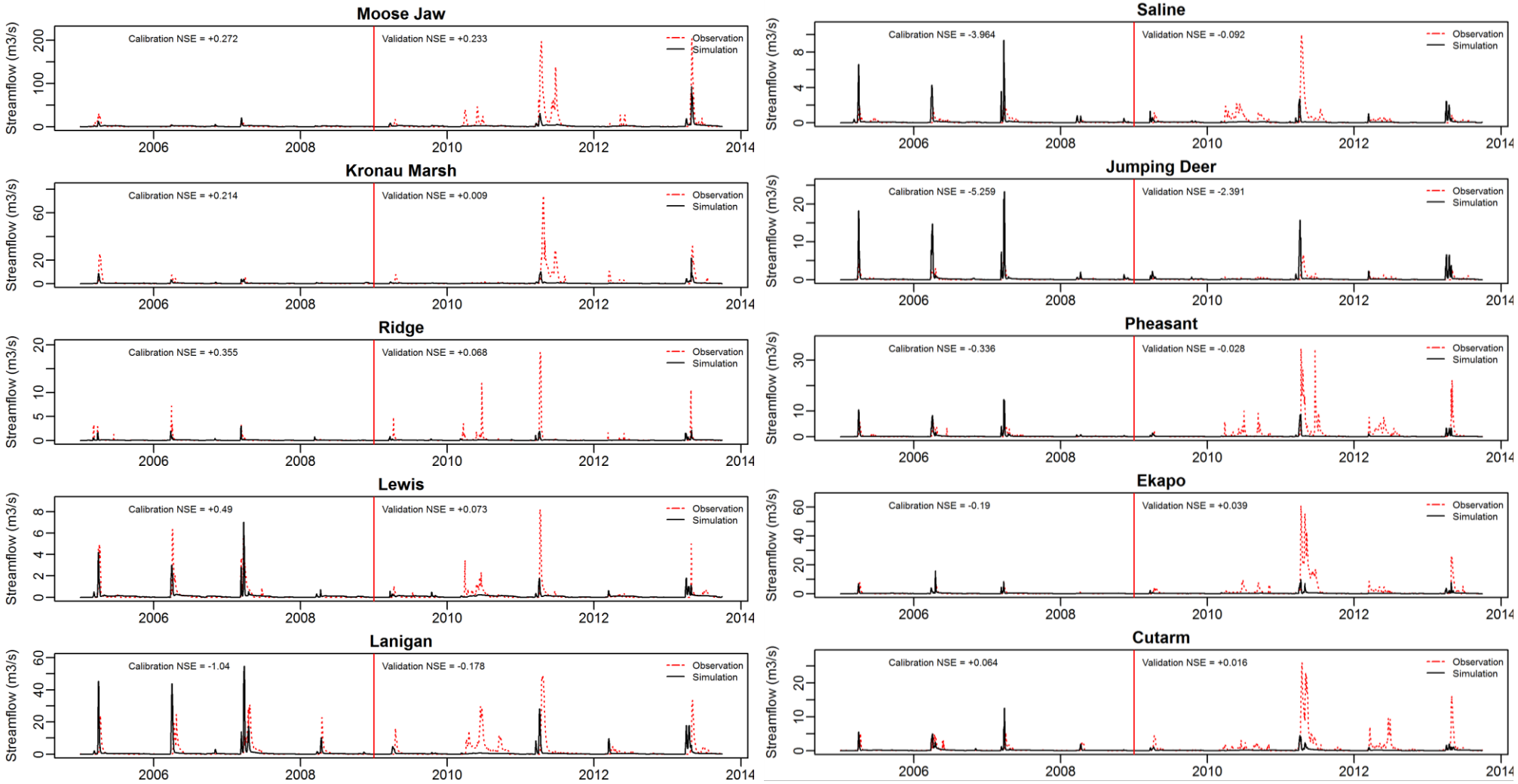

Figure 5.13: Streamflow simulation in the tributaries of the QRB using the hybrid model in the bottom-up approach.

Large-scale hydrological modelling in a prairie watershed is challenging. Developing a hybrid modelling approach for a large-scale prairie watershed is an attempt to simulate the challenges separately and create a common ground so that individual tools can communicate with each other. All the approaches discussed above present different styles of creating a common ground, although the model performance for each case appears unsatisfactory. It is inferred that each tributary sub-basin in a large-scale prairie watershed presents different challenges and addressing them in a similar way may not work. In the Option-II of 'Top-down' approach, separate models were developed for individual tributary sub-basins, which was unable to show a satisfactory validation as well, suggesting that different tributaries need to address differently.

5.2.3 Why is the MESH Model Unsuccessful?

The reason of unsuccessful model validation is possibly related to the hydrological response pattern alteration in the prairies. In a recent work, Savenije and Hrachowitz (2017) provided an opinion that watersheds behave like a meta-organism and they evolve or change their response over a certain period of time. Savenije and Hrachowitz (2017) critically emphasize that the knowledge of hydrology primarily concentrates on correct representation of physics and ignores the representation of ecology, which often plays an important role to change the behavior of a watershed in a long run. Dumanski et al. (2015) conducted a statistical analysis to determine hydrological regime change in the Smith Creek prairie watershed and found that there is a significant increment in rainfall transformation into streamflow, suggesting increased amount of drainage in the prairies. According to Dumanski et al. (2015), year 2010 plays an important role to exhibit an altered hydrological response pattern in the prairies. Figure 5.14 shows the long-term precipitation and streamflow time series (from 1981-2015) near a station close to the outlet of the Moose Jaw River. It is observed that the 90^{th} percentile of daily precipitation varies between 3.42-3.81 mm/d, when averaged over a decadal period shown in the Figure (1981-1991, 1992-2001, 2002-2011, and 2012-2016), suggesting a uniform long

term pattern of extreme precipitation (10% exceedance). However, the 90th percentile of streamflow does not show similar behaviour, and it is observed that the pattern changes over a time period of about 10 years. Streamflow from 1981-1991 and from 2002-2011 show lower values of 90th percentile, indicating low flow periods although few years show flooding in the river (year 1982, 1983, and 2005). However, streamflow from 1992-2001 and from 2012 onward show greater values of 90th percentile flows, indicating high flow periods with few years showing low flows. Now the question is – "why is the streamflow response changing without any significant change of pattern in the precipitation volume?" It is understood that a prairie watershed does not show a conventional rainfall-runoff relation because of complex hydrological features like non-contributing area and surface storage connectivity, which can also be observed in Figure 5.14 as individual peak precipitation does not yield peak streamflow. There are a few possible reasons that a watershed can change the response pattern, such as temperature pattern during the snowmelt season, antecedent soil moisture conditions, mid-winter freeze and thaw, surface drainage connectivity, ecological properties, and human influence. It is possible that the hydrological response is changing because of these reasons acting separately or combined. A comprehensive study is required to identify the most probable reasons for hydrological response change and how they might affect the modelling process. Two major reasons that could cause such a change in hydrological responses are either meteorological or anthropological. Patterns in temperature during snowmelt season and antecedent soil moisture conditions could vastly influence the streamflow and these patterns should be analysed in future studies to identify any changes over a particular time period. It is also known that farmers often dig canals and drain water from neighbouring ponds, which often disrupts natural surface storage connectivity and creates further uncertainties for the model parameterization (Pomeroy et al., 2014; Shook and Pomeroy, 2011). Also, construction of roads and human installations affects prairie drainage. It is a reasonable assumption that the

effect of internally drained ponds and construction is observed after a certain number of years in the means of altered drainage pattern and the effect amplifies over the scale of the basin.

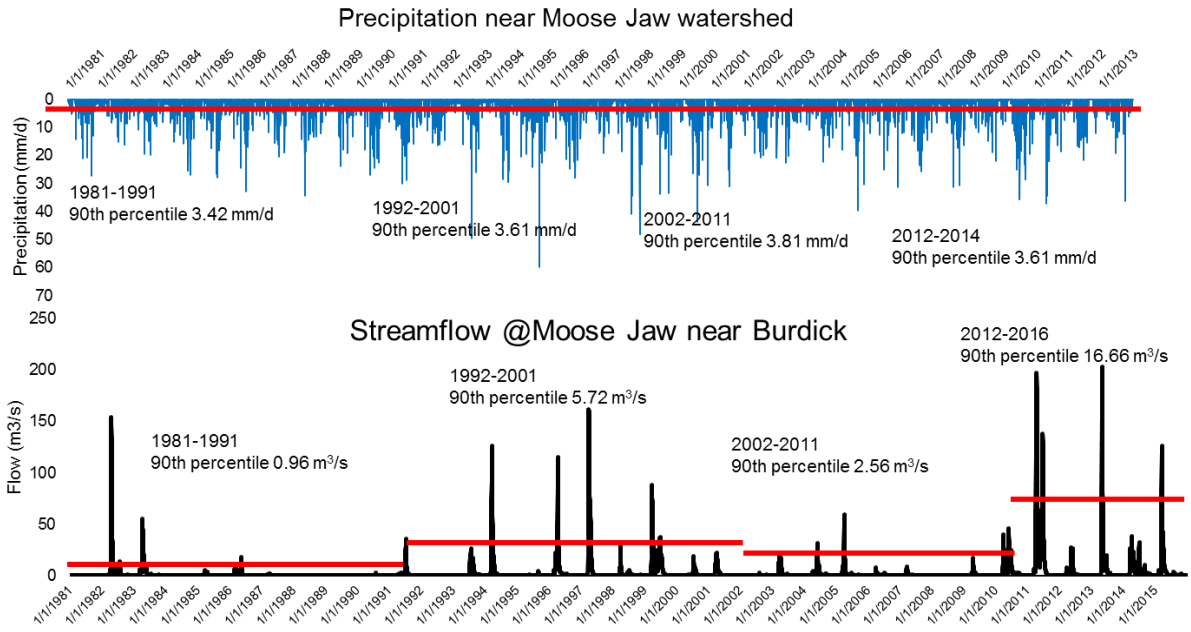

Figure 5.14: Precipitation and streamflow time series near the Moose jaw watershed.

It is possible that the validation of the hybrid model is inefficient because of the altered drainage pattern observed in the prairies. It is unlikely that MESH model can perform well by calibrating from 2004 to 2008 and then validating from 2008 onward because the time periods exhibits different hydrological response patterns. Mekonnen et al. (2016, 2015, 2014) showed a well calibrated hydrological model for the prairies (Moose Jaw and Assiniboine River watershed), however, the modelling period was within 1992-2000 (Mekonnen et al., 2016, 2015) and 2005-2009 (Mekonnen et al., 2014) which shows a uniform drainage pattern according to Figure 5.14. It is possible that these particular models are efficient because of the stationary drainage pattern. Based on these works and Figure 5.14, it is hypothesized that a prairie hydrological model should perform well if - (i) calibrated for more than 20 years to represent the wide range of drainage pattern, or (ii) determining the break point for streamflow alteration and conduct calibration and validation within a period of similar hydrological regime. Here option (i) cannot be tested, because of the unavailability of meteorological data at the time scale required to run

MESH (Hourly gridded data such as CaPA-GEM are available from 2002 onward). However, option (ii) is tested and for this purpose the Moose Jaw watershed was selected. The model setup was similar to the model that was used for Option-II of the top-down approach. The model was calibrated from October 2010 to October 2013 and validated from October 2013 to October 2015. According to Figure 5.15, the model calibrated well with a high NSE (= +0.918). It was also observed that the model performed well during the validation period and a satisfactory NSE (= +0.576) was achieved. The results provide initial verification of the hypothesis of different drainage patterns in different periods. Using this concept and Option-II of the top-down approach, it is possible that a complete hybrid model for the QRB might perform well however, the complete hybrid model was not developed using this hypothesis due to time constraint.

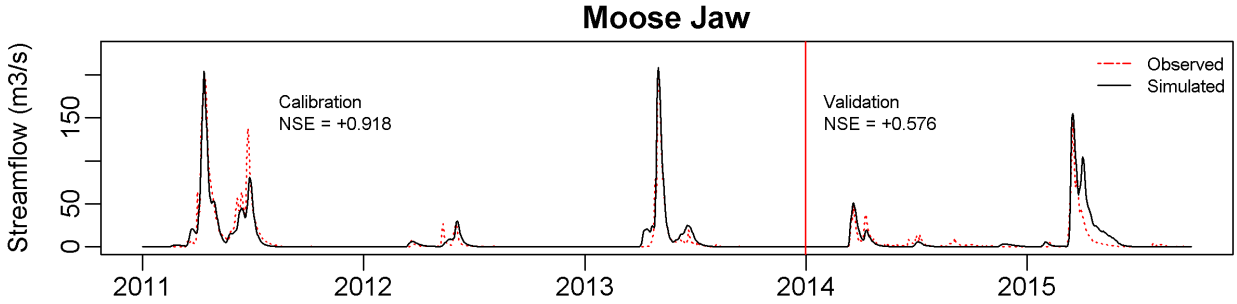

Figure 5.15: Observed and simulated hydrographs for Moose Jaw watershed.

It was understood that streamflow data showed an altered pattern of drainage connectivity from year 2010 onward. Now the question is- 'how the drainage response alteration is explained from a modelling point of view?' To address this, let us look at two separate model results for the Moose Jaw River watershed- (i) model of the Moose Jaw river watershed calibrated from 2004 to 2008 and validated from 2009 to 2014. , which did not show satisfactory validation (from 2009 to 2014) despite acceptable calibration performance (calibration NSE: +0.832, validation NSE: +0.399) (Figure 5.9), and (ii) model of the Moose Jaw river watershed calibrated from 2010 to 2013, which exhibits satisfactory calibration and validation performance from 2014 to 2015 (calibration NSE: +0.918, validation NSE: +0.576) (Figure

5.15). Figure 5.16 shows the comparison of the estimated normalized values of drainage parameters from the two models calibrated based on two different periods (2004-2008 and 2010-2013). The parameter sets for high performing models (NSE > +0.80) were selected for analysis. As the results suggest, the identifiable nature and values change for some of the drainage parameters. For example, the shape factor (b) for GRU-crop and GRU-grass exhibit interchanging identifiability i.e. identifiable in one model and unidentifiable in another model. Surface storage capacity for the non-contributing area (C_{max}_nca) shows increased storage capacity in the first model, whereas in the second model, it shows lower surface storage capacity and is more identifiable. This variation suggests that the non-contributing area holds less amount of water in the latter model, and responds more quickly. However, surface storage capacity for the GRU-crop (C_{max}_crop) is mostly similar and that for GRU-grass (C_{max}_grass) is slightly higher in the second model. The estimated parameters of non-contributing area carry high importance because the proportion for non-contributing area (57%) is comparatively greater than crop (39%) and grass (4%). Similar to C_{max}, limiting snow depth ($zsnl$) also exhibits lower identifiable value from 2010 onwards, suggesting a prompt runoff response during snow melting season. Comparison for the remaining parameters suggest that the model calibrated from 2010 to 2013 shows a lower water holding capacity and faster runoff response whereas the model calibrated from 2004 to 2008 shows a contrasting scenario.

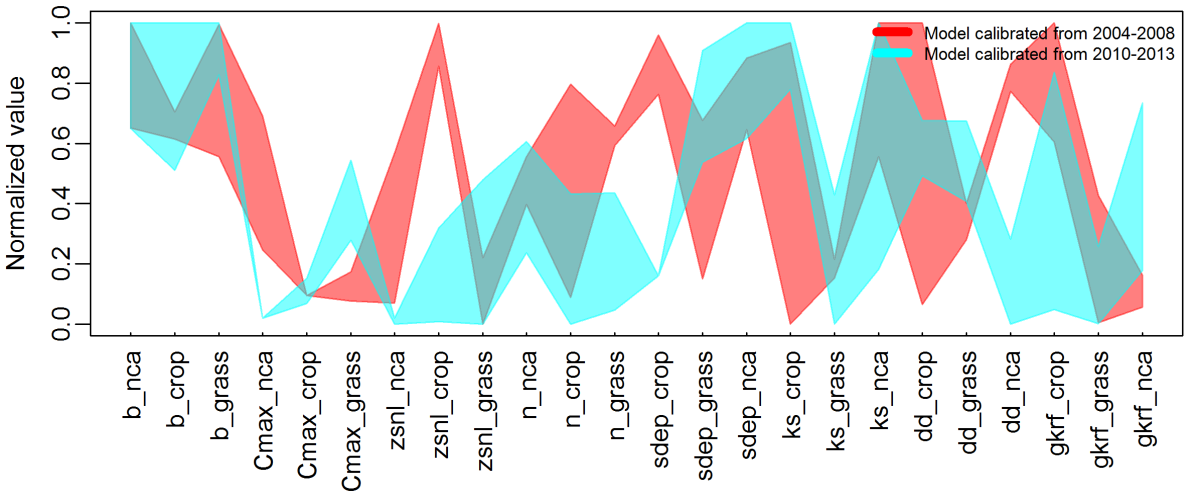

Figure 5.16: Comparison of drainage parameters for the model of the Moose Jaw river watershed was calibrated from 2004 to 2008 and from 2010 to 2013.

The results suggest that the hydrological model parameters are calibrated such that it reduces surface water holding capacity and increases streamflow response during snowmelt period. The change in parameter ranges and subsequent effects on the model performance could be due to changes in drainage patterns within the watershed. However, this cannot be ascertained for the Moose Jaw watershed due to unavailability of information regarding landuse change. Dumanski et al. (2015) observed similar changes in the Smith Creek prairie watershed, where they were able to attribute change in streamflow to reduction in ponded area by 58% and increase in drainage channel length by 780% over last 50 years. Similar observation was reported by Ehsanzadeh et al. (2016, 2012) for multiple watersheds in the prairies. Similar trend is assumed for the Moose Jaw watershed cautiously. A thorough investigation on the isolated and combined effect of meteorological and anthropogenic change could provide conclusive evidence of streamflow pattern change.

Chapter 6: Summary and Conclusion

Developing a hydrological systems model for a large-scale prairie watershed poses a number of challenges, which are mainly fill and spill runoff propagation, dynamic behavior of drainage contribution area, water management and regulation, and uncertainty and unavailability of meteorological data at fine temporal scale. There is a necessity to address some of these challenges and develop a suitable integrated modelling approach for large-scale prairie watersheds. MESH is a well-known hydrological modelling tool in Canada and it has the mechanism to address some of the above-mentioned challenges using different approaches, such as, remote sensing, probabilistic, and data driven approaches. Each approach exhibits its merits and demerits, and there is a scope to improve existing modelling methods for the prairies. The Qu'Appelle River basin (QRB) was selected for this research because it is located in the prairies and contains a complex network of multiple interconnected lakes. Moreover, the QRB represents a classic case of the challenging prairie topography, combined with the cold region hydrological processes. Because the representation of the interconnected controlled and uncontrolled lakes is often difficult to using a hydrological modelling tool, such as MESH, a systems modelling approach for lake operations was developed using system dynamics (SD). Consequently, the SD model was combined with the MESH model that simulates the natural hydrological processes in one hybrid modelling framework. .

6.1 Runoff Generation Algorithms

Runoff generation varies for different ecozones of Canada, and the prime reason is the varying topography, which directly affects the runoff generation and its propagation to the nearest streams. Canadian prairie topography, in particular, is very challenging to be represented in any land surface model to simulate hydrological processes because of the presence of variable contributing area (non-contributing area). In this study, we proposed blending the merits of two

existing runoff generation algorithms (WATROF and PDMROF) to develop LATFLOW, which could be suitable for applications over prairie and non-prairie watersheds. LATFLOW utilizes probabilistic distribution of surface storages with variable capacity to estimate surface runoff and the approximate solution of Richards' equation to estimate interflow. LATFLOW was compared with WATROF and PDMROF through MESH to simulate streamflow in three different watersheds located in two distinct ecozones. This comparison analysis also helped in identifying suitable runoff generation algorithms for prairie and non-prairie watersheds. Results indicated that the physically based runoff generation algorithm (WATROF) performed well for non-prairie watersheds (White Gull Creek) and the probabilistic runoff generation algorithms (PDMROF and LATFLOW) performed better in prairie watersheds (Brightwater Creek and Kronau Marsh). Probabilistic runoff generation algorithms also performed reasonably well in non-prairie watersheds, indicating their ability to represent various types of topography. The LATFLOW algorithm performed better than the PDMROF algorithm at simulating streamflow in prairie watersheds (Brightwater Creek and Kronau Marsh). LATFLOW has the flexibility to use near surface routing during snowmelt season or any rain event, which was achieved by incorporating interflow mechanism. LATFLOW is considered as in-between WATROF and PDMROF as it utilizes the parameterization of PDMROF for overland runoff estimation and the interflow parameterization of WATROF.

6.2 Development of the Lake System Model

In this part of the research, focus was on developing a numerical model for the complex lake system of QRB. There are eight major lakes located in QRB and all of them are connected with each other, creating complex dynamics of lake response. The lake model was intended to simulate the lake operations and interactions by addressing storage area-release relationship. A System Dynamics (SD) approach was used for the lake system model development using a STELLA 10.1 software (cite a reference here for the software developer). The model was

developed using measured inflow from the tributaries, because the primary focus was to model the lake operations and interactions correctly. The model was calibrated and validated using the simulated and measured streamflow at the outlet of the QRB near Welby. The model was evaluated using streamflow at three locations (i.e. Lumsden, Craven, and Welby) for discharge, and at every lake for water level. It was observed that the developed lake SD model was able to simulate streamflow with high accuracy. Prediction of the water level for all the lakes were also good except the Buffalo Pound Lake, where the simulated water level correlated poorly with the measured water level. All the parameters also exhibited identifiability except the evaporation and snowmelt parameters of the Katepwa Lake. Parameter sensitivity analysis showed that the drainage contribution from the ungauged portion of a watershed important for all the lakes, indicating the necessity of estimating these flows using a well-calibrated hydrological model.

6.3 Hybrid MESH-SD Modelling

Following the development of the SD model, a hybrid model was developed to include the lake management information (e.g., lake operations, interaction between multiple lakes) into the hydrological model (MESH). Developing a hybrid model by combining two or more models has a potential to address complex hydrological problems. The MESH models for natural watersheds like the Kronau Marsh and the Brightwater Creek watersheds were efficient at handling the prairie hydrological features. However, it was likely that the complex water resources management would not be addressed appropriately using MESH alone for a large-scale prairie watershed. In the hybrid model, MESH (used for the prairie hydrological Modelling) was coupled with the lake system dynamics (SD) model (used to represent lake operations and interactions). Different approaches of hybridization process were tested, i.e., ‘top-down’ and ‘bottom-up’. In the ‘top-down’ approach, the modelling process initiates from the headwater regions, estimating the outflows from the tributaries (both gauged and ungauged)

using MESH, feeding the estimated outflow to the lake SD model and using of the lake SD model to estimate streamflow at the outlet near Welby. In the 'bottom-up' approach, the modelling process initiates from the outlet by generating a naturalized flow for streamflow near Welby using the lake model, and estimating parameters for the QRB model considering the naturalized flow conditions. Both the approaches were tested and the results indicated that such an approach improves the representation of lakes in the QRB, but does not provide significantly improved performance of the flow prediction at QRB outlet. The performance of the lake SD model shows that it is able to simulate the lake operations and interactions successfully and it can simulate streamflow with high efficiency, however, the problem lies with the simulation of MESH model in the headwater areas. During the validation of MESH model, year 2011 and 2013 were showing distinct peak flows for all the sub-basins of QRB considered in this study, and it was observed that none of these peaks was efficiently estimated using any of the hybridization approaches. It was shown in this study that these approaches of hybridization were able to connect two different modelling platforms to simulate hydrological processes and lake operations simultaneously and simulate streamflow at the outlet of a large-scale watershed. However, they require considerable improvements in the form of better model discretization in MESH to increase their efficiency in simulating natural streamflow.

It appears that the selected time period of the model calibration and validation also posed another challenge due to high variability in the drainage response. The streamflow response appears to be different from year 2010 onward, which made the model validation inefficient, when calibrated using pre- 2010 data. An alternative approach was also tested by calibrating MESH model for the Moose Jaw River watershed (a sub-basin of the QRB) based on 2011 to 2013-time window. This model showed satisfactory validation for 2014-2015, suggests that the developed MESH model can estimate outflow from the tributaries efficiently if calibrated and validated over a stationary time period. The alteration in drainage pattern is observed in the

estimated parameter values of the Moose Jaw river watershed**,** where higher and prompt runoff response is reflected by the parameters governing surface storage when calibrated from 2010 to 2013. Drainage pattern of the Moose Jaw River watershed is likely to have been altered due to anthropogenic activities. The effects of such activities are reflected in terms of lower surface storage capacity, and prompt response during snowmelt and precipitation events. Similar phenomena were observed over other parts of the prairies by many researchers, however, the quantification of such an effect requires further studies.

6.4 Limitations and Future Work

The limitations of this research are related to the modelling assumptions and data preparation processes. Some of the important limitations of this work are listed below.

(i) It was assumed that collected data from ECCC, WSA and relevant websites are already quality controlled. No additional in-depth data checks or bias correction was conducted here.

(ii) The development of LATFLOW only addresses one of the limitations of PDMROF, which is PDMROF's inability to estimate interflow, however, remaining important limitations of PDMROF such as the absence of pond to pond spill path sequence, actual runoff pathway representation, and hysteretic storage-discharge relationship pass into LATFLOW.

(iii) During the development of the lake SD model, it was realized that the operating levels of weirs provided by WSA do not allow for proper simulation of lake elevations, which suggest that either WSA follows different weir guideline information or collected weir elevations are outdated. A trial and error method was used to assume suitable weir elevation that allows for simulating the lake water level efficiently for a longer time period.

(iv) There was a scope to develop the hybrid model using meteorological data from sources other than CaPA-GEM (e.g. ANUSPLIN, hydro-meteorological, and AHCCD data by ECCC).

This was not attempted in this research, because the data preparation processes for MESH and the SD model are fairly complex and time consuming.

The future scope of research in this area could be towards addressing the limitations of the research presented in this thesis as well as towards providing improvements to the hybrid model. The development of LATFLOW is considered as the next development phase in the direction of accurate runoff generation algorithm for the prairies. A hybrid approach was presented in this research; however, the hybrid model could benefit from multiple improvements and these are not tried as part of this research due to time constraints. After developing MESH model for the tributaries using the hydro-meteorological data from 2011 onward, a complete and satisfactory hybrid model is developed, which is an important component of the FloodNet Project 4-3 that motivated the work presented in this thesis.

References

Abbaspour, K.C., Yang, J., Maximov, I., Siber, R., Bogner, K., Mieleitner, J., Zobrist, J., Srinivasan, R., 2007. Modelling hydrology and water quality in the pre-alpine/alpine Thur watershed using SWAT. J. Hydrol. 333, 413–430. https://doi.org/10.1016/j.jhydrol.2006.09.014

Abbott, M.B., Bathurst, J.C., Cunge, J.A., O'Connell, P.E., Rasmussen, J., 1986. An introduction to the European Hydrological System - Systeme Hydrologique Europeen, "SHE", 1: History and philosophy of a physically-based, distributed modelling system. J. Hydrol. 87, 45–59. https://doi.org/10.1016/0022-1694(86)90114-9

Abedini, M.J., 1998. On Depression Storages, Its Modeling and Scale. University of Guelph.

Akaike, H., 1974. A New Look at the Statistical Model Identification. IEEE Trans. Automat. Contr. 19, 716–723. https://doi.org/10.1109/TAC.1974.1100705

Asadzadeh, M., Tolson, B., 2012. Hybrid Pareto archived dynamically dimensioned search for multi-objective combinatorial optimization: Application to water distribution network design. J. Hydroinformatics 14, 192–205. https://doi.org/10.2166/hydro.2011.098

Asadzadeh, M., Tolson, B., 2009. A New Multi-Objective Algorithm , Pareto Archived DDS, in: In Proceedings of the 11th Annual Conference Companion on Genetic and Evolutionary Computation Conference: Late Breaking Papers (GECCO'09). ACM, New York, NY, USA, Montreal, QC, Canada, pp. 1963–1966.

Barlas, Y., 1996. Formal aspects of model validity and validation in system dynamics. Syst. Dyn. Rev. 12, 183–210. https://doi.org/10.1002/(SICI)1099-1727(199623)12:3<183::AID-SDR103>3.0.CO;2-4

Bell, V.A., Kay, A.L., Jones, R.G., Moore, R.J., 2007. Use of a grid-based hydrological model and regional climate model outputs to assess changing flood risk. Int. J. Climatol. 27, 1657–1671. https://doi.org/10.1002/joc.1539

Bell, V.A., Kay, A.L., Jones, R.G., Moore, R.J., Reynard, N.S., 2009. Use of soil data in a grid-based hydrological model to estimate spatial variation in changing flood risk across the UK. J. Hydrol. 377, 335–350. https://doi.org/10.1016/j.jhydrol.2009.08.031

Beven, K., 1989. Changing ideas in hydrology - The case of physically-based models. J. Hydrol. 105, 157–172. https://doi.org/10.1016/0022-1694(89)90101-7

Brannen, R., Spence, C., Ireson, A., 2015. Influence of shallow groundwater-surface water interactions on the hydrological connectivity and water budget of a wetland complex. Hydrol. Process. 29, 3862–3877. https://doi.org/10.1002/hyp.10563

Burnash, R.J.C., Ferral, R.L., McGuire, R.A., 1973. A generalized streamflow simulation system—Conceptual modelling for digital computers.

Campolongo, F., Cariboni, J., Saltelli, A., 2007. An effective screening design for sensitivity analysis of large models. Environ. Model. Softw. 22, 1509–1518.

https://doi.org/10.1016/j.envsoft.2006.10.004

Canadian Hydraulics Center, 2010. Green Kenue Reference Manual. Ottawa, Ontario.

Chen, J., Adams, B.J., 2006. Integration of artificial neural networks with conceptual models in rainfall-runoff modeling. J. Hydrol. 318, 232–249. https://doi.org/10.1016/j.jhydrol.2005.06.017

Chiew, F.H.S., McMahon, T.A., 2002. Modelling the impacts of climate change on Australian streamflow. Hydrol. Process. 16, 1235–1245. https://doi.org/10.1002/hyp.1059

Chow, V. Te, Maidment, D.R., Mays, L.W., 1988. Applied Hydrology, Internatio. ed. McGraw-Hill.

Christiansen, E.A., 1979. The Wisconsinan deglaciation of southern Saskatchewan and adjacent areas. Can. J. Earth Sci. 17, 541–541. https://doi.org/10.1139/e80-052

Chu, J., Peng, Y., Ding, W., Li, Y., 2015. A Heuristic Dynamically Dimensioned Search with Sensitivity Information (HDDS-S) and Application to River Basin Management. Water 7, 2214–2238. https://doi.org/10.3390/w7052214

Chua, L.H.C., Wong, T.S.W., 2010. Improving event-based rainfall-runoff modeling using a combined artificial neural network-kinematic wave approach. J. Hydrol. 390, 92–107. https://doi.org/10.1016/j.jhydrol.2010.06.037

Clark, M.P., Fan, Y., Lawrence, D.M., Adam, J.C., Bolster, D., Gochis, D.J., Hooper, R.P., Kumar, M., Leung, L.R., Mackay, D.S., Maxwell, R.M., Shen, C., Swenson, S.C., Zeng, X., 2015. Improving the representation of hydrologic processes in Earth SystemModels. Water Resour. Res. 51(8), 5929–5956. https://doi.org/10.1002/2015WR017096.Received

Corzo, G., Solomatine, D.P., de Wit, M., Werner, M., Uhlenbrook, S., Price, R.K., 2009. Combining semi-distributed process-based and data-driven models in flow simulation: a case study of the Meuse river basin. Hydrol. Earth Syst. Sci 13, 1619–1634.

Crawford, N.H., Linsley, R.K., 1966. Digital Simulation in Hydrology Stanford Watershed Model 4.

Davison, B., Pietroniro, A., Fortin, V., Leconte, R., Mamo, M., Yau, M.K., 2016. What is Missing from the Prescription of Hydrology for Land Surface Schemes? J. Hydrometeorol. 17, 2013–2039. https://doi.org/10.1175/JHM-D-15- 0172.1

Davison, B., Pohl, S., Domes, P., Marsh, P., Pietroniro, A., MacKay, M., 2006. Characterizing snowmelt variability in a land-surface-hydrologic model. Atmosphere-Ocean 44, 271–287. https://doi.org/10.3137/ao.440305

Dawdy, D.R., O'Donnell, T., 1965. Mathematical Models of Catchment Behavior. J. Hydraul. Div. 91, 123–137.

Díaz-Robles, L.A., Ortega, J.C., Fu, J.S., Reed, G.D., Chow, J.C., Watson, J.G., Moncada-Herrera, J.A., 2008. A hybrid ARIMA and artificial neural networks model to forecast particulate matter in urban areas: The case of Temuco, Chile. Atmos. Environ. 42, 8331–8340. https://doi.org/10.1016/j.atmosenv.2008.07.020

Dingman, S.L., 2002. Physical Hydrology, Second. ed. Waveland Press, Inc., Long Grove, IL.

Dooge, J., 1973. Linear theory of hydrologic systems. USDA Technical Bulletins TB 1468, Washington, D.C.

Dooge, J., 1959. A General Theory of the Unit Hydrograph. J. Geophys. Res. 64, 241–256.

Dornes, P.F., Tolson, B., Davison, B., Pietroniro, A., Pomeroy, J.W., Marsh, P., 2008. Regionalisation of land surface hydrological model parameters in subarctic and arctic environments. Phys. Chem. Earth 33, 1081–1089. https://doi.org/10.1016/j.pce.2008.07.007

Du, J., Xie, S., Xu, Y., Xu, C., Singh, V.P., 2007. Development and testing of a simple physically-based distributed rainfall-runoff model for storm runoff simulation in humid forested basins. J. Hydrol. 336, 334–346. https://doi.org/10.1016/j.jhydrol.2007.01.015

Dumanski, S., Pomeroy, J.W., Westbrook, C.J., 2015. Hydrological regime changes in a Canadian Prairie basin. Hydrol. Process. 29, 3893–3904. https://doi.org/10.1002/hyp.10567

Dunne, T., Black, R.D., 1970. An experimental investigation runol production. Water Resour. Res. 6, 478–490.

Efstratiadis, A., Nalbantis, I., Koukouvinos, A., Rozos, E., Koutsoyiannis, D., 2008. HYDROGEIOS: a semi-distributed GIS-based hydrological model for modified river basins. Hydrol. Earth Syst. Sci. 12, 989–1006. https://doi.org/10.5194/hess-12-989-2008

Ehsanzadeh, E., van der Kamp, G., Spence, C., 2016. On the changes in long-term streamflow regimes in the North American Prairies. Hydrol. Sci. J. 61, 64–78. https://doi.org/10.1080/02626667.2014.967249

Ehsanzadeh, E., van der Kamp, G., Spence, C., 2012. The impact of climatic variability and change in the hydroclimatology of Lake Winnipeg watershed. Hydrol. Process. 26, 2802–2813. https://doi.org/10.1002/hyp.8327

Elliott, J.A., Efetha, A.A., 1999. Influence of tillage and cropping system on soil organic matter, structure and infiltration in a rolling landscape. Can. J. Soil Sci. 79, 457–463. https://doi.org/10.4141/S98-075

Elshorbagy, A., Jutla, A., Barbour, L., Kells, J., 2005. System dynamics approach to assess the sustainability of reclamation of disturbed watersheds. Can. J. Civ. Eng. 32, 144–158. https://doi.org/10.1139/l04-112

Elshorbagy, A., Jutla, A., Kells, J., 2007. Simulation of the hydrological processes on reconstructed watersheds using system dynamics. Hydrol. Sci. J. 52, 538–562. https://doi.org/10.1623/hysj.52.3.538

Fang, X., Minke, A., Pomeroy, J.W., Brown, T., Westbrook, C.J., Guo, X., Guangul, S., 2007. A Review of Canadian Prairie Hydrology : Principles , Modelling and Response to Land Use and Drainage Change. Saskatoon, Saskatchewan.

Fang, X., Pomeroy, J.W., 2009. Modelling blowing snow redistribution to prairie wetlands.

Hydrol. Process. 23, 2557–2569. https://doi.org/10.1002/hyp.7348

Fletcher, E.J., 1998. The use of system dynamics as a decision support tool for the management of surface water resources, in: 1st Int. Conf. on New Information Technolo. for Decision-Making. University of Quebec, Montreal, Canada, pp. 909–920.

Forrester, J., 1961. Industrial dynamics. M.I.T. Press, Cambridge, Massachusetts.

Freeze, R.A., 1972. Role of Subsurface Flow in Generating Surface Runoff 1. Base Flow Contributions to Channel Flow. Water Resour. Res. 8.

Gastélum, J.R., Valdés, J.B., Stewart, S., 2010. A system dynamics model to evaluate temporary water transfers in the Mexican Conchos Basin. Water Resour. Manag. 24, 1285–1311. https://doi.org/10.1007/s11269-009-9497-z

Ghan, S.J., Liljegren, J.C., Shaw, W.J., Hubbe, J.H., Doran, J.C., 1997. Influence of subgrid variability on surface hydrology. J. Clim. 10, 3157–3166. https://doi.org/10.1175/1520-0442(1997)010<3157:IOSVOS>2.0.CO;2

Gonda, J., 2015. Assessing the Tradeoffs of Water Allocation: Design and Application of an Integrated Water Resources Model. University of Saskatchewan.

Granger, R.J., Gray, D.M., 1989. Evaporation from natural nonsaturated surfaces. J. Hydrol. 111, 21–29. https://doi.org/10.1016/0022-1694(89)90249-7

Gray, D.M., 1973. Handbook on the principles of hydrology: with special emphasis directed to Canadian conditions in the discussions, applications, and presentation of data. Water Information Center Inc.

Gray, D.M., Landine, P.G., 1988. An energy-budget snowmelt model for the Canadian Prairies. Can. J. Earth Sci. 25, 1292–1303. https://doi.org/10.1139/e88-124

Gray, D.M., Landine, P.G., Granger, R.J., 1985. Simulating infiltration into frozen Prairie soils in streamflow models. Can. J. Earth Sci. 22, 464–474.

Gray, D.M., Toth, B., Zhao, L., Pomeroy, J.W., Granger, R., 2001. Estimating areal snowmelt infiltration into frozen soils. Hydrol. Process. 15, 3095–3111. https://doi.org/10.1002/hyp.320

Guo, W., Wang, C., Zeng, X., Ma, T., Yang, H., 2015. Subgrid parameterization of the soil moisture storage capacity for a distributed rainfall-runoff model. Water 7, 2691–2706. https://doi.org/10.3390/w7062691

Haghnegahdar, A., Tolson, B., Craig, J.R., Paya, K.T., 2015. Assessing the performance of a semi-distributed hydrological model under various watershed discretization schemes. Hydrol. Process. 4031, n/a-n/a. https://doi.org/10.1002/hyp.10550

Haghnegahdar, A., Tolson, B., Davison, B., Seglenieks, F.R., Klyszejko, E., Soulis, E.D., Fortin, V., Matott, L.S., 2014. Calibrating Environment Canada's MESH modeling system over the Great Lakes basin. Atmosphere-Ocean 52, 281–293. https://doi.org/10.1080/07055900.2014.939131

Hamilton, D.P., Schladow, S.G., 1997. Prediction of water quality in lakes and reservoirs. Part I — Model description. Ecol. Modell. 96, 91–110. https://doi.org/10.1016/S0304-3800(96)00062-2

Hammer, U.T., 1971. Limnological Studies of the Lakes and Streams of the Upper Qu â€™ Appelle River System, Saskatchewan, Canada I . Chemical and Physical Aspects of the Lakes and Drainage System. Hydrobiologia 37, 473–507.

Hassanzadeh, E., Elshorbagy, A., Wheater, H.S., Gober, P., 2016. A risk-based framework for water resource management under changing water availability, policy options, and irrigation expansion. Adv. Water Resour. 94, 291–306. https://doi.org/10.1016/j.advwatres.2016.05.018

Hassanzadeh, E., Elshorbagy, A., Wheater, H.S., Gober, P., 2014. Managing water in complex systems: An integrated water resources model for Saskatchewan, Canada. Environ. Model. Softw. 58, 12–26. https://doi.org/10.1016/j.envsoft.2014.03.015

Hassanzadeh, E., Elshorbagy, A., Wheater, H.S., Gober, P., Nazemi, A., Croke, B., Lecturer, S., Harou, J., 2015. Integrating supply uncertainties from stochastic modeling into integrated water resource management : a case study of the Saskatchewan River Basin. J. Water Resour. Plan. Manag. 142, 1–12. https://doi.org/10.1061/(ASCE)WR.1943-5452.0000581.

Hayashi, M., Van der Kamp, G., Rosenberry, D.O., 2016. Hydrology of Prairie Wetlands: Understanding the Integrated Surface-Water and Groundwater Processes. Wetlands. https://doi.org/10.1007/s13157-016-0797-9

Hayashi, M., Van Der Kamp, G., Rudolph, D.L., 1998. Water and solute transfer between a prairie wetland and adjacent uplands, 1. Water balance. J. Hydrol. 207, 56–67. https://doi.org/10.1016/S0022-1694(98)00099-7

Hayashi, M., van der Kamp, G., Schmidt, R., 2003. Focused infiltration of snowmelt water in partially frozen soil under small depressions. J. Hydrol. 270, 214–229. https://doi.org/10.1016/S0022-1694(02)00287-1

Hesse, C., Krysanova, V., Päzolt, J., Hattermann, F.F., 2008. Eco-hydrological modelling in a highly regulated lowland catchment to find measures for improving water quality. Ecol. Modell. 218, 135–148. https://doi.org/10.1016/j.ecolmodel.2008.06.035

Hewlett, J.D., Hibbert, A.R., 1967. Factors affecting the response of small watersheds to precipitation in humid area, in: International Symposium on Forest Hydrology. Pergamon, New York, pp. 275–290.

Horton, R.E., 1933. The Rôle of infiltration in the hydrologic cycle. Trans. Am. Geophys. Union 14, 446. https://doi.org/10.1029/TR014i001p00446

Horton, R.E., 1907. Weir Experiments , Coefficients , and Formulas, Department of the Interior, United State Geological Survey.

ISEE Systems Inc., 2013. Getting Started with iThink and STELLA 10.

Jain, A., Srinivasulu, S., 2006. Integrated approach to model decomposed flow hydrograph

using artificial neural network and conceptual techniques. J. Hydrol. 317, 291–306. https://doi.org/10.1016/j.jhydrol.2005.05.022

Jajarmizad, M., Harun, S., Salarpour, M., 2012. A Review on Theoretical Consideration and Types of Models in Hydrology. J. Environ. Sci. Technol. 5, 249–261. https://doi.org/10.3923/jest.2012.249.261

Johnson, W.C., Boettcher, S.E., Poiani, K.A., Guntenspergen, G., 2004. Influence of Weather Extremes on the Water Levels of Glaciated Prairie Wetlands. Wetlands 24, 385–398. https://doi.org/10.1672/0277-5212(2004)024[0385:IOWEOT]2.0.CO;2

Karvonen, T., Koivusalo, H., Jauhiainen, M., Palko, J., Weppling, K., 1999. A hydrological model for predicting runoff from different land use areas. J. Hydrol. 217, 253–265. https://doi.org/10.1016/S0022-1694(98)00280-7

Ke, Y., Leung, L.R., Huang, M., Li, H., 2013. Enhancing the representation of subgrid land surface characteristics in land surface models. Geosci. Model Dev. 6, 1609–1622. https://doi.org/10.5194/gmd-6-1609-2013

Keyes, A.M., Palmer, R.N., 1993. The Role of Object Oriented Simulation Models in the Drought Preparedness Studies, in: Water Management in the'90s: A Time for Innovation. ASCE, pp. 479–482.

Kim, T.J., Wurbs, R.A., 2011. Development of monthly naturalized flow using Water Rights Analysis Package (WRAP)-based methods. KSCE J. Civ. Eng. 15, 1299–1307. https://doi.org/10.1007/s12205-011-1184-y

Klemeš, V., 1986. Operational testing of hydrological simulation models. Hydrol. Sci. J. 31, 13–24. https://doi.org/10.1080/02626668609491024

Kotir, J.H., Smith, C., Brown, G., Marshall, N., Johnstone, R., 2016. A system dynamics simulation model for sustainable water resources management and agricultural development in the Volta River Basin, Ghana. Sci. Total Environ. 573, 444–457. https://doi.org/10.1016/j.scitotenv.2016.08.081

Kouwen, N., Soulis, E.D., Pietroniro, A., Donald, J., Harrington, R.A., 1993. Grouped Response Units for Distributed Hydrologic Modeling. J. Water Resour. Plan. Manag. 119, 289–305. https://doi.org/10.1061/(ASCE)0733-9496(1993)119:3(289)

Kulshreshtha, S., Nagy, C., Ana, B., 2012. Present and Future Water Demand in the Qu'Appelle River Basin. Saskatoon.

Li, L., Simonovic, S.P., 2002. System dynamics model for predicting floods from snowmelt in north American prairie watersheds. Hydrol. Process. 16, 2645–2666. https://doi.org/10.1002/hyp.1064

Liang, X., Lettenmaier, D.P., Wood, E.F., Burges, S.J., 1994. A simple hydrologically based model of land surface water and energy fluxes for general circulation models. J. Geophys. Res. Atmos. 99, 14415–14428. https://doi.org/10.1029/94JD00483

Lindenschmidt, K.E., Sydor, M., Carson, R.W., 2012. Modelling ice cover formation of a lake–river system with exceptionally high flows (Lake St. Martin and Dauphin River,

Manitoba). Cold Reg. Sci. Technol. 82, 36–48. https://doi.org/10.1016/j.coldregions.2012.05.006

Liu, Z., Todini, E., 2002. Towards a comprehensive physically-based rainfall-runoff model. Hydrol. Earth Syst. Sci. 6, 859–881. https://doi.org/10.5194/hess-6-859-2002

Lørup, J.K., Refsgaard, J.C., Mazvimavi, D., 1998. Assessing the effect of land use change on catchment runoff by combined use of statistical tests and hydrological modelling: Case studies from Zimbabwe. J. Hydrol. 205, 147–163. https://doi.org/10.1016/S0168-1176(97)00311-9

Lygeros, J., Tomlin, C., Sastry, S., 2008. Hybrid Systems: Modeling, Analysis and Control. Reading 168.

MacDonald, M.K., 2014. Documentation for PBSM in MESH 1.3.008.

MacDonald, M.K., Pomeroy, J.W., Pietroniro, A., 2009. Parameterizing redistribution and sublimation of blowing snow for hydrological models: tests in a mountainous subarctic catchment. Hydrol. Process. 2274, 2267–2274. https://doi.org/10.1002/hyp

Maclean, A.J., 2009. Calibration and Analysis of the MESH Hydrological Model applied to Cold Regions. University of Waterloo.

Maclean, A.J., Tolson, B., Seglenieks, F.R., Soulis, E.D., 2010. Multiobjective calibration of the MESH hydrological model on the Reynolds Creek Experimental Watershed. Hydrol. Earth Syst. Sci. Discuss. 7, 2121–2155. https://doi.org/10.5194/hessd-7-2121-2010

Mahfouf, J.-F., Brasnett, B., Gagnon, S., 2007. A Canadian Precipitation Analysis (CaPA) Project: Description and Preliminary Results. Atmosphere-Ocean 45, 1–17. https://doi.org/10.3137/ao.v450101

Male, D.H., Gray, D.M., 1981. Snowcover ablation and runoff, in: Gray, D.M., Male, D.H. (Eds.), Handbook of Snow: Principles, Processes, Management & Use. Ontario.

Martin, F.R., 2001. The Determination of Gross and Effective Drainage Areas for the Prairie Provinces, Addendum No. 1 to Hydrology Report #104, Hydrology report. Prairie Farm Rehabilitation Administration.

Mekonnen, B.A., Mazurek, K.A., Putz, G., 2016. Incorporating landscape depression heterogeneity into the Soil and Water Assessment Tool (SWAT) using a probability distribution. Hydrol. Process. 30, 2373–2389. https://doi.org/10.1002/hyp.10800

Mekonnen, B.A., Nazemi, A., Mazurek, K.A., Elshorbagy, A., Putz, G., 2015. Hybrid modelling approach to prairie hydrology: fusing data-driven and process-based hydrological models. Hydrol. Sci. J. 1–17. https://doi.org/10.1080/02626667.2014.935778

Mekonnen, M.A., 2011. FROZEN - Areal Snowmelt In ltration into Frozen Soils. Saskatoon, Saskatchewan.

Mekonnen, M.A., Wheater, H.S., Ireson, A.M., Spence, C., Davison, B., Pietroniro, A., 2014. Towards an improved land surface scheme for prairie landscapes. J. Hydrol. 511, 105–

116. https://doi.org/10.1016/j.jhydrol.2014.01.020

Mengistu, S.G., Spence, C., 2016. Testing the ability of a semidistributed hydrological model to simulate contributing area. Water Resour. Res. 1–20. https://doi.org/10.1002/2014WR015716

Meyer, A.F., 1915. Computing run-off from rainfall and other physical data. Trans. Am. Soc. Civ. Eng. 78, 1056–1155.

Mirchi, A., Madani, K., Watkins, D., Ahmad, S., 2012. Synthesis of System Dynamics Tools for Holistic Conceptualization of Water Resources Problems. Water Resour. Manag. 26, 2421–2442. https://doi.org/10.1007/s11269-012-0024-2

Moore, R.B., Johnston, C.M., Robinson, K.W., Deacon, J.R., 2004. Estimation of total nitrogen and phosphorus in New England streams using spatially referenced regression models. US Geol. Surv. Sci. Investig. Rep. 5012, 1–42.

Moore, R.J., 2007. The PDM rainfall-runoff model 11, 483–499. https://doi.org/10.5194/hess-11-483-2007

Moore, R.J., 1985. The probability-distributed principle and runoff production at point and basin scales. Hydrol. Sci. J. 30, 273–297. https://doi.org/10.1080/02626668509490989

Moore, R.J., Bell, V.A., 2002. Incorporation of groundwater losses and well level data in rainfall-runoff models illustrated using the PDM. Hydrol. Earth Syst. Sci. 6, 25–38. https://doi.org/10.5194/hess-6-25-2002

Moore, R.J., Clarke, R.T., 1981. A distribution function approach to rainfall runoff modeling. Water Resour. Res. 17, 1367–1382. https://doi.org/10.1029/WR017i005p01367

Moriasi, D.N., Arnold, J.G., Van Liew, M.W., Bingner, R.L., Harmel, R.D., Veith, T.L., 2007. Model evaluation guidelines for systematic quantification of accuracy in watershed simulations. Trans. ASABE 50, 885–900. https://doi.org/10.13031/2013.23153

Morris, M.D., 1991. Factorial Sampling Plans for Preliminary Computational Experiments. Technometrics 33, 161–174. https://doi.org/10.2307/1269043

Muvundja, F.A., West, A., Isumbisho, M., Kaningini, M.B., Pasche, N., Rinta, P., Schmid, M., 2014. Modelling lake kivu water level variations over the last seven decades. Limnologica 47, 21–33. https://doi.org/10.1016/j.limno.2014.02.003

Nash, J.E., 1957. The form of the instantaneous unit hydrograph, Surface Water, Prevision, Evaporation, Publ. General Assembly of Toronto.

Natural Resources Canada, 2015. Land Cover, circa 2000 - Vector. Canada Centre for Mapping and Earth Observation, digital media [WWW Document]. URL http://wmsmir.cits.rncan.gc.ca/index.html/pub/geobase/official/lcc2000v_csc2000v/doc/LandCoverUNAReport.pdf

Neitsch, S.L., Arnold, J.G., Kiniry, J.R., 2011. Soil and water assessment tool: theoretical documentation, version 2009, Texas Water Resources Institute. Texas.

O'Connell, P.E., Nash, J.E., Farrell, J.P., 1970. River flow forecasting through conceptual models part II - The Brosna catchment at Ferbane. J. Hydrol. 10, 317–329. https://doi.org/10.1016/0022-1694(70)90221-0

Palmer, R., 1994. (ACT-ACF) River basin planning study [WWW Document].

Palmer, R.N., 1995. Willamette River Basin Review Feasibility Study > Portland District > Portland District Announcements [WWW Document]. US Army Corps Eng. URL http://www.nwp.usace.army.mil/Media/Announcements/Article/684784/willamette-river-basin-review-feasibility-study/ (accessed 2.1.17).

Palmer, R.N., Keyes, A.M., Fisher, S., 1993. Empowering Stakeholders Through Simulation in Water Resources Planning.

Papathanasiou, C., Makropoulos, C., Mimikou, M., 2015. Hydrological modelling for flood forecasting: Calibrating the post-fire initial conditions. J. Hydrol. 529, 1838–1850. https://doi.org/10.1016/j.jhydrol.2015.07.038

Peterson, A.M., Helgason, W., Ireson, A.M., 2015. Estimating field scale root zone soil moisture using the cosmic-ray neutron probe. Hydrol. Earth Syst. Sci. Discuss 12, 12789–12826. https://doi.org/10.5194/hessd-12-12789-2015

Peterson, D.W., Eberlein, R.L., 1994. Reality check: A bridge between systems thinking and system dynamics. Syst. Dyn. Rev. 10, 159–174.

Pianosi, F., Rougier, J., Freer, J., Hall, J., Stephenson, D.B., Beven, K., Wagener, T., 2014. Sensitivity Analysis of Environmental Models : A Systematic Review with. Environ. Model. Softw. 290–299.

Pianosi, F., Sarrazin, F., Wagener, T., 2015. A Matlab toolbox for Global Sensitivity Analysis. Environ. Model. Softw. 70, 80–85. https://doi.org/10.1016/j.envsoft.2015.04.009

Pietroniro, A., Fortin, V., Kouwen, N., Neal, C., Turcotte, R., Davison, B., Verseghy, D.L., Soulis, E.D., Caldwell, R., Evora, N., Pellerin, P., 2007. Using the MESH modelling system for hydrological ensemble forecasting of the Laurentian Great Lakes at the regional scale. Hydrol. Earth Syst. Sci. 3, 1279–1294. https://doi.org/10.5194/hess-11-1279-2007

Pohl, S., Davison, B., Marsh, P., Pietroniro, A., 2004. Modelling spatially distributed snowmelt and meltwater runoff in a small Arctic catchment with a hydrology land-surface scheme (WATCLASS). Atmosphere-Ocean 43, 193–211.

Pomeroy, J.W., Fang, X., Westbrook, C.J., Minke, A., Guo, X., Brown, T., 2010. Prairie hydrological model study final report. Saskatoon, Saskatchewan.

Pomeroy, J.W., Gray, D.M., Brown, T., Hedstrom, N.R., Quinton, W.L., Granger, R., Carey, S.K., 2007. The cold regions hydrological process representation and model: a platform for basing model structure on physical evidence. Hydrol. Process. 21, 2650–2667. https://doi.org/Doi 10.1002/Hyp.6787

Pomeroy, J.W., Gray, D.M., Landine, P.G., 1993. The Prairie Blowing Snow Model: characteristics, validation, operation. J. Hydrol. 144, 165–192.

https://doi.org/10.1016/0022-1694(93)90171-5

Pomeroy, J.W., Li, L., 2000. Prairie and arctic areal snow cover mass balance using a blowing snow model. J. Geophys. Res. 105, 26619. https://doi.org/10.1029/2000JD900149

Pomeroy, J.W., Shook, K., Fang, X., Dumanski, S., Westbrook, C.J., Brown, T., 2014. Improving and Testing the Prairie Hydrological Model at Smith Creek Research Basin. Saskatoon, Saskatchewan.

Post, D.A., Jakeman, A.J., 1999. Predicting the daily streamflow of ungauged catchments in S.E. Australia by regionalising the parameters of a lumped conceptual rainfall-runoff model. Ecol. Modell. 123, 91–104. https://doi.org/10.1016/S0304-3800(99)00125-8

Prairie Farm Rehabilitation Administration, 2008. Prairie Farm Rehabilitation Administration (PFRA) Watershed Project - Areas of Non-Contributing Drainage. Canada.

Qin, H.P., Su, Q., Khu, S.T., 2011. An integrated model for water management in a rapidly urbanizing catchment. Environ. Model. Softw. 26, 1502–1514. https://doi.org/10.1016/j.envsoft.2011.07.003

Rao, K.H.V.D., Rao, V.V., Dadhwal, V.K., Behera, G., Sharma, J.R., 2011. A distributed model for real-time flood forecasting in the Godavari Basin using space inputs. Int. J. Disaster Risk Sci. 2, 31–40. https://doi.org/10.1007/s13753-011-0014-7

Razavi, S., Gupta, H. V., 2015. What do we mean by sensitivity analysis? The need for comprehensive characterization of "'global'" sensitivity in Earth and Environmental systemsmodels. Water Resour. Res. 51, 3070–3092. https://doi.org/10.1002/2014WR016527.Received

Refsgaard, J.C., Havnø, K., Ammentorp, H.C., Verwey, A., 1988. Application of hydrological models for flood forecasting and flood control in India and Bangladesh. Adv. Water Resour. 11, 101–105. https://doi.org/10.1016/0309-1708(88)90043-7

Remesan, R., Mathew, J., 2015. Hydrological Data Driven Modelling: A Case Study Approach. Springer, Cranfield, Bedfordshire, UK. https://doi.org/10.1007/978-3-319-09235-5

Richards, L.A., 1931. Capillary Conduction of Liquids Through Porous Mediums. J. Appl. Phys. 1, 318. https://doi.org/10.1063/1.1745010

Saltelli, A., Ratto, M., Andres, T., Campolongo, F., Cariboni, J., Gatelli, D., Saisana, M., Tarantola, S., 2008. Global sensitivity analysis: the primer. John Wiley & Sons Ltd. https://doi.org/10.1002/9780470725184

Saskatchewan Bureau of Statistics, 2012. Saskatchewan Population Report.

Saskatchewan Department of Environment, 1975. Qu'Appelle Conveyence Study.

Saskatchewan Watershed Authority, 2012. Qu'Appelle River Basin Model (Report No. 11-1362-0053). Moose Jaw, SK.

Savenije, H., Hrachowitz, M., 2017. HESS Opinions "catchments as meta-organisms - A new blueprint for hydrological modelling." Hydrol. Earth Syst. Sci. 21, 1107–1116.

https://doi.org/10.5194/hess-21-1107-2017

Shaw, D.A., Dean, D.W., Van der Kamp, G., Conly, F.M., Pietroniro, A., Martz, L., 2012. The Fill-Spill Hydrology of Prairie Wetland Complexes during Drought and Deluge. Hydrol. Process. 26, 3147–3156. https://doi.org/10.1002/hyp.8390

Shaw, D.A., Pietroniro, A., Martz, L.W., 2013. Topographic analysis for the prairie pothole region of Western Canada. Hydrol. Process. 27. https://doi.org/10.1002/hyp.9409

Shook, K., Pomeroy, J.W., 2011. Memory effects of depressional storage in Northern Prairie hydrology. Hydrol. Process. 25, 3890–3898. https://doi.org/10.1002/hyp.8381

Shook, K., Pomeroy, J.W., Spence, C., Boychuk, L., 2013. Storage dynamics simulations in prairie wetland hydrology models: Evaluation and parameterization. Hydrol. Process. 27, 1875–1889. https://doi.org/10.1002/hyp.9867

Shook, K., Pomeroy, J.W., Van der Kamp, G., 2015. The transformation of frequency distributions of winter precipitation to spring streamflow probabilities in cold regions; case studies from the Canadian Prairies. J. Hydrol. 521, 395–409. https://doi.org/10.1016/j.jhydrol.2014.12.014

Simonovic, S.P., Fahmy, H., Elshorbagy, A., 1997. The use of object-oriented modeling for water resources planning in Egypt. Water Resour. Manag. 11, 243–261.

Simonovic, S.P., Rajasekaram, V., 2004. Integrated analyses of Canada's Water resources: A system dynamics approach. Can. Water Resour. J. 29, 223–250. https://doi.org/10.4296/cwrj223

Soulis, E.D., Craig, J.R., Fortin, V., Liu, G., 2011. A simple expression for the bulk field capacity of a sloping soil horizon. Hydrol. Process. 25, 112–116. https://doi.org/10.1002/hyp.7827

Soulis, E.D., Snelgrove, K.R., Kouwen, N., Seglenieks, F.R., Verseghy, D.L., 2000. Towards closing the vertical water balance in Canadian atmospheric models: Coupling of the land surface scheme class with the distributed hydrological model watflood [WWW Document]. Atmosphere-Ocean. https://doi.org/10.1080/07055900.2000.9649648

Spence, C., 2010. A paradigm shift in hydrology: Storage thresholds across scales influence catchment Runoff Generation. Geogr. Compass 4, 819–833. https://doi.org/10.1111/j.1749-8198.2010.00341.x

Spence, C., 2006. Hydrological processes and streamflow in a lake dominated watercourse. Hydrol. Process. 20, 3665–3681. https://doi.org/10.1002/hyp.6381

Spence, C., 2000. The effect of storage on runoff from a headwater subarctic shield basin. Arctic 53, 237–247.

Spence, C., Woo, M.K., 2006. Hydrology of subarctic Canadian Shield: Heterogeneous headwater basins. J. Hydrol. 317, 138–154. https://doi.org/10.1016/j.jhydrol.2005.05.014

Spence, C., Woo, M.K., 2003. Hydrology of subarctic Canadian shield: Soil-filled valleys. J. Hydrol. 279, 151–166. https://doi.org/10.1016/S0022-1694(03)00175-6

Stave, K.A., 2002. Using system dynamics to improve public participation in environmental decisions. Syst. Dyn. Rev. 18, 139–167. https://doi.org/10.1002/sdr.237

Stelfox, H.A., Ironside, G.R., Kansas, J.L., 1991. Guidelines for the integration of wildlife and habitat evaluations with ecological land survey. Wildlife Working Group of the Canada Committee on Ecological Land Classification. Wildlife Habitat Canada and Canadian Wildlife Service (Environment Canada)., Ottawa, Ontario.

Stichling, W., Blackwell, S.R., 1957. Drainage area as a hydrologic factor on the glaciated Canadian prairies. IUGG Proc. 365–367.

Tarnocai, C., 1980. Canadian wetland registry, in: In Proceedings of a Workshop on Canadian Wetlands. Environment Canada., Ottawa, Ontario., pp. 9–39.

Thompson, B.P., Bank, L.C., 2010. Use of system dynamics as a decision-making tool in building design and operation. Build. Environ. 45, 1006–1015. https://doi.org/10.1016/j.buildenv.2009.10.008

Tiwari, M.K., Chatterjee, C., 2010. Development of an accurate and reliable hourly flood forecasting model using wavelet–bootstrap–ANN (WBANN) hybrid approach. J. Hydrol. 394, 458–470. https://doi.org/10.1016/j.jhydrol.2010.10.001

Tolson, B., Shoemaker, C.A., 2007. Dynamically dimensioned search algorithm for computationally efficient watershed model calibration. Water Resour. Res. 43, 1–16. https://doi.org/10.1080/07055900.2014.939131

Torretta, V., Vincenzo, 2014. The Sustainable Use of Water Resources: A Technical Support for Planning. A Case Study. Sustainability 6, 8128–8148. https://doi.org/10.3390/su6118128

Turner, B., Menendez, H., Gates, R., Tedeschi, L., Atzori, A., 2016. System Dynamics Modeling for Agricultural and Natural Resource Management Issues: Review of Some Past Cases and Forecasting Future Roles. Resources 5, 40. https://doi.org/10.3390/resources5040040

Ullah, W., Dickinson, W.T., 1979. Qualitatiove Description of Depression Storage Using a Digital Surface Model. J. Hydrol. 42, 63–75.

Valk, A. van der, 1989. Northern prairie wetlands, 1st ed. . ed. Iowa State University Press, Ames.

Van der Kamp, G., Hayashi, M., 2009. Groundwater-wetland ecosystem interaction in the semiarid glaciated plains of North America. Hydrogeol. J. 17, 203–214. https://doi.org/10.1007/s10040-008-0367-1

Van der Kamp, G., Hayashi, M., 1998. The groundwater recharge function of small wetlands in the semi-arid northern prairies. Gt. Plains Res. 8, 39–56.

Verseghy, D.L., 2011. Class – The canadian land surface scheme (version 3.5), Tecchnical Document. Climate Research Division, Science and Technology Branch, Environment Canada.

Verseghy, D.L., 1991. CLASS-A Canadian Land Surface Scheme for GCMs I. Soil model. Int. J. Climatol. 11, 111–133. https://doi.org/10.1002/joc.3370110202

Verseghy, D.L., McFarlane, N.A., Lazare, M., 1993. Class—A Canadian land surface scheme for GCMS, II. Vegetation model and coupled runs. Int. J. Climatol. 13, 347–370. https://doi.org/10.1002/joc.3370130402

Vionnet, V., Martin, E., Masson, V., Guyomarc'H, G., Naaim-Bouvet, F., Prokop, A., Durand, Y., Lac, C., 2014. Simulation of wind-induced snow transport and sublimation in alpine terrain using a fully coupled snowpack/atmosphere model. Cryosphere 8, 395–415. https://doi.org/10.5194/tc-8-395-2014

Vrugt, J.A., Diks, C.G.H., Gupta, H. V, Bouten, W., Verstraten, J.M., 2005. Improved treatment of uncertainty in hydrologic modeling: Combining the strengths of global optimization and data assimilation. Water Resour. Res. 41.

Ward, A.D., Trimble, S.W., Wolman, M.G., 2004. Environmental Hydrology, 2nd ed. Lewis Publishers, Boca Raton.

Water Security Agency, 2014. Saskatchewan Community Water use records 1999 to 2013 Report 27. Moose Jaw, Saskatchewan S6H 7X9.

Wei, S., Yang, H., Song, J., Abbaspour, K.C., Xu, Z., 2012. System dynamics simulation model for assessing socio-economic impacts of different levels of environmental flow allocation in the Weihe River Basin, China. Eur. J. Oper. Res. 221, 248–262. https://doi.org/10.1016/j.ejor.2012.03.014

Weiler, M., Mcdonnell, J.J., Meerveld, I.T., Uchida, T., 2005. Subsurface Stormflow. Encycl. Hydrol. Sci. 1–14.

White, J.D., Prochnow, S.J., Filstrup, C.T., Scott, J.T., Byars, B.W., Zygo-Flynn, L., 2010. A combined watershed-water quality modeling analysis of the Lake Waco reservoir: I. Calibration and confirmation of predicted water quality. Lake Reserv. Manag. 26, 147–158. https://doi.org/10.1080/07438141.2010.495315

Winz, I., Brierley, G., Trowsdale, S., 2009. The use of system dynamics simulation in water resources management. Water Resour. Manag. 23, 1301–1323. https://doi.org/10.1007/s11269-008-9328-7

Wooding, R.A., 1966. A hydraulic model for the catchment-stream problem. J. Hydrol. 4, 254–267. https://doi.org/10.1016/0022-1694(66)90065-5

Xu, Z., Godrej, A.N., Grizzard, T.J., 2007. The hydrological calibration and validation of a complexly-linked watershed–reservoir model for the Occoquan watershed, Virginia. J. Hydrol. 345, 167–183. https://doi.org/10.1016/j.jhydrol.2007.07.015

Xu, Z.X., Schultz, G.A., Li, J.Y., Ito, K., 2001. Integrated Hydrologic Modeling and GIS in Water Resources Management. J. Comput. … 3801. https://doi.org/10.1061/(ASCE)0887-3801(2001)15

Yassin, F., Razavi, S., Wheater, H.S., Sapriza-Azuri, G., Davison, B., Pietroniro, A., 2017. Enhanced Identification of a Hydrologic Model using Streamflow and Satellite Water

Storage Data: A Multi-criteria Sensitivity Analysis and Optimization Approach. Hydrol. Process. 1–14. https://doi.org/10.1002/hyp.11267

Zehe, E., Becker, R., Bárdossy, A., Plate, E., 2005. Uncertainty of simulated catchment runoff response in the presence of threshold processes: Role of initial soil moisture and precipitation. J. Hydrol. 315, 183–202. https://doi.org/10.1016/j.jhydrol.2005.03.038

Zhao, L., Gray, D.M., 1999. Estimating snowmelt in ® ltration into frozen soils 1842, 1827–1842. https://doi.org/10.1002/(SICI)1099-1085(199909)13:12/13<1827::AID-HYP896>3.0.CO;2-D

Appendix A: Modelling of Cold Region Processes

Cold region hydrology consists few special physical processes (e.g. blowing of snow, infiltration in frozen soil condition), which is generally seen in a location where ice and snow play an important role in the local hydrology. MESH contains special parameterization for some of these processes, which is generally developed using special approaches and adopted during the model development of a cold region watershed. Two such special module was used in this study, which are Prairie Blowing Snow Model (PBSM) and frozen soil infiltration model as the case studies are mainly cold region watersheds. In this section, attempts were made to understand the importance of these modules in MESH.

Prairie Blowing Snow Model

Blowing snow redistribution in the prairie is an important process, where a certain amount of snow gets redistributed by wind force and alters the following spring runoff pattern. MESH implements this model using a subroutine and this component is activated using a flag in MESH environment. This module considers snowfall as input in vertical flux and redistributes using wind force as well as a probability distribution function as horizontal flux. In this study, no measured snow accumulation information was available to validate the simulated snow accumulation. For this reason, simulation of snow accumulation was compared with two separate model runs using PBSM module and not using PBSM module. The intension is to observe any considerable change of snow accumulation because of PBSM module.

Parameterization

The process of blowing snow redistribution was initially parameterized by Pomeroy et al. (1993) and later implemented in the Cold Region Hydrological Model (CHRM) (Pomeroy et al., 2007). Same concept was implemented in MESH with identical parameterization, which is

known as the Prairie Blowing Snow Model (PBSM). This model estimates blowing snow transport and sublimation quantities at the GRU-levels within grid squares. The physical processes assume that wind erode snow from a GRU and sublimates or transported and deposited into downwind GRUs in the same grid square. For an efficient PBSM application, GRUs need to be arranged according to aerodynamic roughness or drifting order. For example, if GRU 1 is bare ground, GRU 2 is shrub, GRU 3 is forest, and snow is transported from bare ground and deposited downwind to shrub & forest. Snow can also be eroded from shrub and deposited in forest. PBSM requires five GRU-dependent parameters, which are fetch, height of vegetation, vegetation density, vegetation diameter, and snow distribution factor. Fetch (distance in meters) is the distance of unobstructed wind flow. The minimum value is 300 m and the maximum value should be at most half the grid square dimension. The height of vegetation (in meters) can vary based on the type of vegetation available in a locality and smaller values will allow more erosion. Vegetation density (number/m^2) can vary from 1 to 500. Vegetation diameter area (in meters) can vary from 0.0 to 2.0 m. Snow distribution factor (*distrib*) controls the inter-GRU snow redistribution within grid squares. Snow can enter GRU 1 from a hypothetical "outside the grid square". The parameter *distrib* is a coefficient that describes the fraction of transported snow deposited into a GRU. For example, if we have three GRUs names A, B & C. Deposition into GRUs will be:

$$Deposition(A) = 0 \text{ , } \textit{if distrib(A) = 0} \quad \text{(A.1)}$$

$$Deposition(B) = \frac{distrib(B)}{distrib(B)+distrib(C)} \quad \text{(A.2)}$$

$$Deposition(C) = \frac{distrib(C)}{distrib(B)+distrib(C)} \quad \text{(A.3)}$$

There are very few applications of PBSM module within MESH model. The values of the parameters are taken from the model results developed in the Cold Region Hydrological Model (CRHM). Though CRHM and MESH are different modelling tools, PBSM module for both

models is based on same principle and the parameterization is also same. Following values for each parameter is fixed-

Table I: Blowing snow parameter values

GRU	Fetch (m)	Vegetation height (m)	Stalk density (#/m^2)	Stalk diameter (m)	Distribution factor
Crop	1000	0.12	320	0.5	0.5
Grass	500	0.4	320	1	1
Wetland	300	1.5	100	1	1
Forest	300	6	100	3	3

According to the PBSM documentation (MacDonald, 2014), PBSM rates are very sensitive to vegetation height. For this reason, vegetation height is considered as a calibration factor here. Calibration range were fixed as: crop 0.05-0.30 m, grass 0.20-0.80 m, wetland 1-2 m, and forest 2-20 m. Other parameters are not recommended for calibration in literature (PBSM documentation).

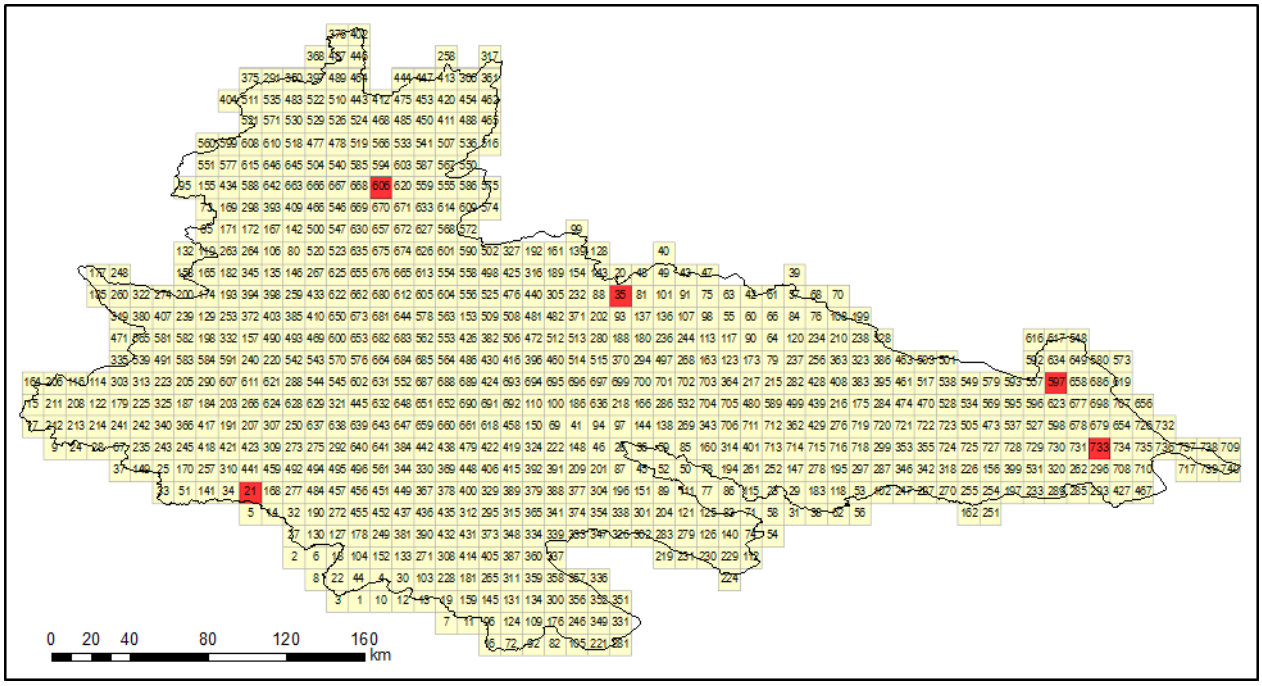

Figure A.1: Location of grid cell where snow accumulation is compared (Highlighted in Red)

Simulation Results

The Qu'Appelle River basin (QRB) MESH model contains 740 grid cell and grid cells are discretized into four different GRUs based on landuse type (Figure A.1). Each grid cell consists

of four landuse type. Crop is dominant landuse type in all grids. The GRUs of QRB are arranged aerodynamically to ensure that blowing snow drifts toward the downwind from crop to grass, grass to wetland, and wetland to forest.

Following Figure illustrates the model outcome at Welby without PBSM and using PBSM module. Apparently, none of the outcome is satisfactory as for both cases model is unable to predict peak flows and low flows efficiently. Calibration NS drops from +0.63 to +0.57 using PBSM module. PBSM module is affecting snowpack development and loses some water via sublimation loss and lowers the simulated peak flow (observed in year 2005, 2006, 2010, and 2014). Also, PBSM is redistributing accumulated snow towards the downwind GRU causing longer recession period of the hydrographs of year 2005, 2006, 2007, and 2013. Validation NS is <0.0, because model is unable simulate year 2014 using PBSM, where model can generate some amount flow in year 2014 without PBSM module.

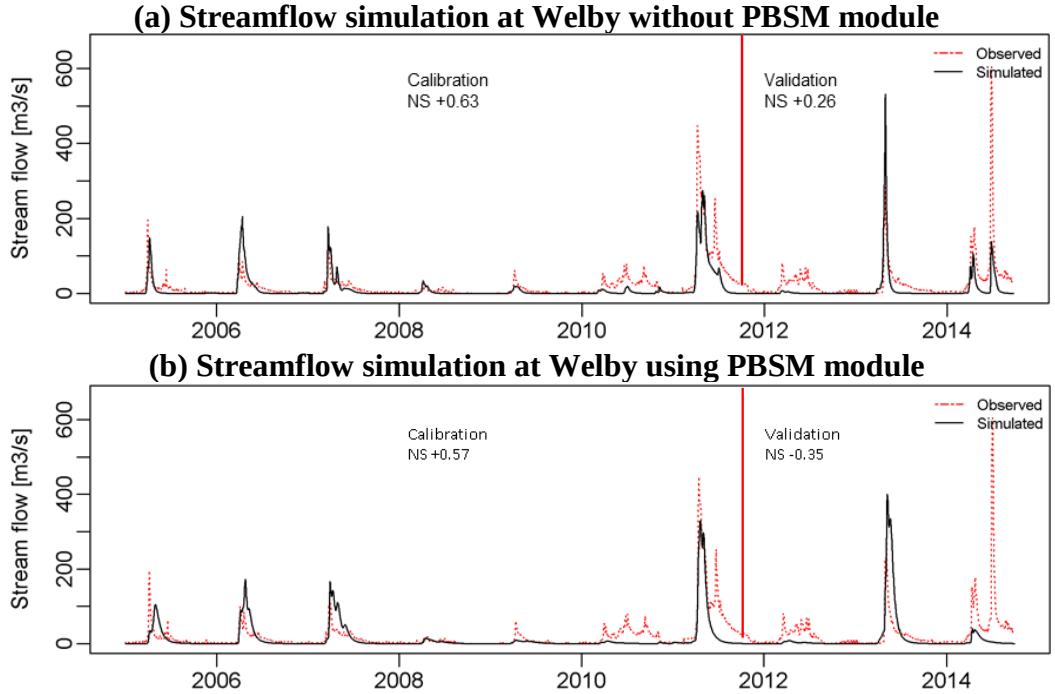

Figure A.2: Streamflow simulation (a) without PBSM and (b) using PBSM module

Similar performance is observed for the prediction of the tributaries (Table-II). Inclusion of PBSM did not add any significant improvements of any of the tributaries and in some cases performance get lowered.

Table II: Model performance at the tributaries

	Calibration NS		Validation NS	
Tributaries	**PBSM off**	**PBSM on**	**PBSM off**	**PBSM on**
Moose Jaw	0.53	0.43	0.39	0.80
Kronau Marsh	0.29	0.20	-2.40	-1.80
Ridge	0.25	0.19	-0.21	-0.25
Lewis	-1.10	-0.44	-0.36	-0.29
Lanigan	-1.70	-2.70	-0.93	-2.00
Saline	-2.30	-2.10	-7.00	-3.50
Jumping Deer	-28.00	-44.00	-16.00	-26.00
Pheasant	-0.49	-0.37	0.35	-0.17
Ekapo	0.58	0.38	0.15	-0.01
Cutarm	0.24	0.12	0.21	-0.02

Figure A.3 shows the snow accumulation in form of snow water equivalent (SWE) in GRUs of different grid cells. MESH accounts for snowpack, ice in soil mass, intercepted snow in vegetation, and stored overland water in ice and snow form in calculation of SWE. In case of blowing snow (using PBSM module), MESH accounts for blowing snow as well. It is observed that up to 20 mm of SWE is drifted from crop land towards grass, wetland, and forest during snow accumulation in each year. Crop, being in the upwind GRU, loses maximum amount of SWE, because it receives SWE only from snowfall. On the other hand, grass receives SWE from upwind GRU and loses SWE to the downwind as well as sublimation, having a small effect due to PBSM module. The most downwind GRU only receives SWE after accounting the sublimation loss by all the GRUs. For this reason, downwind GRU do not receive all the SWE lost by the upwind GRUs. For grid 606, 35, and 21, it appears that wetland accumulates considerably increased amount of SWE though the proportion of wetland appears low compared to crop. This is because wetland stores a significant amount of water overland, which MESH accounts for SWE calculation besides snow depth and stored water in the soil mass. For grid 597 and 733, no wetland exists within the grid cell and a proportionate SWE is appeared to be deposited within each GRU. It appears that crop land is storing a major portion of the SWE compared to downwind GRUs, i.e., grass and forest. because the reason for this is that

crop land occupies a major portion of the area in that particular GRU. The proportion of landuse occupying a specific grid cell is presented in Figure A.3 (values in the parenthesis in legend). It is also observed that blowing snow primarily drifts from crop GRU to other GRUs. The amount of drifted snow is insignificant in other GRUs as there is no distinct difference in the dotted line and solid line in Figure A.3.

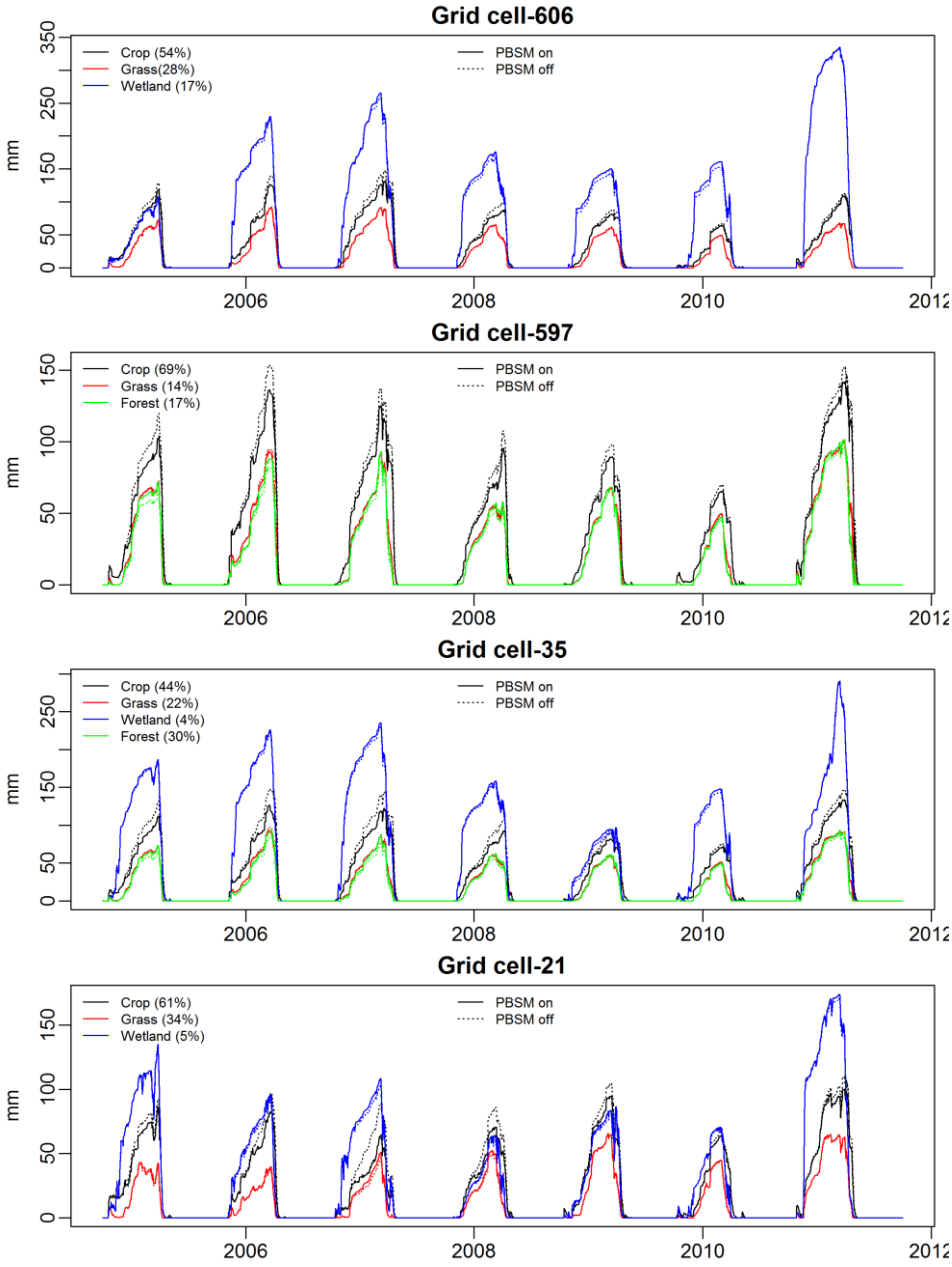

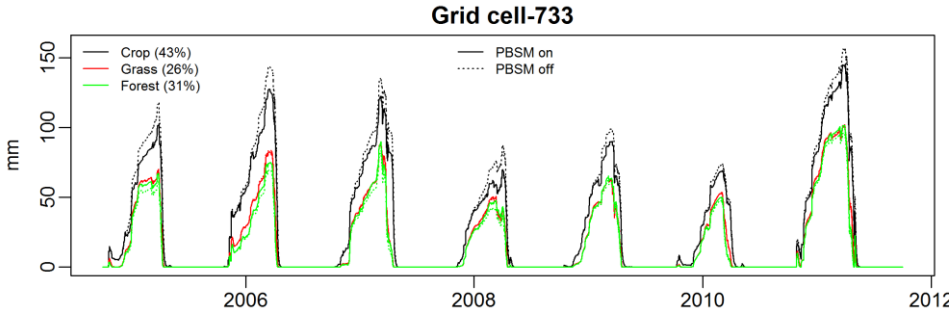

Figure A.3: Snow accumulation for GRUs in different grid cells. Values in parenthesis is proportion of landuse type within that particular grid cell.

PBSM modules redistributes snow within GRUs in a grid cell. It does not have the capability to redistribute snow across grid cells and this limitation is justifiable. When the size of a grid cell is considerably large (for example, this study uses grid cell size of 10km × 10km), it is very unlikely that snow will drift 10 km downwind distance. PBSM also introduces sublimation loss of blowing snow, which affects the snowpack size and spring runoff. It is understood that the effect of PBSM module over a large-scale model with an area of about 50,900 km^2 is insignificant. However, it is possible that model performance can improve with high detailing of model structure with a complex arrangement of GRUs.

Snowmelt Infiltration in Frozen Soil

Infiltration process in the frozen soil is an important hydrological phenomenon in a cold region watershed. MESH has an algorithm which can simulate snowmelt infiltration process through frozen soil (Zhao and Gray, 1999). This algorithm is a general parametric expression for the estimating snowmelt infiltration into different textured frozen soil from measurable physical parameters. According to this algorithm, the infiltration potential of frozen soils is categorized into three groups depending on the surface entry conditions. These groups are- (i) restricted, (ii) limited, and (iii) unlimited (Gray et al., 1985). Restricted group do not allow any water to infiltrate and water entry is impeded by surface conditions such as ice lens formation and the melt water become direct runoff. Limited group allows predominant capillary flow and infiltration is influenced by soil physical property. And unlimited group uses predominant gravity flow and allows most of the melt water to infiltrate. Apparently, limited infiltration potential for frozen soil is the realistic soil condition, however, infiltration potential can vary based on the soil texture. MESH in association with frozen soil infiltration algorithm mimic limited infiltration potential, which is one of the dominant cold region hydrological processes. In this study, no measured infiltration information was available to validation the simulated infiltration. For this reason, simulation of runoff was compared with two separate model runs using the frozen soil infiltration module and not using the frozen soil infiltration module. The intension is to observe any considerable change of runoff because of frozen soil infiltration module.

Parameterization

A parametric equation is required for the limited soils to partition the snowmelt into direct runoff and infiltrated water. According to Gray et al. (1985), cumulative infiltration over time

is estimated by the parametric equation that describes cumulative infiltration into frozen unsaturated soils of limited infiltrability as:

$$INF = C \times S_o^{2.92} \times (1 - S_I)^{1.64} \times \left(\frac{273.15 - T_I}{273.15}\right)^{-0.45} \times t_o^{0.44} \qquad T_I < 273.15 \qquad \text{(A.4)}$$

Where INF is the potential infiltration capacity (mm), S_o is soil surface saturation, $S_I$is the average soil saturation (water and ice) of 0 – 40 cm soil layer at the start of infiltration, T_I is initial soil temperature (K), t_o is infiltration opportunity time (hr), and C is the parametric equation constant and is found to be 2.10 and 1.14 for the prairie soils and forest soils respectively (Gray et al., 2001). $S_I = \frac{\theta_i}{\varphi}$, where θ_i is the average volumetric soil moisture (water and ice) at the start of infiltration (mm^3/mm^3) φ is soil porosity (mm^3/mm^3). The infiltration opportunity time is estimated or accumulated from preliminary model runs such as analyzing the CLASS outputs. It can also be estimated from the snow water equivalent (SWE) using the following empirical correlation (Zhao and Gray, 1999).

$$t_o = 0.65 \times SWE - 5 \qquad \text{(A.5)}$$

Where t_o is in hours and SWE in mm of water. The frozen soil algorithm constraints total infiltration into limited soils by the available water storage capacity. In this study, a fixed porosity of 0.40 was used and complete saturation of soil column was assumed during snowmelt.

Simulation Results

The Kronau Marsh watershed was selected for this study and MESH model simulate the streamflow event of year 2005. Figure A.4 shows the streamflow simulation of MESH with and without frozen soil infiltration algorithm. It is observed that streamflow shows high runoff volume due to the limited infiltrability soil, although the change of streamflow is not significant. Figure A.5 shows the change in amount of overland runoff and interflow using

frozen soil infiltration algorithm. It is observed that overland runoff initiates early because of limited infiltrability (Figure A.5a). As snowmelt cannot infiltrate, most of the water is mainly drains overland. Amount of interflow do not show any change; however, the amount of interflow appears to be increased by an insignificant margin during the recession period of peak flow event. It is probable that the fact of ice lens disappearing from soil column exhibits increased infiltrability compared to traditional infiltration, which do not consider limited infiltration due to frozen soil.

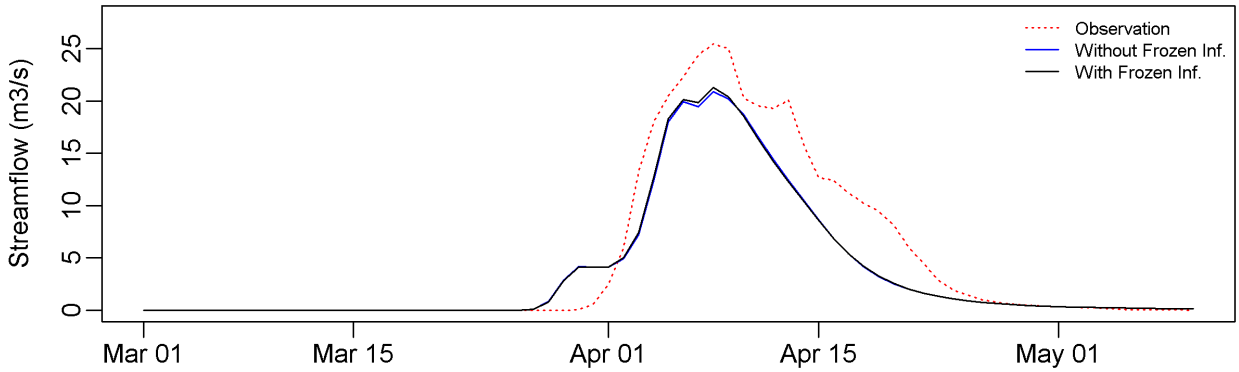

Figure A.4: Streamflow simulation using frozen soil infiltration algorithm in the Kronau Marsh watershed.

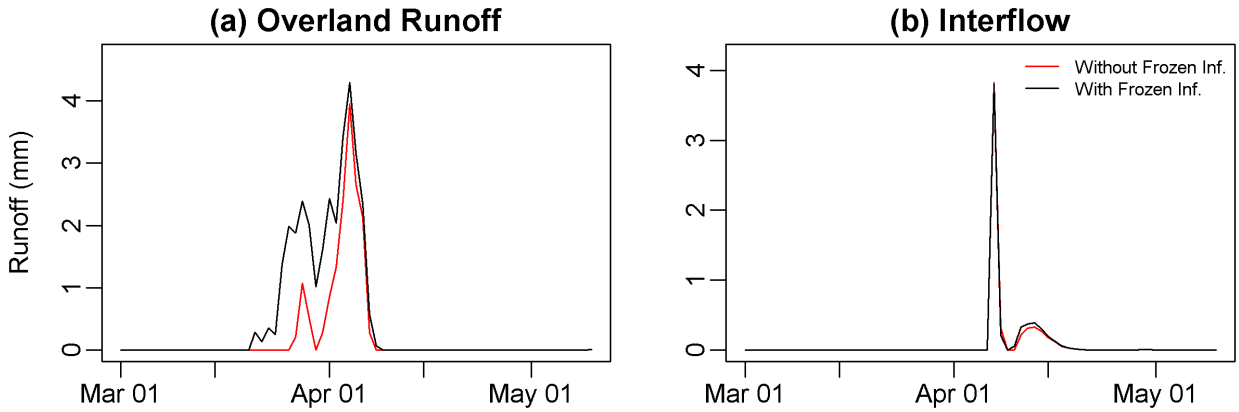

Figure A.5: (a) Overland runoff and (b) interflow simulation using frozen soil infiltration algorithm in the Kronau Marsh watershed.

The main effect of frozen soil infiltration is the limited infiltrability during snowmelt period and early response of runoff as snowmelt can infiltrate into soil. However, this effect may not be visible for a prairie watershed, because there is no guaranty that generated overland runoff may reach to the nearest stream, which is observed in Figure A.4 and Figure A.5a. Although

not a significant change of streamflow simulation is observed for the Kronau Marsh due to the application of frozen soil infiltration algorithm, this type of infiltration process is a signature hydrological process in the cold-region, which need to be addressed in hydrological modelling carefully.

Appendix B: Comparison of Runoff Generation Algorithms

Table B.1: Optimized value of calibration parameters used in the model of the White Gull Creek watershed

Description	Units	GRU	Lower limit	Upper limit	WATROF	PDMROF	LATFLOW	Source
River roughness factor that incorporates a channel shape and width to depth ratio as well as Manning's n	$[m^{0.5}s^{-1}]$		- 0.3	2	1.611	1.621	1.860	User defined
Surface storages connectivity coefficient or shape factor	-	forest	0	30		6.914	4.213	Mekonnen (2014)
		grass	0	30		20.180	13.432	
		wetland	0	5		2.512	0.010	
Maximum surface storage capacity	[m]	forest	0	5		1.719	4.459	Mekonnen (2014)
		grass	0	5		1.698	1.946	
		wetland	0	10		6.463	0.010	
Limiting snow depth below which coverage is less than 100%	[m]	forest	0.05	0.3	0.269	0.118	1.000	User defined
		grass	0.05	0.3	0.258	0.373	0.698	
		wetland	0.05	0.3	0.162	0.147	0.395	
Maximum water ponding depth for snow covered areas	[m]	forest	0.05	0.25	0.368	0.334	0.235	User defined
		grass	0.05	0.25	0.500	0.283	0.254	
		wetland	0.05	0.25	0.311	0.500	0.166	
Maximum water ponding depth for snow free areas	[m]	forest	0.05	0.25	0.090	0.107	0.050	User defined
		grass	0.05	0.25	0.050	0.113	0.190	
		wetland	0.05	0.25	0.050	0.470	0.308	
Manning's n for overland flow	$[ms^{-1/3}]$	forest	0.01	0.05	0.036		0.032	Dingman (2002)
		grass	0.01	0.05	0.022		0.029	
		wetland	0.01	0.05	0.030		0.035	
Soil drainage index. Index 1 allows the soil physics to determine drainage and index 0 completely impede drainage	[]	forest	0	1	0.532	0.367	1.000	User defined
		grass	0	1	0.237	1.000	0.988	
		wetland	0	0.1	0.000	0.380	0.103	
Permeable depth of the soil column	[m]	forest	0	4.1	4.075	3.976	4.100	User defined
		grass	0	4.1	0.010	0.010	0.818	
		wetland	0	4.1	1.250	0.925	1.044	
Saturated surface horizontal soil conductivity	$[ms^{-1}]$	forest	0.0001	0.01	0.00011		0.00311	User defined
		grass	0.0001	0.01	0.00001		0.00112	
		wetland	0.0001	0.01	0.00067		0.08712	
Drainage density, equal to the length of the stream divided by area drained by the stream	$[km/km^2]$	forest	50	120	120.000		111.102	User defined
		grass	50	120	91.405		50.000	
		wetland	50	120	104.961		81.895	
Fraction of the saturated surface soil conductivity moving in the horizontal direction	[]	forest	0	0.8	0.024		0.358	User defined
		grass	0	0.8	0.489		0.106	
		wetland	0	0.1	0.747		0.710	

Table B.2: Optimized value of calibration parameters used in the model of the Kronau Marsh watershed

Description	Units	GRU	Lower limit	Upper limit	PDMROF	LATFLOW	Source
River roughness factor that incorporates a channel shape and width to depth ratio as well as Manning's n	$[m^{0.5}s^{-1}]$	-	0.3	2	2.000	0.651	User defined
Surface storages connectivity coefficient or shape factor	-	crop	0	30	18.505	22.536	Mekonnen (2014)
		grass	0	30	18.064	20.161	
		NCW	0	5	1.083	0.010	
Maximum surface storage capacity	[m]	crop	0	5	0.273	0.687	Mekonnen (2014)
		grass	0	5	0.010	4.636	
		NCW	0	10	4.946	3.191	
Limiting snow depth below which coverage is less than 100%	[m]	crop	0.05	0.3	0.195	0.227	User defined
		grass	0.05	0.3	0.127	0.237	
		NCW	0.05	0.3	0.267	0.292	
Maximum water ponding depth for snow covered areas	[m]	crop	0.05	0.25	0.153	0.207	User defined
		grass	0.05	0.25	0.085	0.055	
		NCW	0.05	0.25	0.237	0.148	
Maximum water ponding depth for snow free areas	[m]	crop	0.05	0.25	0.105	0.097	User defined
		grass	0.05	0.25	0.196	0.092	
		NCW	0.05	0.25	0.206	0.238	
Manning's n for overland flow	$[ms^{-1/3}]$	crop	0.01	0.05		0.022	Dingman (2002)
		grass	0.01	0.05		0.042	
		NCW	0.01	0.05		0.018	
Soil drainage index. Index 1 allows the soil physics to determine drainage and index 0 completely impede drainage	[]	forest	0	1	0.223	0.796	User defined
		grass	0	1	0.747	0.000	
		NCW	0	0.1	0.054	0.059	
Permeable depth of the soil column	[m]	crop	0	4.1	0.531	1.601	User defined
		grass	0	4.1	1.925	0.373	
		NCW	0	4.1	0.349	0.010	
Saturated surface horizontal soil conductivity	$[ms^{-1}]$	crop	0.0001	0.01		0.00585	User defined
		grass	0.0001	0.01		0.01000	
		NCW	0.0001	0.01		0.00052	
Drainage density, equal to the length of the stream divided by area drained by the stream	$[km/km^2]$	crop	50	120		53.016	User defined
		grass	50	120		103.026	
		NCW	50	120		103.698	
Fraction of the saturated surface soil conductivity moving in the horizontal direction	[]	crop	0	0.8		0.376	User defined
		grass	0	0.8		0.039	
		NCW	0	0.1		0.040	

Table B.3: Optimized value of calibration parameters used in the model of the Brightwater Creek watershed

Description	Units	GRU	Lower limit	Upper limit	PDMROF	LATFLOW	Source
River roughness factor that incorporates a channel shape and width to depth ratio as well as Manning's n	[$m^{0.5}s^{-1}$]	-	0.3	2	0.845	0.830	User defined
Surface storages connectivity coefficient or shape-factor		crop	0	30	24.794	10.617	Mekonnen (2014)
		grass	0	30	2.897	13.199	
		NCW	0	5	0.010	4.221	
Maximum surface storage capacity	[m]	crop	0	5	0.274	0.117	Mekonnen (2014)
		grass	0	5	2.507	0.599	
		NCW	0	10	1.673	9.753	
Limiting snow depth below which coverage is less than 100%	[m]	crop	0.05	0.3	0.261	0.260	User defined
		grass	0.05	0.3	0.214	0.148	
		NCW	0.05	0.3	0.300	0.297	
Maximum water ponding depth for snow covered areas	[m]	crop	0.05	0.25	0.080	0.165	User defined
		grass	0.05	0.25	0.242	0.148	
		NCW	0.05	0.25	0.126	0.143	
Maximum water ponding depth for snow free areas	[m]	crop	0.05	0.25	0.173	0.174	User defined
		grass	0.05	0.25	0.098	0.135	
		NCW	0.05	0.25	0.133	0.194	
Manning's n for overland flow	[$ms^{-1/3}$]	crop	0.01	0.05		0.047	Dingman (2002)
		grass	0.01	0.05		0.015	
		NCW	0.01	0.05		0.048	
Soil drainage index. Index 1 allows the soil physics to determine drainage and index 0 completely impede drainage	[]	forest	0	1	0.381	0.745	User defined
		grass	0	1	0.377	0.894	
		NCW	0	0.1	0.058	0.032	
Permeable depth of the soil column	[m]	crop	0	4.1	1.419	1.401	User defined
		grass	0	4.1	1.658	0.045	
		NCW	0	4.1	0.100	2.063	
Saturated surface horizontal soil conductivity	[ms^{-1}]	crop	0.0001	0.01		0.00708	User defined
		grass	0.0001	0.01		0.00010	
		NCW	0.0001	0.01		0.00010	
Drainage density, equal to the length of the stream divided by area drained by the stream	[km/km^2]	crop	50	120		86.112	User defined
		grass	50	120		90.408	
		NCW	50	120		97.756	
Fraction of the saturated surface soil conductivity moving in the horizontal direction	[]	crop	0	0.8		0.077	User defined
		grass	0	0.8		0.709	
		NCW	0	0.1		0.070	

Appendix C: Calibration of QRB using Top-down (Option-I) and Bottom-up approach

Table C.1: Calibration parameter value using 'Top-down' (Option-I) and 'Bottom-up' approach of hybrid model along with their respective range used in QRB

Description	Units	GRU	Lower limit	Upper limit	Top-down (op-I)	Bottom-up	Source
River roughness factor that incorporates a channel shape and width to depth ratio as well as Manning's n	[m0.5s-1]	-	0.3	2	2.00	0.38	User defined
Surface storages connectivity coefficient or shape factor	[]	forest	0.01	30	28.49	25.53	Mekonnen (2014)
		NCW	0.01	5	4.37	1.70	
		crop	0.01	30	17.54	18.99	
		grass	0.01	30	8.90	0.01	
Maximum surface storage capacity	[m]	forest	0.01	5	0.09	4.95	Mekonnen (2014)
		NCW	0.01	10	4.56	0.32	
		crop	0.01	5	0.74	2.25	
		grass	0.01	5	0.42	3.96	
Maximum leaf area index	[]	forest	2	10	5.88	4.93	Verseghy (2011)
		NCW	4	6.5	4.07	5.48	
		crop	2	4	2.83	2.90	
		grass	2	4	2.00	2.97	
Minimum leaf area index	[]	forest	1.6	10	5.34	2.32	Verseghy (2011)
		grass	2	4	3.95	2.15	
		NCW	2	4	2.63	3.75	
Annual maximum canopy mass	[kg/m2]	forest	15	50	26.53	19.39	Verseghy (2011)
		crop	2	5	4.14	3.53	
		grass	1.5	3	1.69	2.76	
		NCW	1.5	3	2.84	1.63	
Annual maximum rooting depth	[m]	forest	1	5	4.18	2.16	Verseghy (2011)
		crop	1.2	5	1.20	2.90	
		grass	0.2	5	0.20	0.28	
		NCW	0.2	5	3.07	2.81	
Natural log of roughness length	[]	forest	-0.22	0.4	0.26	-0.03	Verseghy (2011)
		crop	-2.53	-1	-2.29	-1.58	
		grass	-1.66	-1	-1.54	-1.49	
		NCW	-1.66	-1	-1.17	-1.66	
Average visible albedo when fully-leafed or of the land cover	[]	forest	0.02	0.04	0.04	0.02	Verseghy (2011)
		crop	0.04	0.08	0.08	0.07	
		grass	0.04	0.08	0.05	0.04	
		NCW	0.04	0.08	0.04	0.05	
Average near-infrared albedo when fully-leafed or of the land cover	[]	forest	0.13	0.33	0.17	0.14	Verseghy (2011)
		crop	0.26	0.46	0.26	0.28	
		grass	0.26	0.46	0.32	0.28	
		NCW	0.26	0.46	0.27	0.46	
Limiting snow depth below which coverage is less than 100%	[m]	forest	0.05	0.3	0.05	0.25	User defined
		NCW	0.05	0.3	0.19	0.05	
		crop	0.05	0.3	0.22	0.29	
		grass	0.05	0.3	0.30	0.05	
Maximum water ponding depth for snow covered areas	[m]	forest	0.05	0.25	0.16	0.16	User defined
		NCW	0.05	0.25	0.22	0.13	

Description	Units	GRU	Lower limit	Upper limit	Top-down (op-I)	Bottom-up	Source
		crop	0.05	0.25	0.05	0.09	
		grass	0.05	0.25	0.11	0.09	
Maximum water ponding depth for snow free areas	[m]	forest	0.05	0.25	0.25	0.06	User defined
		NCW	0.05	0.25	0.05	0.25	
		crop	0.05	0.25	0.07	0.15	
		grass	0.05	0.25	0.19	0.16	
Manning's n for overland flow	[ms-1/3]	forest	0.01	0.05	0.04	0.05	Dingman (2002)
		crop	0.01	0.05	0.05	0.03	
		grass	0.01	0.05	0.05	0.04	
		NCW	0.01	0.05	0.02	0.02	
Permeable depth of the soil column	[m]	forest	0.01	4.1	2.50	3.78	User defined
		crop	0.01	4.1	1.11	3.95	
		grass	0.01	4.1	3.29	2.74	
		NCW	0.01	4.1	4.10	1.47	
Saturated surface horizontal soil conductivity	[ms-1]	forest	0.0001	0.01	0.00	0.00	User defined
		crop	0.0001	0.01	0.00	0.00	
		grass	0.0001	0.01	0.00	0.00	
		NCW	0.0001	0.01	0.00	0.00	
Drainage density, equal to the length of the stream divided by area drained by the stream	[km/km2]	forest	50	120	61.87	69.48	User defined
		crop	50	120	99.05	52.38	
		grass	50	120	100.95	91.42	
		NCW	50	120	89.10	120.00	
Fraction of the saturated surface soil conductivity moving in the horizontal direction	[]	forest	0	0.8	0.67	0.58	User defined
		crop	0	0.8	0.80	0.48	
		grass	0	0.8	0.37	0.72	
		NCW	0	0.1	0.00	0.06	
Soil drainage index. Index 1 allows the soil physics to determine drainage and index 0 completely impede drainage	[]	forest	0	1	0.77	0.00	User defined
		crop	0	1	0.00	0.00	
		grass	0	1	0.49	0.98	
		NCW	0	0.1	0.09	0.04	
Percent content of sand in Layer-1		forest	5.8	77.8	32.03	64.09	User defined
Percent content of sand in Layer-2			6.9	72.1	72.10	46.56	
Percent content of sand in Layer-3			7.5	76	44.54	11.61	
Percent content of clay in Layer-1			6.4	78.4	12.79	59.17	
Percent content of clay in Layer-2			10.8	75.6	54.93	30.40	
Percent content of clay in Layer-3			12.2	73.8	31.25	58.85	
Percent content of sand in Layer-1		NCW	2	75	3.99	2.43	User defined
Percent content of sand in Layer-2			2	75	2.00	13.19	
Percent content of sand in Layer-3			2	75	44.44	55.75	
Percent content of clay in Layer-1			20	80	67.78	79.02	
Percent content of clay in Layer-2			20	80	63.33	24.17	
Percent content of clay in Layer-3			20	80	80.00	34.57	
Percent content of sand in Layer-1		crop	5.8	77.8	17.66	59.91	User defined
Percent content of sand in Layer-2			6.9	72.1	54.02	7.33	
Percent content of sand in Layer-3			7.5	76	71.51	9.29	
Percent content of clay in Layer-1			6.4	78.4	68.10	57.72	
Percent content of clay in Layer-2			10.8	75.6	75.60	65.86	
Percent content of clay in Layer-3			12.2	73.8	33.94	30.04	
Percent content of sand in Layer-1		grass	5.8	77.8	72.71	5.80	User defined
Percent content of sand in Layer-2			16.9	72.1	72.10	16.90	
Percent content of sand in Layer-3			7.5	76	46.89	23.88	
Percent content of clay in Layer-1			6.4	78.4	72.58	68.93	
Percent content of clay in Layer-2			10.8	75.6	60.86	75.60	
Percent content of clay in Layer-3			12.2	73.8	36.29	21.43	

Description	Units	GRU	Lower limit	Upper limit	Top-down (op-I)	Bottom-up	Source
Height of vegetation	[m]	crop	0.05	0.3	0.13	0.06	PBSM Documentation
		grass	0.2	0.8	0.77	0.71	
		NCW	1	2	1.17	1.04	
		forest	2	20	6.83	19.56	

Appendix D: Calibration of QRB (Option-I) and selected watersheds (Option-II) using Top-down approach

Table D.1: Calibration parameter values of the MESH models for QRB (Option-I) and its sub-basins (separately calibrated in Option-II) using 'Top-down' approach of hybridization

			Option-I	**Option-II**									
Description	Units	GRU	**QRB**	Cutarm	Ekapo	Jumping Deer	Pheasant	Kronau Marsh	Lanigan	Lewis	Moose Jaw	Ridge	Saline
River roughness factor that incorporates a channel shape and width to depth ratio as well as Manning's n	[$m^{0.5}s^{-1}$]	-	**2.00**	2.00	1.97	2.00	2.00	0.65	1.99	1.63	0.77	2.00	1.78
Surface storages connectivity coefficient or shape factor	[]	forest	**28.49**	15.54	5.10	20.02	17.40						
		NCW	**4.37**	2.49	1.54	3.50	3.76	0.01	0.80	4.76	3.38	3.15	0.01
		crop	**17.54**	9.19	8.09	22.00	4.41	22.54	11.18	28.39	25.51	9.65	29.34
		grass	**8.90**	29.04	17.77	13.40	16.40	20.16	20.55	24.22	26.87	26.23	15.91
Maximum surface storage capacity	[m]	forest	**0.09**	0.20	2.90	2.33	2.33						
		NCW	**4.56**	0.21	5.58	1.49	10.00	3.19	2.48	7.15	0.60	0.12	4.65
		crop	**0.74**	2.82	2.94	0.78	0.45	0.69	3.59	2.80	1.30	1.09	0.90
		grass	**0.42**	3.72	0.01	4.59	3.53	4.64	4.08	4.57	0.26	2.42	3.85
Maximum leaf area index	[]	forest	**5.88**	5.52	7.96	8.54	5.86						
		NCW	**4.07**	5.45	6.46	5.13	6.19	2.00	4.89	5.05	4.28	4.00	4.08
		crop	**2.83**	2.38	2.00	3.27	3.46	5.97	2.67	2.40	3.04	3.90	2.21
		grass	**2.00**	2.21	2.89	2.71	2.00	2.00	2.17	3.98	2.44	2.82	2.65
Minimum leaf area index	[]	forest	**5.34**	8.87	10.00	1.63	10.00						
		grass	**3.95**	2.06	3.97	2.92	3.96	2.80	3.49	2.42	3.17	3.85	4.00
		NCW	**2.63**	3.32	2.37	2.12	2.35	2.80	2.95	3.91	2.05	2.68	3.66
Annual maximum canopy mass	[kg/m^2]	forest	**26.53**	17.41	23.67	32.71	24.54						
		crop	**4.14**	3.38	2.42	2.00	4.89	4.56	2.13	3.56	2.52	2.79	2.12
		grass	**1.69**	1.54	2.05	1.98	1.50	2.44	2.37	2.54	2.90	2.87	2.69
		NCW	**2.84**	2.75	2.12	2.13	2.94	2.44	2.00	2.93	1.84	2.81	1.50
Annual maximum rooting depth	[m]	forest	**4.18**	1.53	2.80	2.90	4.01						
		crop	**1.20**	3.00	3.79	4.19	2.83	2.03	4.61	3.68	1.85	1.37	1.20
		grass	**0.20**	0.20	0.24	1.31	2.15	2.68	2.09	3.29	5.00	4.62	3.47
		NCW	**3.07**	4.02	0.83	2.30	0.47	2.68	4.01	2.05	0.40	3.66	0.56
Natural log of roughness length	[]	forest	**0.26**	-0.09	-0.09	-0.22	0.40						
		crop	**-2.29**	-1.76	-1.60	-1.48	-2.53	-1.01	-1.36	-1.38	-2.16	-1.75	-2.18
		grass	**-1.54**	-1.66	-1.65	-1.16	-1.56	-1.13	-1.40	-1.05	-1.56	-1.00	-1.59
		NCW	**-1.17**	-1.00	-1.39	-1.32	-1.17	-1.13	-1.21	-1.63	-1.00	-1.42	-1.00
Average visible albedo when fully-leafed or of the land cover	[]	forest	**0.04**	0.04	0.04	0.03	0.03						
		crop	**0.08**	0.04	0.05	0.08	0.04	0.06	0.08	0.04	0.06	0.08	0.07
		grass	**0.05**	0.04	0.07	0.04	0.04	0.05	0.05	0.04	0.07	0.05	0.06
		NCW	**0.04**	0.07	0.08	0.07	0.05	0.03	0.06	0.05	0.05	0.06	0.04
	[]	forest	**0.17**	0.30	0.21	0.21	0.19						

			Option-I				Option-II							
Description	Units	GRU	**QRB**	Cutarm	Ekapo	Jumping Deer	Pheasant	Kronau Marsh	Lanigan	Lewis	Moose Jaw	Ridge	Saline
Average near-infrared albedo when fully-leafed or of the land cover		crop	**0.26**	0.35	0.31	0.39	0.39	0.38	0.38	0.31	0.40	0.26	0.29
		grass	**0.32**	0.37	0.43	0.41	0.29	0.37	0.46	0.43	0.46	0.31	0.36
		NCW	**0.27**	0.31	0.26	0.37	0.30	0.25	0.45	0.41	0.45	0.44	0.26
Limiting snow depth below which coverage is less than 100%	[m]	forest	**0.05**	0.19	0.27	0.12	0.27						
		NCW	**0.19**	0.06	0.30	0.05	0.18	0.29	0.30	0.10	0.20	0.10	0.27
		crop	**0.22**	0.15	0.06	0.25	0.18	0.23	0.25	0.20	0.25	0.12	0.23
		grass	**0.30**	0.21	0.05	0.05	0.22	0.24	0.08	0.10	0.08	0.29	0.05
Maximum water ponding depth for snow covered areas	[m]	forest	**0.16**	0.08	0.25	0.18	0.16						
		NCW	**0.22**	0.10	0.22	0.16	0.13	0.15	0.07	0.24	0.13	0.15	0.25
		crop	**0.05**	0.08	0.09	0.07	0.23	0.21	0.22	0.13	0.05	0.11	0.21
		grass	**0.11**	0.10	0.19	0.25	0.07	0.05	0.07	0.08	0.23	0.13	0.05
Maximum water ponding depth for snow free areas	[m]	forest	**0.25**	0.17	0.05	0.16	0.07						
		NCW	**0.05**	0.24	0.12	0.05	0.23	0.24	0.24	0.23	0.16	0.10	0.14
		crop	**0.07**	0.19	0.09	0.20	0.24	0.10	0.17	0.09	0.18	0.09	0.17
		grass	**0.19**	0.15	0.08	0.06	0.25	0.09	0.10	0.23	0.22	0.19	0.13
Manning's n for overland flow	[$ms^{-1/3}$]	forest	**0.04**	0.03	0.04	0.03	0.02						
		crop	**0.05**	0.05	0.05	0.02	0.02	0.02	0.04	0.03	0.03	0.04	0.01
		grass	**0.05**	0.02	0.04	0.02	0.04	0.04	0.02	0.01	0.02	0.04	0.03
		NCW	**0.02**	0.04	0.03	0.04	0.04	0.02	0.04	0.02	0.05	0.03	0.04
Permeable depth of the soil column	[m]	forest	**2.50**	0.10	3.82	2.15	3.48						
		crop	**1.11**	4.10	2.40	3.65	2.27	1.60	3.30	2.78	3.13	2.37	0.95
		grass	**3.29**	2.13	3.87	0.31	2.17	0.37	3.80	0.40	0.87	1.57	1.68
		NCW	**4.10**	1.75	1.13	3.91	2.51	0.01	3.13	2.08	2.66	0.63	0.02
Saturated surface horizontal soil conductivity	[ms^{-1}]	forest	0.0048	0.0083	0.0075	0.0001	0.0033						
		crop	0.0050	0.0005	0.0001	0.0011	0.0036	0.0059	0.0045	0.0063	0.0025	0.0044	0.0001
		grass	0.0041	0.0013	0.0036	0.0017	0.0046	0.0100	0.0014	0.0062	0.0013	0.0055	0.0029
		NCW	0.0018	0.0030	0.0021	0.0045	0.0031	0.0005	0.0086	0.0021	0.0049	0.0032	0.0076
Drainage density, equal to the length of the stream divided by area drained by the stream	[km/km^2]	forest	**61.87**	65.26	120.0	119.3	115.9						
		crop	**99.05**	80.23	54.17	54.72	110.8	53.02	58.19	90.89	51.76	80.06	59.44
		grass	**100.9**	50.00	120.0	84.36	118.8	103.0	75.15	68.76	88.22	86.11	107.2
		NCW	**89.10**	93.07	73.47	96.43	52.49	103.7	95.04	108.9	102.8	100.5	65.59
Fraction of the saturated surface soil conductivity moving in the horizontal direction	[]	forest	**0.67**	0.03	0.42	0.10	0.11						
		crop	**0.80**	0.41	0.26	0.76	0.46	0.38	0.31	0.78	0.37	0.70	0.50
		grass	**0.37**	0.03	0.71	0.25	0.66	0.04	0.52	0.02	0.30	0.78	0.43
		NCW	**0.00**	0.03	0.03	0.09	0.02	0.04	0.02	0.08	0.01	0.01	0.03
Soil drainage index. Index 1 allows the soil physics to determine drainage and index 0 completely impede drainage	[]	forest	**0.77**	0.76	0.26	0.15	0.21						
		crop	**0.00**	0.70	0.42	0.52	0.75	0.80	1.00	0.02	0.00	0.54	0.92
		grass	**0.49**	0.10	1.00	0.79	0.82	0.00	0.96	0.12	0.00	0.72	0.00
		NCW	**0.09**	0.03	0.00	0.08	0.03	0.06	0.00	0.09	0.02	0.00	0.02
Percent content of sand in Layer-1		forest	**32.03**	5.80	75.51	8.49	24.43						
Percent content of sand in Layer-2			**72.10**	37.51	40.23	48.97	68.20						
Percent content of sand in Layer-3			**44.54**	11.89	68.49	19.91	43.45						
Percent content of clay in Layer-1			**12.79**	78.40	36.42	75.97	22.61						

			Option-I			Option-II								
Description	Units	GRU	**QRB**	Cutarm	Ekapo	Jumping Deer	Pheasant	Kronau Marsh	Lanigan	Lewis	Moose Jaw	Ridge	Saline
Percent content of clay in Layer-2			**54.93**	43.06	16.82	60.92	10.80						
Percent content of clay in Layer-3			**31.25**	12.20	15.47	70.01	25.34						
Percent content of sand in Layer-1			**3.99**	15.83	17.58	23.16	11.30	5.72	39.06	18.33	5.27	2.00	2.00
Percent content of sand in Layer-2			**2.00**	47.34	23.84	2.00	2.92	6.69	22.15	29.43	2.00	43.71	70.96
Percent content of sand in Layer-3			**44.44**	50.98	8.97	62.61	2.00	10.47	44.94	51.80	74.60	53.89	2.16
Percent content of clay in Layer-1		NCW	**67.78**	20.05	38.80	75.68	79.26	38.97	65.83	78.36	35.83	47.70	24.30
Percent content of clay in Layer-2			**63.33**	22.24	78.34	43.13	78.06	77.81	79.16	54.18	20.00	27.88	75.45
Percent content of clay in Layer-3			**80.00**	63.92	25.93	73.15	74.22	71.77	59.92	37.04	47.93	46.32	63.25
Percent content of sand in Layer-1			**17.66**	71.13	10.78	32.72	10.90	15.55	19.46	18.93	45.06	64.73	5.80
Percent content of sand in Layer-2			**54.02**	17.51	37.04	41.58	20.88	64.00	20.45	42.26	28.74	11.71	26.88
Percent content of sand in Layer-3			**71.51**	37.94	39.81	28.31	46.33	57.90	75.32	53.29	65.02	33.12	65.40
Percent content of clay in Layer-1		crop	**68.10**	52.92	29.51	6.40	49.68	13.20	26.56	31.10	50.54	31.27	35.81
Percent content of clay in Layer-2			**75.60**	36.39	30.71	21.63	39.04	12.44	19.89	40.69	11.42	63.07	29.27
Percent content of clay in Layer-3			**33.94**	12.86	21.46	49.43	12.20	12.83	23.91	65.20	68.39	25.19	13.92
Percent content of sand in Layer-1			**72.71**	73.91	11.83	72.29	70.83	8.20	75.89	21.54	30.44	43.40	33.81
Percent content of sand in Layer-2			**72.10**	20.73	66.40	50.36	25.38	51.05	47.77	68.79	51.21	37.94	72.10
Percent content of sand in Layer-3			**46.89**	54.16	60.73	53.22	42.21	15.90	43.66	73.67	47.85	25.50	41.50
Percent content of clay in Layer-1		grass	**72.58**	25.34	65.58	51.66	66.98	32.96	50.98	43.51	18.61	6.40	57.14
Percent content of clay in Layer-2			**60.86**	72.94	59.13	48.71	75.60	22.02	49.31	50.79	57.96	34.96	45.52
Percent content of clay in Layer-3			**36.29**	31.76	34.80	16.77	57.32	24.98	70.75	16.01	12.20	71.53	34.42
Height of vegetation	[m]	crop	**0.13**	0.21	0.30	0.14	0.08	0.24	0.20	0.06	0.26	0.22	0.29
		grass	**0.77**	0.74	0.44	0.23	0.76	0.21	0.60	0.35	0.70	0.67	0.33
		NCW	**1.17**	1.79	1.55	1.96	1.48	0.62	1.87	1.68	1.07	1.47	1.64
		forest	**6.83**	2.20	2.00	8.86	9.58						